TOWARDS ENERGY HARVESTING AND INTERFERENCE MITIGATION FOR D2D COMMUNICATION IN 5G

A Thesis submitted in fulfillment of the requirement for the award of the degree of

DOCTOR OF PHILOSOPHY

IN

COMPUTER SCIENCE AND ENGINEERING

Submitted by:

Ishan Budhiraja

(Registration No. : 901703009)

Under the guidance of:

Dr. Neeraj Kumar
Professor, CSED

Dr. Sudhanshu Tyagi
Assistant Professor, ECED

THAPAR INSTITUTE
OF ENGINEERING & TECHNOLOGY
(Deemed to be University)

COMPUTER SCIENCE AND ENGINEERING DEPARTMENT
THAPAR INSTITUTE OF ENGINEERING & TECHNOLOGY,
PATIALA – 147004

March 2021

CERTIFICATE

I, Ishan Budhiraja, Regn. No. 901703009, hereby declare that the thesis entitled **"Towards Energy Harvesting and Interference Mitigation for D2D Communication in 5G"** submitted to the Computer Science and Engineering Department at Thapar Institute of Engineering and Technology, Patiala, Punjab, India is an authenticated record of my own work for the award of the degree of "Doctor of Philosophy" under the supervision of Prof. (Dr.) Neeraj Kumar and Dr. Sudhanshu Tyagi. This report has not been submitted to any other institution for award of any other degree.

Ishan Budhiraja
Regn. No. 901703009

Place: Patiala, Punjab (India)
Date: March 18, 2021

This is to certify that the above statement made by the candidate is correct to the best of our knowledge.

Verified by:

Dr. Neeraj Kumar
(Supervisor)
Professor
CSED
Thapar Institute of Engg. & Tech.
Patiala, Punjab (India)

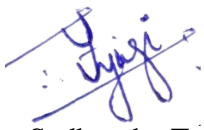

Dr. Sudhanshu Tyagi
(Supervisor)
Assistant Professor
ECED
Thapar Institute of Engg. & Tech.
Patiala, Punjab (India)

ABSTRACT

The exponential growth in the usage of various data-intensive applications such as ultra high definition video transmission, live streaming, augmented reality, virtual reality, real-time video calling, live conferences, and social network services, generate a huge amount of data traffic. This massive increment in data traffic degrades the spectral efficiency. To fulfil the high-end data rate requirements of the aforementioned applications, up-gradation in the existing cellular infrastructure is much needed to meet out the requirements of fifth-generation (5G) networks. Some of the salient features of the 5G networks are high spectral efficiency, massive connectivity, and ultra-reliable low latency. To enhance the spectral efficiency, the researchers from both academia and industry emphasize the usage of device-to-device (D2D) communication.

D2D is supporting to the 5G networks in which nearby user equipment can communicate directly or cooperatively to each other with or without depending upon the base station (BS). It offloads the data traffic to counterbalance the load on the BS using either overlay or underlay paradigm. In overlay scenario, a dedicated spectrum resource is assigned to the D2D users and the rest is used by the cellular mobile users (CMUs). On the other hand, in the underlay scenario, D2D users reuse the spectrum resources assigned to the CMUs which increases network spectral efficiency. Despite these advantages, mutual interference between the D2D mobile users (DMUs) and CMUs has been a challenging issue in the underlaying networks.

Apart from the interference, data management due to massive connectivity is another issue in the 5G networks. The existing underlay D2D cellular infrastructure hugely depends on the orthogonal multiple access (OMA) for spectral reuse. In OMA, one resource block (RB) can serve to one user only, it degrades the spectral efficiency. Also, the OMA supported D2D communication is expensive as connections are limited. To mitigate these issues, power domain non-orthogonal multiple access (PD-NOMA) is used. In PD-NOMA, multiple users are served using different power levels opportunistically as per the channel conditions and quality-of-service (QoS) from a common orthogonal channel. The PD-NOMA based spectrum sharing has considered a better solution for D2D communication in 5G to improve spectrum efficiency, and network connectivity.

Energy is another major issue in D2D communication due to the limited energy storage capability of a battery. To prolong the lifetime of a battery, the wireless powered communication network (WPCN) is used. The WPCN is a harvest-then-transmit protocol and is a combination of the downlink wireless energy transfer (WET) and the uplink wireless information transfer

(WIT). In WET, devices harvest energy from ambient radio frequency (RF) signals to empower their battery, and in WIT, the devices transmit information to the desired user using harvested energy.

In this research work, the following schemes have been proposed to rectify the aforementioned issues:

- Firstly, a “Cross-Layer Interference Management Scheme for D2D Mobile Users Using NOMA" is proposed. In this scheme, the sum rate of the overall network is maximized with respect to the constraints of RB and power allocation. To achieve this goal, the D2D mobile groups (DMGs) are designed between the D2D transmitter (DDT) and DMUs to reduce the intra-user interference using successive interference cancellation (SIC) technique. Secondly, the resource allocation scheme for both the CMUs and DMGs is designed to mitigate the cross-interference using many-to-many mapping scheme. Also, to fully exploit the potential benefits of DMGs and to enhance the spectral efficiency of the DMGs, the group rate selection criterion based RB reuse algorithm among DMGs is proposed. Lastly, for power optimization, the difference of two convex programming approach based on a successive convex approximation with low complexity is used to reduce the co-channel interference.

- The second scheme is “Energy-Delay Tradeoff Scheme for NOMA-Based D2D Groups With Wireless Powered Communication Networks". In this, firstly, the DDTs and CMUs harvest energy from the RF signals of the BS. Then, the CMUs and DDTs transmit the information to the BS and DMUs from the harvested energy using the time division multiple access (TDMA) and PD-NOMA, respectively. Considering both stochastic traffic arrivals and time-varying channel conditions, the stochastic optimization problem is formulated, here, the aim is to maximize the energy efficiency and minimize the delay. The many-to-one matching based subchannel allocation, weighted sum method and Lyapunov optimization scheme are used to estimate the optimal outcome. Further, to obtain the closed-form expression of power and to optimize the time for WPCN, the Lagrangian function has been used.

  To simulate the above two schemes Matlab 2017b and convex optimization (CVX) tools are used, and the parameters used in the simulation are taken from 3GPP urban path loss model (Release- 15 and RAN1).

ACKNOWLEDGMENT

Before discussing my journey of Ph.D., I would like to thank the almighty God who gave me strength and courage to overcome all the obstacles and complete this endeavour. The aim of my life, to be called by the salutation of a 'Doctor', seems to become a reality, when I got admission in Doctorate of philosophy in Thapar Institute of Engineering and Technology, Deemed to be University, Patiala. Research initiated with this startup in my life. Without acknowledging the people who supported me throughout this journey, this task would be incomplete. I know words are never enough to express the gratitude; I am just delivering the phrase for the acceptance of regards.

Firstly, I would like to express my sincerest thanks to my parents. With their consent, support and motivation, I thought to accept this biggest challenge in my life. They have been the true source of real inspiration for me. Secondly, I would like to thank my supervisor, **Prof. (Dr.) Neeraj Kumar (Professor, CSED) and Dr. Sudhanshu Tyagi (Assistant Professor, ECED)**, who have supported me throughout my Ph.D. work with their patience and knowledge; while providing me with the room to work in my own way. Apart from providing me with excellent supervision, active cooperation and constant encouragement throughout this journey, they also shared their invaluable experiences with me to succeed in life. I will always remain indebted to them.

I am very thankful to the examiners **Prof. (Dr.) Sukumar Nandi**, Indian Institute of Technology, Guwahati, India and **Prof. Azzedine Boukerche**, Distinguished University Professor and Canada Research Chair Tier-1 at the University of Ottawa, Ontario, Canada for taking out their valuable time from their busy schedule and evaluating my thesis.

I am also grateful to the head of the department, Prof. Maninder Singh, Associate head, Prof. Inderveer Chana, Ph.D. Coordinator, Dr. Sushma Jain, and members of my doctoral committee, Prof. (Dr.) Rajesh Kumar, Dr. Raman Singh Chauhan, and Dr. M. D. Singh for their constructive suggestions and ensuring the correct pace of my work. I am also obliged to the Director, Prof. Prakash Gopalan, Dean (RSP), Prof. Rafat Siddique and the management of Thapar Institute of Engineering and Technology, who provided me with all the necessary resources and facilities to complete my work.

The chain of my gratitude will definitely be incomplete if I forget to thank my complete family, my honourable father **Shri. G. G. Budhiraja**, my respected mother **Mrs. Anita Budhiraja**, my elder brother Mr. Saurabh Budhiraja, my sister-in-law Mrs. Shalu Budhiraja and my cute niece Yashika Budhiraja, for their unconditional love, support and encouragement in

every phase of my life. It was due to my father's confidence and vision that motivated me to overcome every obstacle during the research. Since then, the journey of Ph.D. has been a sweet and bitter ride at times which leads to a special mention for my mother who stood by me through thick and thin and gave me courage at the times when I felt really low. Her constant motivation showed me the silver lining in the dark clouds.

I would also like to express heartfelt thanks to Prof. Anil Budhiraja (Principal), Seth Jai Prakash Polytechnic, Damla, Yamuna Nagar, Dr. Sudeep Tanwar, (Associate Professor), Nirma University, Gujarat, Dr. Sujit Patel, Dr. Bharat Garg, Dr. Navneet Sharma, and Dr. Shreesh Kumar Rai for providing their valuable guidance and support to me throughout this journey. I would also like to pay my sincere regards to all my relatives and cousins for their constant motivation and support. They made this journey more comfortable with words of encouragement which helped me in finishing my work.

I would also like to thank my friends and colleagues with whom I have travelled this journey of research. A special thanks to my research group, Dr. Anish Jindal, Dr. Aaisha Makkar, Dr. Gagangeet Singh Aujla, Dr. Kuljeet Kaur, Dr. Sahil Garg, Dr. Rajat Chaudhary, and budding doctors Ms. Shubhani Aggarwal, Ms. Arzoo Miglani, Mr. Sandeep Saran, and Mr. Himanshu Sharma. These people have made my research journey more memorable and pleasant. As one cannot mention the names of all well-wishers, friends and beloved ones, I would like to pay my regards to one and all who supported me directly or indirectly during this journey of knowledge.

(**Ishan Budhiraja**)

List of Publications

Journal Publications (SCI/SCIE):

1. **I. Budhiraja**, N. Kumar and S. Tyagi, "Cross-Layer Interference Management Scheme for D2D Mobile Users Using NOMA", in **IEEE Systems Journal**, pp. 1-12, June 2020. (Early Access, DOI: 10.1109/JSYST.2020.2997731).

2. **I. Budhiraja**, N. Kumar and S. Tyagi, "Energy-Delay Tradeoff Scheme for NOMA-based D2D Groups With WPCNs ", in **IEEE Systems Journal**, pp. 1-12, Aug. 2020. (Early Access, DOI: 10.1109/JSYST.2020.2997731)

Contents

List of Figures

List of Tables

List of Abbreviations

Abbreviations	Definitions
3GPP	Third Generation Public Partnership Project
5G	Fifth Generation
5GPPP	Fifth Generation Public Partnership Project
AF	Amplify and Forward
ANOMA	Asynchronous NOMA
AS	Antenna Selection
AWGN	Additive Voice Gaussian Noise
BA	Buffer Aided
BD/BDMA	Beam Division/ Beam Division Multiple Access
BER	Bit Error Rate
BF	Beamforming
BLER	Block Error Rate
BNBF	Best Near Best Far
BOMA	Beam-orthogonal Multiple Access
BRS	Best Relay Selection
BS	Base Station
CAGR	Compound Annual Growth Rate
CAP	Carrier less Amplitude Phase
CCI	Co-channel Interference
CCU	Cell Center User
CDF	Cumulative Density Function
CDMA	Code Division Multiple Access
CD-NOMA	Code Division Non-Orthogonal Multiple Access
CDRT	Co-ordinated Direct and Relay Transmission
CEU	Cell Edge User
CFO	Carrier Frequency Offset
CFR	Co-ordinated Full Duplex Relaying
CMR	Cooperative Multi-relay
CMU	Cellular Mobile User
CNAR	Collaborative NOMA Assisted Relaying
C-NOMA	Cooperative NOMA
CO	Coordinated
CoMP	Coordinated Multipoint Transmission
CQI	Channel Queue Indicator
CR	Cognitive Radio
CrCI	Cross Channel Interference

Abbreviations	**Definitions**
CRN	Cognitive Radio Network
CRS	Cooperative Relay Selection
CS	Compressed Sensing
CS/CB	Coordinated Scheduling/Beamforming
CSC	Coordinated Superposition Coding
CSI	Channel State Information
CSS	Cooperative Spectrum Sensing
CUs	Cellular Users
DC-NOMA	D2D aided Cooperative NOMA
DCO	Direct Current Optical
DDF	Dynamic Decode and Forward
DF	Decode and Forward
DH	Dynamic Hybrid
D-NOMA	Dynamic NOMA
DPA	Dynamic Power Allocation
DPS	Dynamic Power Scheduling
D-R	Destination Relay
DRS	Dynamic Relay selection
DSA	Dynamic Spectrum Allocation
D2D	Device-to-Device
DA-NOMA	Delay Aware NOMA
DBIRA	Dual based Iterative Resource Allocation
DBS	Distributed Base Station
DC	Difference of Two Convex Function
DDT	D2D Transmitter
DMG	D2D Mobile group
DMU	D2D Mobile User
EAB	Enhanced Access Bearing
EE	Energy Efficiency
EEPA	Energy Efficient Power Allocation
EMC	Electromagnetic Capability
EPA	Expectation Propagation Algorithm
ESE	Elementary Signal Estimator
ETT	Equal Transmission Time
FD	Full Duplex
FDMA	Frequency Division Multiple Access
FFR	Fractional Frequency Reuse
F-NOMA	Fixed NOMA
FPA	Fixed Power Allocation
FRAB	Finite Resolution Analog Beamforming
F-SUS	Fairness Oriented Secondary User Scheduling
FTN-FrCT	Faster-Than-Nyquist Fractional Cosine Transform
GF	Grant Free
GFDM	Generalised Frequency Division Multiplexing

Abbreviations	Definitions
GOCA	Group-Orthogonal Coded Access
GP	Gradient Projection
GRPA	Gain ratio Power Allocation
GRSC	Group Rate Selection Criterion
GSM	Global System For Mobile
GSSK	Generalised Space Shift Keying
H2H	Human-to-Human
HAP	Hybrid Access Point
HARQ	Hybrid Automatic Repeat Request
HB	Hybrid Beamforming
HD	High Definition
HD	Half Duplex
HDAF	Hybrid Decode Amplify and Forward
HetNets	Heterogeneous Networks
H-NOMA	Hybrid NOMA
IA	Interference Alignment
IBPA	Inversion-based Pairing Algorithm
ICA	Interference Channel Alignment
ID	Information Decoding
IDMA	Interleave Division Multiple Access
IGMA	Interleave Grid Multiple Access
IMT	International Mobile Telecommunication
IoT	Internet of Things
ITU-R	International Telecommunication Union-Radio
JA-STSK	Joint-Alphabet Space Time Shift Keying
JP	Joint Processing
JT	Joint Transmission
LCRS	Low Code Rate Spreading
LDPC	Low Density Parity Check
LDS	Low Density Spreading
LDS-CDMA	Low Density Spreading-CDMA
LDS-OFDMA	Low Density Spreading-OFDMA
LDS-SVE	Low Density Spreading-Signature Vector Extension
LPMA	Lattice Pattern Multiple Access
LSSA	Low Code Rate and signature based Shared Access
LTE-A	Long Term Evolution Advanced
M2M	Machine-to-Machine
MBMS	Multimedia Broadcast/Multicast Service
MCIK	Multi-carrier shift Keying
MDMA	Multipath Division Multiple Access
MEC	Mobile Edge Computing
METIS	Mobile and Wireless Communication Enablers for the Twenty Information Society
MGF	Moment Generating Function
MIMO	Multiple Input Muliplt Output

Abbreviations	**Definitions**
MINLP	Mixed Integer Non-Linear Programming
mMIMO	massive Multiple Input Multiple Output
MMSE	Maximum Mean Square Error
mMTC	massive Machine Type Communication
mmWave	Millimeter Wave
MPA	Message Passing Algorithm
MRC	Maximal Ratio Combining
MRT	Maximal Ratio Transmission
MSs	Mobile Stations
MTBSA	Matching Theory based Subcahnnel Allocation
MUD	Multi-user Detection
MUI	Multi-user Interference
MU-MIMO	Multi-user MIMO
MUSA	Multi-user Shared Access
MUST	Multi-user Superimposed Transmission
NCC	Non-orthogonal cover codes
NCMA	Non-orthogonal Coded Multiple Access
NI	NOMA Interference
N-NOMA	Network NOMA
NOCA	Non-orthogonal Coded Access
NOMA	Non-Orthogonal Multiple Access
OMA	Orthogonal Multiple Access
OMP	Orthogonal Multi Pursuit
OP	Outage Probability
PAP	Power Allocation Problem
PAPR	Power-to-Average Power Ratio
PBPA	Projection based Pairing Algorithm
PC-NOMA	Polar code-NOMA
PDF	Probability Density Function
PDMA	Pattern Division Multiple Access
PD-NOMA	Power Domain NOMA
PEP	Pairwise Error Probability
PFDM	PU First Decoding Method
PLC	Power Line Communication
PSMA	Power Domain Sparse Code Multiple Access
PSO	Particle Swarm Optimization
PU	Primary users
QAM	Quadrature Amplitude Modulation
QoS	Quality of Service
QPSK	Quadrature Phase Shift Keying
QSI	Queue State Information
RA	Random Access
RA-CEMA	Rate-Adaptive Constellation Expansion Multiple Access

Abbreviations	**Definitions**
RB	Resource Block
RBAP	Resource Block Allocation Problem
RBC	Relaying Broadcast Channels
RDMA	Repetition Division Multiple Access
RIePDMA	Random Interleaver Enhanced PDMA
RSMA	Resource Spread Multiple Access
R-SUS	Reliability Oriented Secondary User Scheduling
SAMA	Successive Interference Cancellation Amenable Multiple Access
SATCOM	Satellite Communication
SBD	Successive Bandwidth Division
SC	Sub-channel
SCMA	Sparse Code Multiple Access
SDN	Software Defined Network
SE	Spectral Efficiency
SFDM	SU First Decoding Method
SGMA	Semi-Grant Multiple Access
SINR	Signal-to-Interference Plus Noise Ration
SSMA	Sequence Spreading Multiple Access
S-NOMA	Secure NOMA
SOMA	Semi-Orthogonal Multiple Access
S-R	Source Relay
SSK	Space Shift Keying
SSMA	Short Sequence Spreading Multiple Access
SU	Secondary User
SWIPT	Simultaneous Wireless Information Power Transfer
TC-NOMA	Turbo Code NOMA
TDMA	Time Division Multiple Access
TTMMA	Trellis Tone Modulation Multiple Access
TW	Two Way
TWR	Two Way Relay
UAV	Unmanned Aerial Vehicle
UWB	Ultra Wide Bandwidth
VNI	Visual Networking Index
VP	Virtual Pairing
WET	Wireless Energy Transfer
WIT	Wireless Information Transmission
WPCN	Wireless Powered Communication Network
WSMA	Welch Bound Spreading Multiple Access
ZFBF	Zero-Force Beamforming

Chapter 1

Introduction

With an exponential growth in the proliferation of smart devices and their associated applications, the amount of data traffic and its requirements for higher data rate applications have been increasing continuously. The increasing demands of the users over the limited spectrum, decrease the spectral efficiency (SE) and energy efficiency (EE) of the wireless network. The Cisco Visual Networking Index (VNI) report of 2017 forecasts that more than 75 billion connected devices will utilize the cellular network services by the end of the year 2023 [1]. This is approximately 40 times more than the traffic available in 2017 as shown in Fig 1.1. This increase in data traffic creates the burden on the spectrum due to which SE and EE degraded. Now, this is a challenge for the researchers of both academia and industry to develop new technologies that efficiently utilize the spectrum. To overcome this problem, researchers proposed a new technology named as D2D communication [2].

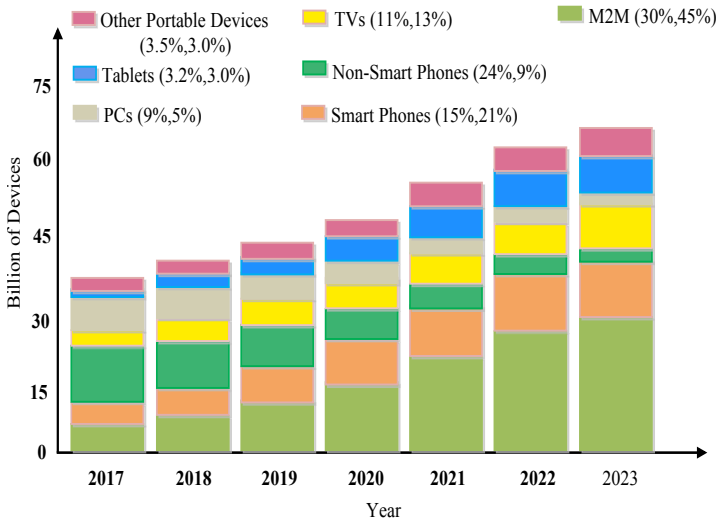

Figure 1.1: CISCO VNI Report

1.1 D2D Commuication

D2D communication is an emerging technology which improves the SE of the network by sharing or reusing the radio resources between DMUs and CMUs. D2D communication is a technique in which proximity user equipments communicate directly to each other without depending upon the base station (BS). This type of communication supports the proximity services which includes social networking applications and public safety communication. To establish a direct link, D2D communication use the licensed (inband) or unlicensed (outband) band with the CUs [2]. Further, inband D2D communication is categorized into two categories: overlay and underlay while outband is categorized as controlled and autonomous. In overlay D2D, a dedicated amount of resource is allocated to their users and the rest of the resources are used by CUs, while in underlay D2D users and CUs both reuse the same resources. For outband, in controlled communication the resources between D2D have managed by the BS while autonomous has managed by the user equipments [3].

1.1.1 Advantages of D2D Commuication

The potential benefits of D2D communication are [3]- [4]: (i) enhance the EE through low power proximity services (ii) enlarge the efficiency of the spectrum by sharing radio resources with CUs (iii) capability to support various types of peer-to-peer services (iv) offload traffic from BSs (v) reduce the latency and improved the QoS of cell edge users (CEUs) for short-distance communication. In spite of the numerous benefits of D2D communication, its performance under ultra-dense network has degraded due to in-cooperation between the adjacent BSs and high interference. Consequently, the SE of the network has to be degraded.

1.1.2 Standards of D2D Communication

Qualcomm was the first organization that proposed very first standard for D2D with a name FlashlinQ. This standard includes the PHY/MAC architecture for D2D communication. 3GPP (Third generation partnership project) was the second organization that developed three standards for D2D communication [3]. In the first standard, 3GPP TR 22.803 (2012) discussed various use cases of D2D. In second, 3GPP TR 23.703(2013) described its detailed architecture and in third, 3GPP Release-12 (ProSe) (2014) investigated the direct communication between the proximity services [4].

1.1.3 Use Cases of D2D Communication

In this the use cases of D2D communication is discussed. The pictorial representation of the use cases is shown in Fig. 1.2

- **Local services:** In this, user equipments (UEs) directly exchange the data with each other without BS. Basic applications of these services are local data transmission, social apps and cellular traffic offloading. For example, in local data transmission, data directly transmitted between UEs on the basis of their proximity. This technique of D2D not only expand the mobile applications but also save the spectrum resources. Which eventually generates, new sources of revenues for operators. In this, the local advertising companies can target users on the basis of their proximity to maximize benefits. Like, a cinema hall in the centre the shopping malls attracts the users' by sending them show-times and promotional tickets.

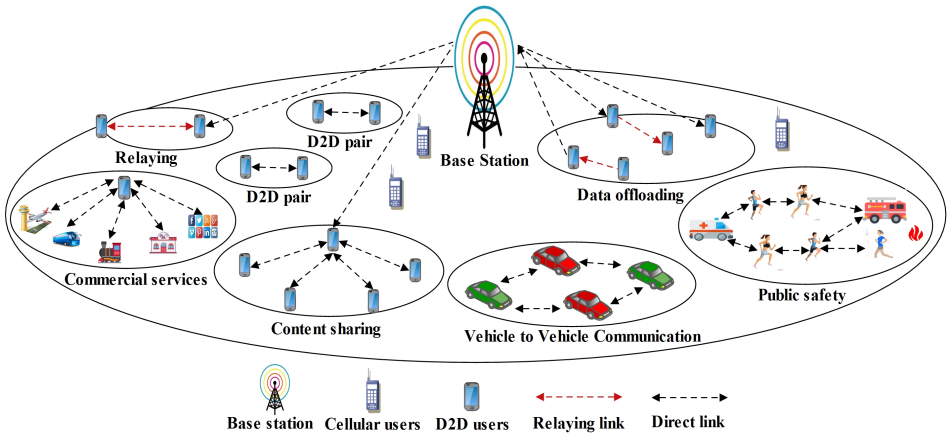

Figure 1.2: General scenario of D2D Communication

- **Emergency Communication:** Under natural calamities such as earthquake, flooding, Tsunami, etc, conventional communication infrastructure gets damaged due to which network disrupted and affect the rescue process. In such situations, with D2D users can establish a multi-hop wireless connection to which ensure smooth communication.

- **Internet of Things Enhancement:** The primary objective of a cellular communication was to set up a network which provides end to end communication between two terminals. The Cisco report [1] forecasts that until 2023, 75 billion wireless devices will be present globally. Out of them, approximately 30 billion may be based on IoT feature. Therefore, using D2D communication technology combined with IoT, a perfect interconnected wireless system can be created. For example, vehicle-to-vehicle (V2V) communication.

- **D2D in multiuser MIMO:** In a regular multi-user MIMO, pre-coding weights have been decided by BSs to provide feedback to terminals. This technique at terminals create the nulls and mitigate interference between UEs but restricted up to single-user MIMO. On the other side, when D2D communication is applied, paired users are formed which

can share the data with the same channel. This enhances the performance of multi-user MIMO system in terms of SE.

1.2 PD-NOMA

In PD-NOMA, each user receives the signals from the BS using multiple resource blocks (RBs), and each RB provides the service to the multiple users. In NOMA, the users' signals are multiplexed at the transmitter using superposition coding and demultiplexed at the receiver using successive interference cancellation (SIC) technique as shown in Fig. 1.3. The use of superposition coding enhances the sum rate, user-fairness, and scheduling flexibility. Moreover, the intra-user interference created by multiplexing can be reduced by the SIC. In PD-NOMA, multiple users are served using different power levels opportunistically as per the conditions and quality-of-service (QoS) from a common orthogonal channel. The NOMA based spectrum sharing has considered a better solution for D2D communication in 5G to improve SE and network connectivity [5].

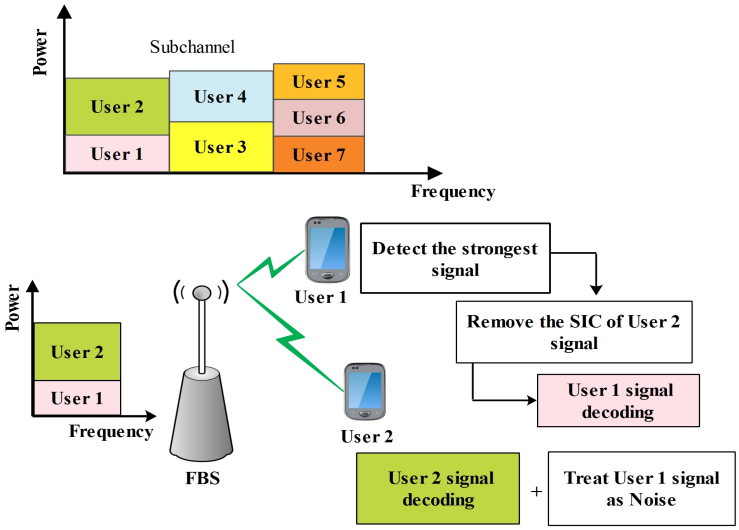

Figure 1.3: PD-NOMA

1.3 Energy Harvesting

Apart from improving SE, EE is another critical issue which needs to be addressed in D2D communication. Generally, electronic devices used for communication are equipped with batteries which have a limited lifetime. To prolong the lifetime of these energy-constrained devices, energy harvesting (EH) is an effective technique [6]. Initially, EH techniques harvest the energy from renewable resources such as sunlight, wind, etc., but these techniques are not reliable due to the dependency on the environment. To overcome this problem, wireless powered

communication networks (WPCN) and simultaneous wireless information and power transfer (SWIPT) were proposed [6], [7]. In WPCN, the devices first harvest energy from the RF signals to store them over downlink and then use the stored energy to transmit the data in the uplink. In WPCN, EH and information decoding process are carried out by different receivers. It is a time-based technique. On the other side, in SWIPT, both the EH and data transmission is carried out from the same RF signals. It is further divided into two schemes: Power splitting (PS) and time splitting (TS). In PS, receiver splits the received power signal into two different ratios, whereas, in TS, the receiver use one antenna to perform both the EH and information decoding [7].

1.4 Thesis Organization

The thesis is organized as follows with the brief description of each chapter:

Chapter 2: Literature Review
This chapter includes a systematic review on variants of NOMA to be used in 5G. The effect of NOMA on D2D communication and other 5G techniques are explored and discussed. A relative comparison of state-of-art approaches is also given in this chapter for the analysis of relative advantages and disadvantages with respect to various evaluation parameters.

Chapter 3: Cross-Layer Interference Mitigation Scheme for D2D Mobile Users Using NOMA
In this chapter, an interference management scheme for D2D mobile users using NOMA in the uplink scenario is explored. The problem of interference in D2D communication arises due to the re-usage of spectrum resources with cellular users. The aim of this chapter is to maximize the sum-rate of the overall network while maintaining the SINR of the CMUs and DMGs. The problem of spectrum reuse is formulated as a mixed-integer non-linear programming form. To address the problem of interference, firstly, the DMGs are formed between the DDT and DMUs to reduce the intra-user interference using the SIC technique. Secondly, the resource allocation scheme for both the CMUs and DMGs is designed to mitigate the cross and co-channel interference using many-to-many mapping scheme. Also, to fully exploit the potential benefits of DMGs, the group rate selection criterion (GRSC) based RB reuse algorithm among DMGs is developed. Lastly, for power optimization, the difference of two convex (DC) functions programming approach based on a successive convex approximation for low complexity (SCALE) is used.

Chapter 4: Energy-Delay Tradeoff Scheme for NOMA-based D2D Mobile Groups with WPCN

In this chapter, a distributed EE and delay tradeoff scheme for NOMA-based DMGs in

wireless powered communication networks is investigated. The DDTs and CMUs harvest energy from the radio frequency signals of the BS. Then, the CMUs and DDTs transmit the information to the BS and DMUs from the harvested energy using the TDMA and NOMA, respectively. The goal of this scheme is to maximize the long-term average EE of each DMG in a distributed manner by maintaining the long-term average EE of each CMU. To achieve this goal, an stochastic optimization problem is formulated which is in the MINLP form. As the optimization problem is in non-linear fractional form, so to convert it into a linear single-objective optimization problem, the weighted sum method is used. Now, to solve the problem, it is divided into three sub-problems (i) Subcarrier allocation (ii) Lyapunov optimization and (iii) Joint time and power allocation. A many-to-one matching based subcarrier allocation scheme is proposed to improve the SE and EE of the network. The Lyapunov optimization approach is used to transforms the stochastic optimization problem into a series of successive deterministic optimization problems. Lastly, to optimize the time and power of DMG across each subcarrier, the Lagrangian method is applied.

Chapter 5: Conclusion and Future Scope
This chapter concludes the thesis by highlighting the contributions made using the proposed schemes. Moreover, this chapter also includes the future directions in the research areas of D2D communication with NOMA and EH in the 5G.

1.5 Summary

In this chapter, the basic idea of using D2D communication, PD-NOMA, and EH are discussed in detail. Moreover, in this chapter, we describe how PD-NOMA solve the problems of inter-user and mutual interference. We have also covered how EH technique improves the energy efficiency of the devices used in short-range communication.

Chapter 2

Literature Review

The exponential growth and usage of smart devices such as smartphones, wearable gadgets, sensors, actuators in Internet-based applications such as ultra HD video transmission, live streaming, augmented reality, virtual reality, real-time video calling, live conferences, and social network services, generates a huge amount of data traffic. It creates an overburden on the LTE/LTE-A spectrum due to which spectral efficiency (SE) of the underlying backbone network infrastructure degrades. According to the CISCO Visual Networking Index (VNI) report [1], it is predicted that smartphones will generate 50 exabytes of data traffic by 2021. Also, from compound annual growth report [1], 2016 forecasts that more than 75 billion connected devices will utilize the cellular network services by the end of the year 2021 as shown in Fig. 2.1. To overcome this problem, various research organizations are keen to use the 5G wireless network that is expected to be fully commercialized by 2020.

To provide a better quality of service (QoS), and quality of experience (QoE) to the end-users, various organizations and countries are putting a lot of efforts on different collaborative projects such as-IMT-2020 (3GPP), 5GPPP/METIS (European Union (EU)), 5G Forums (Korea), and ARIB (Japan). In 2015, International Telecommunication Union-Radiocommunication (ITU-R) officially named the 5G wireless network as IMT-2020 and proposed initial paradigm, key features, and applications [8–10]. The first phase of 5G standard was studied under 3GPP Rel-15 having key features as follows [8] (i) connection density is 10,00000/km^2; (ii) bandwidth is 1 to 2GHz; (iii) data rate is 20/10Gbps (Downlink/Uplink); (iv) latency less than 1ms; (v) Spectral efficiency of 120 bps/Hz; (vi) throughput of 10Gbps; (vii) usage of Massive MIMO that enhances coverage and capacity; (viii) process and transmit information in real-time with high speed up to 1-2Gbps; (ix) frequency band (mmWave) 30 to 300 GHz; (x) Mobility of 500Kmph; (xi) area traffic capacity 10 $Mbits/s/m^2$; and (xii) Energy Efficiency (EE) 50 to 100 times more in comparison to IMT-A.

ITU-R classifies the applications of 5G networks into three broad categories (i) Enhanced Mobile Broadband (eMBB) connection; (ii) Massive machine-type communications (mMTC); and (iii) Ultra-Reliable Low Latency Communication (URLLC). To meet the criteria in 5G, the integration of following technologies, software-defined network (SDN), coordinated mul-

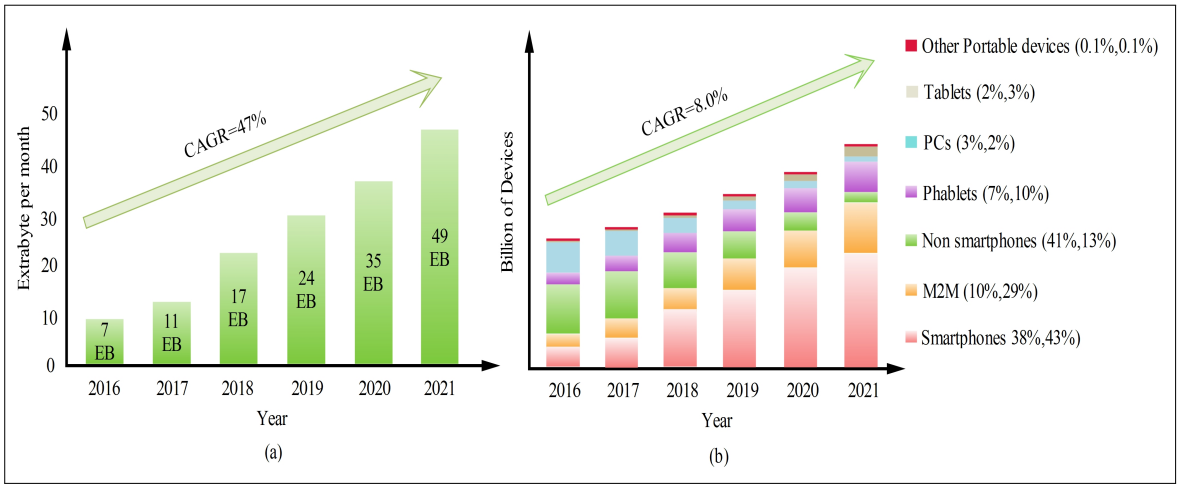

Figure 2.1: CISCO and Compound Annual Growth Report

tipoint (CoMP), cooperative communication, device-to-device (D2D) communication, visible light communication (VLC), machine-to-machine (M2M) communication, cognitive radio network (CRN), small cells, massive multiple-input multiple-output (mMIMO), millimetre wave (mmWave), and vehicle-to-everything (V2X) is greatly needed [8, 10, 11].

The aforementioned integration of different technologies can serve a large number of users from the same resource block (RB) to enhance SE. However, managing asynchronous data generated by machines to provide massive connectivity and diversified QoS to the end-users is a challenging task. To overcome this issue, efficient multiple access (MA) techniques such as Orthogonal multiple access (OMA) and non-orthogonal multiple access (NOMA) are required. Among these two techniques, OMA cannot solve the aforementioned problem due to following reasons (i) bandwidth wastage due to allocation of one orthogonal resource block to each user, and (ii) high signalling overhead and low access efficiency. Hence, NOMA techniques are exploited under the standard 3GPP NR Rel-14 (Downlink) and 3GPP NR Rel-15 (Uplink), especially to handle the aforementioned problems in the 5G environment.

In the NOMA protocol, one resource block (RB) serves more than one users and one user can use more than one RB to improve their data rate. The users' signal is multiplexed at the transmitter side using superposition coding (SC) and demultiplexed at the recipient side using successive interference cancellation (SIC) technique. The usage of SC, enhances the sum rate, user-fairness, and scheduling flexibility. On the other hand, the inter-user interference created by SC multiplexing can be eliminated by SIC. NOMA is broadly classified into two categories: power domain NOMA (PD-NOMA) and code domain NOMA (CD-NOMA). In PD-NOMA, multiple users are served opportunistically as per the channel conditions from a common orthogonal RB. On the other hand, in CD-NOMA, the code spreading sequences are used to serve different users. Different variants of NOMA in these two broad categories are explored and compared in this paper using various evaluation parameters in Sections 3 and 4.

2.1 Scope of the survey

Following are the existing surveys from different the authors addressing various aspects of NOMA [5, 12–22]. Most of these surveys have focused either on CD-NOMA or PD-NOMA alone. But, to the best of our insight, there is no exhaustive survey exists which considered both categories on a common platform. The proposed survey covers most of the variants of NOMA under two broad categories, PD-NOMA and CD-NOMA for 5G networks. The existing survey articles are summarized as follows.

Yunzheng *et al.* [12] reviewed NOMA and waveform modulation schemes for 5G, but the authors do not describe the compatibility of NOMA with 5G. Islam *et al.* [13] surveyed the challenges and implementation issues of PD-NOMA and Liu *et al.* [14] conducted the same on theoretical issues but, the CD-NOMA was partially explored. Ding *et al.* [15], [16] discussed the applications, research, and future challenges of NOMA in 5G. Dai *et al.* [17] analyzed various challenges and solutions for NOMA, but the detailed classification of NOMA was missing in their survey article. Basharat *et al.* [18] focused on the MA schemes of NOMA for 5G along with the discussion on various decoding methods. Aldababsa *et al.* [19] explored the uplink and downlink transmission models for NOMA with their extensions to MIMO and cooperative communication among different devices. Moreover, they discussed the important design challenges and approaches for the Downlink and Uplink NOMA transmissions. But, they have not explored how the compatibility of NOMA with 5G techniques exists. Dai *et al.* [5] focused on PD-NOMA, CD-NOMA as well as all 15 NOMA schemes under Rel-14 3GPP NR. Also, they have explored NOMA for performance gain in different indoor and outdoor scenarios. However, the physical design issues of D2D communication were not explored by the authors. Cai *et al.* [20] explored various modulation techniques of OMA and different MA schemes of NOMA. They have focused on the classification of different NOMA schemes and compared these based on various performance evaluation metrics. But, they have not explored the other challenging applications of NOMA such as D2D communication, M2M communication, and HetNets. Wang *et al.* [21] highlighted the design issues of various NOMA techniques for user separation. Authors focused only on the issues of latency, throughput in PD-NOMA and CD-NOMA. They have also elaborated spatial, hybrid, and network domains. Wu *et al.* [22] presented the technological requirements to enable CD-NOMA and explored its test cases in context with 5G networks but they have not explored PD-NOMA and its compatibility in various 5G techniques. Table 2.1, 2.2 and 2.3 present a summary of these surveys articles with key differences to the proposed survey article.

Fig. 2.2 shows the related surveys articles which also highlights the research gaps in comparison to the proposed survey. The existing surveys on NOMA have mainly concentrated on power domain and code domain. In the proposed paper, we comprehensively studied the different variants of PD-NOMA and CD-NOMA proposed by different authors in context with 5G techniques applicable in various applications.

Table 2.1: Comparison between the proposed and existing NOMA surveys

Year	Authors	Brief			Power Domain				Code Domain					
		1	**2**	**3**	**4**	**5**	**6**	**7**	**8**	**9**	**10**	**11**	**12**	**13**
2015	Yunzheng et al. [12]	✓	×	×	×	×	×	×	MUSA	×	SCMA, PDMA	×	×	×
	Dia et al. [17]	✓	×	✓	✓	✓	×	SoDeMA	×	×	LDS-OFDM, LDS-CDMA, SCMA, PDMA	×	×	×
2016	Zhiqiang et al. [23]	✓	✓	×	✓	✓	x	MIMO	×	×	LDS-OFDM	×	×	×
	Wang et al. [24]	✓	×	✓	×	✓	✓	×	MUSA	RSMA	SCMA, PDMA	×	×	×
	Chunlin et al. [25]	×	×	×	×	×	×	mMTC	MUSA	RSMA	SCMA, PDMA	IDMA	×	×
2017	Ding et al. [16]	✓	×	✓	✓	✓	×	CC, MIMO, CR	×	×	×	×	×	×
	Ding et al. [15]	✓	×	×	✓	✓	×	CR, mmWave, MIMO,SISO, CC	NCMA	x	SCMA, PDMA, LDS	×	LPMA	×
	Islam et al. [13]	✓	x	×	✓	✓	×	CC, CoMP, VLC, SWIPT	×	×	×	×	×	×
	Liu et al. [14]	✓	✓	✓	✓	✓	×	D2D, MIMO, CC, SDN, HetNets, mmWave	×	×	LDS-OFDM, LDS-CDMA, SCMA, PDMA	IDMA	LPMA	×
	Basharat et al. [18]	✓	✓	×	×	✓	×	CR	MUSA		SCMA, PDMA, LDS	×	×	×

Note- 1: Basics, 2: History, 3: Standards, 4: Capacity comparison, 5: DL/UL , 6: MUD Techniques, 7: Compatibility with 5G, 8: Spreading, 9: Scrambling, 10: Coding, 11: Interleaving, 12: Lattice & Beam, 13: Miscellaneous

Notations- ✓: Y, and ×: N

Table 2.2: Comparison between the proposed and existing NOMA surveys

Year	Authors	Brief			Power Domain				Code Domain					
		1	2	3	4	5	6	7	8	9	10	11	12	13
2017	Shan et al. [26]	✓	×	×	×	×	×	HetNets	×	×	×	×	×	×
	Shirvanimogha et al. [27]	✓	×	×	×	×	×	M2M/IoT	×	×	×	×	×	×
	Di et al. [28]	✓	×	×	✓	✓	×	V2X	×	×	×	×	×	×
2018	Cai et al. [20]	✓	×	×	×	×	×	CC, CoMP, MIMO, CR	×	×	LDS-OFDM, LDS-CDMA, SCMA, PDMA	×	LPMA, BOMA	×
	Qi et al. [21]	✓	×	×	×	×	×	×	MUSA, NOCA, NCMA	RSMA	SCMA, PDMA	IGMA	×	×
	Aldababsa et al. [19]	✓	×	×	✓	✓	×	CC, MIMO	×	×	×	×	×	×
	Wu et al. [22]	✓	×	×	✓	×	×	×	MUSA, NOCA, NCMA, FDS, GOCA	RSMA, LSSA	LDS-OFDM, LDS-CDMA, SCMA, PDMA	IGMA, IDMA, LCRS	×	×
	Xiao et al. [29]	✓	×	×	×	×	×	mmWave	×	×	×	×	×	×
	Chandra et al. [30]	✓	×	×	×	×	×	mmWave	×	×	×	×	×	×
	Zhou et al. [31]	✓	×	×	×	×	×	CR	×	×	×	×	×	×
	Wan et al. [32]	✓	×	×	✓	✓	×	CC	×	×	×	×	×	×
	Ali et al. [33]	✓	×	×	✓	✓	×	CoMP	×	×	×	×	×	×
	Zhang et al. [34]	✓	×	×	×	×	×	HeUDNs	×	×	×	×	×	×
	Huang et al. [35]	✓	×	×	×	×	×	MIMO	×	×	×	×	×	×
	Zhong et al. [36]	✓	×	×	×	×	×	MIMO	×	×	×	×	×	×

Note- 1: Basics, 2: History, 3: Standards, 4: Capacity comparison, 5: DL/UL , 6: MUD Techniques, 7: Compatibility with 5G, 8: Spreading, 9: Scrambling, 10: Coding, 11: Interleaving, 12: Lattice & Beam, 13: Miscellaneous

Notations- ✓: Y, and ×: N

Table 2.3: Comparison between the proposed and existing NOMA surveys

Year	Authors	Brief			Power Domain				Code Domain					
		1	2	3	4	5	6	7	8	9	10	11	12	13
2018	Ye et al. [37]	✓	✓	✓	✓	✓	✓	Grant-Free	MUSA, NOCA NCMA, FDS, GOCA	RSMA, LSSA	LDS-SVE SCMA, PDMA	IGMA, IDMA, LCRS	×	×
	Marshoud et al. [38]	✓	×	×	×	×	×	VLC	×	×	×	×	×	×
	Chen et al. [39]	✓	✓	✓	×	×	×	Grant-Free	×	×	×	×	×	×
	Dia et al. [5]	✓	✓	✓	✓	✓	✓	D2D, CoMP, CR, MIMO	MUSA, NOCA NCMA, FDS, GOCA, WSMA	RSMA, LSSA	LDS-OFDM, LDS-CDMA, SCMA, PDMA	IGMA, IDMA, LCRS	LPMA, BOMA	SAMA, SDMA
2019	Shahab et al. [40]	×	×	×	×	✓	×	×	MUSA, NOCA NCMA, FDS, GOCA, WSMA	RSMA, LSSA	LDS-SVE, LDS-OFDM, LDS-CDMA, SCMA, PDMA , SAMA	IGMA, IDMA, RDMA, LCRS	LPMA, BOMA BDMA	×
2020	Our Work	✓	✓	✓	✓	✓	✓	D2D, CC, CoMP, CR, M2M, Grant-Free, SWIPT, WPCN, SISO, MISO, MIMO, mMIMO, VLC, V2X, UAV, MEC, WSX, UDN	MUSA, NOCA NCMA, FDS, GOCA, WSMA	RSMA, LSSA	LDS-SVE, LDS-OFDM, LDS-CDMA, SCMA, PDMA , SAMA	IGMA, IDMA, RDMA, LCRS	LPMA, BOMA BDMA	MDMA, PSMA, SOMA, RA-CEMA, TC-NOMA, PC-NOMA, GSOMA, BDM, NORA, SGMA

Note- 1: Basics, 2: History, 3: Standards, 4: Capacity comparison, 5: DL/UL , 6: MUD Techniques, 7: Compatibility with 5G, 8: Spreading, 9: Scrambling, 10: Coding, 11: Interleaving, 12: Lattice & Beam, 13: Miscellaneous
Notations- ✓: Y, and ×: N

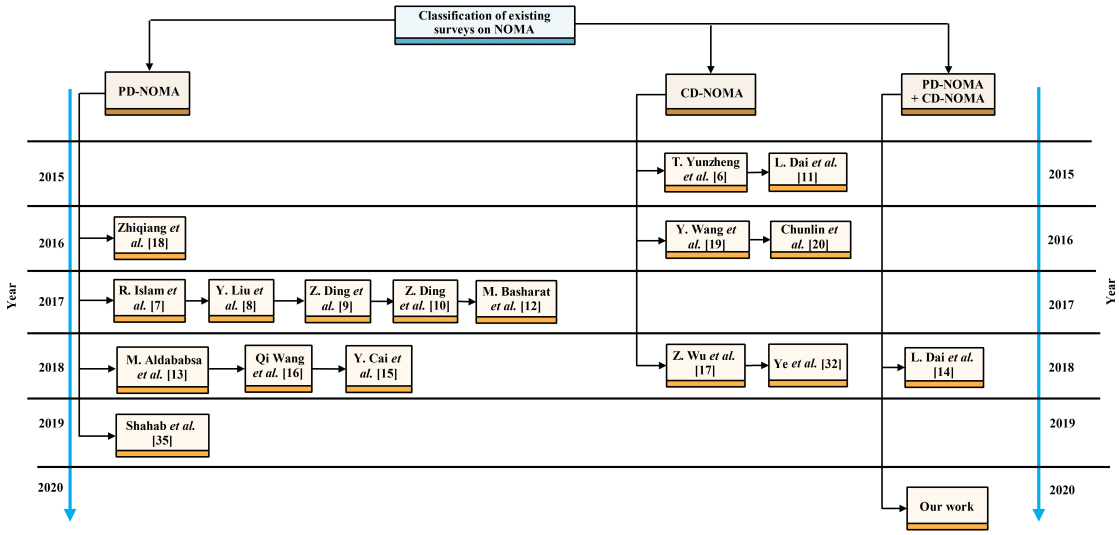

Figure 2.2: Classification of related surveys on NOMA

2.2 Contribution of this Chapter

In this chapter, we present a detailed review of NOMA techniques in the 5G environment. We also highlighted various current challenges and issues for the implementation of various variants of PD-NOMA and CD-NOMA. Moreover, this paper highlights the inadequacy of existing 5G standards in achieving ultra-low latency. Based on the above discussion, the major contributions of this paper are as follows.

- We present a comprehensive review of the PD-NOMA and CD-NOMA to study the various challenges associated with them. The basic principle of NOMA along with its standards, advantages, challenges, and solutions are studied.
- We investigate how PD-NOMA improves the various features of 5G when it is integrated with its different applications. Furthermore, we also studied how PD-NOMA provides better results than that of previous multiple access techniques such as FDMA, TDMA, CDMA, and OFDMA.
- We also explore the concept of CD-NOMA and in-depth explain that how the various variants of CD-NOMA support both the single-carrier and multi-carrier systems. Moreover, we also studied how the variants of CD-NOMA overcome the problems associated with the PD-NOMA.
- Finally, this paper discussed various challenges and open issues related to the PD-NOMA and the CD-NOMA. Along with this we also discussed the potential solutions to overcome the challenges and open issues.

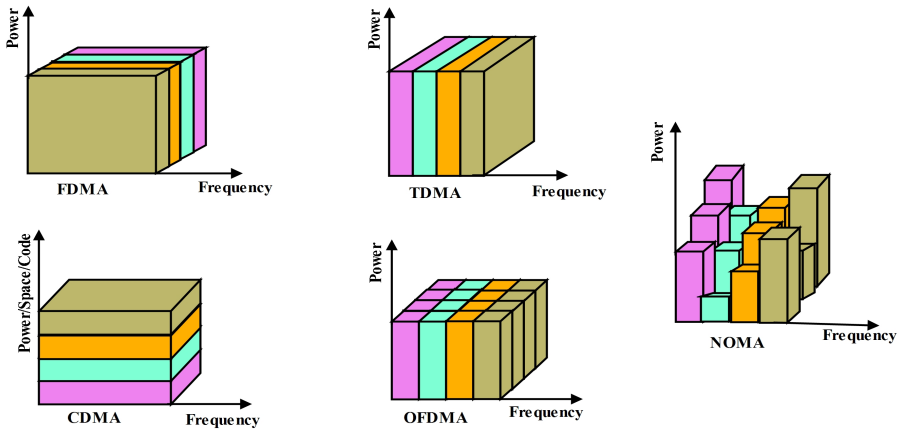

Figure 2.3: Different multiple access techniques

2.3 Background and History of NOMA

This section discusses the background and history of NOMA. In each generation, there is a need for new MA techniques to allow users to reuse the spectrum simultaneously to have a high capacity by allocating the available bandwidth (or channel) among multiple users. This can be done in such a way that QoS of users should not be degraded. In the first generation, a frequency division multiple access techniques (FDMA) was used in which frequency bands were divided into different channels and each channel was allotted to different users. The second generation belongs to global system for mobile (GSM) communications having Time-division multiple access (TDMA) technique, such that each user was allowed to transmit using a common frequency band, but access the channel in a specific time slot. Moreover, this generation also supports code division multiple access (CDMA) technology known as IS-95 or cdmaOne. In the third generation, CDMA was used in which bandwidth was uniformly distributed with the same transmitted power. Users can transmit the data simultaneously using the same frequency band, but with a specific pseudo-random code so that data can be retrieved by the specific user at the receiver side. In the fourth generation, orthogonal frequency-division multiple access (OFDMA) technique was used, where MA was used by allocating the subsets of subcarriers to an individual user. So, the low-data-rate transmissions from different users are possible simultaneously. Using space division multiple access (SDMA) along with MIMO technology, all the users can communicate at the same time using the same channel. This multiple access scheme can be applied for satellite communication to improve the data rate. All the aforementioned MA techniques are shown in Fig. 2.3.

OMA schemes simplify the transceiver design and eliminate co-channel interference. However, the following limitations exist in these schemes. Firstly, the number of users served simultaneously is limited. Secondly, to maintain the orthogonality, a user scheduling along with

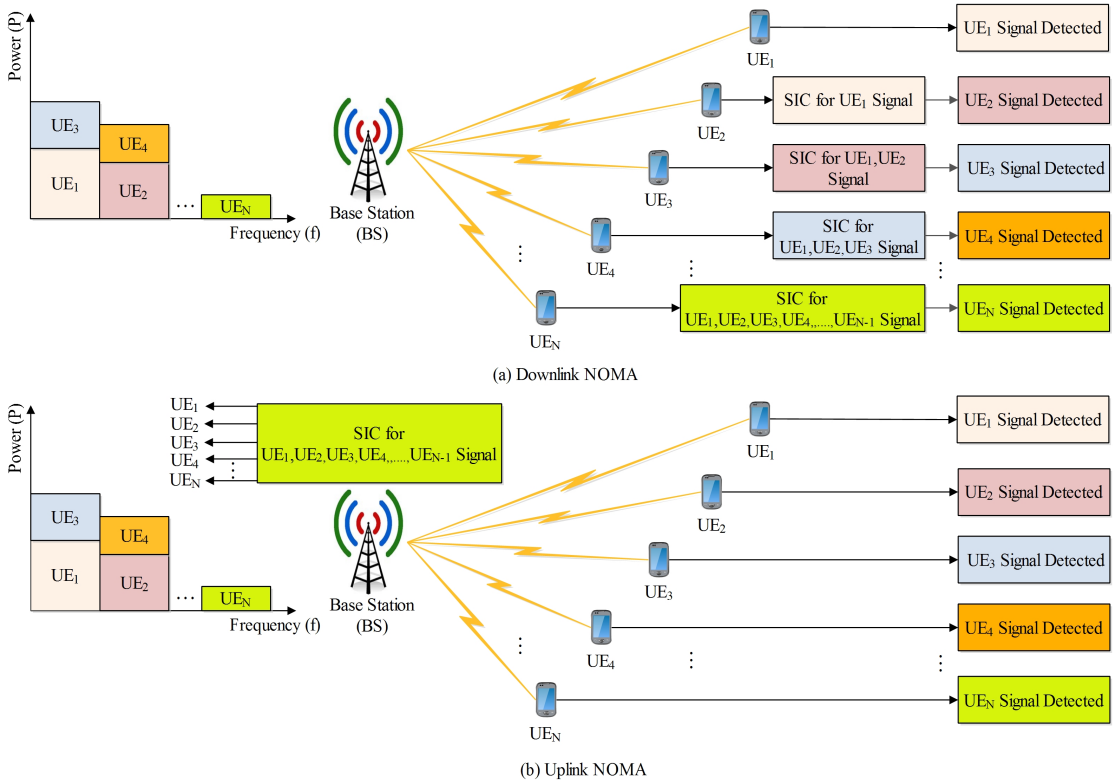

Figure 2.4: Downlink and Uplink NOMA

the strong feedback channels are required. Compared to OMA, NOMA is a better technique for RB allocation, the optimization of a joint power, code signature, and receiver layout. Also, the non-orthogonal behaviour of NOMA decreases the scheduling of multi-user multiplexing and the requirement of a precise channel.

2.3.1 Standards of NOMA

It has been observed from the literature that when NOMA is integrated with eMBB then it improves the user fairness, multi-user capacity, and user experience in ultra-dense networks. On the other side, for mMTC and URRLC, NOMA resolves the issue of massive connectivity along with a large coverage area requirements and provides ultra-reliable link quality with low latency for contention-based grant free transmission. By analyzing the aforementioned benefits of NOMA, 3GPP has developed various standards for both downlink (DL) and uplink (UL) scenarios which are described as follows.

2.3.1.1 NOMA standards for downlink

Multi-user superimposed transmission (MUST) was the first standard proposed by 3GPP for DL scenarios under LTE Release-13. According to the downlink applications, 3GPP divides

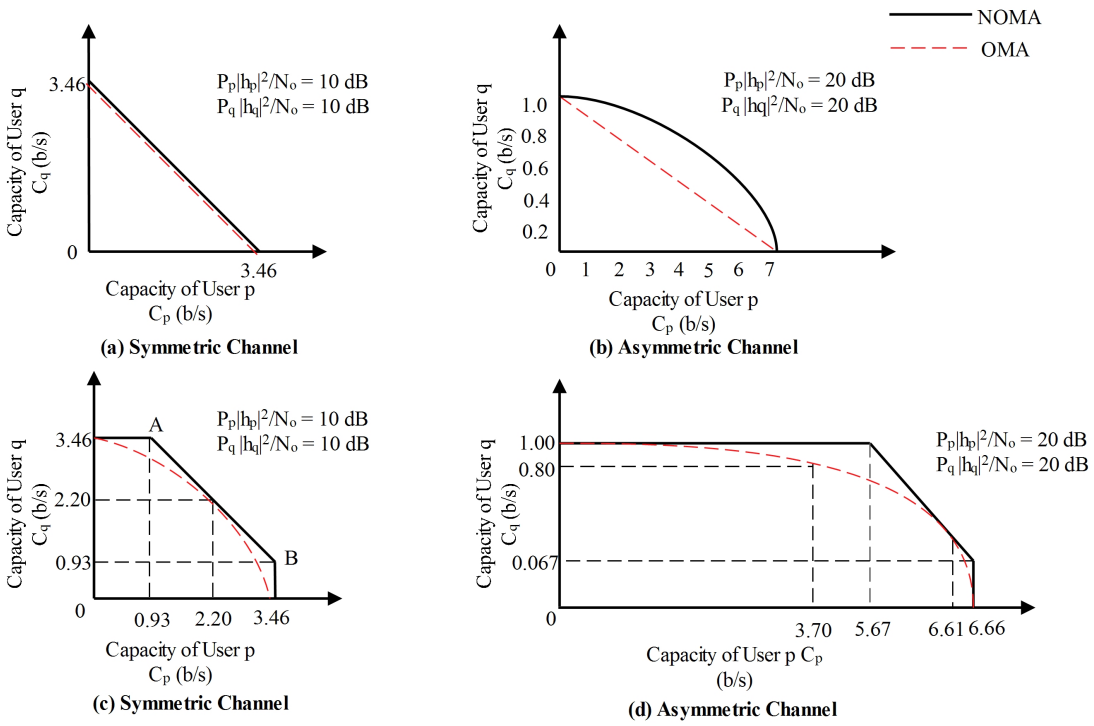

Figure 2.5: Difference between OMA and NOMA

the MUST schemes into three broad categories as, MUST 1, MUST 2, and MUST 3. In MUST 1, coded bits of at least two users are mapped independently to construct the constellation symbols without relying upon the gray mapping. In MUST 2, coded bits of at least two users are mapped together to form the constellation symbols with gray mapping. However, MUST 3 is entirely different from MUST 1 and MUST 2.

2.3.1.2 NOMA standards for uplink

3GPP under Release-14 proposed fifteen NOMA schemes for the uplink scenario which are as follows: SCMA, MUSA, LCRS, FDS, NCMA, PDMA, RSMA, IGMA, LDS-SVE, LSSA, NOCA, IDMA, RDMA, GOCA, WSMA, and NOMA. All these schemes support massive connectivity, large link reliability, and low latency for mMTC to support a grant-free transmission. These schemes were simulated by different companies and predicted that the link-level and system-level simulation of these schemes have higher throughput and gain as compared to OMA techniques. Moreover, these schemes provide large sum-throughput, system capacity, and packet arrival rate (PAR). In Release-15, 3GPP proposed a new UL NOMA scheme which includes the signal processing at transmitter such that the receiver design supports multiple users.

2.3.2 Basic Principle of NOMA

2.3.2.1 Downlink NOMA

In DL scenario, the SC technique is applied at the transmitter side (the BS) to multiplex the signals. These signals have different power allocation coefficients. On the receiver side, a SIC technique is used to separate interfering signals. Power allocations coefficients are allocated as per the channel conditions of users. High power is allocated to the poor channel condition users, whereas low power is allocated to the better channel condition users as shown in Fig. 2.4.

2.3.2.2 Uplink NOMA

In an uplink scenario, each user's equipment (UE) transmit their signals towards the BS. Then, at the BS, SIC technique is used which separates the signals of UEs with their different power allocation coefficients as shown in Fig. 2.4. The signal received at the BS can be represented as follows.

$$r_s = \sum_{p=1}^{N} h_p \sqrt{a_p P_m x_p} + \eta, \tag{2.1}$$

where r_s is the received signal, x_p is the transmitted signal, h_p is the channel gain, a_p is the power allocation coefficient, P_m is the transmitted power of the UE, and η is the additive white Gaussian noise (AWGN).

2.3.3 Capacity Comparison between OMA and NOMA

Fig. 2.5 represents the difference between OMA and NOMA. The mathematical formulation of OMA and NOMA is described as follows:

2.3.3.1 OMA

The capacity of OMA according to the Shannon capacity theorem can be expressed as follows [41]:

$$C_p^{OMA} = b\log_2\left(1+\frac{a_p\rho}{b}|h_p|^2\right), \tag{2.2}$$

$$C_q^{OMA} = (1-b)\log_2\left(1+\frac{a_q\rho}{1-b}|h_q|^2\right), \tag{2.3}$$

where b is the RB allocation coefficients, ρ is the transmit signal-to-noise ratio (SNR) at the BS, a_p and a_q are the power allocation coefficients which satisfy $a_p + a_q \leq 1$, h_p and h_q are the channel gains.

In the absentia of power control at the BS, $\left(\frac{a_p}{b}\right) = \left(\frac{a_q}{1-b}\right) = 1$. So,

$$C_p^{OMA} = b\log_2\left(1+\rho|h_p|^2\right), \tag{2.4}$$
$$C_q^{OMA} = (1-b)\log_2\left(1+\rho|h_q|^2\right). \tag{2.5}$$

2.3.3.2 NOMA

Compared to OMA, the Shannon capacity of NOMA can be expressed as follows:

$$C_p^{NOMA} = \log_2\left(1+\frac{a_p\rho|h_p|^2}{1+a_p\rho|h_p|^2}\right), \tag{2.6}$$
$$C_q^{NOMA} = \log_2\left(1+a_q\rho|h_q|^2\right). \tag{2.7}$$

When SNR becomes high, i.e., $\rho \longrightarrow \infty$ then

$$C_{sum,\infty}^{OMA} \approx \log_2\left(\rho\sqrt{|h_p|^2|h_q|^2}\right), \tag{2.8}$$
$$C_{sum,\infty}^{NOMA} = \log_2\left(\rho|h_q|^2\right). \tag{2.9}$$

So, the capacity sum gain of NOMA over OMA can be described as follows:

$$C_{sum,\infty}^{gain} = C_{sum,\infty}^{NOMA} - C_{sum,\infty}^{OMA},$$
$$C_{sum,\infty}^{gain} = \frac{1}{2}\log_2\left(|h_p|^2|h_q|^2\right), \tag{2.10}$$

When $|h_q|^2 > |h_p|^2$, then capacity of NOMA becomes greater than OMA and this gain becomes more effective at a time when channel conditions of users becomes different. Authors in [42] mathematically proved that NOMA always outperformed the traditional OMA.

2.3.4 Advantages of NOMA over OMA

This section discusses the benefits of NOMA over OMA as follows.

- *High SE:* NOMA provides high SE compared to OMA because, in NOMA, multiple users acquire the services through each RB, whereas in OMA, one RB is allocated to each user which results in wastage of bandwidth [43]. Moreover, NOMA can be easily integrated with other 5G technologies such as mMIMO, mmWave, HetNets, D2D, and CR, to enhance the throughput of the network.

- *Massive connectivity:* NOMA has the abilities to support billion of smart devices using its non-orthogonal characteristics. It is suitable for both the IoT [27] and Tactile Internet [44] because packets are smaller in size and sporadically in nature. In NOMA, multiple

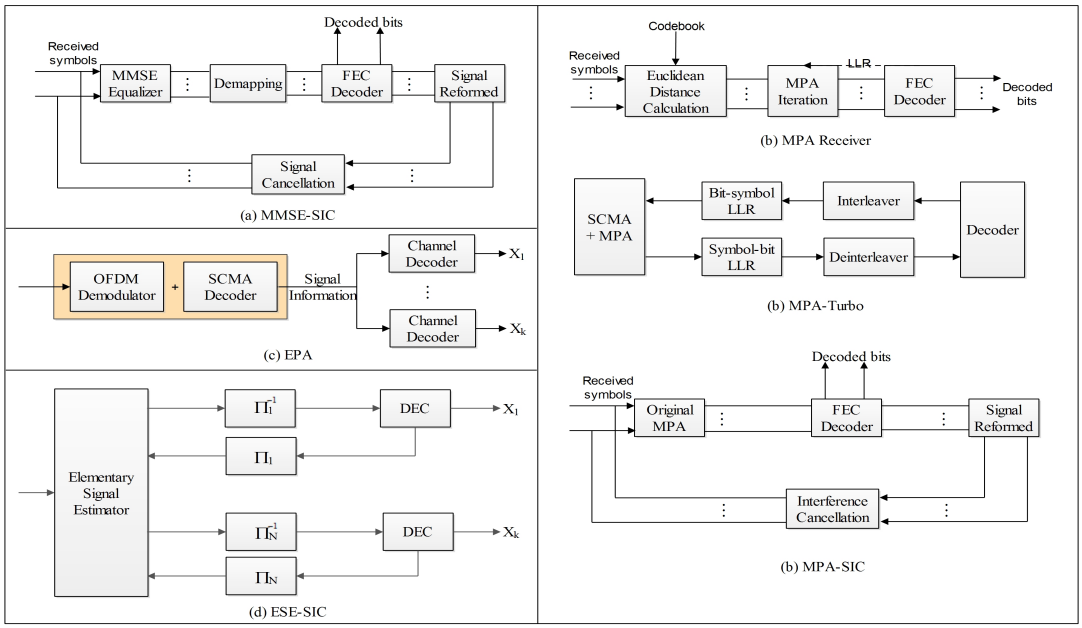

Figure 2.6: Classification of multiuser detection techniques

devices get the services through a single RB by using SC, whereas, in OMA, one device acquires one RB which results in the wastage of RBs.

- *Fairness:* NOMA provides fairness among users, so a large amount of power is allocated to the weak users (having poor channel conditions) and lesser to the strong users. Then, both strong and weak users have guaranteed QoS in terms of throughput. To achieve better fairness among different users, the authors in [45] provide fair power allocation schemes. The co-operative communication and CoMP also plays a vital role to enhance the QoS of the weak users in terms of their fairness [33,46]. Furthermore, to improve the fairness among users, the authors in [47] presented the power allocation scheme under the condition of the average CSI at the transmitter.

- *Ultra Low Latency:* In 5G, latency requirements are more stringent due to the heterogeneous network (HetNet) architecture. OMA techniques are not suitable for such architecture because they are dependent on access-grant request which increases the transmission latency and signalling overhead. In LTE, access grant request takes 15.5ms when data is transmitted [48]. To resolve it, NOMA is used which supports grant free transmission, especially in the UL scenario. Moreover, NOMA also provides flexible scheduling among a large number of devices as per the need of application and QoS of devices.

2.3.5 Multi-user detection techniques

These techniques separate the multi-user signals shared over the same resources. Classification of multiuser detection techniques is as shown in Fig. 2.6. Brief description of these techniques is as follows:

2.3.5.1 The minimum mean square error-successive interference cancellation (MMSE-SIC)

It is an enhanced version of MMSE receiver, where information bits are decoded from those user's signal which is having the highest signal-to-interference noise ratio (SINR) among all the signals. Then, signals of those users are reconstructed and cancelled from the received signals. This process is repeated continuously until the correct signal stream is recovered successfully. Then, the receiver suffers from the problem of error propagation which degrades the QoS of the users. To mitigate it, an SINR difference between the data streams of different users in each round must be sufficiently large to make the receiver suitable for those NOMA schemes that depend upon the diversified channel conditions.

2.3.5.2 Message Passing Algorithm (MPA)

It depends on the non-linear symbol detection scheme. Its structure comprises of sparse spreading sequences having the performance equivalent of maximum-likelihood (ML). It performs the most reliable detection on every resource element to transfer the symbols to the neighbouring elements. The MPA receiver uses the symbol level detection but did not use error-correction of forward error corrections (FECs) to detect the variable data streams of signals. This problem can be resolved by combining MPA with turbo codes and SIC, respectively. In MPA-turbo, the data of MPA is given to the FEC for decoding which is collected as the extrinsic information. Compared to MPA-turbo, MPA-SIC eliminates the multi-user interference (MUI) from the received signals.

2.3.5.3 Estimation propagation algorithm (EPA)

It is implemented at the receiver to reduce the computational complexity and to support SCMA [49]. It was based on variation approximate inference method which was used in the machine learning era [50].

2.3.5.4 Elementary signal estimation-parallel interference cancellation (ESE-PIC)

It was first implemented in interleave-division multiple access (IDMA) to handle a large number of multiplexed users to have a robust performance. In this technique, first ESE detects the transmitted symbols using a linear symbol detector and then at the same time, the detected

symbol de-interleaved to achieve a high gain. Finally, the information received at the decoder is returned to the ESE module for symbol detection.

2.4 Power domain NOMA (PD-NOMA)

In this section, we describe the various variants of PD-NOMA used in 5G as shown in Fig. 2.7. PD-NOMA is a technique which serves multiple users' simultaneously, through the same subchannel by allocating different power levels to them. This technique mainly used in 5G to improve the SE, EE, and reduce the latency. The detailed description of each variant of PD-NOMA is discussed in the following subsections.

2.4.1 D2D Communication

D2D is used to enhance local area services and its advantages in 5G are as follows (i) to enhance the EE by supporting low power proximity service, (ii) to enhance the SE by sharing radio resources with CUs, (iii) to support various peer-to-peer (P2P) services, (iv) to offload the traffic from the BSs, and (v) to reduce latency. However, inter-user and co-channel interference exists due to the reuse of the same RB which degrades the QoS of the CUs and D2Ds users. Hence, it decreases the SE of the communication system. To overcome this issue, researchers integrate NOMA with D2D in 5G. Moreover, it also manages the inter-user interference among the D2D users due to SIC, as shown in Fig. 2.8. To fully exploit the benefits of D2D with NOMA, various NOMA based schemes were proposed which are discussed as follows.

2.4.1.1 MTBSA [51]

In this scheme, the authors proposed the subchannel allocation algorithm based on the many-to-one matching game to overcome the issue of an inter-channel interference in an uplink situation [51]. This scheme reduces the system complexity up to $O(NM^2)$ and also provides stable matching between subchannels and D2D groups. As the number of D2D group increases, this scheme provides better performance. Moreover, this scheme also used to measure the sum rate and provides a good sum rate as compared to the one-to-one matching algorithm and traditional OMA based D2D groups.

2.4.1.2 Q-NOMA [52]

It is for in-band D2D group communication in the overlay cellular network, where clusters of D2D receivers (DRs) are randomly distributed around D2D transmitters (DTs) [52]. In this technique, DTs are located as per Gaussian point process model to obtain users clustering and spatial separation. It provides a better trade-off between the analytical tractability and modelling accuracy. Based on an interference approximation results, the authors in [52]

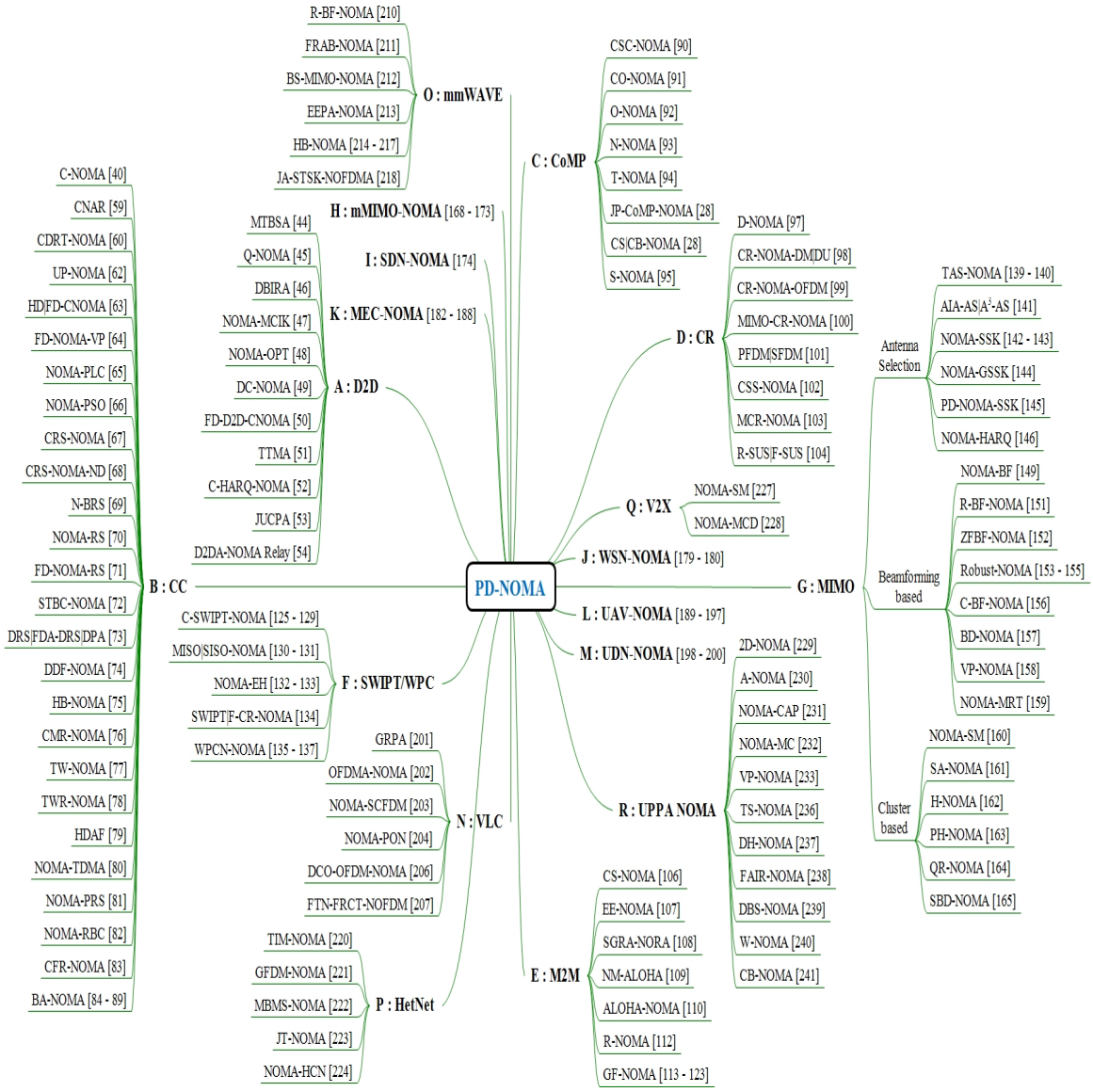

Figure 2.7: A taxonomy of PD-NOMA variants

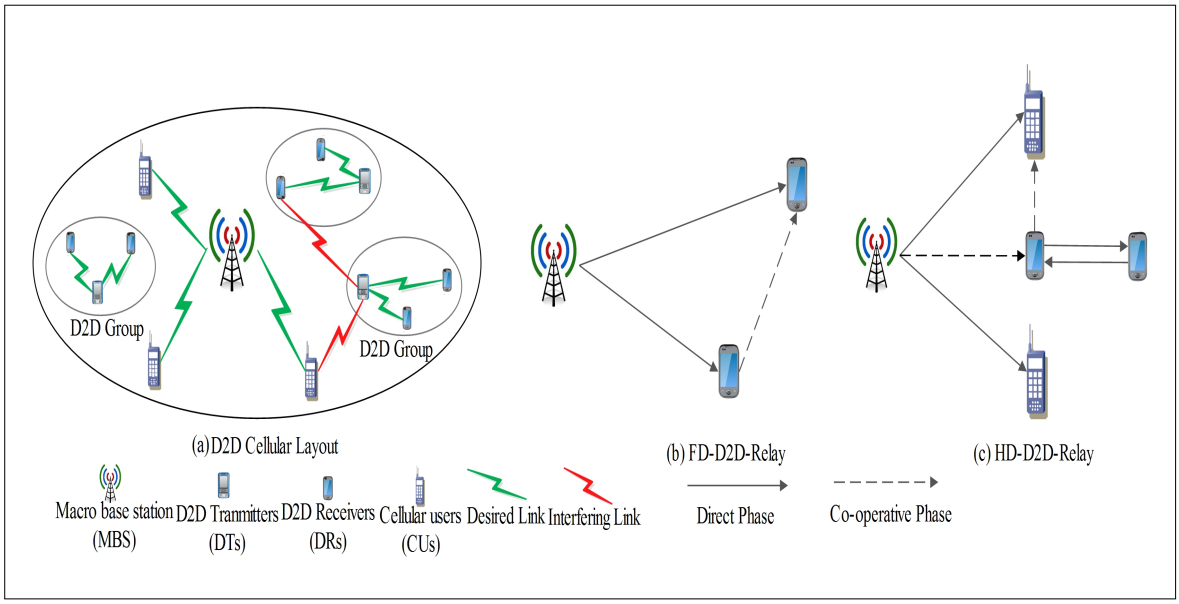

Figure 2.8: D2D-NOMA

demonstrated two closed-form expression for the outage probability of DRs using stochastic geometry: (i) by varying coverage radius RD and (ii) distance between probe DRs and DTs. Performance of Q-NOMA in D2D group communication provides better accuracy and overall less outage probability as compared to conventional paired D2D communication using OMA.

2.4.1.3 DBIRA [53]

It is a dual based iterative resource allocation algorithm (DBIRA) used to reduce the co-channel interference that arises due to the sharing of the same spectrum between the D2D pairs and the CUs [53]. It enhances the sum rate of the D2D pairs with the minimum data-rate requirements of the CUs. The authors used the Okumura-Hata model for simulation and compared the result of DBIRA with the MCU-OFDMA scheme. Moreover, they described the convergence behaviour of the DBIRA algorithm and found a better sum rate. The simulation result proved that the DBIRA algorithm performs better than MCU-OFDMA in the presence of interference. Moreover, it provides a high sum rate for the D2D pairs even if the CUs required large transmit power.

2.4.1.4 NOMA-MCIK [54]

In this, the authors combined the NOMA with the MCIK techniques for proper usage of power and subcarrier index dimensions to reduce the error with a high diversity order. Different sub-carriers were provided to each user, as a result of which interference among D2D under dense deployed areas becomes limited. Its performance was found good in terms of an instantaneous and average pairwise error probability (PEP) over Rayleigh fading channel. It

achieved an acceptable accuracy level of 1dB over high SNR regions for an average PEP.

2.4.1.5 NOMA-OPT [55]

In this, the authors studied a joint time allocation and power control algorithm that was a combination of energy harvesting and NOMA. It has low complexity of an order of $O(LK^2 + LKlog_2\frac{1}{\epsilon})$. Moreover, it was used to improve the EE of the D2D users with the condition to provide guaranteed QoS to the CUs. In this algorithm, both the CUs and the D2D transmitters harvest the energy from a hybrid access point (HAP). It solves two problems of D2D underlaying cellular network: (i) Low system throughput due to limited battery life of users, and (ii) Low data rates of an individual user due to the limited resource of TDMA. These problems were solved by an optimal power allocation of the CUs from the given power of the D2D transmitter. Then, based on optimal conditions, a global optimal solution was proposed for the D2D in the closed-form in terms of power and time resources.

2.4.1.6 DC-NOMA [56]

Kim *et al.* proposed a D2D aided cooperative relaying NOMA scheme (C-NOMA) to improve the SE of the system. It gives an effective method to embrace the non-orthogonal D2D transmission at the relay to have a high sum rate in comparison to the conventional NOMA and C-OMA. Moreover, it provides the sum capacity of the order of $\log SNR$. On the other hand, when a constant power is allocated for superposition coding, DC-NOMA achieves an upper bound scaling capacity of $\frac{1}{2}\log SNR$. The results show that it achieves high ergodic capacity as compared to that of conventional NOMA and C-OMA.

2.4.1.7 FD-D2D-CNOMA [57]

In this, the authors proposed the FD D2D aided cooperative NOMA scheme, where user pairs are predefined and the FD technique is used with the NOMA strong users. The presence of the FD technique at the NOMA-strong users collect the data sent by the BS and transferred it to the NOMA-weak users over the same frequency band. So, the outage performance of the NOMA-weak user improves by reducing the cooperative delay. To improve the performance of this scheme in terms of OP, adaptive multiple access (AMA) scheme was also proposed. It enables the BS to dynamically switch power among the FD-D2D-CNOMA, conventional NOMA, and OMA.

2.4.1.8 TTMMA [58]

Lim *et al.* proposed a NOMA based technique for peer discovery of distributed D2D communication. The performance metrics of peer discovery are range and capacity. To improve the discovery capacity, the authors in [58] explored the non-orthogonal resource allocation and

generated a single tone transmission signal used to solve the problem of the peak to average power ratio (PAPR). To design the discovery procedure concisely, it removed the strict collision detection and collision avoidance problems. The authors also proposed a message-passing algorithm with supplementary schemes for multi-user detection of superimposed multi-access signals. To enhance the discovery capacity, it permits a certain number of mobile stations (MSs) to regulate and transmit their signals on a similar resource section. TTMMA with message passing algorithm enhances the number of discovered devices up to 1.5 times more than the conventional FDMA based discovery from the same resources.

2.4.1.9 Cooperative HARQ assisted NOMA [59]

In this, the authors proposed an interference-aware mathematical scheme based on stochastic geometry for large scale D2D networks. The utilization of stochastic geometry combines the spatial interference correlation at the NOMA receivers and temporal interference co-relation at the HARQ transmission side. The authors also proved that when the effect of aggregated interference and the spatial and temporal interference are ignored then it overestimates and generates misleading design insight. The performance of this scheme was analyzed in terms of outage and throughput limited up to two users. The above assumption of channel gain difference was not always true for the NOMA based D2D scenario. D2D receivers are clustered around D2D transmitters and are situated in the proximity of each other. As a result, they have almost similar channel conditions. It achieved 32% lower outage probability as compared to non-cooperative HARQ assisted NOMA and 47% improvement in long term average throughput (LTAT) as compared to HARQ assisted OMA.

2.4.1.10 JUCPA [60]

Kazmi *et al.* proposed a scheme to mitigate the problem of user clustering and power allocation, where the NOMA technique was applied at the BS. The proposed scheme protects the CUs from interference and enhances the sum rate of the D2D pairs. The authors formulated the problem as a mixed-integer non-linear NP-hard problem. To solve it, the authors divided the problems into two subcategories. In the first category, matching game theory was used for user clustering and subchannel allocation. For user clustering, one-to-many matching theory and for subchannel allocation many-to-one matching game is proposed. In the second category, complementary geometric programming was used to pertain the power of the D2D transmitters (DTs). It has 70% and 90% higher execution gains of the average sum rate in comparison to NOMA and OFDMA, respectively. Furthermore, it improved the network connectivity to serve a large number of users through the same RBs.

2.4.1.11 D2D assisted NOMA Relay [61]

In this, a NOMA technique was integrated with D2D UEs for remote UEs. Due to the utilization of fewer resources, it provides improved SE and high data rate for the farthest UEs in comparison with the traditional D2D relay schemes.

Table 2.4: Parametric analysis of existing NOMA schemes based on D2D

Problem **in D2D**	NOMA **Variant**	Transmission **scenario**	**Techniques**	**Performance metrics**							**Merits**	**Open issues**
				1	**2**	**3**	**4**	**5**	**6**	**7**		
Co-channel interference	MTBSA [51]	Downlink	Joint subchannel and power allocation	✓	×	×	×	×	×	×	Higher sum rate and stable state	Reduced receiver complexity
Co-channel interference	Q-NOMA [52]	Downlink	Power allocation	×	✓	×	×	×	×	×	OP reduced	Can be extended to MIMO systems
Resource Allocation	DBIRA [53]	Downlink	Power control and channel assignment	✓	×	×	×	×	×	×	Higher data rate	Imperfect CSI
Energy and Interference	NOMA-MCIK [54]	Downlink	Joint power control and sub-carrier index activation	×	×	×	×	✓	×	×	Increase the diversity gain and improve CEUs performance	Analyse OP and compute SE by using different detection techniques
Energy harvesting	NOMA-OPT [55]	Downlink/ Uplink	Joint power control and time allocation	×	×	×	✓	×	×	×	Improved EE	Can be extended for multicell network
Capacity scaling	DC-NOMA [56]	Downlink	Power allocation	×	×	×	×	×	×	✓	Higher SE than OMA in low SNR regime	Relay selection needs to be explored
Residual interference & quality of channels	FD-D2D-CNOMA [57]	Downlink	Co-operation	×	✓	×	×	×	×	×	OP reduced and AMA increase the gain	Reduces the complexity
Collision avoidance & detection	TTMMA [58]	NA	Message passing modulation algortihm	×	×	×	×	×	✓	×	Increased the capacity	Proximity services need to be improved
Interbeam & co-channel interference	C-HARQ-NOMA [59]	Downlink	User grouping and power control	×	×	✓	×	×	×	×	Mitigate the interference, improved throughput and reduced OP	Imperfect CSI and Nakagamim fading channel can be explored
Resource Allocation	JUCPA [60]	Downlink	Joint user clustering and power allocation	✓	×	×	×	×	×	×	Mitigate the interference and improved network connectivity	Imperfect CSI
Resource allocation	D2D-relay-NOMA [61]	Downlink	Relaying	✓	✓	×	×	×	×	×	Time slot space reduced upto half and all users achieve diversity order of K	User grouping needs to be explored more

Note- 1: Sum rate, 2: OP, 3: Throughput, 4: EE, 5: PEP , 6: PAPR, 7:Ergodic sum capacity
Notations- ✓: Y, and ×: N

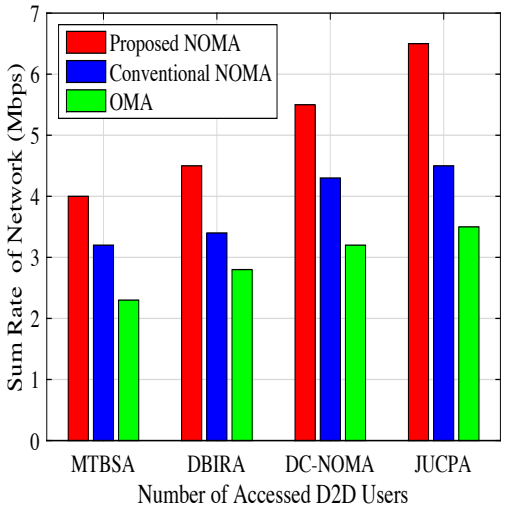

Figure 2.9: Discussion based on classification of D2D communication.

2.4.1.12 Comparison of existing NOMA schemes based on D2D communication

Table 2.4 provides the detailed relative comparison of existing variants of NOMA used in D2D communication using the parameters such as transmission scenario, the technique used, merits, open issues, throughput, EE, PEP, and PARP.

2.4.1.13 Discussion based on classification of D2D communication

Fig. 2.9 shows that the JUCPA achieves 18.2%, 44.45%, and 62.5% higher sum rate as compared to the MTBSA, DBIRA, and DC-NOMA with an increase in the number of accessed D2D users. The reason behind this behaviour is that the JUCPA reduced the co-channel interference among the D2D pairs using the SIC technique Also, the computational complexity achieved by JUCPA is much lower than the MTBSA, DBIRA, and DC-NOMA. These two reasons depict that JUCPA is more suitable for 5G scenario as compared to other ones.

2.4.2 Cooperative Communication

Cooperative communication uses one or multiple relays to enhance the signal strength between the source and destination. It uses two-time frames such that in the first frame, direct phase transmission is used while the second frame is used by relays to forward the information from relays to the final destinations as shown in Fig. 2.10. It has many advantages due to following reasons [62,63] (i) enlarges the coverage area, (ii) enhances the system capacity, (iii) reduces the effect of multipath fading, (iv) resolves the difficulty to mount multiple antennas on small size terminals, and (v) improves the QoS of cell edge users (CEUs). In this technique, relays use two types of protocols, decode and forward (DF) and amplify and forward (AF) to

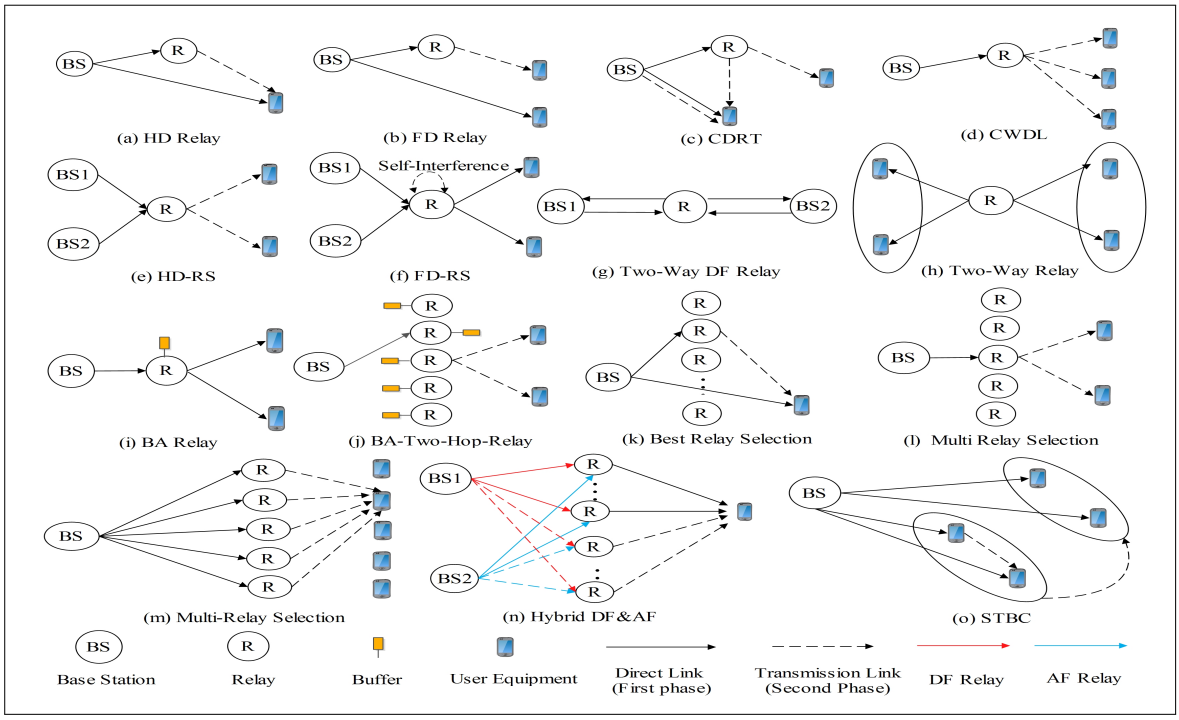

Figure 2.10: Cooperative Communication/Cooperative Relaying systems

transfer the information from source to destination. According to the relaying operation, relays are categorized as half-duplex (HD) and full-duplex (FD). In HD, two-time slots and frequency bands are used for data transmission and reception while in FD, one-time slot and the same frequency band is used [64], [65]. Moreover, the usage of FD increases the SE as compared to HD [66].

To improve the SE of the network, researchers used NOMA with cooperative communication. This integration provides benefits such as reduce system redundancy, fairness, and improved diversity gain for weak users. Considering the aforementioned advantages, the authors have proposed different variants of cooperative NOMA, which are discussed in the sequel.

2.4.2.1 C-NOMA [46]

In this, the authors analyzed the diversity gain to exploit the prior information of the NOMA technique. In this technique, a strong user (having better channel condition) decodes the messages of other users and acts as a relay for weak users (having poor channel condition) to enhance their reception reliability. It improves the diversity gain for all users, but during the cooperative phase, it has been observed that when the data is transmitted from the relay to the weak user, and then it took extra time slots to fulfil the target because relaying operation is carried out serially. A user pairing scheme was used to reduce the complexity of C-NOMA.

2.4.2.2 Collaborative NOMA Assisted Relaying [67]

In this, the collaborative NOMA assisted relaying (CNAR) was proposed for 5G which consists of two NOMA links, which are known as collaborative source-relay (S-R) and relay-destination (R-D). Here, the message of the relay was taken from the S-R NOMA signal and power is adjusted to transmit the remaining part to cell-edge users of the R-D link. In this scheme, relay signals are transmitted and received in a specific frequency band. To achieve the high throughput and to support a large number of users, the FD mode was used in the two-fold antenna relay system for the S-R and the R-D links. In addition to this, the interference was avoided by using separate authorized and unauthorized bands. The execution of the framework was analyzed for OP and ergodic sum capacity. The simulated results show that the proposed framework provides better OP and ergodic sum capacity as compared to OMA. However, it is suitable for short-range communication such as Bluetooth, UWB. Hence, to overcome this problem and to fully exploit the potential benefits of C-NOMA, dedicated relays are proposed with NOMA.

2.4.2.3 CDRT-NOMA [68]

In this, the authors used NOMA in CDRT, where they can communicate directly or indirectly with the BS. To cancel the interference, a NOMA inherent property is used to take the information from other UEs. Its performance was analyzed for OP over frequency flat block fading channels by using DF relaying. In contrast to [68], the authors in [69] analyzed the performance of the above scenario by using AF relaying.

2.4.2.4 UP-NOMA [70]

The authors in this proposed a CDRT protocol using uplink NOMA based on the two-user scenario. In this protocol, a cell center user communicates directly with the BS, whereas CEUs uses HD DF relay to communicate with the BS. Authors analyzed the performance of their scheme in perfect and imperfect SIC scenarios by measuring the ergodic sum capacity.

2.4.2.5 HD-CNOMA/FD-CNOMA [71]

Liu *et al.* proposed a hybrid HD/FD scheme for C-NOMA to resolve the problem of power allocation and to maximize the achievable user rate. In addition to this, a relay selection scheme was also proposed for multiple users. Moreover, an optimal power was allocated by the execution of NOMA-HD and NOMA-FD. It outperformed conventional NOMA, HD-CNOMA, and FD-CNOMA schemes.

2.4.2.6 FD-NOMA-VP [72]

In this, the P nearest and the Q farthest users having similar gain are divided into distinct NOMA clusters using a relay. Clustering was performed using the virtual pairing (VP) scheme between one nearest and multiple farthest users over non-overlapping frequency bands. In FD-NOMA-VP, a dedicated FD relay was used to maintain the communication between the farthest users and the BS whereas, the nearest user communicates directly with the BS. The execution of the proposed framework is analyzed for OP, ergodic sum capacity (ESC), and outage sum potential in conjunction with analytical derivations for each perfect and imperfect interference cancellation (IC) techniques. FD-NOMA-VP achieved tremendous performance gain in comparison to the conventional MA schemes in perfect IC. On the other side, at imperfect IC, the performance degrades due to an increase in the impact of residual interference at the relays.

2.4.2.7 NOMA-PLC [73]

It is a two-stage power allocation NOMA scheme. In the first stage, the source modem transmits two data symbols with different power allocation factors while both the relay and destination receive the superposition coded signal. Then, the destination decodes the signal with a higher power while treating the other as noise. At the relay, the higher power signal is first decoded and then cancelled using the SIC to obtain the second symbol. In the second stage, with the assumption that it is successfully decoded, the relay forwards the second symbol to the destination. The performance of the system was analyzed in terms of the average sum capacity. Two advantages of using the NOMA in PLC are: (i) reduced transmit power at PLC modems which relaxes the electromagnetic compatibility (EMC) problem associated with PLCs, and (ii) better fairness among users since it allows to transmit multiple signals simultaneously to different users (PLC modems) with each user occupying the entire bandwidth.

2.4.2.8 NOMA-PSO [74]

It is applied to the OFDM-based cooperative SATCOM systems to avoid the wasting of resources such as frequency and energy. In [74], NOMA is applied to a multi-satellite cooperative transmission system consisting of GEO and LEO satellites. Due to the presence of NOMA, GEO and the LEO satellites communicate simultaneously to multiple ground users locating in the overlapped coverage area of the satellites. In this case, channel gains from a user to GEO and LEO satellites can be significantly different which makes it feasible and reasonable to apply NOMA to the cooperative system. The authors used the particle swarm optimization (PSO) algorithm and concluded that the performance of their scheme was better than OMA in SATCOM.

2.4.2.9 CRS-NOMA [75]

Kim *et al.* proposed a spatially multiplexed transmissions scheme to enhance the SE. Authors analyzed the achievable average rate for an independent Rayleigh fading channel which shows a better performance of CRS-NOMA as compared to traditional DF scheme.

2.4.2.10 CRS-NOMA-ND [75]

It was based on novel receiver design. Generally, the source simultaneously transmits two symbols by using the superposition code and the relay decodes and forwards the symbols with lower allocated power by using SIC [75]. But, in [76], the destination jointly decodes two symbols from both the directed signal and then forward the signal by using the maximum-ratio combination and SIC. Result of this scheme shows that it outperforms the other schemes for parameters such as ergodic capacity and outage probability when the S-to-R link is better than the R-to-D link.

2.4.2.11 N-BRS [77]

In this, multiple relays are used instead of single, which is an extended version of CRS-NOMA. Among multiple relays, the best relay is selected because best relay selection (BRS) reduces overhead and complexity, while achieves the full diversity order even in the presence of a finite number of interference sources. The performance of this scheme was analyzed in terms of the average rate under independent Rayleigh fading channel. Its simulated results show that N-BRS has more rate gain in comparison to the conventional BRS (C-BRS) when the number of relays becomes large.

2.4.2.12 NOMA-RS/HD-NOMA-RS [78]

This scheme uses NOMA with the HD relay, which uses the dual-hop cooperative relaying. In this scheme, a parallel collaboration between two sources was observed to achieve their objectives. In [78], after having acquired the transmitted symbols in parallel by both the sources with exclusive assigned powers, the relay forwards a superposition coded composite sign using NOMA. Advantage of NOMA-RS is that it has multiple sources in contrast to CRS-NOMA and CRS-NOMA-ND. Results demonstrated that NOMA-RS has a high capacity gain in presence of residual interference and imperfect SIC as compared to conventional NOMA under perfect SIC.

2.4.2.13 FD-NOMA-RS [79]

It consists of FD NOMA and cooperative relay such that two source-destination pairs have a common FDR [79]. FDR demultiplex these symbols and simultaneously transmits a superimposed composite signal to the end locations with a processing delay *tau* using downlink

NOMA. They evaluated the performance of their scheme for ESC, OP, and outage sum capacity. To prove the effectiveness of their scheme, they analytically analyzed their scheme by using both perfect and imperfect SIC conditions. Simulation results of the proposed scheme reveal that it outperforms the HD-NOMA-RS and HD-OMA-RS and improves the 5G systemsâĂŹ performance in comparison to the HD scheme.

2.4.2.14 STBC-NOMA [80]

It is a two-phase cooperative DF relaying scheme which is based on Alamouti (2x1 multiple-input single-output mode) space-time block coded (STBC-NOMA) [80]. To examine the performance of this scheme, a closed-form solution for ergodic sum capacity and outage probability over independent Rayleigh fading channels was studied. At a high SNR, asymptotic approximations for E-SC, OP, and O-SC were also manifested. It acquired significant performance gain using NOMA and the traditional DF relaying schemes as compared to the conventional CRS.

2.4.2.15 DRS-FPA and DRS-DPA [81]

These are DF dual relay selection schemes which use distributive space-time coding for cooperative NOMA [81]. In DRS-FPA scheme, the fixed power is allocated to the system. One relay demultiplexes both the signals of U1 and U2 and finally, the max-min criterion is used to select the best relay. In DRS-DPA, the dynamic power allocation based DF dual relay selection scheme was used, where DPA was used for both hops instead of second hop only. The performance of both schemes was evaluated in terms of a closed-form expression of OP.

2.4.2.16 DDF-NOMA [82]

It is a cooperative NOMA scheme which uses dynamic decode-and-forward (DDF) relay to increase the reception reliability of spatially random users. In DDF-NOMA [82], the user who is close to the BS demultiplexes the superimposed mixture of the users' signals received from the BS using partial reception and then transmits the signal to the farthest user. To overcome the need of channel state information at the BS, random user pairing was used, where users were randomly paired to carried out NOMA transmission with one-bit feedback.

2.4.2.17 HB-NOMA [83]

This scheme uses the benefits of NOMA and TDMA at the relay to improve the throughput of poor channel condition users' [83]. By using the optimum throughput from HB-NOMA relay for each mobile user (MU), the authors investigated the scenario of multi-MUs. To maximize the utility of all MUs in a multi-MUs scenario, the concept of Gradient-projection (GP)-based

multi-MUs scheduling was used. The authors concluded that the GP scheduling scheme improves the total utility of MUs in comparison to the round-robin (RR) scheduling scheme.

2.4.2.18 CMR-NOMA [84]

It is a cooperative multi-relay NOMA-based scheme, where the information of each user in the system is relayed by all other users in an interference-free manner [84]. It establishes cooperation among the users clustered in a NOMA structure. In the cooperation phase, users receive a replica of their signal in a sequential manner starting from the weakest user. It enhances the overall system performance as compared to NOMA and CNOMA schemes at the expense of detection of more signals and the addition of an extra time slot. Moreover, the authors proposed a modified SIC technique to reduce the computational complexity at the receiving UEs.

2.4.2.19 TW-NOMA [85]

It is a two-way DF NOMA scheme, in which an intermediate relay helps two source nodes to communicate with each other [85]. In this scheme, the authors integrated the digital network coding (DNC) to compress received data from these source nodes. Its performance was analyzed and evaluated for OP over Rayleigh fading channels. Simulation results show that TW-NOMA outperformed the conventional two-way scheme using DNC (TWDNC), two-way scheme without using DNC (TWNDNC), and two-way scheme in AF relay systems (TWANC).

2.4.2.20 TWR-NOMA [86]

It is a two-way relay NOMA system where two different NOMA groups exchange message among each other using HD-DF relay [86]. The effect of both the perfect and imperfect SIC was taken to compute the SINR of users. The authors evaluated the closed-form expressions of OP users' signal in terms of the exact and asymptotic way using both the perfect and imperfect SIC. The main aim of this scheme was to provide the solution for decoding order errors due to perfect SIC. The impact of an interference signal (IS) at relays in high SNR regimes and zero diversity order was also studied. The numerical results show that the proposed scheme under perfect SIC and in the absence of IS has a larger sum rate as compared to that of TWR-OMA systems.

2.4.2.21 HDAF [87]

In this, the authors proposed a hybrid relaying scheme, which consists of two sources and one UE. In this scheme, some of the relays worked on the principle of the DF protocol and others on the AF protocol. Improved sum channel capacity and average system throughput were achieved from this scheme as compared to the traditional schemes.

2.4.2.22 NOMA-TDMA [88]

In this, the authors investigated the outage performance over two different NOMA relaying schemes cooperative NOMA and TDMA-NOMA. In this proposal, two relays have been used between the BS and users. The cooperative NOMA took two-time slots, whereas the NOMA-TDMA took three-time slots to complete one round communication. Here, NOMA and dirty parity coding (DPC) are used in the first and second-time slots, respectively. On the other hand in NOMA-TDMA, NOMA was used in the first time slot, and TDMA was used in second and third time slots. Moreover, the authors explored the impact of error propagation in NOMA SIC and it provides better OP as compared to NOMA-TDMA.

2.4.2.23 NOMA-PRS [89]

The authors in this investigated the performance of cooperative NOMA with the AF and partial relay selection (PRS) technique. In this scheme, the BS communicates with two users using a selected relay and also established a direct link with the users. The results show that when the number of relays increases, its performance increases; but at the high SNR region, the performance gain becomes constant after two relays.

2.4.2.24 NOMA-RBC [90]

In this, one BS and two users were used to analyze the performance of cooperative SISO-NOMA relaying. In this proposal, users near to the BS employed the compress and forward protocol and act as an FD relay for the farthest users. The performance of this scheme is analyzed in terms of the achievable rate region of an RBC with the compress-and-forward (CF) relaying and noisy network coding (NNC). From the obtained achievable rate region with CF and NNC, a DPC is also applied at the BS to enhance its performance. It has better results as compared to conventional NOMA.

2.4.2.25 CFR-NOMA (Cooperative full-duplex relaying) [91]

This is an in-band FD relaying scheme with imperfect SIC. In [91], users near to the BS act as the FD relay for the far users. The numerical results of this scheme were analyzed in three conditions using the parameters such as OP and ESC under three conditions. In the first condition, the power of relays and the BS was kept fixed. In the second condition, the power of the BS and relay are optimized to reduce the OP. In the third condition, fairness between the users was taken into account and the power of both the BS and relays was optimized to maximize the individual rate of users.

2.4.2.26 BA-NOMA [92]

Relays transmit and receive the data packets when S-R and R-D links are in outage [92] in buffer aided (BA)-NOMA. It improves the reliability of the relaying systems which increases the throughput of the system. Xia *et al.* [93] proposed a centralized mechanism to select the best relay to exchange the buffer state information between the relay until it becomes empty. Moreover, the authors in [94] proposed a buffer-aided relaying technique which contains one source and two users. In comparison to [94], the authors in [95] proposed a NOMA relay network, where a dedicated relay was used to transmit the information to two users. By using the same scenario of [95], the authors in [96] used an adaptive transmission scheme for a single relay network to maximize the throughput of the cooperative NOMA system to serve two users concurrently. In [97], the authors proposed a multi-relay topology and determined the process of power allocation coefficient. Moreover, they proposed two relay selection algorithms Delay-Aware NOMA (DA-NOMA) and Delay and Diversity-Aware NOMA (DDA-NOMA).

2.4.2.27 DIYA-NOMA [98]

It is a scheme used to improve the network coverage and throughput to provide the quality of service and quality of experience to the end-users by reducing the delay and interference. To achieve the goal, the authors in this proposed the Tactile Internet (TI) driven delay assessment for D2D communication, which works in two phases. In the first phase, a full-duplex communication at relays (intermediate nodes) is used to have the first- and second-hop transmission simultaneously in the same time slot. Then, TI-based communication is used at D2D transmitter to increase the speed of transmission. In the second phase, pricing-based three-dimensional (3-D) matching is proposed to improve the throughput of the cell edge users along with the mitigation of co-channel interference. Also, the power of the D2D transmitter is optimized using successive convex approximation with low complexity, which converts the non-convex optimization problem of subchannel allocation and power control into a convex problem.

2.4.2.28 Comparison of existing NOMA schemes based on cooperative communication

Table 2.6 provides the detailed relative comparison of existing variants of NOMA used in the D2D communication with reference to parameters such as transmission scenario, the technique used, merits, open issues, throughput, EE, PEP, and PAPR.

2.4.2.29 Discussion based on Cooperative Communication Classification

Fig. 2.11 represents the effect on the ergodic capacity with respect to the transmit SINR. The graph shows that when the SINR transmission is low, the ergodic capacity of the network increases rapidly, but as the graph move towards the high transmits SINR region, the EC

Table 2.5: Relative comparison of existing NOMA schemes based on cooperative communication

Problem in cooperative NOMA	**NOMA Variant**	**Performance Metric**	**Advantages**	**Open Issues**
QoS of far users	C-NOMA [46]	Outage Probability (OP) and ergodic sum capacity	(1) Reduce the system complexity 2) maximizes the diversity gain 3) Improves reception reliability of poor connections	1) Multi-antenna at BS 2) optimal power allocation in cooperative NOMA need to be studied.
Multiple CEUs cannot served concurrently	CNAR [67]	Outage probability and Ergodic sum capacity	1) Cell edge users achieved guranteed data rate 2) Provides high throughput	Effect of NOMA interference on CEUs needs to be examined.
Acquiring side information for interference cancellation	CDRT-NOMA [68]	Outage probability and Ergodic sum capacity	1) Imroves the SE 2) capacity gain increases	Can be extended to multicell scenario to achieve high capacity gain.
Capacity gain	UP-NOMA [70]	Ergodic sum capacity	Boost the system capacity for next generation wireless network	Scheme needs to be tested using Nakagami-m Fading channel.
Power allocation	FD/HD-CNOMA [71]	User rate	Maximizes the achievable user rate for the sake of fairness	Resource Allocation scheme need to be designed for the proposed scenario.
Interference cancellation	FD-NOMA-VP [72]	Outage probability, Outage Capacity and Ergodic sum capacity	Provides better results than other pairing schemes	Can be extended for MIMO systems to improve the throughput.
Average Capacity	NOMA-PLC [73]	Average Sum Capacity	1) Reduces the electromagnetic compatibility associated with PLC 2) Relay forwards the two symbols	1) AF protocol need to be examined. 2) Can be extended to FD system.
Limited frequency and energy resources in SATCOM	NOMA-PSO [74]	Sum Rate	This scheme integrates with OFDM based cooperative SATCOM system to avoid wasting resources consisting GEO and LEO satellites	Can be extended to mMIMO systems.
Spatially multiplexed transmissions	CRS-NOMA [75]	Average rate	1) Improves the average channel power of the S-R links 2) Acquires two data symbols during two time slots	Time slots need to be reduced.
Receiver Design	CRS-NOMA-ND [76]	Ergodic sum rate and Outage performance	1) Provides better Ergodic sum rate than CRS 2) MRC scheme is applied at receiver side	Incremental redundancy techniques and source transmission at the second phase need to be studied
Average Rate gain	N-BRS [77]	Average Rate	Reduces overhead and complexity	Best relay position and channel gain need to be examined.
SIC performed for different users	NOMA-RS/HD-NOMA-RS [78]	Ergodic sum capacity	Large number of users can be served at the same time	Outage Probability needs to be evaluated
Spectral efficiency loss in a HD protocol	FD-NOMA-RS [79]	Ergodic sum capacity, Outage probability and Outage sum capacity	Large number of users can be served through the same frequency band	More insights are required for MIMO-NOMA
Spectral efficiency and reliability	STBC-NOMA [80]	Ergodic sum capacity and outage probability	1) Boosts the SE 2) Increases the system reliability	The usage of multiple antenna at the receiver side and its computation complexity using a mathematical analysis needs to be studied
Diversity gain	DRS-FPA/DRS-DPA-NOMA [81]	Outage Probability	1) Improves the system performance 2) Provides high diversity gain using dual relay	Need to study this scheme for Nakagami-m fading channels
Reception reliability of CEUs	DDF-NOMA [82]	Outage Probability	Improves the reception reliability of spatial domain users	This scheme needs to be explored for alternative user pairing strategies exploiting limited CSI knowledge.
Impact of weak channel power gain	HB-NOMA [83]	Throughput	Increases the throughput upto 30% as compared to TDMA	Needs to be investigated in the situation in which different relays select different MUs to provide relay-transmission within a same time-slot.
QoS of strong users	CMR-NOMA [84]	BER and Ergodic sum rate	Modified SIC technique is used to reduce the computational complexity of the receiving UEs	1) Scheme can be extended for MIMO systems 2) It can be evaluated for imperfect CSI.

Table 2.6: Relative comparison of existing NOMA schemes based on cooperative communication

Problem in cooperative NOMA	**NOMA Variant**	**Performance Metric**	**Advantages**	**Open Issues**
Spectral Efficiency at Relays	TW-NOMA [85]	Sum Outage probability	1) Two way DF relay with NOMA is used 2) Provides lower outage probability than TWDNC and TWANC 3) Achieved better performance locate the relay at two suboptimal points between the source nodes	Rician and Nakagami-m Fading channels 2) Imperfect CSI
Residual Interference Signal	TWR-NOMA [86]	Ergodic rate, EE, OP, Delay-tolerant throughput	1) Provides larger rate in absence of SIC at the relay 2) Provides higher throughput with imperfect SIC	Nakagami-m fading channel can be explored
Channel capacity	HDAF-NOMA [87]	Channel capacity and Average system Throughput	It is used to enhance the channel capacity and system throughput for multiple relays	Scheme need to examined over Nakagami-m fding channels.
Outage Performance	NOMA-TDMA [88]	Outage Probability	1) Less Interference 2) SIC error propagation is considered	1) The time slots for transmission can be reduced 2) Power allocation factor can be optimized.
PRS effect	NOMA-PRS [89]	Sum rate, Outage probability, and Ergodic capacity	1) Improved the sum rate and user fairness 2) Performance gain increases with the number of relays.	Can be extended to multiple users
Effect of full duplex relaying	NOMA-RBC [90]	Achievable Throughput	1) Improved the weak user rate 2) Larger gain is achieved using Dirty parity coding and compress-and-forward.	Can be extended to MU-MIMO system
Inband full duplex relaying and Imperfect SIC	CFR-NOMA [91]	Outage probability, ergodic sum rate and Power allocation optimization	1) Near users treated as a full duplex relay for the far users 2) Fairness is examined 3) Maximizes the achievable rate of users	Channel allocation scheme can be explored.
Reliability of relays	BA-NOMA [92]-[97]	Throughput and Outage probability	Improves the QoS and data rate of the Cell edge users	Relay selection can be done more accurately.
Delay and Interference	DIYA-NOMA [98]	Sum Rate and Delay	Improve the coverage network and throughput of the cell edge users	Extend to multi-cell scenario.

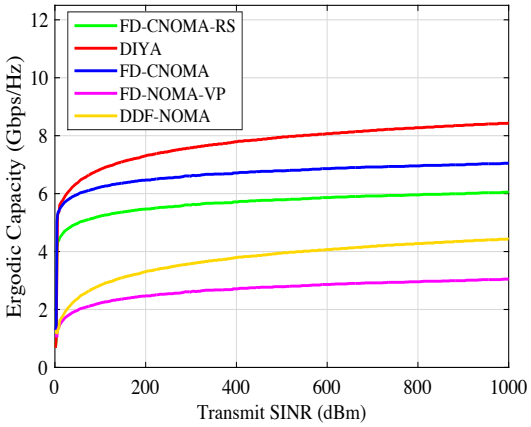

25

Figure 2.11: Classification Comparison on Cooperative Communication

becomes constant. This happened because as the SINR increases, the effect of intra-user interference increases. Also, the result shows DIYA outperforms as compared to the FD-CNOMA, FD-CNOMA-RS, FD-NOMA-VP, and DDF-NOMA. Also, it is evaluated that at 600 dBm, the proposed scheme provides approximately 40% and 45% higher ergodic capacity as compared to the FD-NOMA VP and DDF-NOMA schemes, respectively. This means that DIYA is more suitable for 5G networks.

2.4.3 CoMP

CoMP is an inter-cell technology designed for LTE/LTE-A which enhances the throughput of the users' located at the edges of a cell. In this technology, CEUs not only get the services from the users of the same cell but also the users of other cells via cooperation with each other. This technique reduces the inter-cell interference via sharing the information of users that are using the same channel. However, sharing the same channel by a large number of users of different cells affects the SE of the network. This decrease in SE motivates researchers to integrate NOMA with CoMP, which is a challenging issue due to the following reasons: (i) scheduling the APs (or the BS) and users for the application of the NOMA strategy, (ii) co-channel interference in a multi-cell scenario, and (iii) SIC complexity of NOMA. To resolve these issues, different variants of NOMA are proposed by the researchers which are discussed as follows.

2.4.3.1 CSC-NOMA [99]

In this, the authors proposed a coordinated superposition coding (CSC) scheme in the CoMP network to overcome the issue of not utilizing the same channel by the CEUs and the users nearest to the APs. In this scheme, the superposition algorithm is used for DL transmission through which both the CEUs and the users nearest to the APs can access the common

channel. To achieve it, an Alamouti code (space time code) is transmitted using the NOMA technique, among the CEUs and the users nearest to the APs. Then, the SE of the CoMP network also increases. This scheme outperformed the coherent transmission schemes and has a lower backhaul overhead for the users located at the edges of a cell.

2.4.3.2 CO-NOMA [100]

It is a resource allocation technique for mobile networks, i.e., when NOMA is combined with CoMP, it provides two advantages: (i) a large number of users got the services from limited resources and (ii) less time is taken by the packets to be delivered from source to destination [100]. In this technique, NOMA uses the space domain multiplexing using an appropriate power distribution among user pairs and it combines with it using a coordinated transmission from several RRUs. The upper bound worst-case complexity of this scheme per cluster per RB is given as follows: $O(((K2^{(K-1)}-1)c_{\phi}+c_{eval})|U(c)|)$. In this scheme, with an increase in the number of active users, the throughput per access also increases linearly.

2.4.3.3 O-NOMA [101]

Tian *et al.* proposed Opportunistic-NOMA (O-NOMA) to improve the capacity of CoMP-network which reduces the complexity of the SIC decoding process. Its topology is based on the APs broadcast signal, AP selection, and its cell area. This scheme is divided into two cases: the ideal and non-ideal cases. In the ideal case, each user selects only one AP as per its preferred set while in the non-ideal case, cells overlap with each other and users may select multiple APs. It performs better in terms of OP and the sum rate as compared to JT-NOMA.

2.4.3.4 N-NOMA [102]

It is a technique used for downlink CoMP network with randomly deployed users which consists of SC and distributed analog beamforming at the APs [102]. The SC used by both the CEUs and users nearest to the APs while distributed analog beamforming enhances the QoS of the users located at the edges of a cell. An analog beamforming was used because of two reasons: (i) it reduces the system overhead, and (ii) it utilizes the spatial degree of freedom more efficiently than STBC without using CSI. Its performance was analyzed in terms of closed-form OP because the error probability of detection was tightly bounded and evaluates the outage capacity efficiently. Moreover, they also resolved two challenges: (i) SINR arises due to SC and distributed analog beamforming, and (ii) to capture the impact of random users locations.

2.4.3.5 Multi-Tier NOMA (T-NOMA) [103]

It is a threshold-based multi-tier cluster scheduling strategy [103] which enhances the QoS of the CEUs (poor channel condition). Its model is based on the non-ideal scenario, i.e., the APs are not able to serve all users in the CoMP network. In this strategy, the users who are directly served by the APs are treated as the transmission nodes. These transmission nodes forward a signal to the users who cannot be served by APs. Then, the clusters are divided into different tiers. In the first tier, the clusters are directly served by the APs, whereas in the second tier, the transmission nodes served users in the other clusters and the same process continues in the other tiers. The signals forwarded by the transmission nodes are based on the channel conditions of the nodes and users they served.

2.4.3.6 JP-CoMP-NOMA [33]

In JP-CoMP-NOMA, data is shared between more than one BSs. Based on services provided to users from the active BSs, it is classified into two classes: JT-CoMP-NOMA and DCS-CoMP-NOMA [33]. In JT-CoMP-NOMA, multiple BSs have served both the CEUs, the CCUs using the same RB without interference to each other. Hence, it enhances the signal strength for CEUs, but at the cost of a decrease in the rate for CCUs. To handle it, an organized superposition coding scheme is used for DL to reduce the CSI sharing overhead. Then, the common CEUs among the two cells get the Alamouti coded signals from two BSs while the CCUs get the services from its corresponding BS. JT-NOMA enhances the transmission rates for CEUs without sacrificing the rates for CCUs. In DCS-CoMP-NOMA, user's data is shared between multiple BSs, but transmitted from the selected BS's only. In DCS NOMA, as per order statistics transmitting, the BS dynamically changes over time and provides service to the CEUs which increases the transmission rate.

2.4.3.7 CS/CB-CoMP-NOMA [33]

In this variant, BSs do not share user's data, but they exchange CSI and cooperative scheduling data using an interface X2. Moreover, adjacent BSs does not transmit a superimpose message to NOMA users but transmits a dedicated message to CCUs to ensure data rates for CEUs. Moreover, it improves the QoS of CoMP-NOMA users and provides guaranteed data rates for CEUs. In CB-CoMP-NOMA, only the serving BS has a user's data and based on global CSI, a beamforming decision is made with coordination. To remove the inter-channel interference (ICI), two Interference Alignment algorithms were proposed called an interfering channel assignment (ICA)-CB and interference alignment (IA)-CB. The first algorithm requires global CSI at the BS while the second needs the knowledge of CEUs serving channels at the BS. For the second one, a substantial number of antennas are required to reduce the interfering channels information.

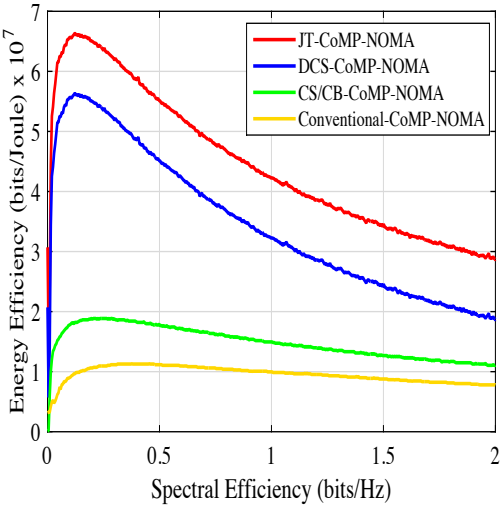

Figure 2.12: Classification Comparison on CoMP

2.4.3.8 S-NOMA [104]

In this, the authors proposed S-NOMA to enhance the security of the physical layer for NOMA-CoMP transmission. They proposed the combination of coordinated user-scheduling and joint transmission strategy to minimize the information-leakage. This scheme protects the target user from untrusted users during the NOMA transmission process. The simulation demonstrates that S-NOMA provides better secrecy OP and sum rate as compared to conventional NOMA.

2.4.3.9 Comparison of existing NOMA schemes based on CoMP

Table 2.7 provides the detailed relative comparison of existing variants of NOMA used in CoMP with reference to parameters such as the transmission scenario, technique used, merits, open issues, throughput, SE, PEP, and PARP.

2.4.3.10 Discussion based on CoMP classification

Fig. 2.12 illustrates the graph of energy efficiency versus spectral efficiency. From the figure, it can be observed that JT-CoMP-NOMA system achieves the best energy efficiency because it involves several base stations for transmission. For the conventional system, a signal generated by neighboring BS will become interference, and thus affects the received signal strength. However, for JT-CoMP-NOMA, it utilizes the neighboring BSs to assist in its transmission process. Also, it does not only mitigate the interference but also successfully eliminate them. At the same time, it converts the interference into a meaningful signal which helps to improve the signal strength. This reason clearly shows that JT-CoMP-NOMA is more suitable for 5G networks.

Table 2.7: Relative comparison of existing NOMA schemes based on CoMP

Problem in CoMP	NOMA Variant	Transmission scenario	Techniques	Performance metrics							Merits
				1	2	3	4	5	6	7	
Sharing of same channel between the cell edge and CCUs	CSC-NOMA [99]	Downlink	Almouti code integrated with APs	✓	×	×	×	×	×	×	Reduces the backhaul overhead for CEUs and improves the reception reliability of CEUs
Inter-cell Interference	CO-NOMA [100]	Downlink	Distributed power allocation	×	×	✓	×	×	×	×	Large number of users can be served and packet travel time from source to destination decreases
Multiuser Interference	O-NOMA [101]	Downlink	Joint muti-cell power allocation	✓	✓	×	×	×	×	×	Mitigates the complexity of SIC, enlarges the system throughput and overcome the muti-user interference
All the users can be served by atleast one AP	T-NOMA [103]	Downlink	Threshold based multi-tier cluster scheduling	✓	✓	×	×	×	×	×	Improves the QoS of the users having very poor channel conditions
Sharing of same channel between the cell edge and CCUs	N-NOMA [102]	Downlink	Fixed power allocation	×	✓	×	×	×	×	×	Improved EE
Inter-cell Interference	JT-CoMP-NOMA [33]	Downlink	Distributed power allocation (Beamforming with known CSI)	×	×	✓	✓	×	×	×	Improves the QoS of CEUs
Inter-cell Interference	CS-CoMP-NOMA [33]	Downlink	Distributed power allocation (Coopertive scheduling with known CSI)	×	×	✓	✓	×	×	×	Reduces the overhead for high mobility CEUs and users data are not shared among the BSs
Inter-cell Interference& detection	CB-CoMP-NOMA [33]	Downlink	Distributed power allocation (Beamforming)	×	×	✓	✓	×	×	×	Reduces the overhead for high mobility CEUs and users data are not shared among the BSs
Inter-cell Interference	DPS-CoMP-NOMA [33]	Downlink	Dynamic point selection (User clustering and power allocation)	×	×	✓	✓	×	×	×	Improved the QoS of the CEUs

Note- 1: Sum rate, 2: OP, 3: Throughput, 4: Spectral Efficiency, 5: PEP , 6: PAPR, 7:Ergodic sum capacity
Notations- ✓: Y, and ×:N

2.4.4 Cognitive Radio

A CR network offers a dynamic spectrum allocation (DSA) technique to make efficient use of spectrum. The two important users in DSA are Primary users (PUs) and secondary users (SUs). PUs are the proprietor of a licensed channel and utilize the spectrum first, while SUs are the opportunistic user whose function is to sense the licensed spectrum without creating interference for the PUs. Moreover, SUs identify the unused channels and keeps a watch on the locally available channel when PUs are absent [105]. Cognitive radio (CR) communications can be classified into three models: interweave, underlay and overlay. In the interweave model, SUs can use spectrum only if PUs are inactive, the activities of PUs are monitored continuously to avoid interference caused transmission of SUs. In the underlay model, SUs transmit with low power as compared to PUs. In the overlay models, codebooks and messages are used to identify the PUs, which in turn reduces the interference. Description of the various CR based NOMA variants are as follow.

2.4.4.1 D-NOMA [106]

In this, the authors proposed a dynamic power allocation scheme, where power allocation coefficients are varied dynamically to the instantaneous channel gains. The scheme provides a guarantee to serve different (strong and weak) users' simultaneously and avoids the situation of getting smaller date rate for weak channel condition users' in F-NOMA, and strong channel condition users' in CR-NOMA. This scheme achieves similar diversity gains like F-NOMA and large diversity gain than CR-NOMA. The performance of D-NOMA is analyzed in terms of OP and average user rate. The authors evaluated the power allocation coefficient for both the DL and UL scenarios and proved that D-NOMA performs better than OMA, F-NOMA, and CR-NOMA. It is suitable for user pairing/clustering algorithm for a large scale network and with the MIMO scenario when the condition of CSI for the transmitter is imperfect.

2.4.4.2 CR-NOMA-D-M and CR-NOMA-D-U [107]

It is a CR inspired NOMA scheme which provides dynamic QoS for multicast and unicast users [107]. In CR-NOMA-D-M, multicast users behave as PUs and the rate of these users is greater than OMA while in CR-NOMA-D-U, unicast users act as PUs. The power allocation coefficients of both these schemes are dependent upon the channel fading gains. The performance of both these schemes illustrated that they provide better results in terms of the diversity order, and secrecy OP as compared to CR-NOMA-F-M and OMA.

2.4.4.3 CR-NOMA-OFDM [108]

It consists of NOMA with cognitive OFDM systems, where the sensed spectrum is split into subcarriers and the NOMA is applied on each subcarrier to give access to multiple users [108]. It maximizes the total weighted capacity of the system by jointly optimizing the sensing duration, user selection, and power allocation. The aforementioned problem is decomposed into three subproblems: (i) the optimal sensing duration is found by the bisection search method, (ii) matching theory is adopted to optimize user selection, and (iii) the difference of convex programming is utilized to obtain efficient power allocation on subcarriers. Finally, an alternate iteration algorithm is also used to derive a joint optimization and to boost SE.

2.4.4.4 MIMO-CR-NOMA [109]

The authors studied an outage oriented joint AS algorithm for MIMO-CR-NOMA networks to maximize the SNR of SUs keeping in view of the QoS of PUs. The authors analyzed the asymptotic closed-form expression for OP and diversity to prove that their scheme performs better in comparison to the OMA scheme.

2.4.4.5 PFDM/SFDM

In [110], the authors proposed a NOMA based CR scheme, where SU access the multiple subchannels both at the present and absent of PU. In this scheme, the SU can transmit the data directly in the subchannel while PU is absent and use NOMA to communicate when the PU is present. To decode the NOMA signals, the PU first decoding method (PFDM) and the SU first decoding method (SFDM) were used at the receiver side. In the PFDM, the PU signal is first decoded and reconstructed, and then the SU signal is decoded by cancelling the PU signal from the received signal. Then, the PU throughput is decreased due to the interference caused by the SU, but the SU achieves perfect throughput. In the SFDM, the SU signal is first decoded and reconstructed, and then the PU signal is decoded by removing the SU signal from the received signal. The SU throughput can be decreased because of the interference brought by the PU, but the PU can achieve perfect throughput.

2.4.4.6 CSS-NOMA

It is a 2-phase overlay cooperative spectrum sharing (CSS) protocol where NOMA is integrated with CRN to raise SE [111]. In this protocol during the first phase, the PU uses the entire time slots and spectrum without leasing them to the SU. On the other side, in the second phase, the SU which coexists with the PU allocates its power to forward the primary symbol and its transmission simultaneously, based on the NOMA approach. In this scheme, three data symbols can be transmitted during the two phases. The performance of this scheme was analyzed in terms of ESC and OP. It achieved a better performance as compared to the TDF, CRS-NOMA, CRS-NOMA-ND, and SC-SS in terms of E-SC, whereas OP depends upon the user target data rates, and the power allocation coefficient.

2.4.4.7 MCR-NOMA [112]

It is a dynamic cooperative scheme, where the multicast SUs serve as relays and collaboratively retransmit the signals intended for the PUs and SUs, respectively. It can be directly applied to current cellular networks, where local SUs may have common packets for nearby receivers. It improves the reliability of secondary multicast transmissions if the signals for both networks are decoded correctly by the SUs. This cooperation is particularly preferred by the primary network when the PU's QoS cannot be met by the primary network itself. In this scheme, three different users scheduling strategies were proposed based on available CSI: instantaneous CSI, partial CSI, and full CSI. It attained a significant performance gain and also achieved the spatial diversity order by opportunistically using the user scheduling strategy as per available CSI.

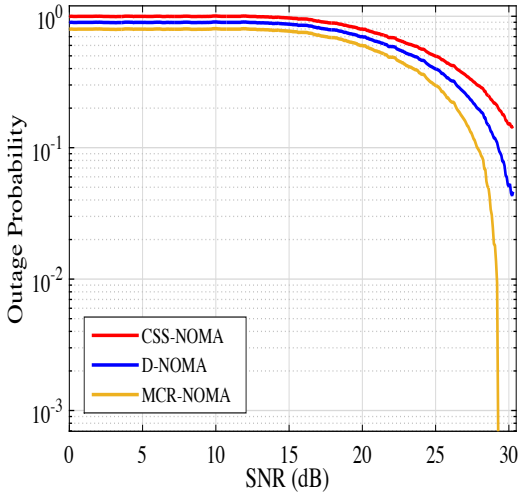

Figure 2.13: Classification Comaprison on CoMP

2.4.4.8 Reliability oriented secondary user scheduling and fairness oriented secondary user scheduling (R-SUS and F-SUS) [113]

The authors introduced the NOMA based cooperative overlay spectrum sharing framework which considered multiple SUs using multi-user diversity for the cooperation between the primary and secondary networks. In this framework, the SUs act as the relays which forward the received signals to PUs using the NOMA protocol. To facilitate the NOMA assisted cooperation, they consist of two SU scheduling schemes: R-SUS and F-SUS. The R-SUS scheme was used to minimize the outage optimal performance for both the PUs and SUs whereas the F-SUS scheme provides an equal opportunity for all SUs for cooperation. For both the schemes, a closed-form expression of primary and secondary OPs was derived and the network diversity order was investigated. The results demonstrated that both the proposed schemes have full diversity orders for PUs and SUs. But, F-SUS loses the OP of SUs in contrast to R-SUS scheme.

2.4.4.9 Comparison of existing NOMA schemes based on cognitive radio

Table 2.9 provides the detailed relative comparison of existing variants of NOMA used in cognitive radio concerning parameters such as transmission scenario, a technique used, merits, open issues, throughput, EE, capacity, and latency.

2.4.4.10 Discussion based on Cognitive Radio classification

Fig.2.13 shows the graph between the outage probability and signal to interference noise. The result implies that MCR-NOMA achieves lower outage probability as compared to the D-NOMA and CSS-NOMA. This happened due to following two reasons: (i) it used round robin

Table 2.8: Parametric analysis of existing NOMA schemes in CR

Problem **in CR**	NOMA **Variant**	Transmission **scenario**	**Techniques**	**Performance metrics**						**Merits**	**Open issues**
				1	**2**	**3**	**4**	**5**	**6**		
QoS of better channel condition is sacrificed	D-NOMA [106]	Downlink	Dynamic power allocation	✓	✓	×	×	×	×	Guaranteed to serve the users having weak channel condition and improves the QoS of users having better channel condition	User pairing /clustering algorithm in a large scale network and can be extended for MIMO with imperfect CSI at transmitter
Multicast-unicast traffic management in MISO-NOMA	CR-NOMA-D-U/CR-NOMA-D-M [107]	Downlink	Power allocation	×	✓	×	×	×	×	Higher data rates are achieved as compared to OMA schemes	Can be extended for MIMO-NOMA and the co-channel interference can be reduces when integrated with OMA schemes
Maximize the total weighted capacity	CR-NOMA-OFDM [108]	Downlink	Joint Bisection search method based sensing duration, matching theory-based user selection and DC programming based power allocation	×	×	×	×	✓	×	Boosts the system capacity of the accessible user	Sensing time can be increased.
Outage oriented antenna selection	MIMO-CR-NOMA [109]	Downlink	Subset based joint antenna selection	×	×	×	×	✓	×	Maximizes the SNR of SU keeping QoS of PU satisfied.	Can be extended to mMIMO.
SU can access the spectrum when PU is idle	PFDM/SFDM [110]	Downlink	Joint spectrum resource and subchannel transmission power allocation, and Sensing time selection	×	×	✓	×	×	×	Enlarges the throughput of PU and SU	Sensing time needs to be increases to improve the performance

Note- 1: Average rate, 2: OP, 3: Throughput, 4: EE, 5: Capacity, and 6: Latency
Notations- ✓: Yes,and ×: No

scheduling to improve the diversity order (ii) it serves both the primary and secondary users simultaneously without consuming additional frequency resource. These reasons clearly show that MCR-NOMA is more suitable for 5G networks.

2.4.5 Machine-to-Machine

In machine-to-machine (M2M), machines can communicate and exchange information with each other with or without human intervention. The presence of an autonomous connection between the machines generates heterogeneous data traffic and imposed a huge amount of traffic in the form of small and frequent data on the UL [114], [227]. In M2M, as per the type of machines and their applications, they require diverse service requirement. To handle the M2M communication in 5G, key challenges are as follows.

Table 2.9: Parametric analysis of existing NOMA schemes in CR

Problem **in CR**	NOMA **Variant**	Transmission **scenario**	**Techniques**	**Performance metrics**						**Merits**	**Open issues**
				1	**2**	**3**	**4**	**5**	**6**		
Primary network performance	CSS-NOMA [111]	Downlink	Cooperative transmission scheme for CRN network	×	✓	✓	×	×	×	An improved win-win situation is achieved and spectrum was utilized efficiently.	FD mode can be used at nodes.
Cooperative transmission for multicast CR	MCR-NOMA [112]	Downlink	Dynamic cooperative and user scheduling schemes are used for spatial diversity	×	✓	×	×	×	×	Improves reception reliability and can access the spectrum simultaneously.	Can be extended to imperfect CSI.
Overlay spectrum sharing for multi-user CRN	R-SUS & F-SUS [113]	Downlink	Cooperative spectrum sharing and two user scheduling schemes (R-SUS & F-SUS) are used.	×	✓	×	×	×	×	R-SUS provides full diversity order, and F-SUS improves the user fairness.	Can be extended to imperfect CSI.

Note- 1: Average rate, 2: OP, 3: Throughput, 4: EE, 5: Capacity, and 6: Latency
Notations- ✓: Yes,and ×: No

- *Control overhead:* In M2M, control overhead needs to be minimized because payload data generated by most of the M2M applications is small in size.
- *Scalability:* The data traffic generated by devices are dynamic. Therefore, the capacity of the network must be large so that the network can easily tolerate the changes in the node density with small information exchange.
- *Energy efficiency:* The devices used in M2M are battery operated and have a limited lifetime. To improve the EE of devices, the energy spent on radio access and data transmission need to be controlled.
- *Transmission latency:* To minimize the transmission latency in M2M, the channel access delay needs to be reduced.
- *Random access and resource allocation:* The numbers of radio resources available in 5G are limited. Therefore, an effective resource allocation scheme is required to control and exchange the messages. Proper management of resource allocation prevents co-channel interference.

To overcome the aforementioned challenges in M2M, researchers integrated NOMA with M2M communication and proposed different variants which are described as follows.

2.4.5.1 CS-NOMA [115]

It is an asynchronous CDMA uplink transmission scheme to enable joint detection of active users with their data [115]. In this scheme, a new version of the spreading technique called low

spreading sequence (LCS) was introduced. For LCS signature, mutual coherence is non-zero but far less than 1 due to which the number of LCS signature exceeds the value of N, which results in a high system overload. In this proposal, CS-MUD is deployed in the BS to recover a sparse signal. The estimation of the sparse signal can be achieved by an orthogonal matching pursuit (OMP) algorithm. To analyze the recovery of sparse signal in the presence of noise two conditions have been used, which are coherence property and restricted isometry property. Moreover, this variant with perfect CSI and imperfect CSI attains a high system overload when the active users are relatively sparse. It also enhanced the SE, mitigate the control overhead, and reduced the transmission latency.

2.4.5.2 EE-NOMA [116]

It is an energy minimization scheme for M2M communication in an UL scenario [116]. In this scheme, the authors assumed that the UE acts as machine type communication gateway (MTCG) which can decode and forward information of machine type communication devices (MTCDs) and its data directly to the BS. Then, an efficient energy network for M2M communication can be achieved using MTCD and UE rate constraint. It consumes less energy as compared to the existing NOMA and TDMA schemes. Moreover, when the number of MTCDs increases and reaches up to 100, and then 0.18 Joule amount of energy is consumed which is lower as compared to the traditional schemes.

2.4.5.3 Spatial group based random-non-orthogonal resource allocation access (SGRA-NORA) [117]

It consists of non-orthogonal resource allocation (NORA) with the spatial group based random access (SGRA) [117] to resolve two shortage problems of random access (RA) (i) Preamble collision (PA) problem which arises due to limited RA in preambles on physical RA channels (PRACH), and (ii) Congestion and overload problem which arises due to limited physical UL shared channel (PUSCH) resources. The aforementioned problems can be solved in three steps: (i) by using a large number of the preamble, (ii) non-orthogonally allocation of the same PUSCH resource blocks (RBs) to a group of machine nodes belonging to distinct spatial groups, and (iii) decoding of multiple received RA data by using SIC. It effectively utilizes both the PRACH and PUSCH and has a high RA success probability within a limited RBs allotted for M2M communication and outperformed the conventional RA scheme.

2.4.5.4 NM-ALOHA [118]

The authors in this used the NOMA technique to multichannel ALOHA for the RA scheme which effectively increases the number of subchannels by using multiple subchannels and power levels for RA. It provides a higher throughput as compared to multichannel ALOHA

by using different power levels. Moreover, it improves the number of subchannels without expanding the bandwidth and reduces the transmission power because its transmission power was based on NOMA.

2.4.5.5 ALOHA-NOMA [119]

Pure ALOHA integrated with PD-NOMA was proposed to provide scalability, EE, and high throughput MAC protocol to handle the requirements of low complexity devices for IoT applications [119]. Moreover, the presence of the SIC receiver at the gateways reduced the retransmission of IoT devices and avoids the continuous listening of the channel. This happened because it is difficult to separate the multiple signals which are transmitted in the same frequency band at the same time interval. Then, the number of active IoT devices cannot be estimated due to its throughput degraded. To overcome it, a dynamic frame structure with robustness was proposed which calculates the number of active IoT devices transmitted in ALOHA using multi-hypothesis. It has less time for payload transmission and also protects the degradation in throughput. It outperformed pure ALOHA. When five active users are successfully separated via SIC, the throughput achieved by pure ALOHA was 0.18, while in ALOHA-NOMA, it was 1.27.

The author in [120] proposed an uncoordinated random access protocol for the enhancement of ALOHA-NOMA which provides an IoT gateway to determine the number of active IoT devices following are the advantages of this scheme (i) easy estimation of the SIC power levels, and (ii) signals transmitted by different IoT devices in the same time and frequency can be easily separated. It has a throughput gain of 5.5dB over conventional slotted ALOHA.

2.4.5.6 RNOMA [130]

It was based on grant free property and used to solve two problems of mMTC (i) massive connectivity, and (ii) signalling overhead. In this technique, each user randomly transmits the same packet on each RU as per their optimized probability. Moreover, the interference at the receiver can be removed by using intra and inter-RU SIC. It performed better than slotted ALOHA in terms of reduced signalling overhead.

2.4.5.7 GRANT-FREE NOMA [121–129, 131–133]

In human-to-human (H2H) communications, devices are lesser in numbers, but they generate data with high data rates and large packet sizes [122]. In contrast to H2H, transmission and arrival of data packets in mMTC are smaller in sizes [124]. In this technique, controlling the signal overhead and accessing the channel are the major issues of mMTC. Generally, in grant-based transmission, users require four-step random access (RA) procedure to access the channel. In the case of mMTC, it is not possible to establish a dedicated connection for the data transmission because signalling overheads for coordination are proportional to the number of

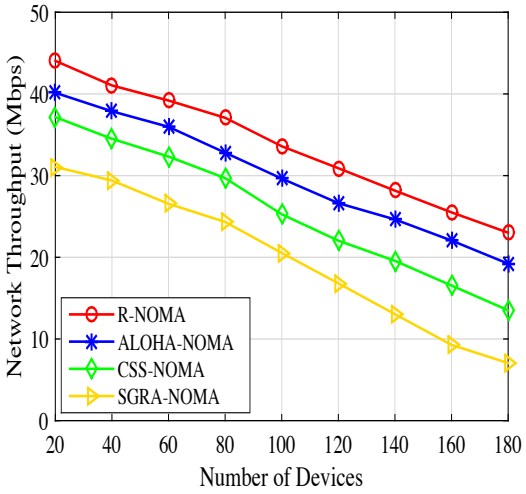

Figure 2.14: Discussion based on classification for M2M Communication

devices. Therefore, a grant-free transmission is a viable solution for mMTC.

In grant-free transmission, devices directly communicate with each other without depending upon the BS permission [125], the devices can transmit data in a UL scenario in an arrive-and-go manner [125, 126]. However, the contention is the main problem which needs to be resolved because multiple users transmit using the same channel and at the same time. The authors in [127, 128] proposed two grant-free techniques. The first one is based on mMIMO and the second is based on NOMA principle [129]. In the first technique, the spatial degree of freedoms was exploited, while in the second, the MUD techniques were explored.

Integration of NOMA with grant-free transmission results into low latency, low signalling overhead, less devices cost, and reduced in device energy consumption. The authors in [121] applied a PD-NOMA with grant-free to increase the number of connections by assuming that the BS knows the CSI of both the transmitter and receivers to achieve an optimal subchannel and power allocation. But, these techniques are not suitable for grant-free due to large signalling overhead. This issue was addressed by [131, 132] which integrates the CD-NOMA with grant-free, where a compressive sensing technique for MUD was used. But, the requirement of users prior information makes the design and computational complexity of the receiver as two challenging problems.

Jiang *et al.* [133] proposed a distributed NOMA, power MA, grant-free NOMA framework with a hybrid transmission scheme to mitigate the problems of a high collision probability which arises due to grant-free random access. It also reduces the number of MTCDs by dividing the cell into different layers based on different power levels. Moreover, to improve the throughput, they proposed an Enhanced Access Barring (EAB) mechanism to control the congestion and to reduce the overhead. To reduce the receiver side computational complexity, the author used MUD based on the different power levels of devices. The authors in [123]

proposed a technique to resolve the issue for an increase in the number of admitted users for grant-free access.

Table 2.10: Relative comparison of existing NOMA schemes based on M2M communication

Problem in M2M	NOMA variants	Transmission scenario	Techniques	Performance metrics							Merits
				1	2	3	4	5	6	7	
Latency and overhead	CS-NOMA [115]	Uplink	LCS and OMP algorithm	×	×	×	×	✓	×	×	Improve the SE and avoid the control signaling overhead and reduce the transmission latency.
Energy efficiency	EE-NOMA [116]	Uplink	Time scheduling and power control	×	×	×	✓	×	×	×	Energy reduced up to 0.18J for 100 MTCDs less than the conventional schemes
PA and PUSCH shortage problem	SGRA-NOMA [117]	Uplink	Resource allocation	×	✓	×	×	×	×	×	RA success probability reaches up to 90% with 30 RBs, which is significantly higher than 30% of the conventional RA scheme
Latency	ALOHA-NOMA [119]	Uplink	dynamic frame structure	×	×	✓	×	×	×	×	Enhances the throughput and minimizes the retransmissions of IoT devices
Signalling overhead	R-NOMA [130]	Uplink	Power control and frame structure	×	×	✓	×	×	×	×	Grant-free property of NOMA reduced the signalling overhead

Note- 1: Sum rate, 2: RA Success Probability, 3: Throughput, 4: EE, 5: Latency, 6:PAPR, and 7:Ergodic sum capacity.
Notations- ✓: Yes, and ×:No

2.4.5.8 Comparison of existing NOMA schemes based on M2M Communication

Table 2.10 provides the detailed relative comparison of existing variants of NOMA used in M2M communication using parameters such as the transmission scenario, technique used, merits, throughput, EE, sum rate, and latency.

2.4.5.9 Discussion based on classification for M2M Communication

Fig. 2.14 represent the variation in network throughput with respect to the number of devices used in communication. The graph implies that when the number of devices in network are less in number then the throughput is high whereas when the number of devices increases continuously the throughput start decreases. Also, the graph shows that R-NOMA performs better than the three schemes named as ALOHA-NOMA, CSS-NOMA, and SGRA-NOMA because it utilize the grant free NOMA scheme which reduced the interference among the devices, resulting into decrease in signaling overhead.

2.4.6 SWIPT and WPCN

Apart from improving SE, EE is another critical issue which needs to be addressed in the 5G wireless network. Generally, most of the devices used for communication are equipped

with batteries which have a limited lifetime, as shown in Fig. 2.15. So, to prolong the lifetime of these energy-constrained devices, energy harvesting (EH) is an effective technique. Initially, EH techniques harvest the energy from renewable resources such as sunlight, wind, but these techniques are not reliable as they depend upon the environment. In contrast to this, SWIPT emerges as the popular EH technique, where nodes or terminals harvest the energy from electromagnetic radiation of RF signals during data decoding. It harvests the energy even from the interfering signals. It was observed in C-NOMA that when strong users acted as a relay for weak users and then their batteries drained with a fast rate. So, the signal strength of both the strong and weak users degraded. This problem motivates the researchers of both academia and industry to use SWIPT with C-NOMA to enhance network EE as follows.

2.4.6.1 C-SWIPT-NOMA [134–138]

The combination of SWIPT with NOMA was first explored in [137], in which users were randomly located. In this technique, strong users at the time of relaying harvest the energy from RF signals of the BS and then forward the data to the weak users. In [136], the authors designed a transceiver for C-NOMA, where multiple antennas were used with the BS and a single antenna with other users. To maximize the rate of relays, the authors in [136] designed joint transmitter beamforming, power splitter, and receiver filter scheme with the QoS constraint of weak users and power constraint of the BS, respectively. Moreover, a zero-forcing (ZF) beamforming design was developed at the transmitter side. These two schemes outperformed the direct transmission scheme.

In contrast to [137], the authors in [134] investigated the impact of user association. In this technique, the authors proposed three types of users' selection scheme (RNRF, NNNF, and NNFF) based on the euclidean distance from the BS. It has lower OP and higher system throughput as compared to the random selection users scheme. Moreover, the presence of SWIPT technique reduced the effect of low diversity gain as compared to conventional NOMA. Similar to [134], the authors in [138] proposed a best near and best far (BNBF) user selection scheme which achieved a diversity order of $M+1$ without being depended upon the number of the nearest users. In this technique, M represents the number of farthest users. In [135], the authors explored the performance of C-SWIPT-NOMA having a BS and two users. Users near to the BS act as relays having multiple antenna while the user farthest from the BS had a single antenna only. Moreover, they used beamforming and random selection strategies to analyze the performance of their scheme in terms of OP to have better results in comparison to the other two schemes.

2.4.6.2 C-SWIPT-MISO/SISO-NOMA [139, 140]

In [139], the authors implemented the TAS scheme with MISO-NOMA used with the hybrid SWIPT protocol. They divided the TAS scheme into two criteria: criterion-I and criterion-II.

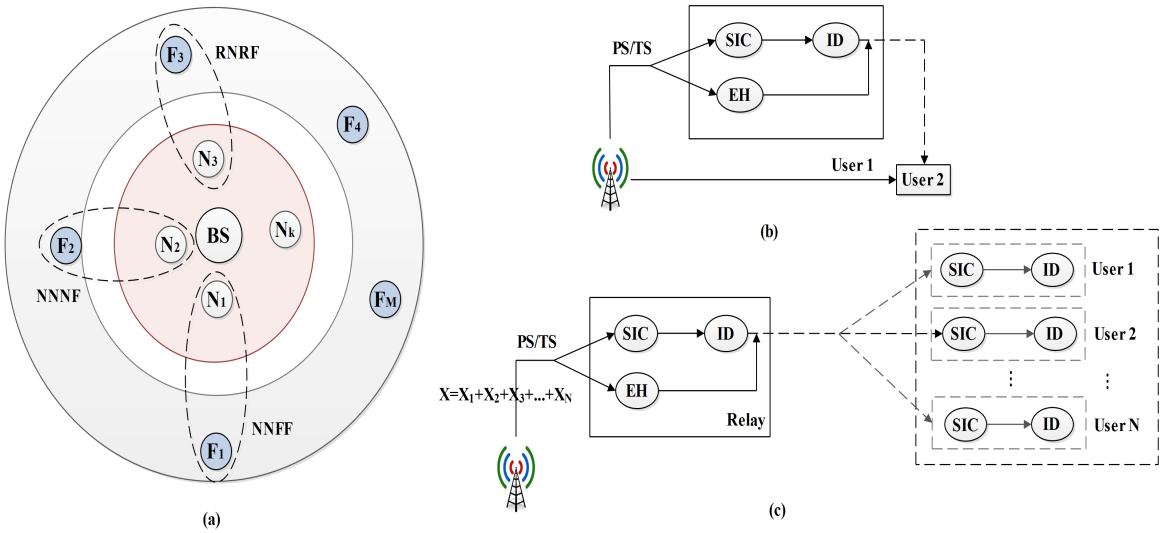

Figure 2.15: Block diagram of SWIPT

In both these criteria, they selected an antenna which provides a channel having the best fading condition from the source to the farthest users and the nearest users, respectively. Hybrid SWIPT was used with the nearest users to power the relaying operation, but for the farthest users, criterion-I and criterion-II achieved a diversity order of $K+1$ and 2 while for the nearest users it becomes 1 and K, where K represents the number of transmit antennas at the BS. In contrast to [139], the authors in [140] implemented the C-SWIPT-NOMA transmission strategy with MISO and SISO techniques. First of all, a power splitting technique was used at the EH relays. Using it, the relays forward the information by harvesting the energy from the RF signals only and protect the consumption of their battery. Second, MISO technique was studied to maximize the data rate of strong users. To achieve the target, the authors first proposed the semi-definite relaxation (SDR) technique to reduce the quadratic terms related to the beamformers and applied the exhaustive search to achieve the global optimal solution. Moreover, to reduce the high complexity of the exhaustive search, the SCA based iterative algorithm was proposed to obtain the stationary point. Third, the SISO technique was used in the transmission strategy to study practical applications. It outperformed the existing schemes and maximizes the data rate of strong users with the condition to provide guaranteed QoS to weak users.

2.4.6.3 NOMA-EH [141, 142]

Similar to C-SWIPT-NOMA, the authors in [141, 142] combined SWIPT with NOMA, where relay nodes (strong users) were equipped with EH techniques which provide communication between the BS and multiple users. In this technique, multiple antennas were used at both the BS and users side. Moreover, transmitting antenna selection (TAS) and maximal ratio combining (MRC) techniques were also used at the BS and multiple users. Performances of these schemes were analyzed in terms of a closed-form expression of outage over Rayleigh and

Nakagami-m fading channel distribution, respectively. It outperformed the SE and user fairness as compared to OMA-EH.

2.4.6.4 SWIPT-F/CR-NOMA [143]

In this, the authors explored the impact of two types of power allocation scheme in C-SWIPT-NOMA. The first scheme was based on fixed power and second on the CR. In this scheme, from source to relay Nakagami-m and from the relay to users, Rayleigh fading distribution was used. In SWIPT-F-NOMA, users power allocation coefficients were fixed and more power was allocated to the weak users as compared to strong users. On the other hand, in SWIPT-CR-NOMA, power allocation coefficients were opportunistic. It provides different trade-offs among user fairness, reception reliability, and system complexity. Both the proposed schemes lower the OP but achieved the same diversity gain as compared to SWIPT-OMA.

2.4.6.5 SWIPT-NOMA-HETNET [144, 145]

In these authors proposed an energy-efficient resource allocation scheme for simultaneous wireless information and power transfer (SWIPT)-Non-orthogonal multiple access (NOMA) based femtocells users with imperfect channel state information. A dynamic resource allocation scheme by using SWIPT and NOMA with femtocells is investigated. An energy efficiency is calculated with the help of Dinkelbach technique, also many-to-many matching technique is used to develop the subchannel allocation. The preference list of macro-users and femto-users have been developed on the basis of their harvested energy from the MBS and FBS radio frequency signals. To optimize the power of FBs, SCALE is applied to convert the non-convex problem into convex. The optimal value of power is calculated by using Lagrangian dual decomposition method with KKT conditions.

2.4.6.6 WPCN-NOMA [146–148]

In the WPCN model, the users transmit the data signals towards the BS as well as harvest the energy from the signals to charge their batteries. But, on the other side, the receivers cannot transmit the data along with energy harvesting. To overcome it, the authors in [146] used the WPCN with NOMA in a UL scenario having one BS and multiple EH users. In this technique, the users harvest the energy from the BS by using the harvest-then-transmit protocol scheme. The authors in [146] proposed two types of decoding strategies to improve the individual data rate of users and to provide fairness among them. It provides improvement in EE, user fairness, and throughput as compared to TDMA. In contrast to [146], the authors in [148] proposed a joint time allocation (uplink), energy beamforming, and receiver beamforming (downlink). It outperformed fixed power allocation and OMA schemes. In [147], the authors proposed a resource allocation scheme to mitigate the doubly near-far-effect. They also proposed joint power

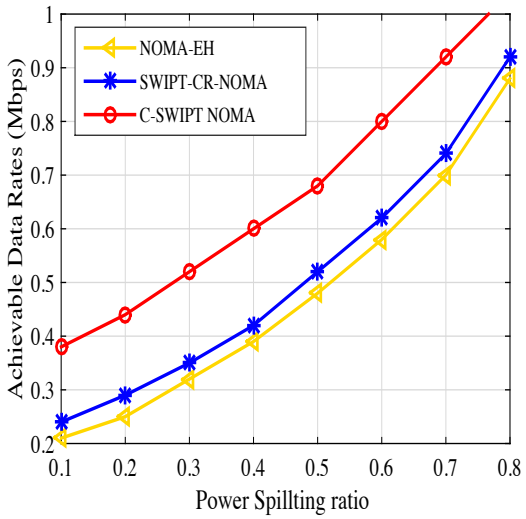

Figure 2.16: Classification Comaprison on SWIPT-NOMA

allocation with the duration of energy harvested and information transmission. Compared to TDMA, it achieved a higher rate for CEUs with better fairness.

2.4.6.7 Discussion based on SWIPT-NOMA classification

Fig. 2.18 shows the variation in rate of energy harvesting with respect to the power splitting ratio. The graph implies that C-SWIPT-CNOMA provide beeter performance as compared to that of the SWIPT-CR-NOMA and NOMA-EH. The reason behind this effect is that in C-SWIPT-NOMA the pairing schemes among the users were performed on the basis of their Euclidean distance from the BS. The authors in [134] investigated the pairing schemes more efficiently and proposed three strategies whose description are as follows: 1) random near user and random far user (RNRF), in which pairing is assigned randomly; 2) nearest near user and nearest far user (NNNF), in which the nearest near and far users to the BS are paired; and 3) nearest near user and farthest far user (NNFF), in which a near user that is closest to the BS is paired with a far user that is farthest from the BS. It is shown that the best pairing strategy is NNNF, in the sense that it minimizes the outage probability and maximizes the achievable rates for both near and far users, which are derived in closed-form. Also, this work concludes that by carefully choosing transmission rates and power splitting coefficients, one can achieve guaranteed performance results without the need to use the near usersâĂŹ own energy to power the relay phase transmission. This shows that C-SWIPT-NOMA are more suitable for 5G Scenario.

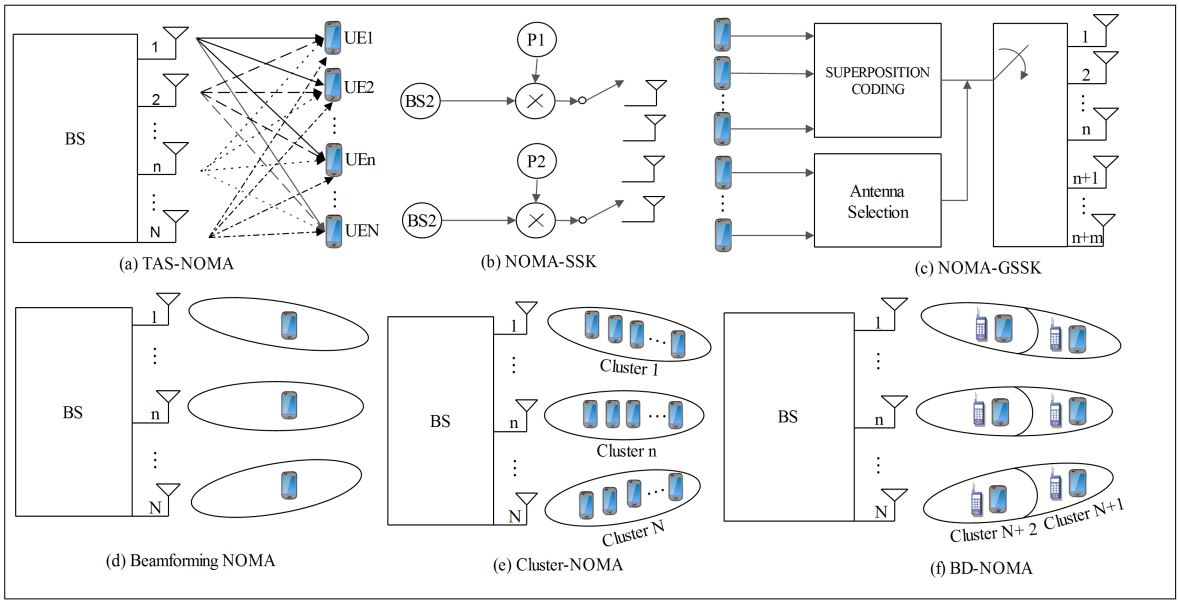

Figure 2.17: Block diagram of MIMO-NOMA: (a) TAS-NOMA, (b) NOMA-SSK, (c) NOMA-GSSK, (d) Beamforming NOMA, (e) Cluster-NOMA, and (f) BD-NOMA

2.4.7 MIMO

In MIMO, multiple antennas are used at both the transmitter and receiver side. It plays a vital role in 5G wireless communication due to following reasons: (i) enlarge the coverage area, (ii) minimize the errors arise due to multipath fading, (iii) provide high data rate, (iv) reduce bit error rate performance, (v) improved QoS for CEUs, and (vi) lower the outage probability. However, inter-user, inter-cluster, and intra-user interference are the major issues that need to be addressed in MIMO due to matrix form of channels. These interferences in MIMO reduce the network SE and degrades the QoS of CEUs. To resolve these issues, NOMA is integrated with MIMO, but in NOMA user requires special attention at the time of power allocation and channel ordering. Hence, to resolve this issue, an efficient antenna selection and beamforming technique is required in the NOMA based MIMO system.

2.4.7.1 Antenna selection based MIMO-NOMA

Antenna selection is a technique which plays a key role to maintain the diversity of the MIMO system [149] to reduce the adverse effects such as cost, complexity, and power consumption generated due to the usage of multiple antennas simultaneously. Researchers used MIMO technique in the OMA system, but cannot achieve a remarkable gain in comparison to MIMO-NOMA, due to the presence of inter-user interference. So, to overcome this problem, the following variants are proposed.

2.4.7.2 TAS-NOMA [150–152]

It is a transmit antenna selection based scheme [150], in which the authors investigated the performance of the MISO-NOMA system in a DL scenario. In this scheme, multi-antenna is used at the BS side and a single antenna at each mobile userâĂŹs side as shown in Fig. 2.17. In TAS-OMA, an antenna having the highest SINR at the BS side was selected, whereas, in TAS-NOMA, an antenna which provides the maximum sum rate was selected. Moreover, the authors in [151] proposed a user scheduling algorithm for the mMIMO-NOMA system. In contrast to [150], the authors also analyzed the sum rate. In this scheme, the authors proposed an algorithm for two cases, single-band two users and multi-band multi-users. In the first case, a search algorithm was proposed to search antennas which provides the highest channel gains, whereas, in the second case, a joint user and antenna selection algorithm was proposed to compute the normalized value of the desired antenna user-pair channel gain. The pair having the highest channel gain was selected. This scheme not only improves the system performance but also reduces the system complexity. The authors concluded that the TAS-NOMA scheme provides better performance in comparison to the OMA based user and antenna selection schemes. However, the authors in [150] and [151] did not explore the system performance analytically which was resolved in [152].

2.4.7.3 AIA-AS/A^3-AS [152]

In this, the max-min-max and the max-max-max algorithms were proposed for the two user NOMA system. The max-min-max algorithm was used to improve the instantaneous channel gain of weak channel condition users while max-max-max was used for strong channel condition users. The author applied this scheme to a model in which multiple antenna was equipped with both the BS and mobile users. They evaluated the asymptotic closed-form expressions for both the algorithms and also analyzed its average sum rate. The numerical results show that the max-min-max algorithm has better fairness and the max-max-max algorithm has a larger sum-rate than the pre-existing schemes.

2.4.7.4 NOMA-SSK [153, 154]

It is a technique which is used to improve the SE of CEUs by combining NOMA with space shift keying (SSK) [153]. It is a type of MIMO technique which transmits information using the antenna index as compared to traditional modulation schemes [154]. The major advantages of SSK are that it reduces the receiver complexity and transmitter overhead. On the other hand, it has been observed that the number of transmit antennas used in SSK must be a power of two due to its characteristics, which is its major limitation.

2.4.7.5 NOMA-GSSK [155]

This technique overcomes the limitation on the number of transmits antennas of NOMA-SSK. To enhance the SE of CEUs, the authors in [155] proposed NOMA-GSSK. In this proposal, multiple transmit antennas are used, unlike NOMA-SSK. In this scheme, both power and spatial domains are used to multiplex the users since it provides high SE, high EE, and low BER as compared to NOMA-SSK and MIMO-NOMA. In addition to these features, this scheme also reduces the complexity of the system by reducing the number of SIC steps.

2.4.7.6 PD-NOMA-SSK [156]

In this, the authors proposed a scheme for group communication. To carry out group communication, the number of resources available for users is limited due to different power levels requirements of users through the PD-NOMA system. As a result, cryptographic keys cannot be distributed efficiently among users. By analyzing this problem, the authors in [156] integrated the SSK modulation scheme with PD-NOMA to fulfil the demand of high SE. Also, to enhance the system throughput, the authors multiplex PD-NOMA-SSK with MU-MIMO techniques. The numerical results proved that the proposed PD-NOMA-SSK and PD-NOMA-SSK with MIMO enhanced SE by two to three times in comparison to the conventional NOMA and NOMA with MIMO techniques.

2.4.7.7 NOMA-HARQ [157]

In this, the authors investigate the HARQ design for downlink NOMA with single user-MIMO (SU-MIMO). The authors proposed this scheme to avoid inter-stream and inter-user interference. To handle the retransmission issue in MIMO-NOMA systems, the authors studied the impact of user pairing, precoding matrix adaptation and transmission power assignment (TPA) ratio adaptation. The results showed that the HARQ probability of NOMA is much higher than that of OFDMA, and flexible retransmission strategies could increase performance gain. Moreover, the authors also proposed an enhanced HARQ algorithm, where opportunistic HARQ combined with the TPA scheme to achieve higher performance gain than the existing algorithm.

2.4.7.8 Discussion based on Antenna Selection Based MIMO-NOMA

Fig. 2.18 shows the variation in spectral efficiency with respect to the E_b/N_o. The graph implies that PD-NOMA-SSK achieves better spectral efficiency than the GSSK and SSK because in PD-NOMA-SSK, a spatial domain technique is integrated along with PD-NOMA and SSK modulation. This combination increase the system spectral efficiency up to 2 to 3 times by using MIMO multiplexing technology. Also, to mitigate the near-far effect, in this a user-grouping strategies were used which improve the throughput 20% higher than the GSSK and

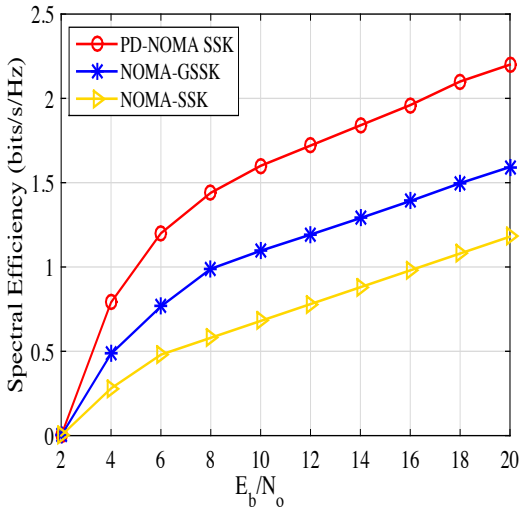

Figure 2.18: Classification Comaprison on SWIPT-NOMA

SSK. This comparison shows that PD-NOMA-SSK is suitable for 5G network.

2.4.7.9 Beam-forming based MIMO-NOMA

Multicast beamforming is a technique used in MIMO-NOMA to enhance the sum capacity of the system especially for the case of multi-users. It can be classified as single and multi-beams. In a single beam, a common single beam is allocated to all users in a group while, in multi-beams, different beams are applied to each group of users [158, 159].

2.4.7.10 NOMA-BF [160, 161]

In this, the authors studied the beamforming technique for the multi-user MIMO-NOMA system in a downlink scenario. In this scheme, the same beam is shared by a pair of users who have different channel conditions. The authors proposed the user clustering and power allocation algorithm to reduce the inter-cluster and inter-user interferences. This scheme maximizes the sum capacity of the system. In contrast to [160], the authors in [161] studied the usage of multicast beam-forming in the MISO-NOMA system for two-users. The transmitter of the BS is equipped with multi-antenna which broadcast the information using the multi-resolution technique. In this technique, the low priority signal is forwarded to the weak users (poor channel quality) whereas, both high and low priority signals are transferred to the strong users near to the BS. In this scheme, the authors integrated a minimum power beamforming technique with SC to resolve the problem of power allocation and beamforming vectors for both the users. Moreover, a closed-form expression for an optimal power allocation is also elaborated.

2.4.7.11 Random-BF-NOMA [162]

The authors studied the use of random beamforming technique at the BS side. In this scheme, a single beam with the same power allocation coefficient is allocated to each user in a cluster. To mitigate the inter-cluster and inter-beam interference in a MIMO-NOMA system, the authors in [162] proposed a spatial filter. In addition to this, the authors also applied the concept of fractional frequency reuse (FFR) to improve the power allocation among multiple beams.

2.4.7.12 ZFBF-NOMA [163]

The authors in this applied zero-forcing beamforming (ZFBF) technique for multi-user MIMO-NOMA system in a downlink scenario. This technique mitigates inter-cluster interference especially when the users have different channel conditions. In [163], the authors proposed dynamic power allocation and user clustering algorithm to mitigate the interference and to achieve the maximum throughput. The paper aimed to maximize system capacity.

2.4.7.13 Robust-BF-NOMA [164–166]

It was observed that most the researchers have worked on the beamforming design of NOMA when the BS knows the perfect CSI of the users. However, in practice, it is difficult for the BS to know the perfect CSI of the users due to channel estimation and quantization errors. So, to resolve the problem of norm-bound channel uncertainties, robust beamforming technique based on the worst-case optimization framework was studied in [164]. They studied the robust beamforming in the downlink multiuser-MISO-NOMA system. In this scheme, a single beamformer was used for all users located in the same cluster. In contrast to [164], the authors in [166], optimized the power of beamformer while maintaining the data rate of each user. In this scheme, the signal for each user was transmitted with a dedicated beam-former. Differing from [164] and [166], the authors in [165] studied the robust beamforming technique in MIMO-NOMA system using the cutting set method.

2.4.7.14 Co-ordinated beamforming NOMA (C-BF-NOMA) [167]

In [167], the authors investigated the problem of inter-cell interference in a multi-cell MIMO-NOMA based system. The authors proposed two algorithms named as interference channel alignment CBF (ICA-CBF) and interference alignment CBF (IA-CBF) algorithms. In these schemes, two BSs mutually coordinate with each other in terms of their beamforming vectors to improve the QoS of CEUs without sharing the data between cells. Both these algorithms eliminate the intercell and inter-cluster interference whereas SIC technique of NOMA mitigates the intra-cluster interference. The first algorithm uses full CSI at the BS while the second uses the knowledge of channel gains of CEUs. The numerical results show that both

these algorithms performed better than traditional NOMA and OMA. These schemes improved the throughput and increased the number of served users.

2.4.7.15 BD-NOMA [168]

The authors observed that BDMA and NOMA could not directly be combined in the case of long term feedback based beamforming due to the problem of short-term channel variation. To resolve this issue, the authors in [168] used short term feedback with FDD-MU-MIMO system which had multiple channel indicators (CQIs). For this, NOMA with BDMA can be used which is known as BD-NOMA. In BD-NOMA, distinctive power is allocated to near and far users over each beam to mitigate the inter-beam and intra-beam interference at the same time. Moreover, the authors also proposed a weighted minimum mean square error (MMSE) based algorithm to solve the joint user selection and power allocation problem for BD-NOMA. The numerical results show that BD-NOMA for low interbeat interference (IBI) achieved 20% WSR gain over BDMA when equal power is allocated over each beam while the proposed scheme shows that BD-NOMA for high IBI achieved 10% WSR gain over BDMA.

2.4.7.16 VP-NOMA [169]

This is a hybrid NOMA transmission scheme designed for the MU-MISO system [169]. The basic idea behind this scheme was to minimize the total transmit power by using the beamforming matrix and power allocation technique. To minimize the transmit power; the authors designed a low-complexity greedy iteration algorithm to generate beamforming vectors. The numerical results showed that the vector-perturbation (VP)-NOMA reduces the transmit power as compared to NVP-systems.

2.4.7.17 NOMA-MRT [170]

In this, the authors investigated the design of the adaptive transmission mode, that switching between MMSE-BF and NOMA-MRT to maintain the achievable rate. The objective of the scheme was to achieve the maximum weighted sum rate for MISO downlink systems. Also, the authors proposed that when the channel vectors of the two users are highly correlated and perfectly aligned with each other, and MMSE-BF achieved an almost equal rate like NOMA-MRT. On the other hand, when two channels are orthogonal, MMSE-BF outperformed the NOMA-MRT.

2.4.7.18 Discussion based on Classification of Beamforming MIMO-NOMA

Fig. 2.19 represents the graph between the outage probability and SNR. The result in the graph shows that C-BF-NOMA is suitable for 5G networks where high massive connectivity, and low outage probability are required. The reason behind such behaviour is that this scheme

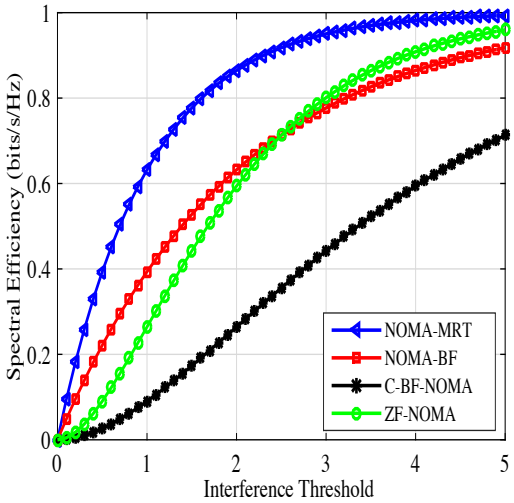

Figure 2.19: Classification Comaprison on VLC Communication

perfectly deals with the inter-cell interference, and increase the cell-edge users' throughput, which in turn improves user fairness. In addition, when the number of users in a network increases, then this scheme performs better than the others because in this SIC and interference alignment technique are used to cancel the intra cluster interference and inter-cluster interference, respectively.

2.4.8 Cluster based MIMO-NOMA

In this scheme, the users are partitioned into several different clusters, the appropriate beams related to the corresponding clusters are designed. Cluster-based MIMO-NOMA (CB-MIMO-NOMA) effectively suppress the inter-cluster interference through an appropriate transmit precoder and detector. This technique ensured that the beam related to the particular cluster should be orthogonal to the users in other clusters. Due to cluster isolation, the difference between the users' channel conditions also increases. With this, the intra-cluster interference can be also mitigated from the SIC technique of NOMA.

2.4.8.1 NOMA-SM [171]

SM is energy-efficient MIMO techniques in which both amplitude-phase modulation and an index of transmit antennas are used to transmit the information bits. It was found that when OMA integrated with SM, low SE was achieved; while when transmit antenna grouping (TAG) integrates with SM, severe interuser interference was obtained. To overcome these problems, the authors in [171] integrate NOMA with SM in a downlink MU-MIMO scenario. With this scheme, the inter-user interference can be eliminated by deploying the SIC technique on the user's side. Moreover, to achieve high SE, the authors in [171] proposed a low complex power

allocation scheme based on symbol rate error analysis. The authors also proposed the user pairing scheme to address the near-far effect. The numerical results show that NOMA-SM achieved better results than OMA-SM and TAG-SM.

2.4.8.2 SA-NOMA [172]

It is a technique used in the MIMO-NOMA system to eliminate inter-cluster interference. The authors in [172] applied this technique in a single cell framework to study the outage performance of both uplink and downlink MIMO-NOMA transmissions. In this scheme, stochastic geometry was used to study the impact of users' random locations and interferers. Moreover, the authors proposed two power allocation schemes to provide better trade-offs between users' fairness and throughput. The fixed power allocation (FPA) technique was used to have different QoS requirements while CR-inspired power allocation technique assures that users' QoS requirements must be fulfilled instantaneously. In [172], the authors also combined the SA-NOMA technique with the usersâĂŹ precoding selection scheme to fully exploit the spatial degree of freedoms of MIMO systems.

2.4.8.3 H-NOMA [173]

It is a precoding algorithm having low complexity as compared to DPC and ZFBF. It is based on the quasi degradation concept and is suitable for practical scenarios. The application of this algorithm was studied in [173] with the sequential user pairing technique for the two-user MISO-NOMA system. It optimizes QoS for two users and minimizes the transmit power having bound on data rates. The authors numerically and analytically analyzed the performance of H-NOMA using average transmit power and outage probability. The results show that H-NOMA outperformed both DPC and ZFBF.

2.4.8.4 PH-NOMA (Projection Hybrid-NOMA) [174]

It is an algorithm which combines Hybrid NOMA (H-NOMA) precoding and conventional ZFBF algorithm and was proposed to mitigate inter and intracluster interference for the multi-user MISO-NOMA system [174]. Moreover, to reduce overall interference and to achieve low complexity, PH-NOMA with projection-based pairing algorithm (PBPA) and inversion based pairing algorithm (IBPA) are combined using the properties of quasi-degradation. The performance of these algorithms was analysed in terms of outage probability and diversity gain. To analyse the efficiency of these proposed BF algorithms, various performance evaluations are performed.

2.4.8.5 QR-NOMA [175]

The authors investigated the outage performance by using the precoding matrix and power allocation scheme. In this scheme, one transmitter sent information to two users where one user received data (small packet) at a low rate and the other a higher rate. The presence of a precoding matrix in this scheme reduces the user's effective channel gain but improves the signal strength of the second user's. With this scheme, the potential of NOMA can be gained even when the participating users have similar channel conditions.

2.4.8.6 SBD-NOMA [176]

The authors in this proposed a scheme for an uplink MIMO-NOMA system with a fixed set of power allocation coefficients. It is hybrid multiple access schemes which inherit the advantages of both orthogonal and non-orthogonal transmissions. In this scheme, the authors partitioned the available bandwidth among the users into identical orthogonal sub-bands according to their CSI information. As a result, inter-cluster interference is eliminated and an improved QoS is achieved. With this scheme, the number of MUDs reduces, which results in reduced receiver complexity. Moreover, the authors also developed a user pairing technique to reduce the inter-cluster interference. To derive the outage probability, the probability density function (PDF) of the received SINR was approximated by a gamma function under Rayleigh fading distributions.

2.4.9 Comparison of existing NOMA schemes based on MIMO

Table 2.12 provides the detailed relative comparison of existing variants of NOMA used in MIMO using parameters such as transmission scenario, advantages, open issues, outage probability, bit error rate, throughput, EE, sum rate, UL, and DL.

2.4.10 massive MIMO

In 5G, massive MIMO (mMIMO) is a key enabler with large antenna diversity at a lower cost [177], [178], [179]. Its advantages are as follows (i) improvement of SE and EE of the network, (ii) reduction in latency, (iii) mitigation of an inter-cluster and inter-user interference, (iv) robustness against intentional jamming, and (v) improved SNR for the receiver. The authors in [180] integrated NOMA with mMIMO with limited feedback. In this technique, the transmitter of the BS consists of a large number of antennas as compared to the number of users. To simplify the design, it decomposed the channels of massive MIMO-NOMA into multiple SISO-NOMA channels. Its performance was analytically derived in terms of an exact expression of OP and diversity order.

In [181], the authors combined NOMA and IDMA technique for MU-mMIMO transmission. In this technique, the gain of the MU-mMIMO transmission was affected at a large rate

Table 2.11: Relative comparison of existing NOMA schemes based on MIMO

Problem in MIMO	**NOMA variants**	**Scenarios**	**TS**	**SR**	**OP**	**EE**	**BER**	**SE**	**Th**	**Advantages**	Open Issues
Multiple antennas at Transmitter enhance the complexity, cost and consumption	TAS-NOMA [150]	MU-MISO	DL	✓	×	×	×	×	×	Reduces the complexity, cost and power consumption	Imperfect CSI and need to find the ESC and OP
Joint antenna selection at both the BS and users	$AIA - A^3 - AS$ [152]	MU-MIMO	DL	✓	×	×	×	×	×	AIA-AS provide better user fairness and $A^3 - AS$ provide near-optimal sum-rate performance	Imperfect CSI
Low SE of CEUs	NOMA-SSK [153]	MU-MIMO	DL	×	×	✓	✓	✓	×	Reduces decoding complexity at the receivers and reduce the interference of CEUs.	Power allocation scheme need to be determined.
Low SE of CEUs	NOMA-GSSK [155]	MU-MIMO	DL	×	×	✓	✓	✓	×	Reduces the computational complexity	Need to study the scheme with SIC
Secure group communication	PD-NOMA-SSK [156]	MU-MIMO	DL	×	×	×	✓	✓	×	Improves the network throughput	Study the power allocation problem for multiple adjacent users
Inaccurate MCS selection problem originated from implicit feedback	NOMA-HARQ [157]	SU-MIMO	DL	×	×	×	×	✓	×	Improved the cell throughput by 4% and cell edge throughput by 5% than HARQ algorithm	Extension to MU-MIMO system.
Inter cluster and Inter user interference	NOMA-BF [160]	MU-MIMO	DL	✓	×	×	×	×	×	Increases the number of supportable users and QoS of the weak users can be guaranteed	Imperfect CSI and SIC need to be studied.
Inter-cluster and inter user interference	NOMA-BF [161]	MU-MISO	DL	✓	×	×	×	×	×	Minimizes the total transmit power	Extension to MU-MIMO and mMIMO systems.
Inter cluster and Inter beam interference	RANDOM-BF-NOMA [162]	MU-MIMO	DL	×	×	×	×	×	✓	Reduces the CSI feedback and increase the throughput of CEUs	Performance over imperfect SIC is need to be evaluated.
Inter cluster	ZF-BF-NOMA [163]	MU-MIMO	DL	×	×	×	×	✓	✓	Maximizes the overall throughput in a cell	Multicell scenario need to be investigated
Worst case uncertainties	ROBUST-BF-NOMA [164]	MU-MISO	DL	✓	×	×	×	×	×	Investigate the scheme with imperfect CSI and maximizes the worst case achievable sum rate	Extend the scheme for MU-MIMO scenario, and need to eliminate the NOMA interference arise due to imperfect SIC.
	ROBUST-BF-NOMA [166]	MU-MISO	DL	×	✓	×	×	×	×		
	ROBUST-BF-NOMA [165]	MU-MIMO	DL	✓	×	×	×	×	×		
Inter cell and inter cluster interference	C-BF-NOMA [167]	MU-MIMO	DL	×	×	×	×	×	✓	Increases the CEUs throughput and improves the user fairness	Need to eliminate the NOMA interference arise due to imperfect SIC.

Note- 1: Sum rate, 2: Outage Probability, 3: EE, 4: Bit error rate, 5: Spectral efficiency, 6:Throughput
TS: Transmission scenario, DL: Downlink, UL: Uplink
Notations- ✓: Yes, and ×: No

Table 2.12: Relative comparison of existing NOMA schemes based on MIMO

Problem in MIMO	**NOMA variants**	**Scenarios**	**TS**	**SR**	**OP**	**EE**	**BER**	**SE**	**Th**	**Advantages**	Open Issues
Inter and intra beam interference	BD-NOMA [168]	MU-MIMO	DL	✓	×	×	×	×	×	Performance gain increases from 10% to 20%	Investigate short term feedback with long term feedback and random user distribution with more users and clusters need to be studied
Transmit power	VP-NOMA [169]	MU-MISO	DL	✓	×	×	×	×	×	Minimizes the total transmit power	System may be extended to MU-MIMO.
Sum rate	NOMA-MRT [170]	MU-MISO	DL	✓	×	×	×	×	×	Adaptive switching method maximizes the weighted sum rate	Need to be extended for MIMO and mMIMO systems.
Inter-user interference	NOMA-SM [171]	MU-MIMO	DL	×	×	×	✓	×	×	Enhanced SE and eliminate inter-user interference	Need to increase the number of radio frequency at the transmitter side.
Inter-cluster interference	SA-NOMA [172]	MU-MIMO	DL/UL	x	✓	×	×	×	×	Provides large diversity gain	Imperfect CSI and SiC need to be studied.
Transmission power	H-NOMA [173]	MU-MISO	DL	×	✓	×	×	×	×	Reduced the transmission power	Same scenario need to studied for MIMO-NOMA system
Inter and Intra cluster interference	PH-NOMA [174]	MU-MISO	DL	✓	✓	×	×	×	×	Minimizes the total power consumption and eliminate the inter cluster interference	Same scenario need to studied for MIMO-NOMA system
Small packet transmission	QR-NOMA [175]	MU-MIMO	DL	×	✓	×	×	×	×	QoS of the users can be guaranteed, suitable for critical and real time applications, and channel conditions of user's are different.	Similar scheme need to be applied for V2X system.
Resource allocation	SBD-NOMA [176]	MU-MIMO	UL	✓	✓	×	×	×	×	Reduced receiver complexity and provides better sum rate	The system need to be studied for imperfect CSI, and Nakagami-m fading channels need to be examined.

Note- 1: Sum rate, 2: Outage Probability, 3: EE, 4: Bit error rate, 5: Spectral efficiency, 6:Throughput
TS: Transmission scenario, DL: Downlink, UL: Uplink
Notations- ✓: Yes, and ×: No

with perfect CSI at the BS. To resolve it, the authors used IDMA and iterative data aided channel estimation (DACE) scheme with imperfect CSI which provides high throughput and robustness against the pilot contamination problem. It is observed that for 5G networks, group-oriented applications were used with a multicast infrastructure used in 5G applications. The authors in [182] implemented a multicast 5G infrastructure with the combination of NOMA and mMIMO techniques. In [182], the authors proposed a hybrid unicast/multicast precoding scheme based on NOMA. The scheme first separates unicast users in NOMA and non-NOMA types and then eliminates the signal leakage using null space and SIC technique. Moreover, to enhance SE, it superimposed the NOMA users signals on to the multicast users signals.

The concept of SA-MIMO-NOMA was used in [172], and the authors in [183] designed an interference cancellation combining (ICC) matrix to eliminate the intra-pair-interference in the mMIMO-NOMA system to limit the number of antennas between the BS and users. Moreover, to enhance the sum rate and to decrease OP, the authors proposed a user pairing and pair scheduling algorithm (UPaS) which selects the first and second user of each group. In [184], the authors analyzed the performance of massive access MIMO system instead of mMIMO. In this scheme, a Gaussian message passing iterative detection (GMIPD) algorithm was used for mean and variance computation as compared to the mean square error multiuser detection scheme used in [185].

In [186], distinctive power is distributed to various users. According to the increase in allocated power, each user was arranged within each sub-band along with the NOMA encoding scheme. In this scheme, the transmission was divided into two phases: In the first phase, a NOMA encoding strategy was used to encode the data and transmitter was used to handover this to relay while in the second phase, a relay transfers the encoded data to the receiver. In this way, the edge users have a fast transmission rate, where the relays are the CCUs or the access point. Moreover, it extends the coverage area and enhances the QoS performance for CEUs. In this NOMA scheme, the authors applied the maximum mean square error (MMSE)-SIC technique at the receiver side to decrypt the data and determined the closed-form expression for SINR, system capacity, and sum rate.

2.4.11 Software Defined Networking

Xu *et al.* [187] proposed an evaluation criterion to analyze the performance gain of NOMA over TDMA. Authors in [187], first illustrated the relationship between the capacity region of Gaussian BC and two rate regions using NOMA and TDMA. Then, they proposed an evaluation criterion for NOMA using wireless fading scenarios. This evaluation criterion was used to study statistically the sum rate and individual data rates. Moreover, the authors also proposed a user pairing and optimum power allocation scheme for the DL scenario and analytically showed that NOMA with TDMA outperformed the other schemes using parameters such as the sum rate and data rate.

2.4.12 Wireless Sensor Networks

Wireless Sensor Networks (WSNs) are low cost and low-power homogeneous or heterogeneous sensors which are used for sensing, computations and short-range wireless communications [188], [189]. But, the key challenges of these sensors are their energy depletion which results in limited lifetime [190], [191], [192]. To resolve these issues, NOMA technology is integrated with WSN. For example, the authors in [193], investigate the problem of maximizing the EE of NOMA based WSN. They used energy harvesting to improve the energy of the sensors. To solve this problem, the authors proposed a particle swarm optimization based algorithm. The simulated results showed that the proposed algorithm achieved the convergence equivalent to the global optimum solution. In [194], the authors studied the problem of interference due to the sharing of spectrum between the sensors and other sources by using stochastic geometry. The main aim of this scheme was to provide the massive connectivity between the sensors using NOMA. Also, the authors in [194] evaluated the performance of the proposed scheme using OP, average link throughput and energy consumption efficiency where results showed that NOMA performed better than OMA. In [195], the authors proposed a solution to maximize the lifetime of a single hop WSN. The authors in [196] proposed a power allocation scheme for NOMA based underwater acoustic sensor networks. The equal transmission times (ETT) power allocation scheme prevents resource wastage by ensuring the same transmission time between each transmission path.

2.4.13 Mobile Edge Computing

NOMA and Mobile Edge Computing (MEC) are integrated to avoid the delay and to reduce the energy consumption of the MEC network [197]. In [198], the NOMA-based MEC network was used such that the SIC based BS is selected to perform the computation tasks from different users to ensure the offloading. In contrast to [198], the authors in [199], analytically proved that the latency and energy consumption are reduced when uplink and downlink NOMA are combined with MEC. The authors in [200] and [201] studied the NOMA-based MEC networks to minimize time and energy consumption. It was found that the authors from [198–201] applied NOMA only on one group of users and ignored the time allocation procedure among different group of users. So, to resolve this issue, the authors in [202] proposed the resource allocation scheme among different groups of users by using uplink NOMA transmission over MEC. The main aim was to provide an energy-efficient scheme which provides better results in comparison to the conventional OMA. In [203], the energy consumption of NOMA-MEC networks was minimized by assuming that each user has access to multiple bandwidth resource blocks. To minimize the energy consumption of the network, the authors in [204] combine EH technique with the NOMA-based full-duplex MEC network. They achieved the target by using power control, time scheduling and computation capacity allocation.

2.4.14 Unmanned Aerial Vehicles

To improve the coverage and SE of 5G, Unmanned Aerial Vehicle (UAV) communication with NOMA technique plays a vital role. Since NOMA works effectively under asymmetric channel conditions, so this property of NOMA is suitable for UAVs due to high mobility which enhances the performance gain of the network [205]. In [206], the authors studied the bit allocation and trajectory optimization framework for UAV mounted cloudlet for offloading applications in NOMA. The results demonstrated that the proposed scheme enhances the EE of mobile users. The authors in [207] deployed the fixed-wing UAV communication with NOMA for ground users which are located at the areas where the BS coverage does not exist. The authors also proposed a multiple access mode selection (NOMA/OMA) scheme to ensure guaranteed communication for ground users as per their outage probability requirements. In contrast to [206] and [207], the authors in [208] investigated the NOMA with an aerial BS, where they addressed the problem of coverage and capacity by assuming performance thresholds for both cell-edge as well as the CCUs.

In [209], the authors applied the NOMA technique with UAV to enhance the coverage of user region which is densely packed such as stadium, malls or a concrete area. Furthermore, a beam scanning approach was used to find the optimal area that radiates within the user region. Based on this, a hybrid transmission strategy was applied to all the users at a time in the presence of NOMA. The result showed that user distance feedback is a better alternative in comparison to full CSI feedback especially for the rapid fluctuation channels for NOMA rather than OMA. In [210], the authors studied the three cases of NOMA enabled UAV communication. In the first case, the author evaluated the performance of NOMA enabled UAV communication by using stochastic geometry for position estimation of UAVs and ground users. In the second case, they investigated the two-dimensional (2D) model for position estimation of UAVs by assuming that UAV can fly at a fixed height. In the last and third case, they analyzed how machine learning algorithms can be applied for UAVs localization. Authors in [211] applied MIMO-NOMA on UAVs by using stochastic geometry, by considering the locations of NOMA users and interference sources. In [212], the authors applied the concept of NOMA transmission with UAV assisted wireless backhaul network and proposed a novel cooperative NOMA strategy to boost the performance of the system. Authors in [213] proposed a cooperative NOMA scheme to eliminate the uplink interference arise due to sharing of the same channel between the UAV's LOS and the BS cellular-connected users. In contrast to [213], the authors in [214] studied the UAV uplink communication in the cellular network. In this scheme, UAVs have multi-antennas to transmit multiple data streams to a large number of ground base stations to serve a terrestrial user at the same time over the same frequency band. Also, the authors in [214] proposed a NOMA based transmission strategy which is used to mitigate the signals received from the UAVs and the terrestrial users' signals.

2.4.15 Ultra-Dense Network

Ultra-Dense Network (UDN) is a technology which is used in 5G to reduce the distance between the BS and users. This technique not only increases the number of connections between the BS and users but also improves the data rate of the CCUs and CEUs, respectively. In [215], the authors used the concept of PD-NOMA in UDN for multi-user access. The authors applied the matching algorithm for resource allocation and the difference of two convex programming for power allocation. By using these two concepts, the authors enhanced the throughput of the network. In contrast to [215], the authors in [216] also enhanced the throughput of the network by using the PD-NOMA based user-centric framework. In this scheme, they converted the mixed-integer non-linear programming (MINLP) problem into an access points grouping problem. To solve this problem, a low complexity based sub-optimal matching algorithm was implemented. Then, the authors in [217] proposed the concept of user pairing and designed a new resource allocation algorithm to have a flexible configuration in heterogeneous UDN.

2.4.16 Visible Light Communication

Visible Light Communication (VLC) is a small cell technology used in 5G to provide ubiquitous broadband connectivity for indoor areas. It has an unlicensed spectrum of an order of terahertz (430 THz-790 THz) which is currently unused in wireless communication. As per the report of [1], it was found that 70% of the data traffic is originated from indoor areas. So, when VLC is integrated with the existing fibre networks, its unlicensed spectrum offload the data traffic. Generally, light-emitting diode (LEDs) are used to provide VLC in both the indoor and outdoor scenarios. Using LEDs, the cost of broadband connection reduces and the speed of data transmission over white light increases. This consists of two techniques namely as, intensity modulation (IM) and direct detection (DD). In IM, the intensity of light generated by LEDs varied as per the location of users whereas, in DD, photo-detectors are used at the receiver side which detects the variation in the intensity of light. The light signals from LEDs cannot penetrate through the walls, so intercell interference does not exist. Due to this advantage, visible light provides secure communication and improved the QoS of the CEUs. Despite the aforementioned benefits, VLC has limitations which need to be addressed to fully exploit its potential benefits. The major limitations of VLC are (i) it has narrow modulation bandwidth due to which achievable data rate cannot be achieved and (ii) in multiple cells scenario the problem intercell interference becomes severe. So, to resolve these problems, integration of NOMA is required with the following example researches.

2.4.16.1 Gain ratio power allocation [218]

It is a gain ratio power allocation (GRPA) scheme where power allocated to k^{th} user is given by $P_k = (\frac{h_1}{h_k})^k P_{k-1}$. The authors in [218] assumed that the user's actual channel conditions are

based upon the fair power allocation among them. To avoid overlapping between the cells, a cell zooming technique was proposed, where transmitting angles of the LEDs are adjusted to control the size of cells. Sometimes, adjusting the transmitting angles may affect the width and intensity of beams, resulting in the undesired illumination across the indoor space. So, to overcome this issue, a location-based user association strategy was proposed. With this strategy, users may remain connected with those two LEDs which create an overlapping area. Moreover, to enhance the performance of CEUs, tunable FOVs were used to decrease the number of handovers at the PDs.

2.4.16.2 OFDMA-NOMA [219]

It is a hybrid multiple access technique designed for bidirectional VLC transmission [219]. The combination of both these techniques enlarges the capacity of the system to provide services to a large number of users. It provides high SE, high throughput, and high tolerance against multipath induced distortion. Performance of the proposed scheme was experimentally demonstrated using the optimum power allocation ratio (PAR). The results show that the PAR values for both uplink and downlink transmission were about 0.25. Moreover, to eliminate the inter-user interference, the authors in [219] also investigated the effect of channel estimation. The obtained results demonstrated that the channel estimation like intra-symbol frequency averaging (ISFA) and minimum mean square error (MMSE) perform better than least square.

2.4.16.3 NOMA-SCFDM [220]

In this, the authors combined the NOMA technique with single carrier frequency division multiplexing (SCFDM). Similar to [219], this scheme also provides high SE, high throughput, and high tolerance against multipath induced distortion but it lowers the value of PAPR. The authors experimentally demonstrated the feasibility of this scheme and proved that it provides better results in comparison to the NOMA-OFDM in terms of BER.

2.4.16.4 NOMA-PON [221]

The authors proposed a single carrier transmission-based NOMA for bidirectional passive optical network (PON) transmission. In this scheme, power domain-based SC technique was used to multiplex the optical network units (ONUs) signals at the transmitter side and frequency domain successive interference cancellation (FD-SIC) used to separate the ONU signals at the receiver side. So, all ONUs efficiently utilized the whole time-frequency resources. To provide better trade-offs between the system throughput and user fairness, an efficient power allocation technique was proposed. The main aim of the proposed scheme was to achieve an optimum PARs. Also, the authors also proposed a polarization dimension and joined detection techniques to enlarge the transmission capacity and analyse the BER, respectively. The results

show that the optimum power difference between two ONUs for upstream was 7 dB and optimum PARs for downstream was 0.25. The BER performance for both these streams equals to 10^{-3}. In contrast to [221], the authors in [222] integrate MIMO and polarization interleaving technique with the NOMA-PON transmission scheme so that capacity of the system can be increased and a large number of users can be served. Moreover, the authors also studied the MIMO channel estimation technique concerning ISFA and MMSE to eliminate the inter-user interference and the crosstalk between polarizations. The results showed that for four users, the proposed transmission scheme achieved an optimum PAR of 0.42.

2.4.16.5 DCO-OFDM-NOMA [223]

Direct current biased optical orthogonal frequency division multiplexing (DCO-OFDM) technique was used in the VLC system to convert the bipolar OFDM signal into unipolar one. In [223], the authors integrated NOMA technique with DCO-OFDM to enhance the system SE. In this scheme, the authors studied the impact of clipping in terms of attenuation factor and clipping noise, through asymmetrical double clipping technique. They have analysed the scheme in terms of achievable rate regions and proved that it outperformed the OMA-DCO-OFDM.

2.4.16.6 FTN-FrCT-NOFDM [224]

Faster-than-Nyquist-Fractional cosine transform-non-orthogonal frequency-division multiplexing (FTN-FrCT-NOFDM) scheme provide real-valued signal as compared to FrFT-NOFDM [224]. It can be directly applied to the VLC system without up-conversion, which makes it more suitable for cost-sensitive VLC systems. It consumes lesser bandwidth as compared to FrFT-NOFDM, resulting in low-frequency distortion and high SE. The simulated results show that FrCT-NOFDM performs better in terms of BER as well as achieved higher security than FrFT-NOFDM.

2.4.16.7 Comparison of existing NOMA schemes based on VLC Communication

Table 2.13 provides the detailed relative comparison of existing variants of NOMA used in VLC with reference to parameters such as the transmission scenario, technique used, merits, throughput, EE, capacity, latency, and open issues.

2.4.16.8 Discussion based on Classification of VLC Communication

Fig. 2.20 shows the effect of varying the SNR on the bite error rate. The result implies that GRPA achieves lower BER than the OFDMA-NOA, NOMA-SCFDM, and NOMA-PON. The reason behind such a behaviour is that in GRPA, the user's actual channel conditions are based upon the fair power allocation among them. To avoid overlapping between the cells, a cell

Table 2.13: Parametric analysis of existing NOMA schemes in VLC

Problem **in VLC**	NOMA **Variant**	Transmission **scenario**	**Techniques**	**Performance metrics**						**Merits**	**Open issues**
				1	**2**	**3**	**4**	**5**	**6**		
Narrow modulation bandwidth	GRPA [218]	Downlink	Gain ratio power allocation	×	×	✓	×	×	×	Maximize the users' sum rate and decrease the number of handover by tuning the field of views (FOVs)	Scheme needs to be analyzed for UL scenario.
Flexible bandwidth allocation	NOMA-OFDMA [219]	UL & DL	Hybrid scheme for VLC transmission.	×	×	✓	✓	✓	×	Efficient channel estimation are used to eliminate the inter-user interference and improved system capacity.	Outage probability needs to be derived.
Lower BER & Less tolerant to LED nonlinearity	NOMA-SCFDM [220]	Downlink	Integrate NOMA with SCFDM	×	✓	✓	✓	×	×	Improved BER than NOMA-OFDM.	Can be extended to Multi- carrier frequency division multiplexing.
Broadband Access	NOMA-PON [221]	Downlink & Uplink	Single carrier transmission with NOMA and FD-SIC	✓	×	×	✓	×	×	Lower BER and PAPR is achieved.	Needs to be analyzed the throughput.
Effect of clipping	DCO-OFDM [223]	Downlink	Clipping process is proposed	×	×	×	×	✓	×	Enlarge the achievable rate region and provide unipolar signal.	Dynamic power allocation scheme is required.
Higher bandwidth	FTN-FrCT-NOFDM [224]	Downlink	Joint spectrum resource and subchannel transmission power allocation, and Sensing time selection	✓	×	×	×	×	×	Directly used in VLC systems without upconversion, cost sensitive, and save the limited bandwidth	An effective algorithm is required to mitigate the inter cluster interference.

Note- 1: Bit error rate (BER), 2: High Tolerance 3: Throughput, 4:PAPR, 5: Capacity 6: Spectral Efficiency
Notations- ✓: Yes,and ×: No

zooming technique was used, where transmitting angles of the LEDs are adjusted to control the size of cells. Also, adjusting the transmitting angles may affect the width and intensity of beams, resulting in the undesired illumination across the indoor space. So, to overcome this issue, a location-based user association strategy was used. Furthermore, GRPA FOV tuning can be used to decrease the number of handovers occurs in the system. These advantages show that GRPA is more suitable for 5G network as compared to the other one.

2.4.17 Millimeter Wave

The frequency range of Millimeter Wave (mmWave) in the electromagnetic spectrum is from 30-300GHz [225], [227] which shows that it provides a huge amount of bandwidth for 5G to handle the high data rate. In spite of its large bandwidth, it has some disadvantages like poor foliage penetration and free-space path loss [226], which degrades the QoS to the end-users in

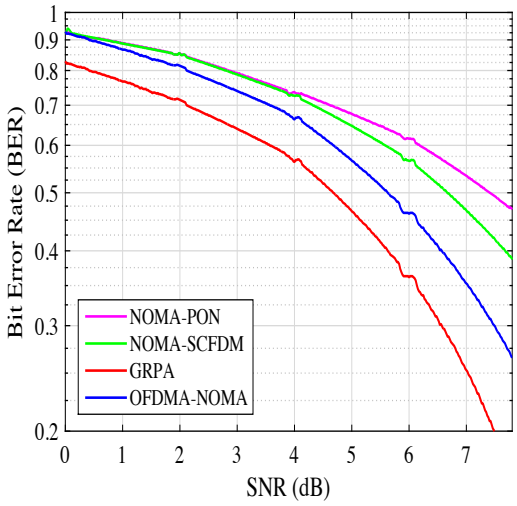

Figure 2.20: Discussion based on classification for VLC Communication

ultra-dense networks. To overcome these disadvantages of mmWave, various the authors integrated NOMA. When NOMA is integrated with mmWave then it provides the following benefits: (i) supports massive connectivity, (ii) amenable with mmWave correlated channels, (iii) increased the throughput due to reduction in inter-beam interference, (iv) reduced the hardware cost. By exploring these advantages, the authors provided the following variants of NOMA with mmWave.

2.4.17.1 Random-BF-NOMA [228]

In this, the authors studied the combination of mmWave with NOMA. In this scheme, the BS without knowing the CSI generates a single random beam for each user. Due to the presence of mmWave, the beam behaves like a directional antenna and users having low signal strength do not take part in the scheduling. As a result, the overhead of the system gets reduced. To analyze the performance of this technique, the authors used thinning scheme aided stochastic geometry model to study the blockage features of mmWave. Moreover, to reduce the system overhead, the authors' proposed two beamforming techniques (i) low feedback transmission scheme, and (ii) one-bit feedback scheme. In the first scheme, the BS already knows the users' distance, while in the second scheme, one user sends one bit as feedback to the BS. The authors also investigated the scenario of multiple beams generation from the BS, where the presence of mmWave suppressed the inter-beam interference. The numerical results showed that the proposed schemes outperformed the traditional mmWave-OMA schemes. In contrast to [228], the authors in [229] studied the user scheduling and power allocation algorithms for mmWave NOMA systems with random beamforming under partial CSI feedback. To achieve the suboptimal and low complexity solution, the authors used the matching theory for user scheduling and successive convex approximation for power allocation. In addition, the proposed mmWave

NOMA systems is capable of outperforming conventional mmWave orthogonal multiple access (OMA) systems in terms of sum rate and the number of served users.

2.4.17.2 FRAB-NOMA [230]

The authors studied the effect of combining NOMA with finite resolution analog beamforming (FRAB) technique. In this scheme, users' channel conditions do not match with each other. The authors proved that when NOMA exploited with FRAB, multiple users easily shared the single beam in an efficient manner and can communicate concurrently due to which the degree of freedom induced by mmWave decreases. The numerical results of FRAB with NOMA outperformed the conventional NOMA schemes.

2.4.17.3 Beamspace MIMO-NOMA [231]

This scheme was proposed to overcome the limitation of mmWave. In this scheme, the number of users who take part in the beamspace-MIMO scheme must be larger than the number of available resource blocks. The authors in [231] integrated NOMA with beamspace-MIMO to get the high spectrum and EE. So, to reduce the inter-beam interference, a precoding scheme based on the principle of zero-forcing was designed. Moreover, to allocate the power dynamically, they proposed a low complexity based iterative optimization algorithm to have a high sum rate.

2.4.17.4 EEPA-NOMA [232]

In this, the authors optimized the problem of EE in the mmWave-mMIMO-NOMA system. They integrated NOMA in this system to correlate the usersâĂŹ channel. To reduce the complexity of the hardware, the authors applied a low RF chain structure at the BS with the hybrid analog/digital precoding scheme. Firstly, paired users were formed in a cluster based on channel correlation and gain difference. Then, analog beamforming was applied in each cluster as per their codebooks. Also, to reduce the inter-cluster interference, the ZF precoding scheme was applied at the strong channel condition users. Moreover, the authors proposed an iterative power allocation algorithm per cluster to maximize the EE of the usersâĂŹ as per their QoS requirements. The numerical results show that the proposed scheme provides better EE as compared to OMA schemes.

2.4.17.5 HB-NOMA [233–236]

In the above-mentioned schemes, the authors combined NOMA with mmWave by using only baseband precoders/combiners. Also, the authors in [233] and [235] proposed hybrid beamforming (HB) in mmWave-NOMA systems. In [233], the authors studied the joint power allocation and beamforming scheme to maximize the sum rate of two-user mmWave NOMA

using an analog beamforming structure with the phased array. In [235], the authors analyzed that when HB is integrated with the mmWave-NOMA system, then digital precoders of the BS are not perfectly aligned with the user's effective channel. Based on the imperfect aligned beams, the authors in [235] also proposed a power allocation algorithm to maximize the sum rate of the system. But, they did not consider the effect of imperfect beamforming for analysis of the sum rate. Also, the authors in [236] provide the imperfect correlation in HB for multi-users. In this proposal, the authors first formulated the expressions of the sum rate for HB-NOMA and then proposed a sub-optimal algorithm to maximize it. Then, they derived a lower bound for the achievable rate by assuming that the angle between the highest channel gain MUs and the other MUs is non-zero. The results obtained show that the proposed scheme has a loss in terms of data rate due to inter-cluster interference between the MUs. In addition to [236], the authors in [234] studied the impact of imperfect correlation between the effective channels. They maximized the sum rate of the HB-NOMA system in three steps using power constraints. In the first step, they used analog precoders/combiner, and in the second step, digital precoders are used and at last a sub-optimal power allocation was introduced. Also, they proposed a lower bound for each user under perfect and imperfect correlation. The results obtained demonstrated that with perfect correlation the sum rate is equivalent to digital precoders while with imperfect correlation, it depends on the correlation factor. The obtained results show that the proposed scheme has an optimal sum rate as compared to conventional HB-OMA systems.

2.4.17.6 Cluster-based mmWave NOMA [237]

In this, the authors investigated the designs of user clustering and power allocation algorithms for mmWave-NOMA systems where the users follow a spatial clustering distribution model. Motivated by the combinatorial feature of NOMA, the authors proposed a machine-learning framework for effective user clustering in mmWave-NOMA systems. Channel correlations provides an efficient measurement that facilitates the implementation of K-means based clustering. Furthermore, for each cluster, the authors developed a closed form expression for the optimal power allocation, assuming that the power is equally allocated over each cluster. Simulation results revealed that the proposed K-means enabled machine-learning framework for mmWave-NOMA systems outperforms mmWave-OMA systems.

2.4.17.7 JA-STSK-NOMA [238]

In this, the authors studied the JA-STSK and JA-MS-STK schemes with NOMA to replace the STSK scheme in MC-IDMA and SC-IDMA, respectively. The objective of the proposed scheme was to acquire high throughput without high complexity. Also, the authors proved that when JA-STSK and JA-MS-STK schemes are integrated with fair algorithm, these have higher throughput as compared with the random selection algorithm. Moreover, they also demonstrated that when MC-IDMA is integrated with IRCC, then the proposed scheme provides an

increase in throughput with lesser in decoding complexity as compared to OMA. The results obtained show that this scheme provides a reduction in computational complexity with respect to CFRs and have a significant BER performance.

2.4.18 Heterogeneous Networks

Heterogeneous Networks (HetNets) in 5G is used to enhance the coverage and capacity for the users in an ultra-dense network [239], [240]. In these networks, low power BSs such as FBS and PBS are deployed under MBS. The presence of low power BSs near to the UE also improves EE due to less battery power consumption. But, the problem of co-channel and cross-channel are severe in these networks which in turn affects SE. To fully exploit the potential benefits of this network, the authors integrated NOMA with HetNets and proposed the following variants .

2.4.18.1 TIM-NOMA [241]

This is a hybrid scheme in which Topological Interference Management (TIM) and NOMA mitigate intercell interference and intra-cell interference, respectively, in a heterogeneous network [241]. It is applied to HetNets using user pairing and Kronecker Product representation. This scheme has twice the sum rate as compared to TDMA for high SNR values and also enhances the performance of cell-edges users of femtocells in terms of fair power allocation and QoS.

2.4.18.2 GFDM-NOMA [242]

It is a combination of generalised frequency division multiplexing (GFDM) and NOMA technique. GFDM is used to cover the OFDM and single carrier frequency domain while NOMA improves the system capacity by serving a large number of users from the same RB. The authors in [242] proposed a joint subchannel and power allocation scheme in this technique to handle two types of heterogeneous traffic, elastic and streaming. The main aim of this scheme was to maximize the weighted sum rate for elastic traffic users to minimize the sum rate for streaming users with subject to the constraint of subchannel and transmit power allocation. The numerical results demonstrated that the proposed scheme achieved approximately 31% enhancements in sum rate in comparison to OMA.

2.4.18.3 MBMS-NOMA [243]

In this, the authors explored how NOMA enhances the performance of a multimedia broadcast/multicast service (MBMS) system in HetNets. With this NOMA, two transmission techniques were studied, non-orthogonal multi-rate MBMS transmission (NOMRMT) and non-orthogonal multi-service MBMS transmission (NOMSMT). In this proposal, the authors pro-

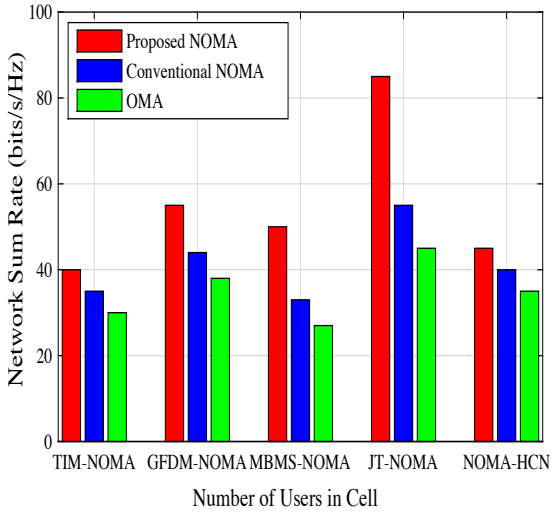

Figure 2.21: Discussion based on HetNets classification

posed stochastic geometry and developed a tractable model to analyze the performance by using synchronous and asynchronous transmissions. The numerical results demonstrated that the proposed MBMS-NOMA scheme outperformed the MBMS-OMA.

2.4.18.4 JT-NOMA [244]

The authors in [244] analysed the impact of power allocation to NOMA users in a multi-cell network. In JT-NOMA, all BSs in coordination with each other perform joint transmission for the remote users in a particular cell using the same RB. With this scheme, the SIC technique is not only used to separate the signals for remote users but is also helpful in decoding the signals for far users. In this way, it mitigates the inter-cell interference and enhances the performances of all NOMA users. The numerical results showed that this scheme enhances the coverage and throughput for each user in HetNets.

2.4.18.5 NOMA-HCN [245]

In this, the authors proposed HetNets, where the first tier consists of MBS and second-tier has various FBS using NOMA. With this scheme, the authors offload the traffic from MBS. The main aim of the authors was to enhance the fairness and performance gain of the users located at the edge of FBS cell by using CCUs. The numerical results showed that the proposed scheme provides an improvement in terms of ergodic rate and user fairness.

2.4.18.6 Discussion based on HetNets classification

Fig.2.21 represents the graph between the sum rate and number of users in the networks. The graph implies that JT-NOMA outperforms than the TIM-NOMA, GFDM-NOMA, MBMS-

NOMA, and NOMA-HCN. The happened because this scheme mitigate not only the inter cell co-channel interference but also overcome the problem arise from the channel fading. Furthermore, in this scheme, all void BSs can do joint transmission to enhance the signal power of the farthest user in a cell, which improves the throughput of the users in dense network with a moderate user intensity. It shows that JT-NOMA is suitable for 5G network as compared to the rest of the HetNets classification.

2.4.19 Vehicle-to-Everything

Vehicle-to-Everything (V2X) communication is a newly emerging technology in 5G which is used to provide improved user's travel experience along with security, safety and internet access services [246], [247], [248]. In spite of these advantages, energy-saving, low latency, and faster packet transmission and reception in an ultra-dense network of V2X are the issues which are required to be addressed. To resolve these issues, the authors integrated NOMA with this technique. When NOMA is integrated with V2X, then it resolved the problem of data congestion by accessing the channel non-orthogonally [249], [250] and provides following benefits (i) reduction of the transmission latency, (ii) support for massive connectivity and (iii) enhanced SE and EE. But, the problems of improvement in link reliability, enhancement of bandwidth efficiency and reduction in collision still need to be resolved. So, following variants of NOMA in V2X communication are proposed.

2.4.19.1 NOMA-SM [251]

To improve the link reliability and to fulfil the high bandwidth requirements for V2V communication, the authors in [251] used NOMA with SM and massive TA. But, still, there are many challenges which need to be resolved. For example, the authors in [251] proposed a new NOMA-SM scheme for V2V scenario with correlated Rician channel, and analytically derived the ergodic capacity of NOMA-SM by using Monte Carlo simulation. The results obtained show that the proposed NOMA-SM scheme provides an improvement in robustness against the spatial and temporal effects of the V2V channel. Moreover, a power allocation algorithm was proposed to satisfy the QoS of low priority flow and to maximize the throughput of high priority flow.

2.4.19.2 NOMA-MCD [252]

In this, the authors amalgamate NOMA with the mixed centralized/distributed (MCD) scheme. The main aim of this scheme was to provide decreased access collision along with the increase in reliability of the network. In this scheme, time and frequency resources were used by the BS in a non-orthogonal manner whereas, dynamic power control along with the iterative control signalling was used by the vehicles to achieve better performance. Also, the

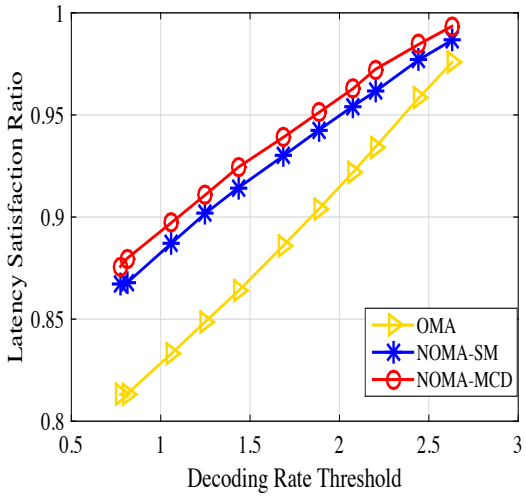

Figure 2.22: Discussion based on classification of V2X

authors studied the scheduling and resource allocation problem in a cellular V2X broadcasting system. To resolve this, they used two multi-dimensional stable roommates (MD-SR) schemes. Then, the authors proposed a novel rotation matching algorithm. The numerical results show that the NOMA-MCD scheme reduces the latency and enhances the packet reception reliability in comparison to OMA based V2X schemes.

Table 2.14: Relative comparison of existing NOMA schemes based on V2X

Problem **in M2M**	NOMA **variants**	Channel **fading**	**Techniques**	**Performance metrics**			**Merits**
				1	**2**	**3**	
Inter antenna interference (IAI) and Doppler and fading effects	NOMA-SM [251]	Rician channel fading	Distributed power allocation	✓	×	×	Improved the link reliability and bandwidth efficiency of V2V transmissions, eliminates the IAI, and reduces the transmission latency.
Scheduling and resource allocation	NOMA-MCD [252]	Rayleigh channel fading	Rotation matching algorithm for sub-channel allocation and Tx-Rx selection and time slot allocation algorithm	×	✓	✓	Reduces the access latency, improves the packet reception probability, and reduces the access collision

Note- 1: BER, 2: Packet reception reliability, 3: Latency
Notations- ✓: Yes, and ×:No

2.4.19.3 Comparison of existing NOMA schemes based on V2X

Table 2.14 provides a detailed relative comparison of existing variants of NOMA used in V2X using parameters channel fading, technique used, merits, bit error rate, latency, and packet reception reliability.

2.4.19.4 Discussion based on Classification of V2X

Fig.2.22 shows the effect on latency with respect to the decoding rate threshold. The graph implies that NOMA-MCD performs better than NOMA-SM and OMA with an increase in decoding rate. This happened because NOMA-MCD reduced the packet collision up to a larger extent in comparison to the NOMA-SM and OMA schemes. This reason makes NOMA-MCD to be more suitable for 5G networks.

2.4.20 User pairing and power allocation variants

2.4.20.1 2D-NOMA [253]

It consists of both power and code domain NOMA techniques [253]. The power domain NOMA produces multi-level modulation while code domain generates sparse spreading code words. It was used to reduce the inter-user interference and to increase the Euclidean distance of superimposed signals. To reduce the effect of deep fading, quadrature components of multiple sparse code multiple access (SCMA) code-words were interleaved before the transmission. At the same time, according to the quality of the channels, the window size of interleaving can be adjusted. For this scheme, mixed integer optimization technique was formulated to enhance its data rate. The mixed integer optimization consists of power allocation, power splitting and codebook assignment. The simulated results show that this scheme outperformed its counterparts in terms of data rate.

2.4.20.2 Ashynchronous NOMA (ANOMA) [254]

In this, the authors proposed this scheme to mitigate mutual interference between users by applying different artificial symbol-offset between packets. Also, to simplify the signal detection, a precoding technique at the BS and a whitening-and-decomposing (WD) detection technique along with SIC applied at the receiver's side. The proposed scheme investigated at both the Rayleigh and Gaussian fading distributions. The numerical results showed that ANOMA outperformed synchronous NOMA (SNOMA).

2.4.20.3 NOMA CAP [255]

The authors in this integrated NOMA with multiband carrierless amplitude phase modulation (multiCAP) scheme to improve the netwrok capacity. The objective the scheme was to provide the dynamic resource allocation to fulfill the data rate requirements of users in an ultra-dense network. The authors experimentally demonstrated that the proposed scheme over a W-band mmWave and fibre system, by assuming six 1.25GHz multi-bands and two NOMA levels with quadrature phase shift keying. The numerical results showed that in a highly dense network, the proposed scheme provides an aggregated transmission rate of 30Gbps.

2.4.20.4 NOMA-multicast (MC) [256]

The authors proposed a scheme to mitigate the problem of content caching, where extra radio resource blocks are occupied to push the content objects to the edge devices to optimize the spectrum efficiency. With this scheme, both the multicasting and content pushing phases can be performed simultaneously. Authors in this scheme first studied the single cell scenario and then extend it to the multi-cell by using stochastic geometry to have an optimal outage probability. Moreover, to enlarge the performance gain of the proposed scheme, they proposed a joint power allocation and content matching design. Also, they proposed two distributed optimization algorithms based on Galey-Shapley matching technique.

2.4.20.5 Virtual pairing (VP)-NOMA [257]

The authors introduced a virtual user pairing scheme. In this scheme, similar channel gain CCUs form a pair with the single CEU to enhance the SE of the system. In contrast to [257], the authors in [258] and [259] also proposed a user pairing scheme on behalf of channel gain difference in between the FUs. They also proposed even and odd number of FUs in a femtocells.

2.4.20.6 TS-NOMA [260]

In [260], the authors proposed a variant of NOMA to investigate a time sharing (TS) based user pairing strategy to accommodate similar gain user. This NOMA variant reduces the computational complexity issue of VP-NOMA. With this scheme, one cell center user forms a pair with two or more CEUs in a time sharing manner. The numerical results showed that it outperformed C-NOMA and OMA with respect to ergodic sum capacity.

2.4.20.7 Dynamic Hybrid (DH)-NOMA [261]

It is a dynamic power allocation scheme for hybrid NOMA, applied when channel gain of strong users becomes worst with respect to threshold value for weak users [261]. When this condition occurs then conventional OMA scheme is used to serve the users otherwise, NOMA is used. The numerical results showed that this scheme provides better trade-offs between two user individual rates in comparison to F-NOMA and CR-NOMA. A better outage performance is achieved in comparison to OMA using the outage probability.

2.4.20.8 FAIR-NOMA [262]

It is a fair power allocation scheme applied for two users in a downlink NOMA transmission scenario [262]. The main aim of the scheme was to achieve a guaranteed capacity for users in OMA. Moreover, this scheme does not require any CSI like other NOMA techniques which results in high performance gain. The numerical results showed that FAIR-NOMA enhanced the sum capacity of the network and capacity of users in comparison to the OMA.

2.4.20.9 Distributed base station (DBS)-NOMA [263]

It is a distributed power allocation scheme designed to minimize the total power transmission in each cell by using various resource allocation techniques [263]. Different from the other NOMA techniques, in this scheme, SIC decoding technique is applied at both paired UE sides. Moreover, the authors also proposed mutual SIC technique with suboptimal power adjustment to provide better trade-offs between complexities and transmit power.

2.4.20.10 Wavelet NOMA (W-NOMA) [264]

The authors integrated NOMA with wavelet OFDM. They proposed this scheme to mitigate the interference, to improve the bandwidth, and to enhance the MU capacity. Also, they proposed a dual PHY layer transceiver for WOFDM based pulse shaping methods to reduce the latency. The performance of the scheme was analyzed using BER. The numerical results showed that the proposed scheme is compatible with 4G networks and provides the improved robustness, higher SE, and lower PAPR in comparison to the conventional NOMA but at the cost of increased hardware complexity.

2.4.20.11 Contention-based NOMA

Contention based uplink (CB UL) access is an effective technique which was designed to reduce the access latency and uplink access signaling overhead as compared to conventional dedicated scheduling request (DSR) technique. This technique is effective under low traffic load but it was found that when traffic load increases then the performance of this technique is degraded due to an increase in collisions. To overcome this issue, the authors in [265] integrated NOMA with contention based uplink transmissions. NOMA with CB UL reduces the bad collisions and enables the good collisions without knowing which UEs will conduct the CB UL transmissions. In this way, NOMA enhances the performance of the CB UL transmission and reduces the latency. Moreover, the authors also proposed two effective algorithms for user pairing between the downlink SNR information at UE and scheduling information at evolved-Node-B (eNodeB). The numerical results showed that this scheme reduces the latency and improves the SE network.

2.5 Code domain NOMA (CD-NOMA)

CD-NOMA is a technique in which user specific spreading sequences are used to multiplex the signals at the transmitter side. The main advantages of this technique are: (i) low-density, (ii) low inter-correlation, and (iii) support grant free access. CD-NOMA is an advanced version of CDMA which was proposed in 90's. With respect to CDMA, in CD-NOMA receiver's has to detect the active codes of the receivers and has to estimate their data. In CD-NOMA,

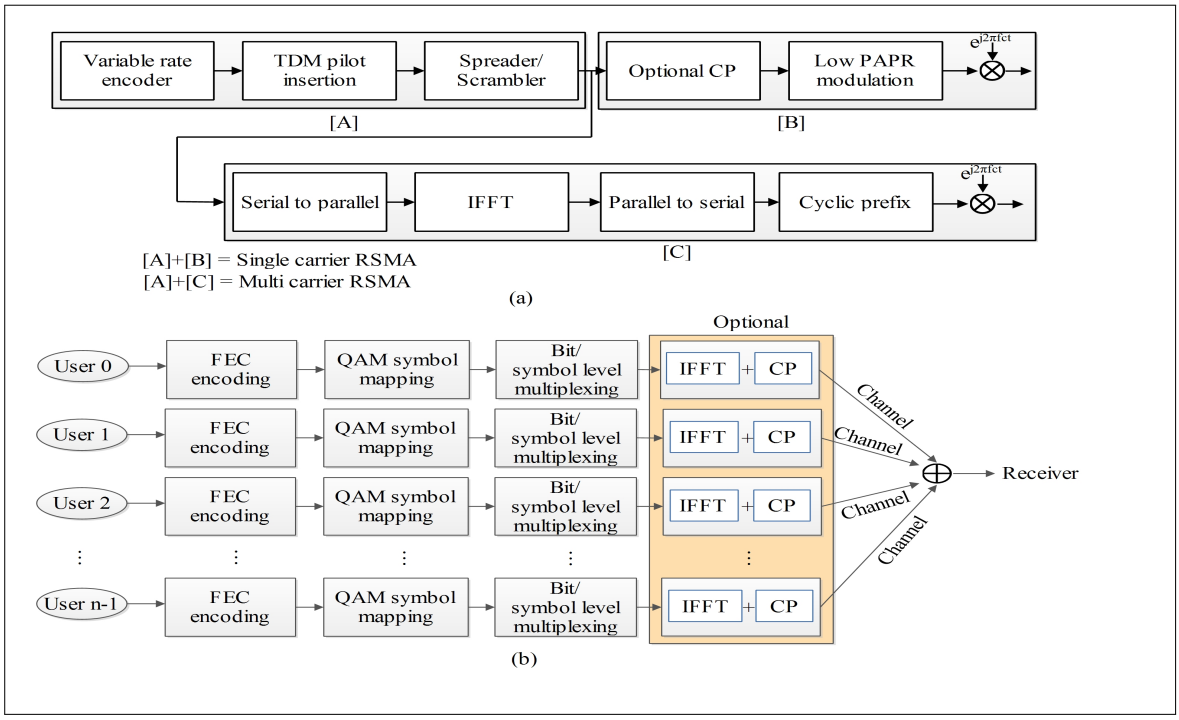

Figure 2.23: Block diagram of (a) Resource spread multiple access (RSMA), and (b) Low code rate and signature based shared access (LSSA)

compressive sensing (CS), Gaussian random, and sparse codes are the backbone of this technique. It has five variants: (i) Scrambling-based NOMA, (ii) Interleaving-based NOMA, (iii) Spreading-based NOMA, (iv) Coding-based NOMA, and (v) Lattice and Beam based NOMA. The detailed description of each variant is is shown in Fig. 2.24, and discussed in the following sections.

2.5.1 Scrambling based NOMA

Scrambling based NOMA has types: Low code rate and signature based shared access (LSSA) and Resource spread multiple access (RSMA). RSMA was designed by Qualcomm, whereas LSSA was designed by ETRI. The block diagrams of RSMA and LSSA are shown in Fig. 2.23. In these schemes, different scrambling structures and low rate channel coding are used for each user. Both are long sequence and bit level based NOMA, respectively. In RSMA, the long sequence of user signature are used which results into high latency and decoding complexity at the receiver side. These issues can be resolved using the LSSA scheme, where the length of the user signature is reduced. To separate the user's signatures at the receiver side, the elementary signal estimator (ESE) and minimum mean square error with successive interference cancellation (MMSE-SIC) were used [266]. The detailed description of RSMA and LSSA is as follows:

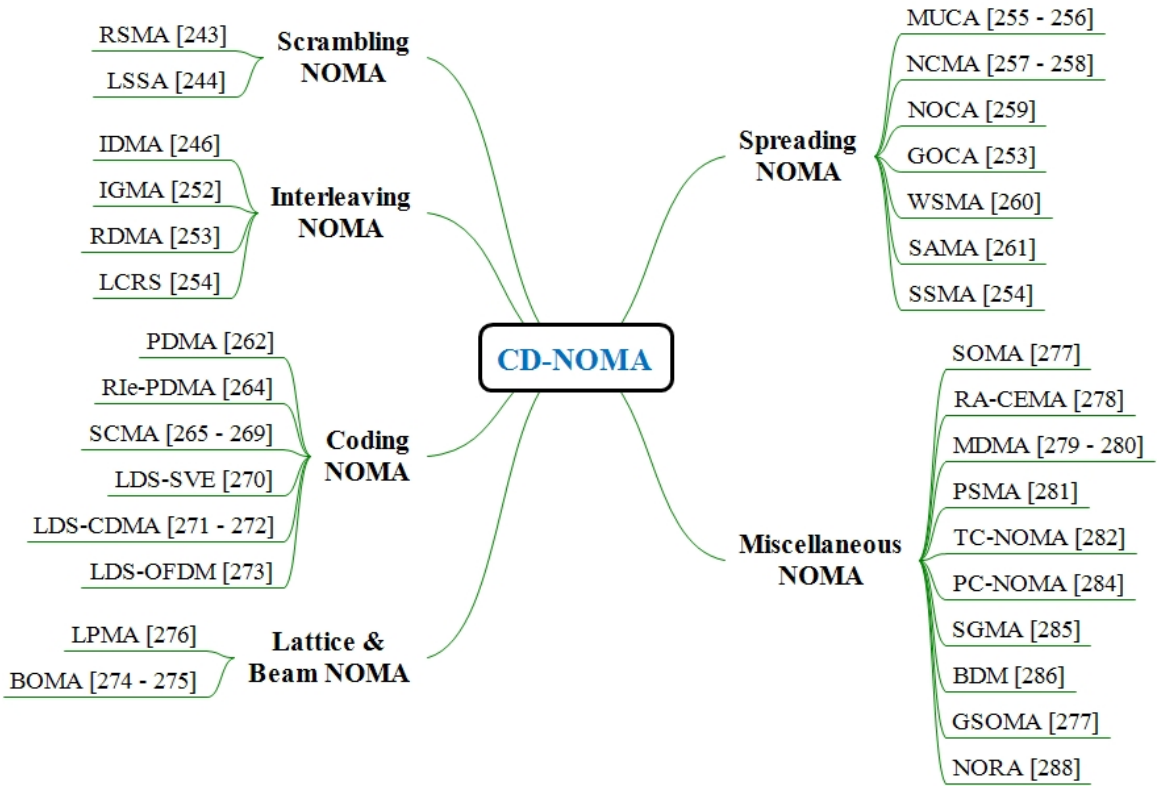

Figure 2.24: Detailed taxonomy of CD-NOMA variants

2.5.1.1 Resource spread multiple access

It uses long spreading or scrambling sequence, where sequences of each user are broadcasted in the form of signals over the available bandwidth. As a result, full diversity and low forward-error-correction (FEC) are achieved. To separate the signals of different users at the receiver side, different scrambling or sequences are used. In this scheme, every user transmit their data at any time. To reduce the multi user interference (MUI), scramblers can be replaced by different interleavers. As per the requirements of an applications, it is categorized into two types: single carrier (SC) and multi carrier (MC) RSMA [267] each of which is described as follows.

(a) *Single carrier resource spread multiple access:* It is suitable for the uplink scenario to reduce the peak-to-average-power ratio (PAPR). In this technique, a single carrier modulation is used to extend the coverage of transmitting data and to reduce the UEs battery power consumption. To separate the signals of SC-RSMA, the matched filter is used at the receiver side. Moreover, it supports grant free and asynchronous transmission to reduce the signalling overhead because it does not depend upon joint detection and synchronization requirements.

(b) *Multi carrier resource spread multiple access:* It is suitable for the downlink scenario and is used to reduce the complexity of the receiver. In this technique, data is splited into multiple layers (virtual layers) for each user which reduces the latency and increases the SE. Its

complexity is higher than SC-RSMA.

2.5.1.2 Low code rate and signature based shared access

It is suitable for asynchronous uplink transmission [268], where each user's signal is encoded by a low rate channel encoder. Then, the user specific signature is multiplexed with the output of channel encoder to mitigate the MUI. To achieve it, the vector length of each user signature pattern is the same and should be unknown to other users. In this technique, the BS separates the signals of different user's by correlating them with the user's specific signature patterns even though the transmission time for each user is different. Moreover, it supports multi-carrier variant to fully exploit the frequency diversity, resulting into a large bandwidth and lower latency.

2.5.2 Interleaving-based NOMA

It consists of four types of NOMA schemes, interleave division multiple access (IDMA), interleave-grid multiple access (IGMA), repetition division multiple access (RDMA), and low code rate spreading (LCRS). IGMA is designed by Samsung, IDMA by Nokia, RDMA by Mediatek, and LCRS by Intel, respectively. Common features of these schemes are: (i) different channel inter leavers are used for overlapped multiple users, and (ii) a low-rate channel coding for multi-user decoding. Detailed description of these schemes is as follow.

2.5.2.1 Interleave division multiple access

In this scheme, user's signals are separated from each other by using different interleaving patterns. The structure of IDMA is as shown in Fig. 2.25. This scheme was first investigated by Li *et al.* [269] to improve the performance of asynchronous CDMA. Similar to CDMA, it also reduces the effect of fading and ICI. In comparison to CDMA, it achieved a $\frac{E_b}{N_o}$ gain of 1dB at a BER of 10^{-3} in highly loaded systems having a normalized user-load of 200% [270]. In contrast to [269], the authors in [271] explored more features of IDMA such as EE, frequency diversity, and rate adaption. In [272], the authors investigated that the IDMA achieved the capacity equals to Gaussian MAC when an iterative decoding strategy was used with an interleaved low-rate codes. In [273], the authors proposed a user specific interleaver designed to solve the problem of memory cost and also reduces the signalling overhead between the BS and users. In [274], the authors explored the additional features like robustness and user overload tolerance. Moreover, the authors in [275], discussed the concept of IDMA in both single path and multipath fading channels, which provides a large diversity gain as compared to bit-interleaving scheme.

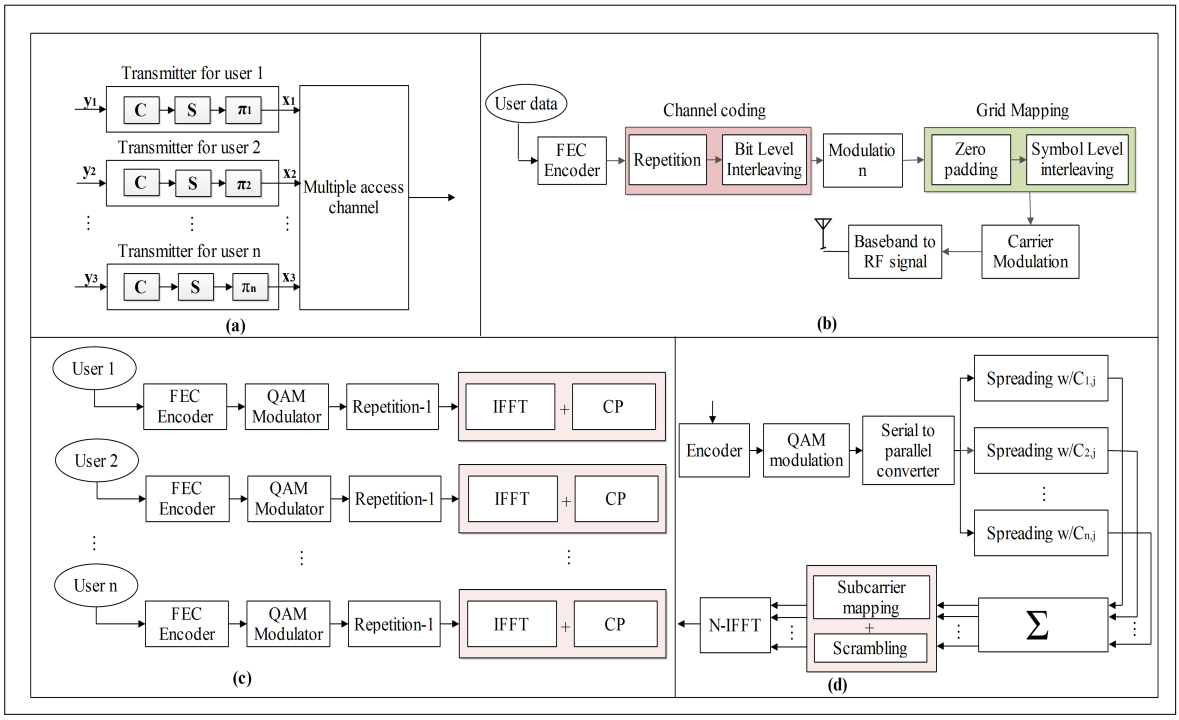

Figure 2.25: Interleaving-based NOMA schemes for (a) IDMA, (b) IGMA, (c) RDMA, and (d) LCRS

2.5.2.2 Interleave-grid multiple access

The structure of IGMA is as shown in Fig. 2.25, where at the transmitter side, bit-level repetition, channel encoding, zero-padding, modulation, bit-level interleaving, and symbol level interleaving are used sequentially by each user. In this technique, sparse grid mapping patterns, bit level interleavers, and the mixture of both were used to separate the signals streams of various users. Bit level interleavers/grid mapping patterns support different connection density patterns. It creates a trade-off between sparse resource mapping and the channel coding gain. The presence of sparse grid mapping patterns reduces the detection complexity and symbol-level collisions with respect to IDMA [276]. Finally, the symbol level interleaving in IGMA, randomizes the symbol sequence order which helps to combat the frequency selectivity and ICI.

2.5.2.3 Repetition division multiple access

It is a special type of cyclic interleaving scheme [277] in which the symbol-level interleaving scheme, is used instead of bit-level interleaving. In this scheme, a different user's signals are distinguished from each other by using cyclic-shift repetition pattern which provides a complete randomized MUI along with time and frequency diversities. The transmission structure of IDMA is as shown Fig. 2.25. Its structure is simpler in comparison to IDMA and RSMA,

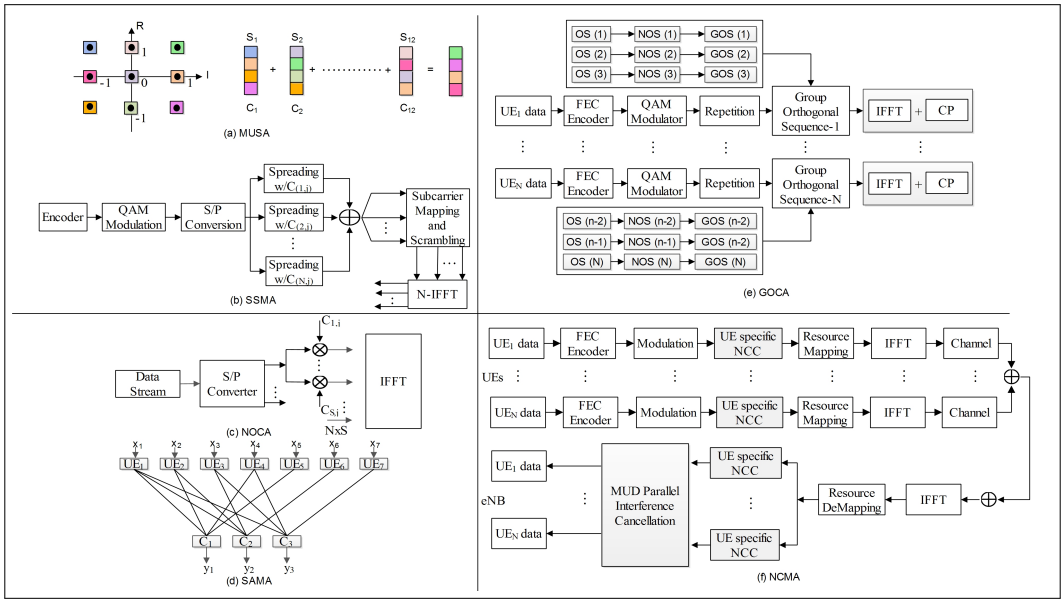

Figure 2.26: Structure of: (a) MUSA, (b) SSMA, (c) NOCA, (d) SAMA, (e) GOCA, and (f) NCMA

and it provides low signalling overhead due to the absence of user-specific scrambling and interleaving patterns. Moreover, a SIC technique is employed at the receiver side to separate the each user's data from the superimposed signal.

2.5.2.4 Low code rate spreading

In this scheme, data bits are transmitted over the entire non-orthogonal transmission area by using low-rate coding and bit-level repetition [278]. It provides the maximum coding gain, where MMSE-SIC is used at the receiver side to detect the multiuser signal [269].

2.5.3 Spreading-based NOMA

Spreading-based NOMA is categorized in to seven different types such as multi-user shared access (MUSA), non-orthogonal coded multiple access (NCMA), non-orthogonal coded access (NOCA), group orthogonal coded access (GOCA), welch-bound spreading multiple access (WSMA), successive interference cancellation amenable access (SAMA), and sequence spreading multiple access (SSMA). The detail description of all these techniques is described as follows.

2.5.3.1 MUSA

It supports low cross correlation-based short complex spreading sequences such as spreading sequences are non-sparse in nature to reduce the interferences. An example of MUSA with

its complex sequences is as shown in Fig. 2.26 (a). At the transmitter side, after encoding and modulation, the modulated symbols of each user are spread by using the property of complex sequences $\{-1, 0, +1\}$. Then, these spreading sequences are passed through the same radio resources. On the other hand, at the receiver side, SIC is used which separates the superimposed multiuser signals [279], [280]. In this scheme, each user randomly selects one spreading sequence form a sequence pool consists of multiple spreading sequences. Then, each user uses a different spreading sequence for different symbols, to mitigate the average MUI and to enhance the performance level of the system. The advantages of MUSA are as follows (i) suitable for mMTC because it supports grant-free transmission, (ii) Less collisions due to same spreading sequences, (iii) User detection can be carried out without the knowledge of spreading code, and (iv) It can handle 700% user overload on multipath fading channel due to high-frequency diversity.

2.5.3.2 NCMA

It uses dense spreading sequences similar to MUSA, but its main goal was to minimize the MUI and to handle the high overloading capacity [281]. In this technique, spreading sequences are obtained by solving the Grassmannian line packing problem to maximize the minimum chordal distance between spreading codes. The spreading sequences of NCMA are known as non-orthogonal cover codes (NCC) which are found to be suitable to predict the interference level [282]. The structure of NCMA is as shown in Fig. 2.26 (f). At the transmitter side, the modulated symbols are spread by using the NCC. Also, to reduce the PAPR, an additional FFT operation is performed before the IFFT. On the other hand, a PIC detector is used at the receiver's side to decode the superimposed signals. Advantages of NCMA are: (i) Improved throughput and (ii) enhanced connectivity with a small loss of block error rate (BLER).

2.5.3.3 NOCA

It used the property of low cross-correlation which operates in both time and frequency domain. In this scheme, before transmitting a sequence, its modulated symbols are spread according to the non-orthogonal sequences [283]. Its spreading sequences are the reference signals defined in LTE which are generated by the cyclic shifts of a bases sequence. The minimum spreading factor of NOCA is taken as 6. In this technique, first of all, a modulated symbol is converted into a parallel subsequence using an S/P converter. Then, each subsequence is spread by non-orthogonal sequences and then mapped onto different sub-carriers. Then, at the receiver side, the minimum mean square error with parallel interference cancellation (MMSE-PIC) is used to separate each user's signal. It is used to mitigate the inter-cell interference because it supports a large number of spreading sequences and can also handle high overload easily as shown in Fig. 2.26 (c).

2.5.3.4 GOCA

It is an updated version of RDMA [277], in which modulated symbols are spread using a group orthogonal sequences into shared time and frequency resources after repetitions. The structure of GOCA is as shown in Fig. 2.26 (e). Moreover, it uses a two-stage method to produce grouped orthogonal sequences which are used in the first stage, whereas non-orthogonal sequences in the second stage. Its spreading sequences are suitable for a group of multiple users. It uses an MMSE-SIC to decode the user's signal.

2.5.3.5 WSMA

Its spreading sequence was based on Welch bound which reduces the cross-correlation of spreading sequences [284]. In this technique, the MMSE-SIC technique is used at the receiver side to decode the user's signals. Moreover, its spreading sequence has a low cross-correlation as compared to the spreading sequences of MUSA.

2.5.3.6 SAMA

This scheme is a combination of signature matrix and SIC based iterative message-passing algorithm [285]. The structure of SAMA is as shown in Fig. 2.26 (d). In this technique, the symbols of each user are designed based on their diversity orders in the frequency domain. The SIC based iterative message-passing algorithm eliminates the MUI and enhances the diversity gain and transmission rate for multi-users. Let us consider an uplink scenario consists of N users and J orthogonal OFDM subchannels. Its model is based on MUSA, but in SAMA spreading sequences for users are equal to one. The spreading matrix in SAMA is represented as $S = \{s_1, s_2, .s_N\}$. The advantages SAMA matrix are (i) maximizes those number of groups which are having a different number of $1's$ in their spreading sequences, and (ii) it minimizes the number of the overlapped spreading sequences which are having the same number of $1's$ in their sequences. The number of users based on N orthogonal subchannels is given as follows.

$$\binom{J}{1} + \binom{J}{2} + .. + \binom{J}{J} = 2^J - 1. \tag{2.11}$$

If J=2 and K=3, then spreading matrix can be calculated as follows:

$$S_{2,3} = \begin{pmatrix} 1 & 1 & 0 \\ 1 & 0 & 1 \end{pmatrix}$$

2.5.3.7 SSMA

It is a short sequence spreading multiple access technique which directly spreads the modulated symbols with multiple orthogonal codes. Then, it transmits the spread symbols in time-frequency resources allocation for non-orthogonal transmission [278]. Its structure is as shown

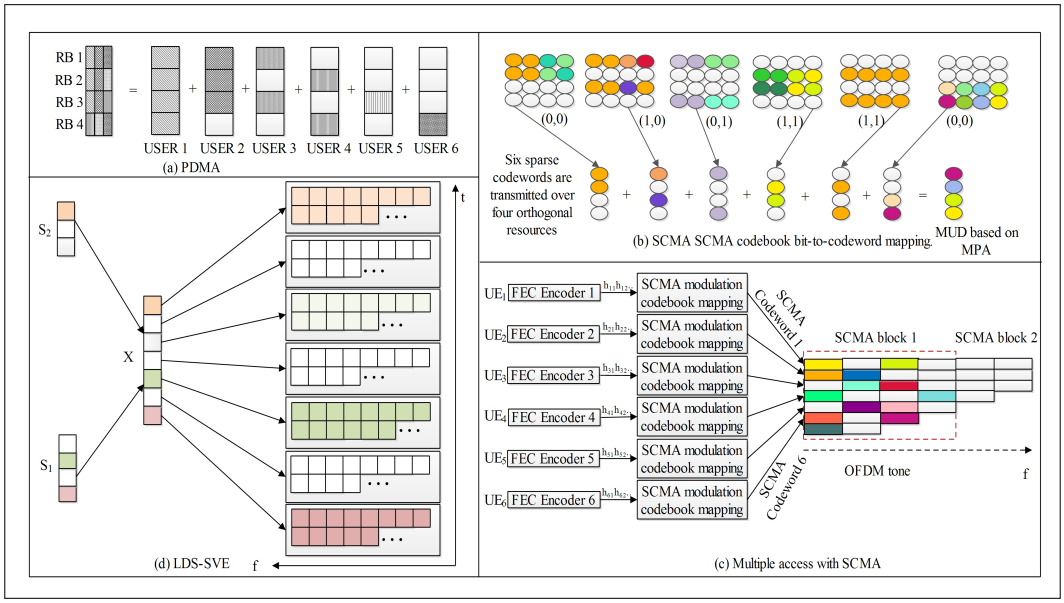

Figure 2.27: Transceiver block diagram for (a) PDMA (b) Bit-to-codeword mapping in SCMA (c) Multiple access with SCMA, and (d) LDS-SVE

in Fig. 2.26 (b). It behaves like NOCA when the user-specific sequences are used to decrease the MUI..

2.5.4 Coding-based NOMA

It consists of PDMA, SCMA, and LDS-SVE which are designed by CATT, Huawei, and Fujitsu, respectively. The transceiver block diagrams of these schemes are shown in the structure of GOCA is shown in Fig. 2.27. It is used to design a sparse codebook overlapped in the multiple (space, code, time or frequency) domains for the multiple users. In all these schemes, a message-passing algorithm (MPA) was used at the receiver side for MUD. These schemes have high complexity which varies exponentially with the size of the codebook. To reduce the complexity from exponential to linear, a novel expectation propagation algorithm (EPA) was proposed in [49]. This algorithm is based on an approximate interference method and was mostly used in machine and deep learning era.

2.5.4.1 PDMA

It is an MC-NOMA scheme based on SAMA technique [285]. This technique utilizes the resources in the multiple domains consists of power/code/spatial or their combinations. In this technique, user signals can be multiplexed into different subcarriers which increases the number of accessed users. It supports unequal diversity at the transmitter side, but equal diversity at the receiver side. In PDMA, at the transmitter side, non-orthogonal patterns are used to maximize the diversity to minimize the correlations among the users, whereas, at the receiver side, SIC is

used to decode the irregular sparse signatures [286]. An example of PDMA which consists of six users and four subcarriers is shown as follows:

$$G_{PDMA} = \begin{bmatrix} 1 & 1 & 1 & 0 & 0 & 0 \\ 1 & 1 & 0 & 1 & 0 & 0 \\ 1 & 1 & 1 & 0 & 1 & 0 \\ 1 & 0 & 0 & 1 & 0 & 1 \end{bmatrix}$$

where 1 represents that the subcarrier is occupied by a users. PDMA cannot ensures strict sparsity constraints. In downlink PDMA, the signal received at the i^{th} user through all the subcarriers is represented by follows:

$$y_i = diag(g_i)G_{PDMA}x + n_i. \tag{2.12}$$

In uplink NOMA, the signal received at the b^{th} BS is represented as follows:

$$y_b = (g_b \odot G_{PDMA})x + n_b, \tag{2.13}$$

where $x = [x_1, x_2, x_3, ..., x_I]^T$, n=$[n_1, n_2, n_3, ..., n_I]$ represents the noise and g_i and g_b represents the channel gain between the BS and i^{th} user and channel gain between the all the users and uplink, respectively. The numerical results of [287] show that PDMA in an uplink and downlink scenario achieved a normalized throughput of 200% and 50%, respectively as compared to LTE.

2.5.4.2 RIePDMA

It is a random interleaved enhanced PDMA scheme used to provide the massive connectivity [288]. It is designed by inserting interleavers between the PDMA encoder and the channel encoder. The random interleaver in RIePDMA reduces the two effects of a channel: (i) fading effect and (ii) interference-effect. During the mitigation, RIePDMA does not disturb the order of encoded bits. It enhances the performance of the network as compared to PDMA to support massive connectivity.

2.5.4.3 SCMA

It was proposed by Nikopour *et al.* [289] to decrease the complexity of receiver and to improve the reliability in high overhead conditions [290] [291]. It uses the coded bits to multidimensional modulation symbols, as per predefined sparse codebook [292], rather than sequentially conducting modulation and low density spreading. The authors in [293] proposed that to perform multiplexing in SCMA, both the multidimensional constellation and resource element mapping are essential. The transmission process of SCMA is as shown in Fig. 2.27 (b). In [292], the authors proposed a new codebook design for SCMA based on rotation, shuf-

fling, and permutation. The SCMA also can provide the large performance gain by allowing the pairing among symbols located in multiple radio resources is as shown in Fig. 2.27 (b). In this scheme, the message passing algorithm (MPA) is used at the receiver side to detects the multiple data streams in the form of symbol-level. The example of the SCMA matrix is given as follows:

$$G_{SCMA} = \begin{bmatrix} 1 & 1 & 1 & 0 & 0 & 0 \\ 1 & 0 & 0 & 1 & 1 & 0 \\ 0 & 1 & 0 & 1 & 0 & 1 \\ 0 & 0 & 1 & 0 & 1 & 1 \end{bmatrix}$$

In SCMA, at the receiver side, MPA enlarges the computational burden when the number of multiplexed users are more. To handle the computational complexity of the receiver two technique are used (i) the sparseness level of SCMA code-words and (ii) the use of multidimensional constellations with a low number of projection points per dimension. SCMA is a multiple access that promises some significant advantages such as-to support large levels of connectivity, provides reduced transmission latency, and it is also able to provide energy saving. Block diagrams of SCMA with multiple access are shown in Fig. 2.27 (c).

2.5.4.4 LDS-SVE

It is an extension of LDS and is designed to produce a large user signature vector [294], where several element signature vectors are transformed and concatenated into a large signature vector. It applies the user signature vector over the RBs to use the time and frequency diversity on the basis of their channel conditions as shown in Fig. 2.27 (d).

2.5.4.5 LDS-CDMA

It is an advanced version of CDMA and is based on low density parity-check (LDPC) codes [295], [296]. In this scheme, orthogonal variable spreading factor (OVSF) codes are used, whereas in conventional CDMA, dense spreading sequences are used to eliminate the interference. To achieve the performance equivalent to maximum-likelihood (ML) detection, a MPA is used at the receiver side to demultiplex the signals.

2.5.4.6 LDS-OFDM

It is a mixture of LDS-CDMA and OFDM to support multiple carrier scenarios [297]. Similar to LDS-CDMA, in this scheme, a sparse coding sequences are implemented at the transmitters side and MPA detection at the receivers side. In this technique, the data stream mapping consists of two steps. In the first step, data bits are spreaded by using low density spreading techniques and in the second step, each bit of data streams is transmitted over different subchannels using OFDM modulator.

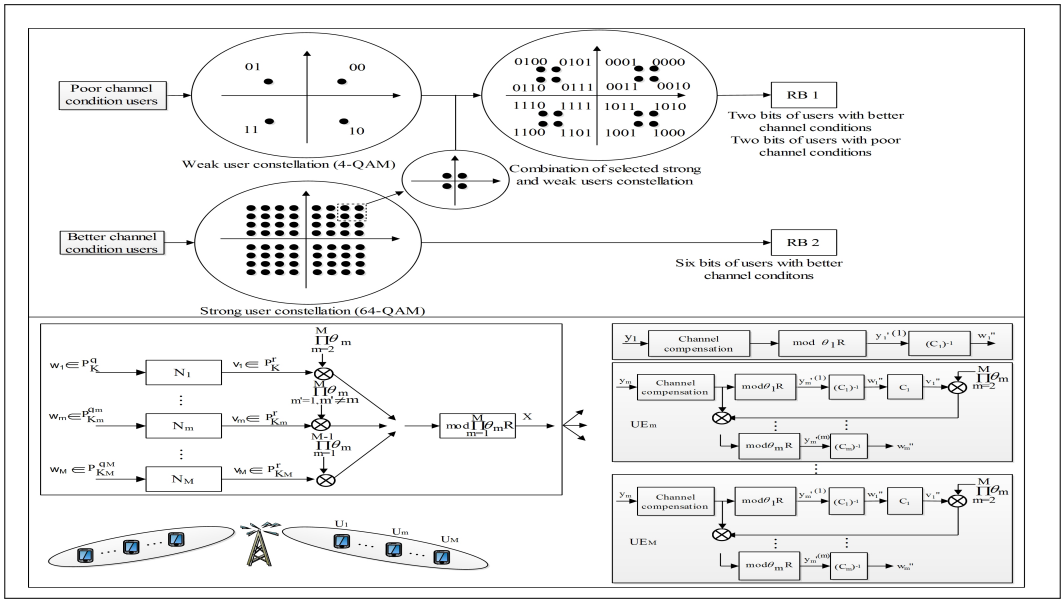

Figure 2.28: Block diagram of Lattice and Beam-based NOMA for (a) BOMA, and (b) LPMA

2.5.5 Lattice and Beam-based NOMA

When the users have similar channel conditions, the performance of NOMA degrade with respect to the OMA. To address this problem, researchers proposed the geometrical separation technique in between the users during superposition transmissions. This technique uses beams to form a cluster among the users having different channel conditions. Despite the advantage, this technique does not cope up when the user density and traffic demand increases due to the following reasons: (i) complexity increases, and (ii) co-channel interference arises in between the users of neighboring clusters. To overcome this issue, a new multiple access technique LPMA is introduced. On the other side, BOMA is a technique in which separate tiled building blocks are used for the poor CSI users with respect to the good CSI users. In this way, this technique improves the BER performance of poor CSI users.

The detail description of both these techniques is described as follows.

2.5.5.1 BOMA

It multiplexes the user signals of perfect CSI with the imperfect CSI to improve their capacity, as shown in Fig. 2.28 (a). In this scheme, the imperfect CSI achieves the BER performance similar to the perfect CSI by using a minimum Euclidean distance. In this, the building blocks of perfect CSI users are used with the constellation of imperfect CSI users to attain a similar BER [298], [299]. In the case of imperfect CSI user, the constellation point is the center of the building block and tiled building block can be treated as interference. Moreover, as the size of the building block gets decreases then the performance to detect the degradation becomes minimum. This scheme is suitable for massive MIMO technique and high-frequency

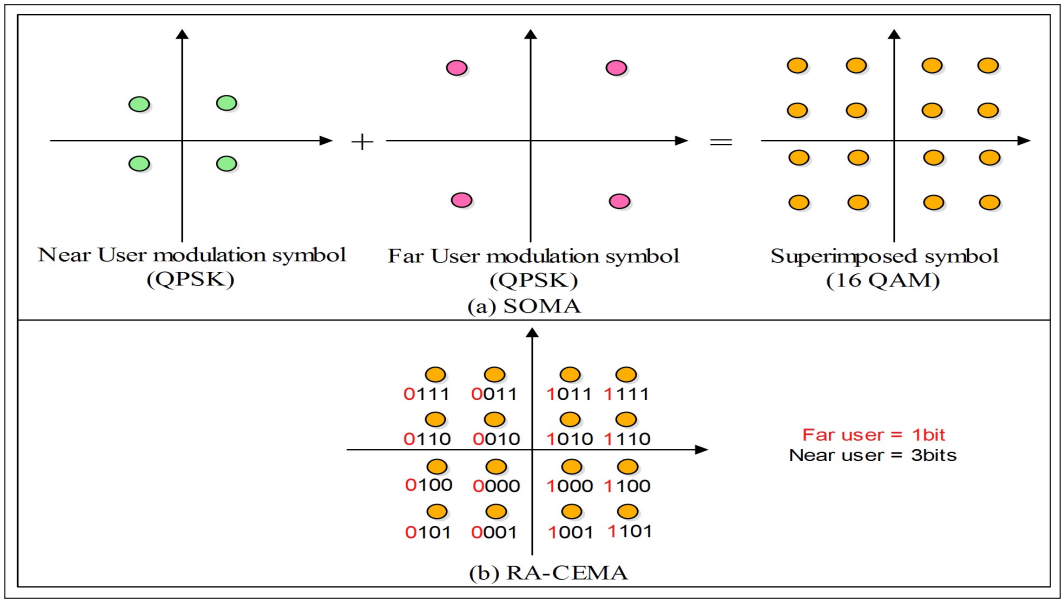

Figure 2.29: Block diagram of (a) SOMA, and (b) RA-CEMA

band signals.

2.5.5.2 LPMA

This scheme was proposed by [300] by considering a non-orthogonal multi-user transmission scheme for downlink scenario. It is suitable for both PD-NOMA and CD-NOMA to increase their multiplexing gain. Its usage in the power domain scheme enhances the throughput by superimposing different-power streams, whereas its usage in the code domain improves the security of codes by using the linear combination of lattice codes. LPMA use lattice coding at the transmitter side to encode the information of users and SIC at the receiver side to decode the information. In comparison to PD-NOMA, LPMA provides better performance gain with respect to the increase in channel quality difference of users. Moreover, it provides high encoding and decoding complexity as compared to CD-NOMA.

2.5.6 Comparison of existing CD-NOMA schemes

Table 2.16 provides the detailed relative comparison of existing variants of CD-NOMA using parameters, transmission type, carrier type, receiver used, technique used, and merits and demerits of each variants.

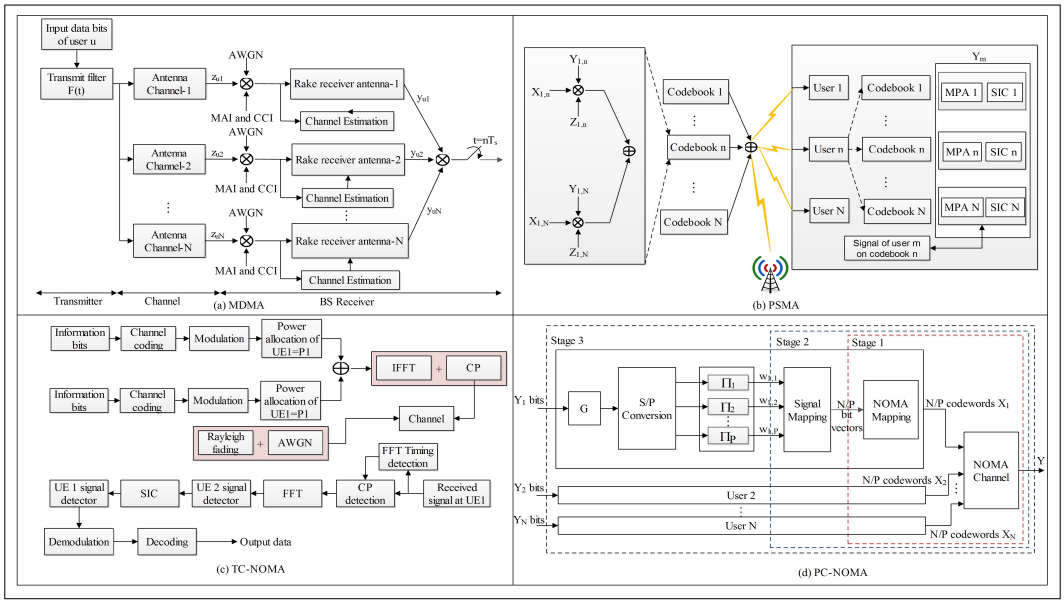

Figure 2.30: Block diagram of (a) MDMA (b) PSMA (c) TC-NOMA, and (d) PC-NOMA

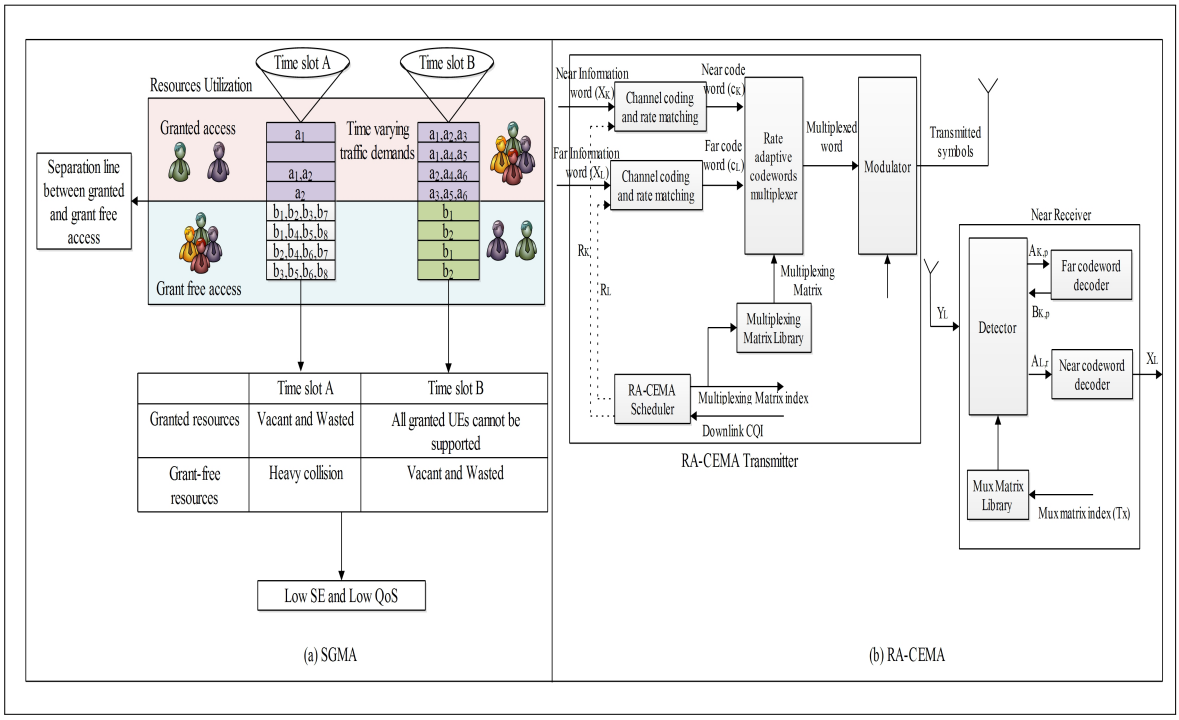

Figure 2.31: Block diagram of (a) SGMA, and (b) RA-CEMA

Table 2.15: Relative comparison between different CD-NOMA schemes

Type	Acronym	Organization	Carrier type	Transmission Type	Receiver used	Technique used	Merits	Demerits
Short spreading sequence	MUSA	ZTE	SC		MMSE-SIC	Short complex sequence	Block error rate (BLER) low, Large number of user access	High interference between users, Optimal spread symbols
	NOCA	Nokia	SC	Uplink	MMSE-SIC	Zadoff-Chu sequence	Reduce the PAPR	-
	NCMA	LGE	SC	Uplink	MUD+IC	Grassmannian line packing	Optimal non-orthogonal sequence	Transmitter overhead is high
	SSMA	Intel	SC	Uplink	MUD+IC ; MMSE-SIC	Orthogonal or quasi-orthogonal codes	Receiver complexity is low	Performance depends upon actual sequence length.
Long spreading sequence	GOCA	Mediatek	SC	Uplink	SIC	Group-based orthogonal/non-orthogonal sequences	Inter-group orthogonality	-
	WSMA	Ericsson	SC	Uplink/Downlink	MMSE-SIC	Welch bound coding	Receiver complexity is low	-
Coding	PDMA	CATT	MC	Uplink/Downlink	Belief Propagation (BP) [MPA-IC]	Irregular LDS	Provide Multidimensional diversity, Receiver complexity low, Irregular protection	Optimal pattern design
	SCMA	Huwaei	MC	Uplink/Downlink	MPA+IC	Multidimensional modulation	Signal space diversity gain	Optimal codebook design
	LDS-SVE	Fujistu	SC	Uplink/Downlink	MPA+IC	LDS and User signature vector extension (SVE)	Large diversity	Define LDS code and signature vector extension method
	LDS-CDMA	Fujistu	SC	Uplink/Downlink	MPA+IC	Sparese spreading CDMA	CSI independent	Redundant coding
	LDS-OFDM	Fujistu	MC	Uplink/Downlink	MPA+IC	Sparse spreading OFDM	CSI independent, provide wideband signals	Redundant coding

Table 2.16: Relative comparison between different CD-NOMA schemes

Type	Acronym	Organization	Carrier type	Transmission Type	Receiver used	Technique used	Merits	Demerits
Lattice and Beam	LPMA		SC	Uplink/Downlink	SIC	Multilevel lattice code and multiplexing in power and code domain	User clustering independent	Specific channel coding
	BOMA		SC	Uplink/Downlink	SIC	Tiled building block	Receiver complexity low, easy structure	User pairing dependent
Interleaving	IGMA	Samsung	SC	Uplink/Downlink	MPA	Bit-level Interleaving(permutation matrix)	Low coding rate,Sparse grid Mapping	Transmitter overhead is high
	IDMA	Nokia	SC		Elementary signal estimator(ESE)+IC (IMD)	Bit-level Interleaving	Large diversity gain/ Low coding rate, Randomized the mutual interference	Interleaving design
	RDMA	Mediatek	SC	Uplink	SIC	Cyclic shift based time-frequency repetition	Easy implementation	-
	LCRS	Intel	SC	Uplink	ESE-PIC	Bit-level spreading	High code gain	Users' separation at receiver depends upon its structure
Scrambling	RSMA	Qualcomm	SC	Uplink	Matched filter + IC (MMSE-SIC; ESE-PIC)	Low cross-correlation Sequence scrambling	Fit for asynchronized scenario	Not suitable for SE, and requires synchronous multiplexing with OFDM
	LSSA	ETRI	SC	Uplink	MMSE-SIC	User-specific bit-level inter leaving/permutation pattern	Low rate FEC code or moderate one with repetition, Large number of signatures	-
Power domain	PD-NOMA	NTT DoCoMo	SC	Uplink/Downlink	SIC	Signals separated through different power levels	High SE and low outage probability	Error propagation

2.6 Miscellaneous

2.6.1 SOMA

In this variant, each user's data rate is independently modulated in a QAM constellation. Then, based on appropriate power allocation coefficients, the data rate is summed up to generate the higher-order QAM modulation, as shown in Fig. 2.29 (a). This technique was designed to address the uplink capacity shortage problem in mMIMO [301]. The main difference between SOMA and NOMA is the symbol constellations. In NOMA, the post superposition symbol constellation mappings are divided with SIC without gray mapping, whereas in SOMA, it depends upon gray mapping.

2.6.2 RA-CEMA

It is used to generate a superimposed symbol. It also transmits the QAM modulation, but differs from SOMA, because the mapping of the coded bits of each user is adaptively controlled as per the user's channel condition to enhanced and control the data rate of the system. The authors in [302] used RA-CEMA to mitigate the problem of amplitude weighted (AW) NOMA which arises during the transmission for degraded broadcast channel. By using RA-CEMA, the authors applied the multiplexing technique over UEs signals to store their codewords and then map the columns into constellation symbols. The results show that RA-CEMA performs similarly like other conventional schemes on the basis of their superposition coding, but overcome the potential standardized problems which arise due to the usage of unconventional constellations.

2.6.3 MDMA

Hsiao *et al.* [303] proposed a scheme which combine mmWave technique with mMIMO at the BS. It reduces the multiple access interference (MAI) of cellular mobile radio and enhances the processing gains of the system by using multiple antennas at the BS as shown in Fig. 2.30 (a). The presence of mmWave in this scheme improves the channel bandwidth to provide high data transmission, whereas massive antennas at BS are used to reduce the MAI to improve the capacity of the system. In MDMA, users are separated from each other by their distinct multipath structures. Moreover, the authors in [304] explored the feasibility and of applications of MDMA.

2.6.4 PSMA

It was proposed by Moltafet [305] to improve the network SE. The authors used a combination of PD and CD NOMA to transmit the multiple signals over a subcarrier simultaneously.

In this scheme, PD-NOMA was used to send the signals to users via different power levels and SCMA was used to provide the same codebook to multiple users. Fig. 2.30 (b) shows the usage of the same codebook by multiple users. In SCMA, the usage of the same codebook produces interference among each other. To overcome it, PSMA reused a codebook in the coverage area of each BS more than once which enhanced the network SE. In this technique, at the receiver side, MPA based SIC detector is used to separate the signal of each user. The performances of PSMA was evaluated through the heterogeneous cellular network in terms of the system sum-rate and QoS of users by considering system-level and transmit power constraints, respectively. The numerical results show that the PSMA in comparison with SCMA and PD-NOMA improved the SE up to 50%.

2.6.5 TC-NOMA

These codes are error-correcting codes and theoretically produced the results equivalent to ShannonâĂŹs capacity theorem. This extraordinary performance is due to the use of two encoders and an interleaver at the transmitter and two decoders and a de-interleaver at the receiver [306]. The block diagram of NOMA with turbo coding is as shown in Fig. 2.30 (c). According to [307], performance results show that the NOMA with turbo codes outperformed than NOMA without coding and the BER is reduced at the receiver side.

2.6.6 PC-NOMA

It is based on channel polarization, where the combination of binary polar codes and signal modulation decomposed the original NOMA channel into multiple bit polarized channels by using a three-stage channel transform (user$\rightarrow$ signal $\rightarrow$ bit) partitions [308]. The authors proposed two schemes. In the first scheme, channel transformation-sequential user partition (SUP) and the parallel user partition (PUP) is used. In the SUP based PC-NOMA system, a worst-goes-first strategy was proposed to determine the user partition order which improves the system performance by the enhanced polarization effect among the user synthesized channels. At the receiver side, a joint successive cancellation detection and decoding scheme was developed. Its was analyzed through channel polarization principle. On the other side, in the PUP based PC-NOMA system, a parallel detection scheme was developed to reduce the processing latency. The numerical results show that PC-NOMA scheme outperformed than TC-NOMA in terms of block error ratio and throughput.

2.6.7 SGMA

This technique was proposed by [309] to ensure the QoS of users. The goal of the proposed scheme was to reduce the latency and signalling overhead, as shown in Fig. 2.31 (a). In this scheme, complete or part of the available resources can be shared by both the grant access

and grant free access scheme [309]. Let X be the number of RBs/subcarriers of the wireless network, D^g and D^{gf} represents the demand set of grant access and grant free access, respectively, R^g and R^{gf} represents the available resources set for grant access and grant free access, respectively and M shows the mapping between the demand set and available resources, i.e., $D^g \xrightarrow{\text{M}} R^g$ and $D^{gf} \xrightarrow{\text{M}} R^{gf}$. Then, according to SGMA, $\forall R^g \neq \emptyset, R^{gf} \neq \emptyset \rightarrow R^g \cap R^{gf} \neq \emptyset$. SGMA decreases the BER and improves the throughput of the network as compared to SCMA, PDMA, MUSA, and IDMA.

2.6.8 BDM

Bit division multiplexing (BDM) is a physical layer subchannel technique used to overcome the limitations of time-division multiplexing (TDM) [310]. This technique enhances the transmission efficiency of scalable video broadcasting. It can be easily applied to higher-order constellations because it provides the flexibility in channel resource allocation using the conventional hierarchical modulation technique. BDM also assigns the fixed number of bits from the multiple symbols over the sub-channels by exploiting the inherent characteristics of high order modulation schemes, i.e., multiple unequal error protection. In contrast to TDM, BDM increases the transmission rate by decreasing the SINR across the multiple sub-channels.

2.6.9 GSOMA

It is an amalgamation of SOMA and conventional TDD [301, 311]. It was observed by the authors in [301] that when in any group only one user is left and no blanking was used then GSOMA behaves like SOMA, whereas when only one group is left with the maximum number of users, GSOMA behaves like conventional TDD. Therefore, a properly designed GSOMA is required which provides the advantages of both SOMA and conventional TDD. GSOMA enhances the aggregate rate with respect to conventional TDD when more groups are to be scheduled. Similar to conventional TDD, in GSOMA, pilot sequences are also mutually orthogonal which allows joint channel estimation without interference for all users in each group. The authors in [301] proposed a general framework of GSOMA and show that it works better than the TDD and conventional SOMA.

2.6.10 NORA

This random access scheme was proposed by [312] to reduce the large random access (RA) delay so that the performance between the UEs to carried out mMTC can be improved. The key idea behind this scheme was to overcome the congestion problem by using the SIC technique. First of all, it identifies the multiple UEs with an identical preamble by using the difference between their time of arrival. Then, NORA enables power domain multiplexing to avoid the collision between the UEs and use SIC technique at the BS for preamble detection. Using

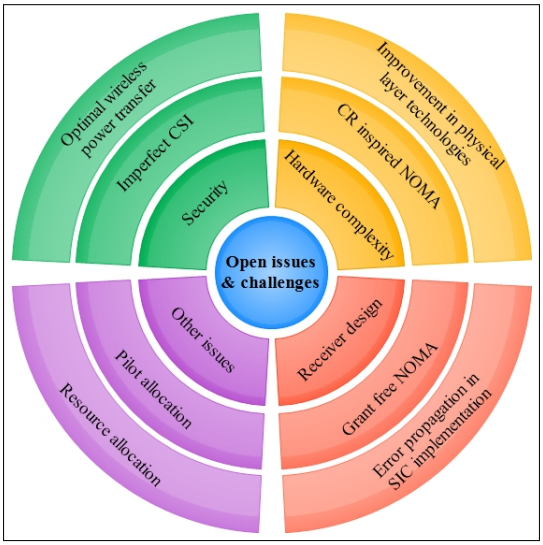

Figure 2.32: Open issues and research challenges

NORA, multiple UEs simultaneously received the message by using limited PUSCH resources. In comparison to ORA, this scheme provides 30% increase in throughput of RA process and also reduce the required preamble transmissions and access delay up to half when the total number of UEs is near the RA throughput.

2.7 Open issues and Challenges

Use of NOMA variants for 5G environment is still in its infancy. A number of open issues and research challenges need to be addressed to realize its effect feel to the end-users. In December 2015, Huwaei proposed three variants of MA-NOMA, SOMA, and RA-CEMA. Most of the work has been done only in PD-NOMA and CD-NOMA. This section discusses the current and future communication challenges by the use of NOMA variants as shown in Fig. 2.32.

2.7.1 Optimal wireless power transfer

This technique improves the lifespan of energy-constrained devices. Energy harvesting is based on the solar, wind, and thermoelectric effects, but these are not feasible as they rely on the location, environment and day time. To overcome it, harvesting from RF signals has been used so that the energy of the battery constrained devices can be improved. The implementation of NOMA with WPT for IoT application is an open issue which needs to be resolved to improve the network EE. In spite of an improvement in EE, the management of co-channel interference along with energy harvesting is also an open issue.

2.7.2 Imperfect CSI

It has been observed that in NOMA lots of work already done by the researchers with perfect CSI for resource allocation and multi-user detection. However, perfect CSI is not possible due to feedback and channel estimation errors. It has been observed that when users CSI is not known then it results in interference. This happened because, with imperfect CSI, signals received from other user's signals cannot be removed completely. So, to handle the model with imperfect CSI, there is a need of perfect joint precoders to remove the interfering signals from the BS and a more advanced channels estimation algorithm to attain the more accurate channel information. Considering the aforementioned discussion, it is an open issue which needs to be resolved to reduce the effect of errors.

2.7.3 Security

In each generation of wireless communication system, security is an important issue which needs to be addressed. The signal broadcasted through wireless channel requires significant attention as it is vulnerable to eavesdropping. The author in [313] proposed an appealing technique to improve the security of the wireless channel by using the cryptographic technique at the physical layer. In contrast to [313], the authors in [314] proposed a solution to improve the secrecy of the network. Moreover, it improves the capacity of the channels with respect to eavesdropper's channel, but with a change in generation, new techniques are required to improve the physical layer security.

In NOMA, the security of the physical layer is not exploited to its full potential. In [315], the authors discussed the physical layer security issue by using stochastic geometry in a large scale network employing a single antenna at NOMA users. In this technique, the BS communicates with the NOMA users which are distributed randomly in a cell. To improve the security of the physical layer, a protected zone is used around the BS so that the intended users acquire more capacity in comparison to eavesdrop users. The authors in [316] implemented a multiple antenna-based NOMA and proposed a technique to improve the security of the physical layer. In this technique, the authors generated an artificial noise around the BS to decrease the capacity of eavesdropper's channel. In [317], the authors explored the security issue in SISO-NOMA networks, but still, security is an open issue for NOMA technique especially for the cases of MIMO and mMIMO.

2.7.4 Improvement in Physical layer technologies

The pre-existing NOMA schemes worked either on bit-level or symbol level operations; as a result, they did not provide a global optimal design. To overcome this issue, a joint technique which consists of both bit and symbol level needs to be designed, but it is sensitive towards certain channel conditions and needs further attention to cope up with the practical scenarios.

Despite the design at the transmitter side, the detection of signals at the receiver side is another physical layer technology which needs to be improved. The traditional technique requires a large number of iterations to detect the symbol and encode the channel which increases latency. Hence, the reduction in latency and complexity are the open issue which needs to be addressed to improve the system reliability.

2.7.5 CR inspired NOMA

NOMA is suitable for 5G applications that improve the SE. When NOMA is integrated with CR, it guaranteed the QoS for the poor channel condition users as it treats those users as a PU, but the performance of the SU can be degraded as they get services only after the weak channel condition user's QoS is met. This is the reason why CR-NOMA cannot fulfil the QoS requirements of all users which needs to be addressed.

2.7.6 Hardware Complexity

In NOMA, the presence of SIC detector increases the hardware complexity which first separates the high power level signals as compared to the lower power level to obtain users data. It has been observed that when there is a number of users or a fast signalling transmission is required then the detection delay increases which can affect the battery of the UEs. Hence, to implement the NOMA in ultra-dense networks, UEs must be equipped with sufficient battery which is practically impossible. To resolve it, fair power allocation and effective user clustering techniques are required.

2.7.7 Error propagation in SIC implementation

When SIC is carried out at the receiver side, then the users with better channel conditions subtracts the signals of weak channel condition users' to estimate their data rate. But, in practical situations, the SIC detection affects the receiver because it is not possible for NOMA system to ideally estimate the channel. This happened due to hardware complexity, timing offset (TO), carrier frequency offset (CFO) type related impairments. So, error propagation and erroneous detection usually occur in the SIC process. To resolve the aforementioned issue as well as to enhance the QoS, an improvement in the estimation quality of mentioned hardware impairments is needed.

2.7.8 Grant free NOMA

In OMA, the access grant-based transmission in an uplink scheduling and downlink resource allocation results into high transmission latency and signalling overhead. However, there is a requirement of an MA technique which overcomes the grant free transmission and

provides low transmission latency and low signalling overhead. The aforementioned issues are resolved with the usage of NOMA to ensure the massive connectivity for the case, where short packets are to be transmitted. Therefore, a contention-based NOMA is a promising solution for the scenarios, where one or more pre-configured resources are allocated to contending users. It was also found that integrated protocols such as random back-off techniques suitably eliminate the non-orthogonal collisions which become helpful in a rate reduction of dropping packets. Moreover, NOMA removes the dependency to access the grant procedure due to which BS cannot obtain any information related to the users, Hence, to overcome this issue there is a need of compressed sensing (CS) based algorithms due to the sparsity of user activity.

2.7.9 Receiver design

The SIC employed receiver, the complexity and error propagation degrade the performance of the users. Therefore, to overcome this issue, a more accurate non-linear detection algorithm with high performance is required which reduces the influence of the error propagation. However, the MPA-based receiver has high complexity, but it efficiently removes the error propagation issue by using the Gaussian distribution approximation technique. It provides more accurate and better results when the number of connections increases. Moreover, it was also found that MPA simultaneously decodes and detect the data symbols especially for the graphs having variable and observation nodes. These receivers also decode, demodulate, and exchange the data symbols more efficiently to improve the performance of signal detection. But, the issues such as efficient receiver design, error propagation, and signal detection accuracy need to exploited to strengthen the performance at the receiver side.

2.7.10 Resource allocation

It is used to assign the radio resources to users which improves their throughput, data rate, EE, and user fairness. When the number of users becomes large in a multi-cell scenario, then the resource allocation to users becomes a difficult task as the spectrum has limited radio resources. NOMA has efficiently utilized the resources due to its capability to serve multiple users simultaneously by using different power levels. However, assigning resources to users using NOMA technique is quite complex due to the presence of co-channel and cross-channel interference. To mitigate these interferences, a proper resource allocation scheme is required which reduces the impact of error propagation.

2.7.11 Pilot Allocation

The transmission of multiple signals are carried out in an overlapped fashion due to which the problem of intra-user interference and error propagation becomes severe. It results in a degradation in performance of NOMA as compared to OMA systems. To implement error

and interference-free NOMA, the positions of the pilot and its allocation is an important issue which needs to be reinvestigated. It also reduces the error and enhances the performance of the NOMA based system.

2.7.12 Other issues

It has been observed that NOMA enhances the SE and EE of the network when these are used in HetNets, UAVs, V2X, and WSNs. However, NOMA improved the system efficiency of these applications, but still, there are various open issues which need to be addressed such as-in V2X and UAVs, mobility of the vehicles and co-channel interference, whereas, in HetNets, co-channel, cross channel, and NOMA interference is severe. All these issues need to be addressed to improve the data rate, SE, EE, reliability, throughput, and OP of the system.

2.8 Summary

In this paper, different NOMA variants for 5G environment are explored. The survey is divided into four parts. The first part of the survey discussed the background and standards of NOMA in detail. NOMA history is analyzed on the basis of year-wise improvements in traditional techniques. Then, the capacity comparison of OMA and NOMA and advantages of NOMA over OMA are analyzed. The second part of the paper discussed the NOMA variants in the power domain. Then, NOMA in D2D communication, cooperative communication, cognitive-communication, M2M communication, SWIPT, MIMO, mMIMO, SDN, MEC, UAVs, VLC, mmWave, Het Nets, and V2X are discussed. The comparative analysis of the existing variants of NOMA is performed on the basis of transmission scenario, techniques used, throughput, sum-rate, EE, latency, capacity, and random access probability. The third part of the survey discussed the code domain NOMA variants. Finally, the open issues and challenges of code and power domain variants of NOMA are discussed.

2.9 Research Gaps

After a detailed analysis of the aforementioned existing proposals, following research gaps need to be addressed during the implementation of PD-NOMA-based D2D users underlaying cellular networks.

- **Interference Management**: When D2D users share the same RBs with CMUs the interference occurs. In downlink transmission, CMUs receive interference from DDTs whereas D2D users receive interference from BS. On the other hand in uplink transmission, BS receives the interference from DDTs and D2D users receive interference from

CMUs transmitter. Apart from the above interference, intra-user interference (Interference among D2D users) is a challenge which needs to be addressed for D2D communication. PD-NOMA with SIC technique handle this interference efficiently, but to handle co-channel and cross channel interference in D2D in the presence of PD-NOMA is a challenging task.

- **Resource Allocation**: To improve the spectral efficiency of a network, a proper resource allocation scheme among D2D users and CMUs is required. Generally, there are two types of resource allocation techniques for D2D communication: orthogonal and non-orthogonal. In orthogonal, the large number of radio resources are allocated to the CMUs and rest used by the D2D users. Whereas, in non-orthogonal, D2D users and CMUs share the same radio resources. In D2D communication, radio resources are allocated in the form of a centralized or distributed manner. In centralised, resources are allocated to D2D users and CMUs by BS. This supports a large number of users but device complexity is high. On the other hand, in distributed, message passage algorithm is required to mitigate the interference but in this case, device complexity becomes high. Work had been done in both the centralized and distributed considering the OFDMA techniques. For 5G network, OFDMA is not suitable to serve a large number of users from the same RB, therefore PD-NOMA is used. Some works have been proposed for resource allocation in PD-NOMA based D2D network but still, proper resource allocation schemes are required to enhance the sum rate and throughput of the users.

- **Power Control**: To efficiently utilize the resources, the power of DDTs must be controlled. If DDTs are randomly deployed under cellular networks, the performance of the network degraded due to co-channel interference. To fulfil the signal-to-interference ratio (SINR) requirements of cellular users, DDTs need to limit their power. The power optimization techniques can improve the throughput and EE of the network. Same can be used to mitigate co-channel interference. In 5G, especially for a multi-cell scenario, an effective power control scheme needs to be addressed.

- **Energy Efficiency**: D2D communication enlarges the EE of the network due to short-distance communication but they have limited battery lifetime. Generally, D2D communication depends on peer discovery and communication protocols. When protocols force user equipments to make fast pairing and ask for frequent data transmission than battery consumed at a faster rate. Along with the above issue, it is also not possible to change and charge the batteries of devices after a frequent interval of time, resulting in a higher cost. So, to prolong the lifetime of mobile devices there should be an optimal wireless power transfer. This technique improves the lifespan of energy-constrained devices. Energy harvesting is based on the solar, wind, and thermoelectric effects, but these are not feasible as they rely on the location, environment and day time. To overcome it, harvest-

ing from RF signals has been used so that the energy of the battery constrained devices can be improved. The implementation of PD-NOMA with WPCN for D2D application is an open issue which needs to be resolved to improve the network EE.

2.10 Objectives

Following are the research objectives finalized by the research committee:

1. To study and explore the effect of NOMA with D2D and other 5G techniques.
2. To design a joint sub-channel allocation and power control scheme for NOMA based D2D communication network to mitigate the interference.
3. To develop a resource allocation scheme for D2D network using energy harvesting technique.
4. To validate the proposed solutions by selecting various performance evaluation metrics in different scenarios.

2.11 Methodology for objective 1

This objective aims to study the effect of NOMA with D2D and other 5G techniques. First of all study the available reviews on NOMA. Second, search the parameters on which the reviews are not available. From the existing schemes, search and study all the different parameters. On the basis of available parameters, find those which have not been studied till yet. After that, a systematic review will be prepared on the above-said parameters which are not studied. The review will consist of all the existing schemes proposed by various authors. The review covers the different challenges and also open various issues.

2.12 Methodology for objective 2

When NOMA integrated with D2D technique then it enhances the spectral efficiency of the network. With NOMA, a large number of users can be served from the same RBs. As various D2D users reuse the same RB with the CUs, the problem of NOMA and co-channel interference becomes a challenging issue. To overcome the problem of NOMA interference proper scheduling between the D2D users will be required. To handle the co-channel interference, a proper sub-channel allocation will be needed to properly reuse the spectrum. To fulfil the minimum QoS requirement of CUs, the power of DTs must be controlled. This objective aims to design a joint sub-channel and power control scheme to handle the interference. To achieve the desired goal, the first step is to study and analyse the issues of interference between D2D and

CUs. Secondly, the study of various existing schemes to allocate a sub-channel. Third, study the various schemes for controlling the power of the DTs. Then a joint sub-channel and power control scheme will be developed. Finally, analyse the performance evaluation of the proposed scheme with the existing NOMA and OMA based scheme with respect to the parameters such as - sum rate, outage probability and so on.

2.13 Methodology for objective 3

The objective aims are to design a resource allocation scheme using EH technique to improve the energy efficiency of the UEs. To achieve this objective, we will integrate a SWIPT technique with D2D. SWIPT is a new emerging technique which may harvest the energy from the radio frequency signals. The major challenge is to tackle the energy consumption of UEs at running of high multimedia applications as they have limited battery power.

Our task is to develop an energy-efficient resource allocation algorithm which maximizes the energy efficiency of the D2D and CUs respectively. For this, first of all, study the various energy-efficient scheme proposed for D2D. Second, study the various aspects of SWIPT and its advantages of integrating with D2D. Third, develop the proposed scheme consisting of SWIPT with D2D. At last, analyse the performance of the proposed scheme with the existing schemes in terms of energy efficiency.

2.14 Methodology for objective 4

To achieve this objective, the proposed schemes will be tested for it accuracy and efficiency using realistic parameters. Since the target scheme comprises of both the D2D and CUs (two-tier network), so the proposed scheme will be simulated on the MatLab tool to demonstrate the performance evaluation. On the MatLab tool, a program will be designed to test the various performance metrics in different scenarios.

Chapter 3

Cross-Layer Interference Management Scheme for D2D Mobile Users Using NOMA

D2D communication is a promising technology in which the spectrum resources are reused efficiently with cellular mobile users (CMUs) in an underlay of the 5G network. Using it, network capacity and spectral efficiency increases but it introduces the co-channel interference. Moreover, massive connectivity has not been fully exploited for efficient spectral efficiency usage in the existing solutions. The main goal of the chapter is to maximize the sum-rate of the overall network while maintaining the SINR of the CMUs and DMUs.

The key components of the chapter are as follows:

- Firstly, we design an optimal DDT-DMUs grouping scheme to reduce intra-user interference using SIC decoding order. To design the DMGs, following cases are considered (i) when strong DMU equals to the weak DMU (ii) strong DMU is larger than the weak DMU, and (iii) strong DMU is less than weak DMU in a cell.
- NOMA is integrated with DMGs so that the DDT in each DMG can serve more than one DMUs using the same RB. Based on the network model, a mixed-integer non-linear programming (MINLP) problem is formulated. To solve this problem, it is decomposed into two sub-problems: RB allocation problem (RBAP) and power allocation problem (PAP) for CMUs and DMGs, respectively.
- To solve the RBAP for both the CMUs and DMGs, firstly, we use the many-to-many mapping scheme to assign the RBs. Secondly, to reduce the co-channel interference among the DMGs, the GRSC based Greedy algorithm is proposed to reuse the RB. In this, the DMGs can exchange the RBs among each other based on its channel conditions to achieve the maximum sum rate.

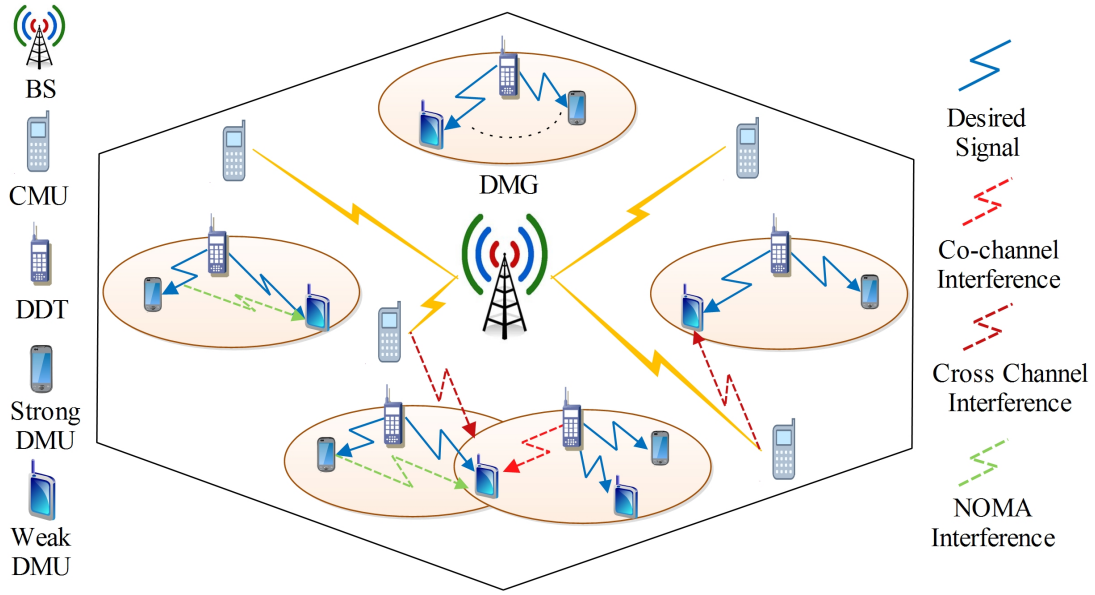

Figure 3.1: System Model

- For PAP, the difference of two convex (DC) programming approach based on SCALE is used. Then, an efficient iterative algorithm is designed to obtain a near-optimal value of power allocation.
- Simulation results show that in comparison to the state-of-art schemes, our proposed algorithm achieves superior sum rate for DMGs while ensuring the SINR requirement of the CMUs.

3.1 System Model

In this section we discuss the various components of the proposed system model as shown in Fig. 3.1.

3.1.1 Network Model

Assume a single cell uplink transmission scenario in a cellular network, as shown in Fig. 3.1, which consists of a BS denoted by b, $\mathcal{I}$ CMUs, and $\mathcal{J}$ DMGs. The BS b is located at the center, whereas $\mathcal{I} \in \{1,2,\ldots,i,\ldots,I\}$ CMUs and $\mathcal{J} \in \{1,2,\ldots,j,\ldots,J\}$ DMGs are uniformly distributed in a cell as shown in Fig.3.1. Each DMG consists of one DDT, and $\mathcal{R} \in \{1,2,\ldots,r,\ldots,R\}$ DMUs. The location of DDTs and DMUs are varying as they are moving with very low velocity. For simplicity, DDT is represented as $\mathcal{J} \in \{1,2,\ldots,j,\ldots,J\}$. $\mathcal{I}$ CMUs and $\mathcal{J}$ DMGs used OFDMA techniques to communicate with the BS, whereas the DDT in each

DMG has NOMA to communicate with respective DMUs. Assume that CMUs and DDTs use $\mathcal{N} \in \{1,2,\ldots,n,\ldots,N\}$ orthogonal uplink RBs to communicate with the BS, and respective DMUs. If B is the total bandwidth, then w=($\frac{B}{N}$) is the bandwidth equally assigned to each RBs. Also, assume that the CSI of all the CMUs, DDTs, and DMUs is known to the BS through their pilot signals. In this, we fixed the phase rotation and have not considered its effect on the NOMA multiplexing. Moreover, in this paper, the quasi-static Rayleigh fading channel model is used, where the channel coefficients are constant for each channel and follow Gaussian complex distribution. The Rayleigh fading is a statistical model for a propagation environment on the radio signal. Assume that the magnitude of a signal passing through a communication channel has varied randomly. Rayleigh fading is most suitable to the situation when no dominant propagation is available for the line of sight between the transmitter and receiver.

3.1.2 Signal Model

In order to form a NOMA-based DMG, a minimum two users in each group are required, i.e.,

$$2 < \sum_{r=1}^{R} \rho_{j,r}^{n} < R, \tag{3.1}$$

where R is the number of DMUs in each DMG, and $\rho_{j,r}^{n}$ is the DDT-DMUs grouping indicator which is defined as follows:

$$\rho_{j,r}^{n} = \begin{cases} 1, & \text{if the } r^{th} \text{ DMU is grouped to the } j^{th} \text{ DDT,} \\ 0, & \text{otherwise.} \end{cases}$$

3.1.2.1 CMU

The signal received at the BS b from the i^{th} CMU over the n^{th} RB is given as follows:

$$y_{i,b}^{n} = |g_{i,b}^{n}|\sqrt{P_{i}^{n}}x_{i,b}^{n} + \underbrace{\sum_{j=1}^{J} \rho_{j,r}^{n}\phi_{j,i}^{n}|g_{j,b}^{n}|\sqrt{P_{j}^{n}}x_{j,b}^{n}}_{\text{Interference from DMGs}} + \underbrace{\xi_{i,b}^{n}}_{\text{AWGN}}, \tag{3.2}$$

where

$$\phi_{j,i}^{n} = \begin{cases} 1, & \text{if the } i^{th} \text{ CMU and the } j^{th} \text{ DDT reuse the} \\ & n^{th} \text{ RB,} \\ 0, & \text{otherwise.} \end{cases}$$

Now, the SINR using Eq. (3.2) is calculated as follows:

$$\Gamma_{i,b}^{n} = \frac{P_i^n |g_{i,b}^n|^2}{\sum_{j=1}^{J} \rho_{j,r}^n \phi_{j,i}^n P_j^n |g_{j,b}^n|^2 + \sigma_{i,b}^2}. \tag{3.3}$$

where P_i^n and P_j^n denote the transmit power of the i^{th} CMU, and the j^{th} DMG, respectively. $|g_{i,b}^n|^2 = |\hat{g}_{i,b}^n|^2 d_{i,b}^{-\eta}$, and $|g_{j,b}^n|^2 = |\hat{g}_{j,b}^n|^2 d_{j,b}^{-\eta}$. Here $\hat{g}_{i,b}^n$ and $\hat{g}_{j,b}^n$ are small scale fading with $\hat{g}_{i,b}^n \sim \mathcal{CN}(0,1)$ and $\hat{g}_{j,b}^n \sim \mathcal{CN}(0,1)$. $d_{i,b}$ and $d_{j,b}$ are the distances between the i^{th} CMU and the b, and between the j^{th} DMG and the b. η is the path loss exponent.

3.1.2.2 DMUs in DMG

In PD-NOMA, the superposition coding is used at the DDT to multiplex the power signal, and SIC is used at the $\mathcal{R}$ DMUs to reduce the intra-user interference. The multiplexed signal transmitted by the DDT using superposition coding towards the $\mathcal{R}$ DMUs with different power allocation coefficients is given as follows.

$$\alpha_{j,1} x_{j,1}^n + \alpha_{j,2} x_{j,2}^n + \cdots + \alpha_{j,r_s} x_{j,r_s}^n + \alpha_{j,r_w} x_{j,r_w}^n \cdots + \alpha_{j,R} x_{j,R}^n, \tag{3.4}$$

where $\{\alpha_1, \alpha_2, \ldots, \alpha_R\}$ and $\{x_1, x_2, \ldots, x_r\}$ represents the power allocation coefficients and the messages for DMUs. r_s and r_w denotes the strongest and weakest DMU associated with the DDT. If channel gain of DMUs in the DMG is represented as $|g_{j,1}^n| \geq |g_{j,2}^n| \geq \cdots \geq g_{j,r_s}^n \geq g_{j,r_w}^n \cdots \geq |g_{j,R}^n|$, then the signal received at r_w DMU in the j^{th} DMG over the n^{th} RB is same as given in [98].

$$y_{j,r_w}^n = \underbrace{\sqrt{P_j \alpha_{j,r_w}} |g_{j,r_w}^n| x_{j,r_w}^n}_{\text{Desired Signal}} + \underbrace{\sum_{r=2}^{R} \sqrt{P_j \alpha_{j,r_s}} |g_{j,r_s}^n| x_{j,r_s}^n}_{\text{NOMA Interferece } (I_{j,r_s}^{no})} + \underbrace{\sum_{j' \neq j}^{J} \phi_{j',j}^n \sqrt{P_{j'}} |g_{j',j,r_w}^n| x_{j',j,r_w}^n}_{\text{Co-channel Interference } (I_{j,1}^{co})}$$

$$+ \underbrace{\rho_{j,r}^n \phi_{j,i}^n \sqrt{P_i} |g_{i,j,r_w}^n| x_{i,j,r_w}^n}_{\text{Cross channel interference } (I_{j,r_w}^{cr})} + \underbrace{\xi_{j,r_w}^n}_{\text{AWGN}}, \tag{3.5}$$

where $\phi_{j',j}^n$ represents the co-channel interference, which is given as:

$$\phi_{j',j}^n = \begin{cases} 1, & \text{if the } (j')^{th} \text{ and the } j^{th} \text{ DDT reuse the} \\ & n^{th} \text{ RB}, \\ 0, & \text{otherwise.} \end{cases}$$

$|g_{j,r_w}^n| = |\hat{g}_{j,r_w}^n| d_{j,r_w}^{-\eta}$, $|g_{j,r_s}^n| = |\hat{g}_{j,r_s}^n| d_{j,r_s}^{-\eta}$, $|g_{j',j,r_w}^n| = |\hat{g}_{j',j,r_w}^n| d_{j',j,r_w}^{-\eta}$,and $|g_{i,j,r_w}^n| = |\hat{g}_{i,j,r_w}^n| d_{i,j,r_w}^{-\eta}$. Here $\hat{g}_{j,r_w}^n \sim \mathcal{CN}(0,1)$, $\hat{g}_{j,r_s}^n \sim \mathcal{CN}(0,1)$ $\hat{g}_{j',j,r_w}^n \sim \mathcal{CN}(0,1)$, and $\hat{g}_{i,j,r_w}^n \sim \mathcal{CN}(0,1)$. $d_{j,r_w}^{-\eta}$ is the distance between the j^{th} DMG and the r_w DMU, $d_{j',j,r_w}^{-\eta}$ is the distance between the $(j')^{th}$ DMG

and the r_w DMU of the j^{th} DMG, and $d_{i,j,r_w}^{-\eta}$ is the distance between the i^{th} CMU and the r_w DMU of the j^{th} DMG.

For successful SIC, the SINR of r_s DMU should be greater than or equal to the SINR of remaining DMU's, i.e.,

$$\frac{|g_{j,r_s}^n|^2 P_j \alpha_{j,r_s}}{I_{j,r_s}^{no} + I_{j,r_s}^{co} + I_{j,r_s}^{cr} + \sigma^2} \geq \sum_{r=2}^{R} \frac{|g_{j,r_w}^n|^2 P_j \alpha_{j,r_w}}{I_{j,r_w}^{no} + I_{j,r_w}^{co} + I_{j,r_w}^{cr} + \sigma^2}. \tag{3.6}$$

So, Eq. (3.6) can be rewritten as follows.

$$\Delta(\phi) = |g_{j,r_s}^n|^2 (I_{j,r_w}^{no} + I_{j,r_w}^{co} + I_{j,r_w}^{cr} + \sigma^2) - \sum_{r_w=2}^{R} |g_{j,r_w}^n|^2 (I_{j,r_s}^{r,no} + I_{j,r_s}^{co} + I_{j,r_s}^{cr} + \sigma^2) \geq 0 \tag{3.7}$$

After successful SIC, the r_s DMU remove the interference from r_w DMUs to decode its own information. Therefore, received SINR at the r_s DMU using Eq. (3.5) is expressed as follows:

$$\Gamma_{j,r_s}^n = \left(\frac{|g_{j,r_s}^n|^2 P_j \alpha_{j,r_s}}{I_{j,r_s}^{co} + I_{j,r_s}^{cr} + \sigma^2} \right). \tag{3.8}$$

Similarly, the SINR received at the remaining DMUs is calculated as follows:

$$\Gamma_{j,r_w}^n = \sum_{r=2}^{R} \left(\frac{|g_{j,r_w}^n|^2 P_j \alpha_{j,r_w}}{I_{j,r_w}^{r,no} + I_{j,r_w}^{co} + I_{j,r_w}^{cr} + \sigma^2} \right). \tag{3.9}$$

3.1.3 Data Rate and Sum Rate Calculation

According to the principle of Shannon, the data rate of the i^{th} CMU using Eq. (3.3) is given as follows:

$$R_{i,b}^n = \log_2(1 + \Gamma_{i,b}^n). \tag{3.10}$$

Similarly, the data rates of DMUs in a DMG using Eq. (3.8) and Eq. (3.9) are expressed as follows:

$$R_{j,r_s}^n = (1 + \Gamma_{j,r_s}^n). \tag{3.11}$$

$$R_{j,r_w}^n = \sum_{r_w=2}^{R} (1 + \Gamma_{j,r_w}^n). \tag{3.12}$$

Now, the sum-rate of $\mathcal{I}$ CMUs and $\mathcal{J}$ DMGs having $\mathcal{R}$ DMUs is given as follows:

$$R_{i,b}^n = \sum_{i=1}^{I} \log_2(1 + \Gamma_{i,b}^n). \tag{3.13}$$

$$R_j^n(\rho, \phi, \alpha) = \sum_{j=1}^{J} \left(\rho_{j,r}^n \phi_{j,i} (R_{j,r_s}^n + \sum_{r_w=2}^{R} R_{j,r_w}^n) \right). \tag{3.14}$$

The sum-rate of overall single cell network is calculated as follows:

$$R^n_{i+j}(\rho,\phi,\alpha) = \sum_{i=1}^{I}\left(R^n_{i,b} + \sum_{j=1}^{J}\rho^n_{j,r}\phi_{j,i}(R^n_{j,r_s} + \sum_{r_w=2}^{R}R^n_{j,r_w})\right). \tag{3.15}$$

3.1.4 Problem Formulation

Our goal is to maximize the sum-rate of the overall network while maintaining the SINR of CMUs and DMGs. The mathematical problem formulation of the proposed model is given as follows:

$$\begin{aligned}
P.F. \quad &: \quad \max_{\rho,\phi,\alpha} R^n_{i+j}(\rho,\phi,\alpha), && (3.16)\\
s.t.\ \mathbb{C}_1 \quad &: \quad 2 < \sum_{r=1}^{R}\rho^n_{j,r} < R, && \forall \mathcal{J},\\
\mathbb{C}_2 \quad &: \quad \sum_{j=1}^{J}\rho^n_{j,r} \le 1, && \forall \mathcal{J},\\
\mathbb{C}_3 \quad &: \quad R^n_{i,b} \ge R^{n,\min}_{i,b}, && \forall \mathcal{I},\mathcal{N},\\
\mathbb{C}_4 \quad &: \quad \sum_{j=1}^{J}\phi_{j,i}p_j|g^n_{j,i}|^2 \le I^{th}_i, && \forall \mathcal{I},\\
\mathbb{C}_5 \quad &: \quad \Delta(\phi) \ge 0, && \forall \mathcal{J},\\
\mathbb{C}_6 \quad &: \quad R^n_{j,r_s} \ge R^{\min}_{j,r_s}, R^n_{j,r_w} \ge R^{\min}_{j,r_w}, && \forall \mathcal{N},\\
\mathbb{C}_7 \quad &: \quad \phi^n_{j,i}, \phi^n_{j',j} \in \{0,1\}, && \forall \mathcal{I},\mathcal{J},\mathcal{N},\\
\mathbb{C}_8 \quad &: \quad \sum_{i=1}^{I}\phi^n_{j,i} \le S_{\max}, && \forall \mathcal{I},\mathcal{N},\\
\mathbb{C}_9 \quad &: \quad \sum_{j=1}^{J}\phi^n_{j,i} \le T_{\max},, && \forall \mathcal{J},\mathcal{N},\\
\mathbb{C}_{10} \quad &: \quad P^n_i \le P^{n,\max}_i, && \forall \mathcal{I},\\
\mathbb{C}_{11} \quad &: \quad \alpha_{j,r_s} + \sum_{r_w=2}^{R}\alpha_{j,r_w} \le 1, && \forall \mathcal{J},\mathcal{R},\\
\mathbb{C}_{12} \quad &: \quad \alpha_{j,r_s} \ge 0, \sum_{r_w=2}^{R}\alpha_{j,r_w} \ge 0, && \forall \mathcal{J},\mathcal{R}.
\end{aligned}$$

In the above problem, $\mathbb{C}_1$ ensures that a minimum of two DMUs must be grouped with each DDT to perform downlink NOMA. $\mathbb{C}_2$ implies that each DMU must be connected with one DDT. $\mathbb{C}_3$ denotes the minimum data rate requirement of CMU. $\mathbb{C}_4$ represents the aggregated interference threshold for CMUs. $\mathbb{C}_5$ defines the successful SIC, and $\mathbb{C}_6$ describes the minimum SINR requirement of r_s and r_w DMUs in each DMG. $\mathbb{C}_7$ ensures that each RB cannot be used by more than one CMU and DMG, respectively. $\mathbb{C}_8$ and $\mathbb{C}_9$ implies that $S_{\max}$ is the maximum

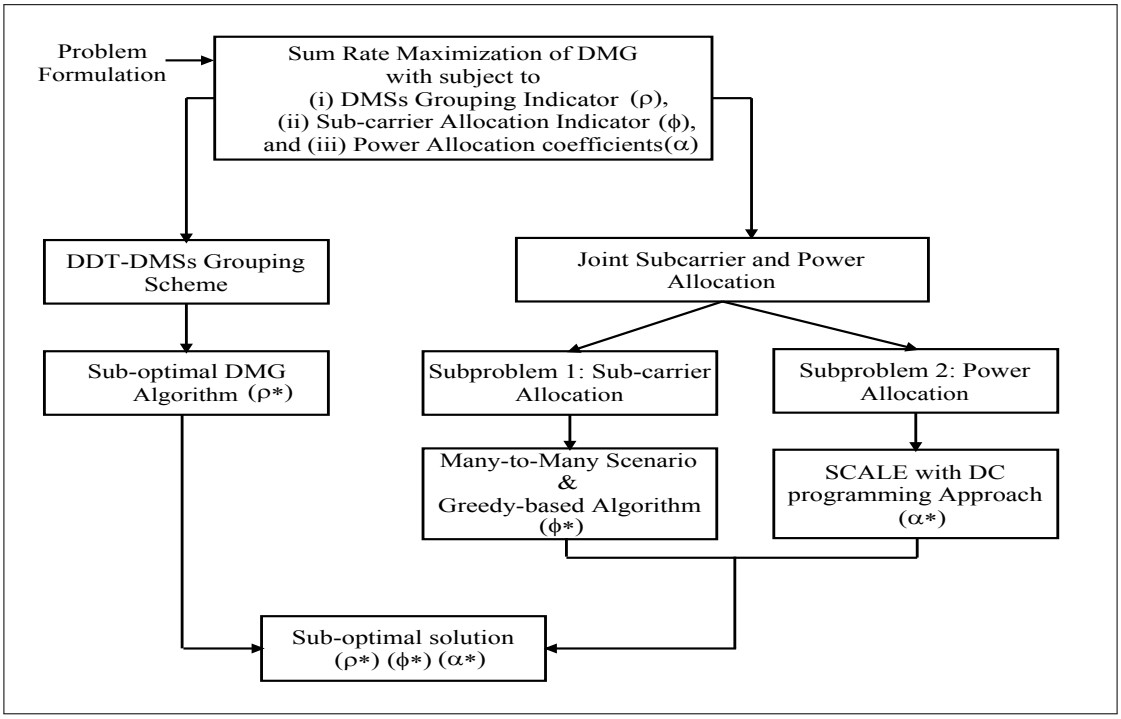

Figure 3.2: Systematic flow of the Proposed Scheme

number of DMGs which share the same RB and $T_{\max}$ is the maximum number of RBs which can be reused by the DMGs. Constraints $\mathbb{C}_{10}$ and $\mathbb{C}_{11}$ ensures the upper limit of the transmission power of CMUs and DDTs, and $\mathbb{C}_{12}$ ensures the non-negative power transmission.

3.2 Proposed Scheme

The optimization problem formulated in Eq. (3.16) is the MINLP problem due to the binary integer and a continuous variable in constraints $\mathbb{C}_5$, $\mathbb{C}_9$, and $\mathbb{C}_{10}$, respectively. Due to this, the problem becomes an NP-hard and cannot be solved directly. Therefore, to solve this problem, we divide it into two sub-problems: (i) DDT-DMUs grouping, and (ii) resource allocation. The resource allocation problem is still combinatorial. So, it is further divided into two sub-sub-problems: (i) RBAP to provide the RBs to CMUs and DMGs, and (ii) PAP to control the power of CMUs and DDTs. To solve the RBAP, the many-to-many mapping scheme is used. Further, to reuse the RBs, the GRSC based Greedy approach is applied. Next, for PAP, DC programming based SCALE is used. The execution of the proposed scheme is as shown in Fig. 3.2.

Algorithm 1 Suboptimal DDT-DMU Grouping Algorithm

Initialization: $r_s, r_w \in \mathcal{R}$ = Indices for strong and weak DMU in each DMG;
Set $G = \{\emptyset\}$; Set of groups; Set $q = 0$; Number of groups formed;
d_{j,r_s} = Distance between the j^{th} DDT and the r_s^{th} DMU;
d_{j,r_s} = Distance between j^{th} DDT and r_w^{th} DMU; and g_{j,r_s},
g_{j,r_w} = Channel gain of the strong and weak DMU from the j^{th} DDT.
Output: $\rho_{j,r}^{n*}$.

$q = 0$
Sort the DMUs in ascending order on the basis of their channel gain.
for $(j = 1, j \leq \mathcal{J}, j{+}{+})$ **do**
  if $(r_s = r_w)$ **then**
    for $(r_s = 1; r_s \leq \mathcal{R}; r_s{+}{+})$ **do**
      for $(r_w = r_s; j \leq \mathcal{R}; r_w{+}{+})$ **do**
        if $(d_{j,r_w} - d_{j,r_s} > 0)$ **then**
          $\Delta\{g_j^{(r_s,r_w)}\} = ||g_{(j,r_s)}| - |g_{(j,r_w)}||$
        else
          $\Delta\{g_j^{(r_s,r_w)}\} \neq ||g_{j,r_w}| - |g_{j,r_s}||;$
        end if
        $q = q + 1;$
        $(r_s, r_w)_c \leftarrow \arg\max\{\Delta\{g_j^{(r_s,r_w)}\}\};$
        $G \leftarrow G \cup (r_s, r_w)_c;$
      end for
    end for
  else
    if $(r_s > r_w)$ **then**
      for $(r_s = 1; r_s \leq \mathcal{R}; r_s{+}{+})$ **do**
        for $(r_w = r_s; j \leq \mathcal{R}/2; r_w{+}{+})$ **do**
          if $(d_{j,r_w} - d_{j,r_s} > 0)$ **then**
            $\Delta\{g_j^{(r_s,r_w)}\} = ||g_{(j,r_s)}| - |g_{(j,r_w)}||$
          else
            $\Delta\{g_j^{(r_s,r_w)}\} \neq ||g_{j,r_w}| - |g_{j,r_s}||;$
          end if
          $q = q + 1;$
          $(r_s, r_w)_c \leftarrow \arg\max\{\Delta\{g_j^{(r_s,r_w)}\}\};$
          $G \leftarrow G \cup (r_s, r_w)_c;$
          The Remaining r_s DMU served by the BS using the OMA
        principle to maintain their minimum data rate requirements.
        end for
      end for
    else
      for $(r_s = 1; r_s \leq \mathcal{R}/2; r_s{+}{+})$ **do**
        for $(r_w = r_s; r_w \leq \mathcal{R}; r_w{+}{+})$ **do**
          if $(d_{j,r_{w1}} - d_{j,r_s} > 0$ && $d_{j,r_{w2}} - d_{j,r_s} > 0)$ **then**
            $\Delta\{g_j^{(r_s,r_{w1})}\} = ||g_{(j,r_s)}| - |g_{(j,r_{w1})}||$
            $\Delta\{g_j^{(r_s,r_{w2})}\} = ||g_{(j,r_s)}| - |g_{(j,r_{w2})}||$
          else
            $\Delta\{g_j^{(r_s,r_{w1})}\} \neq ||g_{j,r_{w1}}| - |g_{j,r_s}||;$
            $\Delta\{g_j^{(r_s,r_{w2})}\} \neq ||g_{j,r_{w2}}| - |g_{j,r_s}||;$
          end if
          $q = q + 1;$
          $(r_s, r_{w1})_q \leftarrow \arg\max\{\Delta\{g_j^{(r_s,r_{w1})}\}\};$
          $(r_s, r_{w2})_q \leftarrow \arg\max\{\Delta\{g_j^{(r_s,r_{w2})}\}\};$
          $G \leftarrow G \cup \{(r_s, r_{w1})_q, (r_s, r_{w2})_q\};$
          The Remaining r_w DMU served by the BS using the OMA
        principle to maintain their minimum data rate requirements.
        end for
      end for
    end if
  end if
end for

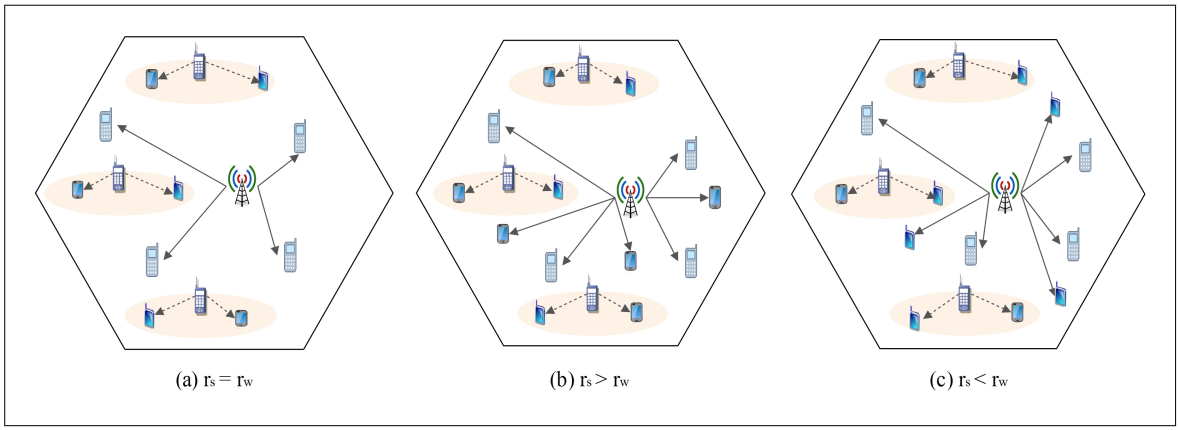

Figure 3.3: (a)-(c) Cases of DDT-DMUs Grouping Scheme

3.2.1 DDT-DMUs Grouping

In this subsection, we optimize the DMU grouping indicator, keeping the RB allocation and power allocation factor constant, i.e., $\phi_{j,i} = \phi^*_{j,i}$, and $\alpha_j = \alpha^*_j$.

$$\begin{aligned} DMG \quad &: \quad \max_{\rho} R_{i+j}(\rho), \\ s.t. \quad &\quad \mathbb{C}_1, \mathbb{C}_2. \end{aligned} \tag{3.17}$$

To optimize the value of ρ, a suboptimal grouping scheme is designed in between the DDT and DMUs to form the DMGs. The main aim of this scheme is to reduce the intra-user interference by properly utilizing the SIC technique. To develop the DMGs, we propose following three cases: (i) $r_s = r_w$, (ii) $r_s > r_w$, and (iii) $r_s < r_w$ shown in Fig. 3.3.

Algorithm 1 suggests the DDT-DMUs grouping scheme. To group the DMUs with the DDT, channel gain and distance between the DDT and DMU have been considered. The DMU near to the DDT have high channel gain whereas, the DMUs far from the DDT have low channel gain. During DMG formation, each DDT uses an equal number of strong and weak DMUs. The detailed execution of Algorithm 1 is as follows: First of all, as per the DMUs channel condition, sort the strong and weak DMUs in descending order, i.e., from the strong to the weak. Now, the DDT computes the difference between the highest channel gain and the lowest channel gain of the DMUs based on their distance from it using Euclidean distance formula. According to this difference, the sum-rate of the strong and weak DMU is calculated. If the sum-rate satisfies the individual SINR requirement of the DMU, then the group is formed between the DDT and their strong and weak DMUs, otherwise, DMUs search the next best DDT to form the group. This process continues until all the groups are not formed. In case, if the number of strong DMUs is larger than the weak DMUs in a cell then after grouping, remaining strong DMUs are served from the BS using OMA to fulfil their minimum data rate requirements. Similarly, if the number of weak DMUs is large in number than the strong DMUs then after grouping,

remaining weak DMUs get the services from the BS using OMA.

3.2.2 Resource Allocation

This subsection covers detailed discussion on RBAP and PAP.

3.2.2.1 RB Allocation Problem

In order to solve the RBAP for both CMUs and DMGs, we assume that the CMUs, and DDTs transmit with power, P_i^n=$P_i^{*n} = \frac{P_i^{n,\max}}{I}$, $\forall \mathcal{I}$, and $P_j^n \alpha_{j,r} = P_j^n \alpha_{j,r}^* = \frac{P_j^{n,\max} \alpha_{j,r}^{\max}}{J}$ across all the RBs. Thus, the problem formulated in Eq. (3.16) can be reformulated as:

$$\begin{aligned} RBAP \quad &: \quad \max_{\phi} R_{(i+j)}^n(\phi), \\ s.t. \quad &\quad \mathbb{C}_4, \mathbb{C}_5, \mathbb{C}_7 - \mathbb{C}_9. \end{aligned} \tag{3.18}$$

The RBAP is a non-convex due to the presence of binary integer $\{0,1\}$ variables and inter-

Algorithm 2 RB Allocation For CMUs

Initialization: $\mathcal{A}_i^n$ = Set of RBs already allocated to CMUs; $\mathcal{B}_i^n$ = Subset of CMUs that allowed to use RBs; N = Set of unused RBs, $\forall N \in \mathcal{N}$; Set $R_{i,b}^n = 0$; Initial value of achievable data rate of i^{th} CMU.

Output: $n^* \leftarrow i^*$.

```
while (A_i^n ≠ ∅ && ∃B_i^n ≠ ∅) do
    for (i = 0, i ≤ I, i++) do
        i* ← arg max R_{i,b}^n.
    end for
    for (n = 0, n ≤ N, n++) do
        n* ← arg max g_{i*,b}^n.
    end for
    Allocate n* ← i*.
    Update A_i^n, B_i^n & N.
    Compute R_{i*,b}^{n*} using (3.10).
    Set R_i^n = R_i^n + R_{i*}^{n*}.
end while
```

ference term in denominator of $R_{(i+j)}^n(\phi)$. The exhaustive search method is suitable to solve this type of problem. However, the complexity of this method increases exponentially with an increase in the number of DMGs, which makes it unsuitable for the ultra-dense networks. Therefore, to reduce the complexity and to make the problem tractable, we use the many-to-many mapping scheme for RB allocation of both the CMUs and DMGs. Further, to fully exploit the potential benefits of multiple DMGs, the GRSC based Greedy approach is used to reuse the RBs already occupied by the CMUs.

The detailed discussion on the RB allocation for CMUs is given in the Algorithm 2. Here,

our goal is to fulfil the minimum required data rate of all CMUs by allocating RBs to them. Therefore, firstly we compute the data rate of $\mathcal{I}$ CMUs. Then we search the n RBs as per their highest channel gain and allocate n^*, the highest channel gain RBs to i^* CMUs to provide them with the maximum achievable data rate. This process continues until all the RBs are allocated to the CMUs. The complexity of Algorithm 2 is $\mathcal{O}(N\mathcal{I})$, which means that it takes at most $N\mathcal{I}$ times to complete the task.

In Algorithm 3, the RBs are allocated to the DMGs. In this, first of all, the channel gain of RBs and the data rate of all j DMGs are computed. Then we identified S_{max}, the set of DMGs having higher data rate among the j DMGs. Then the n^* highest channel gain RB to S_{max} DMGs from the set of $\mathcal{F}_j^n$ is computed. Here, S_{max} represents the upper limit of DMGs allotted to each RB. The complexity of Algorithm 3 is $\mathcal{O}(N\mathcal{J}\mathcal{R})$.

Algorithm 4 improves the data rate of DMGs by reusing the RBs which are already occu-

Algorithm 3 RB Allocation For DMGs

Input: $n^* \leftarrow i^*$; RBs allocated to CMUs.
Initialization: $\mathcal{E}_j^n$ = Set of RBs already allocated to DMGs; $\mathcal{F}_j^n$ = Subset of DMGs that allowed to use RBs; N = Set of unused RBs, $\forall N \in \mathcal{N}$; Set $R_{j,r}^n$ is the achievable data rate of j^{th} DMG; Set S_{max} is the maximum limit of DMGs allocated to each RB.
Output: $n^* \leftarrow j^*$

1: **while** $(\mathcal{E}_j^n \neq \emptyset \;\&\&\; \exists \mathcal{F}_j^n \neq \emptyset)$ **do**
2: **for** $(n = 1, n \leq \mathcal{N}, n{+}{+})$ **do**
3: Compute $n^* \leftarrow arg\max\ g_{j,r}^n$;
4: **for** $(j = 1, j \leq \mathcal{J}, j{+}{+})$ **do**
5: **for** $(r = 1, r \leq \mathcal{R}, r{+}{+})$ **do**
6: Compute $j^* \leftarrow arg\max R_{j,r}^n$
7: Compute $S_{\max} \leftarrow \{j^*\}$
8: **if** $(\sum_{j=1}^{J} \phi_{j,i}^n \leq S_{\max})$ **then**
9: Allocate $n^* \leftarrow S_{\max}$;
10: Set $\mathcal{F}_j^n = \mathcal{F}_j^n - S_{\max}$;
11: **end if**
12: **end for**
13: **end for**
14: **end for**
15: Update $\mathcal{E}_i^n, \mathcal{F}_i^n,\ \&\ N$.
16: **end while**

pied by the CMUs. Firstly, we sort the DMGs which are not using the T_{max} RBs (line number 4). DMGs allowed reusing the T_{max} RBs those already occupied by CMU if following conditions are satisfied: (i) the data rate of the DMGs must be improved, and (ii) the minimum required data rate of CMUs cannot be degraded. Without violation of any conditions, reuse of the $T_{\max}$ RBs is terminated. The process continued for the next DMGs available in sequence. Also, when the CMU is not occupied by the $T_{\max}$ RBs, then the set of sorted DMG reuse the $T_{\max}$ RBs until it improves the sum-rate of the DMUs available in DMGs. Reuse of the n^{th} RB terminates if it fails to provide an improvement in the sum-rate. This process continued for the

Algorithm 4 GRSC based RB resue Algorithm

Initialize $\mathcal{A}_i^n$ = Set of RBs already allocated to CMUs; $\mathcal{E}_i^n$ = Set of RBs already allocated to DMGs; $\mathcal{F}_i^n$ = Subset of DMGs that allowed to reuse $T_{\max}$ RBs; H_{i+j}^n = Subset of CMU $\cup$ DMGs that allowed to reuse $T_{\max}$ RBs; $\tilde{\mathcal{D}}$ = Set of DMGs want to reuse the $T_{\max}$ RBs; and set $n^* \leftarrow i^*$, and $n^* \leftarrow j^*$.

Output: Reuse n^*.

1: **for** $(n = 1; n \leq T_{\max}; n{+}{+})$ **do**
2: Set $i^* \leftarrow \{i : T_{\max} \in \mathcal{A}_i^n\}$.
3: Set $\tilde{\mathcal{D}} = \mathcal{D}$.
4: Select $j^* = arg\max \frac{g_{j,r}^n}{\sum_{h \in H_{i+j}^n} g_{j,h}^n}, \forall j \in \tilde{D}$.
5: Allocate $n \leftarrow j^*$.
6: Calculate $\Delta\bar{R}_{i+j}^n$ using (15).
7: **if** $(i^* \neq \emptyset)$ **then**
8: Recompute R_{b,i^*}^n using (9).
9: **if** $(\Delta\bar{R}_{i+j}^n > 0$ && $R_{b,i^*}^n \geq R_{b,i^*}^{n,req})$ **then**
10: $n \leftarrow j^*$.
11: Update E_i^n, F_i^n, H_{i+j}^n, & $T_{\max}$.
12: $R_j^n = R_j^n + R_{j^*}^n$;
13: $\tilde{D} = \tilde{D} - \{j^*\}$.
14: Go to Line 4.
15: **else**
16: **if** $(\Delta\bar{R}_{i+j}^n \leq 0$ || $R_{i^*}^n < R_{i^*}^{n,req})$ **then**
17: Go to Line 1
18: **end if**
19: **end if**
20: **else**
21: **if** $(i^* = 0)$ **then**
22: **if** $\Delta\bar{R}_{i+j}^n > 0$ **then**
23: $n \leftarrow i^*$
24: Update E_i^n, F_i^n, H_{i+j}^n, & $T_{\max}$.
25: $R_j^n = R_j^n + R_{j^*}^n$;
26: $\tilde{D} = \tilde{D} - \{j^*\}$.
27: Go to Line 4.
28: **else**
29: **if** $\Delta\bar{R}_{i+j}^n \leq 0$ **then**
30: Go to Line 1.
31: **end if**
32: **end if**
33: **end if**
34: **end if**
35: **end for**

next DMGs available in sequence.

Thus, to check whether the reuse of $T_{\max}$ RB improves the data rate of DMGs or not, the following equation is used.

$$\Delta R_j^n = \sum_{n=1}^{T_{max}} \Bigg[\log_2 \left(1 + \frac{P_j^{n,max} g_{j,r}^n}{\sum_{h \in H_{i+j}^n} g_{j,h}^n + \sigma^2} \right) + \sum_{h \in \mathcal{F}_j^n} \log_2 \left(1 + \frac{P_h^{n,max} g_{h,r}^n}{P_j^{n,max} g_{j,h}^n + \sum_{h' \neq h}^{H_{i+j}^n} P_h^{n,max} g_{h,r}^n + \sigma^2} \right)$$

$$- \sum_{h \in \mathcal{F}_j^n} \log_2 \left(1 + \frac{P_h^{n,max} g_{h,r}^n}{\sum_{h' \neq h}^{H_{i+j}^n} P_h^{n,max} g_{h,r}^n + \sigma^2} \right) \Bigg]. \tag{3.19}$$

The complexity of Algorithm 4 is $\mathcal{O}(N\mathcal{R})$.

3.2.2.2 Power Allocation Problem

The closed-form expression of each DMU power is required to improve the sum-rate of the network. After RB allocation, it has been observed that the problem in (3.16) is still non-convex due to co-channel interference. So, to address it, the DC programming based SCALE [318] approach is used.

$$\begin{aligned} PAP\ 1 \quad &: \quad \max_{\alpha} \sum_{n=1}^{\mathbb{N}} \sum_{j=1}^{J} R_j^n(\alpha), \\ s.t. \quad &\quad \mathbb{C}_3, \mathbb{C}_6, \mathbb{C}_{10} - \mathbb{C}_{12}. \end{aligned} \tag{3.20}$$

According to equation (3.14), the PAP can be rewritten as follows:

$$\begin{aligned} PAP\ 1 \quad &: \quad \max_{\alpha} \sum_{n=1}^{\mathbb{N}} \left(R_{j,r_s}^n + R_{j,r_w}^n \right), \\ s.t. \quad &\quad \mathbb{C}_3, \mathbb{C}_6, \mathbb{C}_{10} - \mathbb{C}_{12}. \end{aligned} \tag{3.21}$$

Now, the Eq. (3.21) in DC function [319] using constraint $\mathbb{C}_6$ is written as follows:

$$= \sum_{n=1}^{\mathbb{N}} \log_2 \left(\frac{|g_{j,r_s}^n|^2 P_j \alpha_{j,r_s} + I_{j,r_s}^{co} + I_{j,r_s}^{cr} + \sigma^2}{I_{j,r_s}^{co} + I_{j,r_s}^{cr} + \sigma^2} \right) - \log_2 \left(\frac{|g_{j,r_w}^n|^2 P_j \alpha_{j,r_w} + I_{j,r_w}^{no} + I_{j,r_w}^{co} + I_{j,r_w}^{cr} + \sigma^2}{I_{j,r_w}^{no} + I_{j,r_w}^{co} + I_{j,r_w}^{cr} + \sigma^2} \right), \tag{3.22}$$

$$= g_j(\alpha) - f_j(\alpha), \tag{3.23}$$

where $g_j(\alpha)$ and $f_j(\alpha)$ are the concave functions and is expressed as follows:

$$g_j(\alpha) = \sum_{n=1}^{\mathbb{N}} \left(\log_2(|g_{j,r_s}^n|^2 P_j \alpha_{j,r_s} + I_{j,r_s}^{co} + I_{j,r_s}^{cr} + \sigma^2) - \log_2(I_{j,r_s}^{co} + I_{j,r_s}^{cr} + \sigma^2) \right), \tag{3.24}$$

$$f_j(\alpha) = \sum_{n=1}^{\mathbb{N}} \left(\log_2(|g^n_{j,r_w}|^2 P_j \alpha_{j,r_w} + I^{no}_{j,r_w} + I^{co}_{j,r_w} + I^{cr}_{j,r_w} + \sigma^2) - \log_2(I^{no}_{j,r_w} + I^{co}_{j,r_w} + I^{cr}_{j,r_w} + \sigma^2) \right). \tag{3.25}$$

Now, the Eq.(3.24) and Eq.(3.25) are expressed as follows:

$$g_j(\alpha) = \sum_{n=1}^{\mathbb{N}} (\log_2(|g^n_{h,r_s}|^2 P_h \alpha_{h,r_s}) - \log_2(I_{h,r_s} + \sigma^2). \tag{3.26}$$

$$f_j(\alpha) = \sum_{n=1}^{\mathbb{N}} (\log_2(|g^n_{h,r_w}|^2 P_h \alpha_{h,r_w}) - \log_2(I_{h,r_w} + \sigma^2), \tag{3.27}$$

where $h = (i \cup j)$.

Similar to $\mathbb{C}_6$, the constraint $\mathbb{C}_3$ in a DC form is expressed as follows:

$$\sum_{i=1}^{I} \sum_{n=1}^{\mathbb{N}} R^n_{i,b} = \sum_{i=1}^{I} \sum_{n=1}^{\mathbb{N}} \log_2 \left(1 + \frac{P_i |g^n_{i,b}|^2}{\sum_{j=1}^{J} \phi^n_{j,i} P_j |g^n_{j,i}|^2 + \sigma_i^2} \right),$$

$$= g_i(P) - f_i(P), \tag{3.28}$$

The expression for $g_i(P)$ and $f_i(P)$ are given as follows:

$$g_i(P) = \sum_{n=1}^{\mathbb{N}} \log_2 \left(P_i |g^n_{i,b}|^2 + \sum_{j=1}^{J} P_j |g^n_{j,i}|^2 + \sigma_i^2 \right). \tag{3.29}$$

$$f_i(P) = \sum_{n=1}^{\mathbb{N}} \log_2 \left(\sum_{j=1}^{J} P_j |g^n_{j,i}|^2 + \sigma_i^2 \right). \tag{3.30}$$

As $h = (i \cup j)$, therefore, the Eq. (3.29) is rewritten as follows:

$$g_i(P) = \sum_{n=1}^{\mathbb{N}} \log_2 \left(P_{h,i} |g^n_{h,i}|^2 + \sigma_i^2 \right). \tag{3.31}$$

Now, the gradient of $f_i(P)$ and $f_j(\alpha)$ is expressed as follows [320] [321]:

$$\nabla f_i(P) = \sum_{n=1}^{\mathbb{N}_i} \left(\frac{1}{\sum_{j=1}^{J} P_{j,i} |g^n_{j,i}|^2 + \sigma^2} \right) \vec{e}_i. \tag{3.32}$$

$$\nabla f_j(\alpha) = \sum_{n=1}^{\mathbb{N}_j} \left(\frac{1}{\sum_{h \in H} |g^n_{h,r_w}|^2 P_h \alpha_{h,r_w}} - \frac{1}{I_{h,r_w} + \sigma^2} \right) \vec{e}_j, \tag{3.33}$$

where $\vec{e}_i$ and $\vec{e}_j$ are column vector with $\mathcal{N}(\mathcal{I} + \mathcal{J})$ elements which are defined as follows:

$$\vec{e}_i = \begin{cases} \frac{|g^n_{j,i}|^2}{\ln 2}, & j \in \mathcal{J}, n \in \mathbb{N}, \\ 0, & \text{otherwise.} \end{cases} \text{ and } \vec{e}_j = \begin{cases} \frac{|g^n_{h,r_w}|^2}{\ln 2}, & h \in H, n \in \mathbb{N}, \\ 0, & \text{otherwise.} \end{cases}$$

An iterative sequence of $\{P^t\}$ and $\{\alpha^t\}$ alongwith the first order Taylor expansion of approximate $f_i(P)$ and $f_j(\alpha)$ can be expressed as follows:

$$f_i(P) \approx f_i(P^t) + \nabla f_i^T(P^t)(P - P^t), \tag{3.34}$$

$$f_j(\alpha) \approx f_j(\alpha^t) + \nabla f_j^T(\alpha^t)(\alpha - \alpha^t). \tag{3.35}$$

Therefore, the *PAP* 2 in (3.21) is reformulated as follows:

$$\begin{aligned} PAP\ 2 \quad &: \quad \sum_{j=1}^{J} g_j(\alpha) - f_j(\alpha^t) - \nabla f_j^T(\alpha^t)(\alpha - \alpha^t), \\ s.t.\ \mathbb{C}_1 \quad &: \quad g_i(P) - f_i(P^t) - \nabla f_i^T(P^t)(P - P^t) \geq R_i^{min}, \\ &: \quad \mathbb{C}_{10} - \mathbb{C}_{12}. \end{aligned} \tag{3.36}$$

The *PAP* 2 in Eq. (3.36) becomes a standard convex optimization problem that can be solved using Algorithm 5. Execution of Algorithm 5 is given as follows:

Algorithm 5 consists of two stages. (i) Initialization stage, and (ii) Updated stage. In

Algorithm 5 Power Allocation Algorithm for CMUs and DMGs

Input: $\mathcal{I} \in \{1,2,...,i,...,I\}$ =Number of CMUs; $\mathcal{J} \in \{1,2,...,j,...,J\}$ = Number of DMGs; $\mathcal{N} \in \{1,2,...,n,...,N\}$ = Number of RBs; and α_j = Power allocation factor.
Initialization: ε_{max}=Maximum Tolerance value; δ_{max}= Maximum number of Iterations; $\delta = 0$=Iteration index; Set $R(0) = \sum_{j=1}^{J} g_j(\alpha(0)) - f_j(\alpha(0))$ at $\alpha(0)$.
Output: α_j^*.

1: **repeat**
2: Compute $\nabla f_j(P)$ and $\nabla f_i(\alpha)$ using (3.32) and (3.33).
3: Solve (3.36) to obtain α_j^*.
4: $\delta = \delta + 1$.
5: Obtain $\alpha_j^\delta = \alpha_j^*$.
6: Compute $R^\delta = \sum_{j=1}^{J} g_j(\alpha^\delta) - f_j(\alpha^\delta)$
7: **until** $|R^\delta - R^{\delta-1}| \leq \varepsilon_{max}$.

the initialization stage, the value of the $R(0)$ is computed at $\alpha(0)$, where $\alpha(0)$ is the power allocation factor at zero. On the other side, in the updated phase, first of all, the value of $\nabla f_i(P)$ and $\nabla f_j(\alpha)$ are computed using Eq. (3.32) and Eq. (3.33), respectively. Then the optimal power allocation factor, i.e., α_j is computed using Eq. (3.36). The procedure continues until the difference between the values of R_j^n in the current iteration and that between the previous iteration is less than the maximum threshold value.

To solve the PAP formulated in Eq.(3.36), we used interior-point method. The interior-point method complexity is estimated as $\mathcal{O}(\upsilon^{1/2}(\upsilon + \phi)\phi^2)$. In this expression, ϕ and υ represents the number of variables and inequality constraints. After solving the PAP formulated in Eq. (3.36), we find that the complexity is $\mathcal{O}((N(I+J)+2I+J)^{1/2}(2N(I+J)+I+2J)(I+J)^2N^2)$.

Theorem 1. *The SCALE based DC programming approach proposed in Algorithm 5 provides a sequence of appropriate solutions for convergence to a global optimal solution* α^*.

Proof. According to [319], [320] if $f_i(P)$ becomes the concave function, then its super gradient $\nabla f_i(P)$ is expressed as follows.

$$f_i(P) + f_i(P^t) + \nabla f_i^T(P^t)(P - P^t). \tag{3.37}$$

Now, it is proved that, if $g_i(P) - f_i(P^t) - \nabla f_i^T(P^t)(P - P^t) \geq R_i^{n,min}$, then $g_i(P) - f_i(P) \geq R_i^{n,min}$. It ensure that the solution obtained during each iteration must lie with in a feasible region.

Similarly, if the function $f_j(\alpha)$ becomes concave, then its super gradient $\nabla f_j(\alpha)$ given as follows.

$$f_j(\alpha) + f_j(\alpha^t) + \nabla f_j^T(\alpha^t)(\alpha - \alpha^t). \tag{3.38}$$

Now, we have

$$\begin{aligned} R_j^{t+1} &= \sum_{j=1}^{J} \left[g_j(\alpha^{t+1}) - f_i(\alpha^{t+1}) \right] \\ &\geq \sum_{j=1}^{J} \left[g_j(\alpha^{t+1}) - f_i(\alpha^t) - \nabla f_j^T(\alpha^t)(\alpha^{t+1} - \alpha^t) \right] \\ &\geq \sum_{j=1}^{J} \left[g_j(\alpha^t) - f_i(\alpha^t) - \nabla f_j^T(\alpha^t)(\alpha^t - \alpha^t) \right] \\ &= \sum_{j=1}^{J} \left[g_j(\alpha^t) - f_i(\alpha^t) \right]. \end{aligned} \tag{3.39}$$

Eq. (3.39) shows that the data rate of DMGs should be either improved or remains the same at each iteration. The data rate is improved only when the constraint formulated in $PAP:1$ must be compact and the value obtained during each iteration from the solution of $PAP:3$ should be located within a feasible region. The power allocation technique used in Algorithm 4 finally provides the optimal power allocation α^*. □

The Algorithm 6 consists of two steps. (i) Initialization step and (ii) RB and power allocation factor step. In the initialization step, the CSI is sent by the DMUs and CMUs to DDTs and BS, respectively. Then the groups are formed using the Algorithm 1 to apply the NOMA so that sum-rate of DMGs can be improved. Afterwards, RBs are allotted to the CMUs and DMGs from Algorithms 2, 3, and 4 using the current power allocation factor α. Lastly, the α^* is estimated from the Algorithm 5 based on ϕ. This process continues up to the maximum number of iterations δ_{max} until the maximum sum-rate is achieved.

Algorithm 6 Joint User Grouping and Resource Allocation Algorithm

Input: $\rho_{j,r}$ = DDT-DMUs grouping indicator; α_j = Power allocation factor; and $\phi_{j,i}$ = RB allocation factor.

Initialization: $\delta = 0$; Iteration index; δ_{max}; Maximum number of Iterations; and BS estimate the CSI of all the CMU, DDTs, and DMUs using their pilot signals.

Output: $\phi^*_{j,i}, \alpha^*_j$.

1: **for** $(\delta = 1; \delta \leq \delta_{max}; \delta{+}{+})$ **do**
2: Call Algorithm 6 to develop the DMGs.
3: Call Algorithm 1, 2, and 3 to update the RB allocation factor $\phi_{j,i}$.
4: Call Algorithm 4 to update α at given ϕ.
5: **end for**

3.3 Performance Evaluation

In this section, the performance of the proposed scheme is evaluated. This section consists of two subsections (i) Numerical settings, and (ii) Results and Discussion.

3.3.1 Numerical Settings

The parameters used in simulation are based on 3GPP urban path loss model (Release 15 and RAN1) [322], [323] as shown in Table 3.1. Assume a hexagonal cell of inter-site distance 500 m in which the BS is situated at the centre, and the DDTs and CMUs are uniformly distributed. Further, consider that the BS, CMUs and DDTs are equipped with an Omni-directional single antenna. To design the DMG we adopt the grouped distribution model [324]. According to the grouped distribution model, DDT is situated at the centre, and DMUs are uniformly distributed within a disk. We also assume that both the CMUs and DMUs are moving with a very low velocity. We used the RB with 180 kHz wide in frequency. The RBs are either 12×15 KHz or 24×7.5 kHz subcarriers. The number of subcarriers used per RB for the channels and signals is 12, as used in [325], [326], [327]. To show the effectiveness of the proposed scheme, we compared it with the existing joint user clustering and power allocation (JUCPA) [60], and joint spectrum and power allocation (JSPA) [328].

3.3.2 Results and Discussion

3.3.2.1 Convergence Analysis

Fig.3.4(a) represents the cumulative distribution function with the number of iterations. The graph shows the convergence behaviour of the Algorithms 1, 2 and 3 with different number of DMGs. The plotted CDF shows that the proposed RB allocation algorithm takes a lesser number of iterations to converge. For example, when the number of DMGs in a cell is 9, on an average 40, the number of iterations is used by the proposed algorithm to converge. Moreover, the graph shows that when the number of DMGs in a cell increases, the number of iteration

Table 3.1: Simulation Parameters

Parameters	**Values**
Cell Layout	Hexagonal
Radius of cell (Inter-site Distance)	500 m
Radius of DMG	10∼50 m
Number of CMUs ($\mathcal{I}$)	1∼16
Number of DMGs ($\mathcal{J}$)	1∼16
Bandwidth (B)	180KHz
Subcarrier spacing (w)	15 KHz
One Resource block	12 subcarriers
Number of RBs ($\mathcal{N}$)	10
SINR threshold of CMU (I_i^{th})	5 dBm
Number of DMUs in each DMG ($\mathcal{R}$)	4
Maximum Transmit power of DMGs ($P_j^{\max}$)	25 dBm
Maximum Transmit power of CMU ($P_i^{\max}$)	25 dBm
Noise power spectrum density, (N_o)	-174 dBm
DMU Noise figure	5 dB
Maximum error tolerance (ε)	10^{-4}
Minimum data rate requirement of CMU ($R_{i,b}^{n,\min}$)	5∼20 bps/Hz.
Minimum data rate requirement of DMUs in each DMG ($R_{j,r}^{n,\min}$)	5∼20 bps/Hz.
Multipath fading	Unit Mean
Log-Normal Shadowing Standard Deviation	8 dB
User speed	Very Low velocity

steps also increases. The reason behind such behaviour is that the probability of reusing the RBs increases which result in an increase in the iteration steps.

Fig.3.4(b) shows the convergence behaviour of the Algorithm 4 with respect to the data rate requirements of DMGs. The graph shows that an optimal power allocation is achieved for the small number of iterations, but as the data rate requirements of DMGs increases, the convergence rate also decreases. The reason behind such behaviour depends upon the availability of RBs. When the data rate requirements of DMGs increases then they have to reuse the best possible RB as per its availability to meet their data rate requirements. As the number of DMGs in a cell increases, the possibility to find the best RB decreases due to an increase in co-channel interference. As a result, the data rate of DMGs starts decreasing and gets saturated after a certain number of iteration steps.

The graph plotted in Fig.3.4(c) describes the convergence behavior of the CMUs with respect to their minimum data rate requirements, i.e., $R_{i,b}^{n,\min} = 5\ bps/Hz$. It implies that the CMUs within a small number of iterations converge to the minimum required data rate. The reason behind such behaviour is the availability of a large number of spectrum resources for CMUs. CMUs are primary ones which access the best possible RB based on channel gain to meet their minimum data rate requirements.

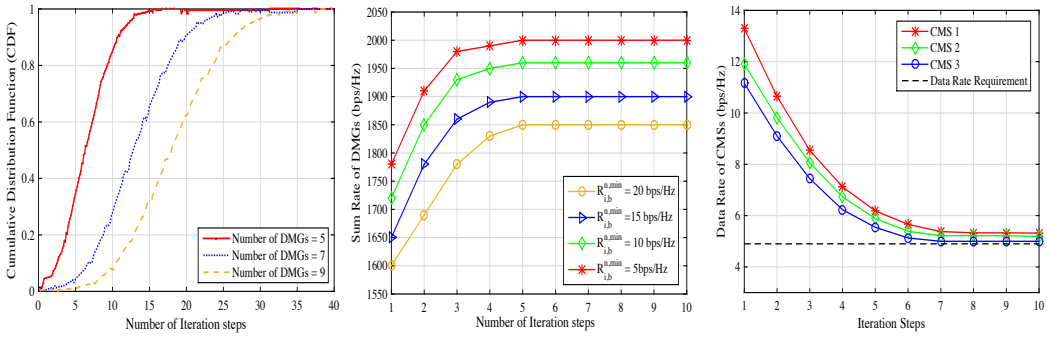

Figure 3.4: Comparative Analysis (a) Convergence behaviour of the RB allocation algorithms in terms of CDF at $P_j = 10 \sim 15dBm$ (b) Convergence testing of the sum-rate of DMGs at $\mathcal{I} = 4$, $\mathcal{J} = 5$, $\mathcal{N} = 4$, and $P_i^{\max} = P_j^{\max} = 25dBm$ (c) Convergence testing of the data rate of CMUs at $\mathcal{I} = 4$, $\mathcal{J} = 5$, $\mathcal{N} = 4$, $P_i^{\max} = P_j^{\max} = 25dBm$, & $R_{j,r}^{n,\min} = 5bps/Hz$.

3.3.2.2 Comparison of the proposed Scheme with the state-of-the art schemes

We compared the proposed scheme with the pre-existing NOMA and OFDMA schemes. The results obtained are discussed as follows.

Fig. 3.5(a) shows the effect on the sum-rate of DMGs with an increase in the number of DMGs in a cell. The results show that as the number of DMGs in a cell increases, the sum-rate of the DMGs increases. This is due to the fact is that as the number of DMGs in a cell increases, the best possible RB is allotted to it using the Algorithm 3 in the proposed scheme. But, after a certain increase in the number of DMGs, the sum-rate of DMGs becomes saturated. The reason behind this change is an increase in co-channel interference. Moreover, the results obtained show that when the number of DMGs in a cell increases up to 12, then the proposed scheme has 4.54% and 22.72% higher sum-rate than the JUCPA and JSPA, respectively. The reason behind this is that the proposed scheme handles co-channel interference much better than the JUCPA and JSPA. Also, in JUCPA, the problem of intra-user interference among CMUs is severe along with co-channel over RBs, and in JSPA the D2D can access only one RB due to OFDMA technique.

Fig. 3.5(b) depicts the effect on the sum-rate of DMGs with an increase in the number of CMUs in a cell. The results obtained show that as the number of CMUs in a cell increases, the sum-rate of DMGs starts decreasing. The reason for such behaviour is due to the fact that when the number of CMUs in a cell increases, they capture a large part of spectrum resources to attain their minimum required data rate. As a result, only a few numbers of resources remains left for DMGs due to which the problem of the cross and co-channel interference becomes severe and sum-rate gets degraded. However, the results obtained shows that when the number of CMUs in a cell increases up to 12, the proposed scheme has 2.78% and 22.22% higher sum-rate than JUCPA and JSPA, respectively. The reason behind such a behaviour is that we have used the many-to-many mapping among RBs and DMGs whereas, in JUCPA, the one-to-many,

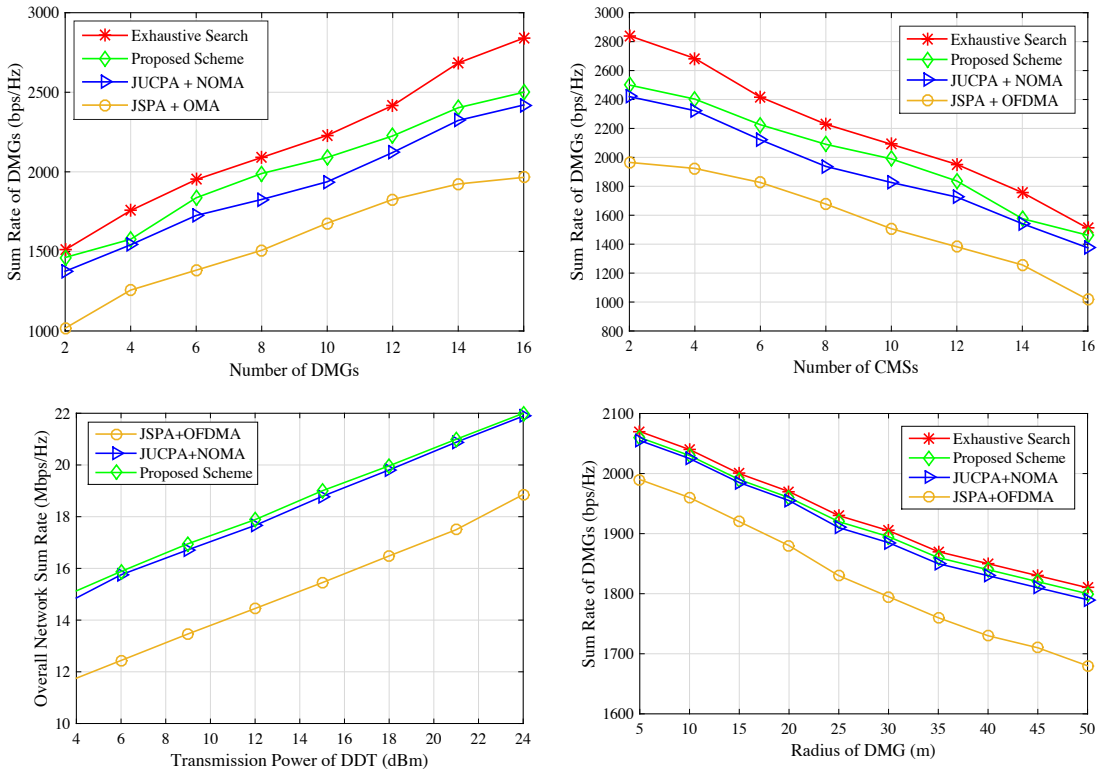

Figure 3.5: Comparative Analysis (a) Impact on the sum-rate of DMGs versus number of DMGs. (b) Impact on the sum-rate of DMGs with respect to the number of CMUs (c) Impact on sum-rate with respect to DDT transmit power (d) Variation in sum-rate with respect to the radius of DMGs at $P_i^{\max} = P_j^{\max} = 25dBm$.

and JSPA, the one-to-one mapping among RBs and DMGs is used.

Fig. 3.5(c) shows the effect of DDT transmit power on the overall sum-rate of the network. It can be observed from the results obtained that when the DDT transmits with the fixed power allocation coefficient, then the lower sum-rate is as observed in Fig. 3.5(c). On the other side, when the DDT transmits with the dynamic power allocation coefficients then the proposed scheme has better sum-rate as compared to that of JUCPA and JSPA, respectively. The reason for such behaviour is due to the fact that with the dynamic power allocation coefficients, an improved SINR is received at the DMUs. The graph obtained in 3.5(c) clearly shows that when the transmission power of DDT becomes 15dBm, the proposed scheme provides 1.136% and 18.69% higher sum-rate in comparison to the JUCPA and JSPA. The reason behind this is that in the proposed scheme, we optimized the transmit power of both the DDT and CMU whereas, in JUCPA and JSPA only the transmit power of DDT is optimized.

Fig. 3.5(d) depicts the effect on the sum-rate of DMGs with variation in its radius. The results show that when the radius of the DMG increases, the sum-rate starts decreasing. The reason for such behaviour is due to the fact that as the radius increases, the distance between DDT and their respective DMUs increases due to which SINR decreases. Also, the graph

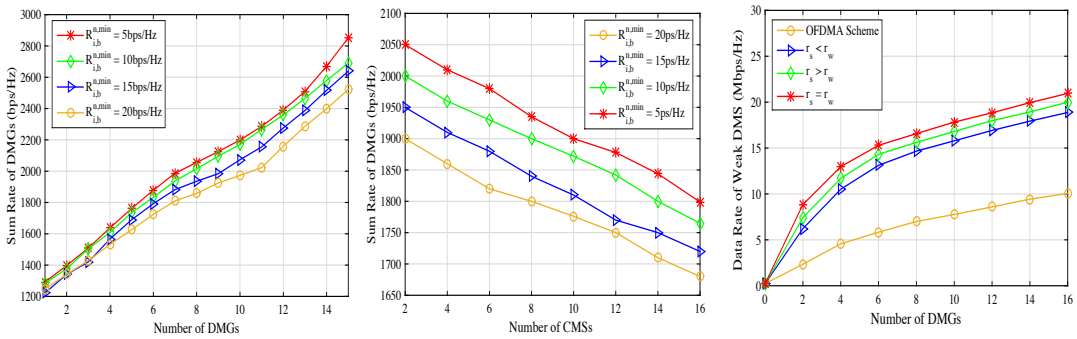

Figure 3.6: Comparative Analysis (a) Sum rate of DMGs versus number of CMUs at different values of $R_{i,b}^{n,\min}$ (b) Sum rate of DMGs versus number of DMGs at different values of $R_{i,b}^{n,\min}$ (c) Data Rate of Weak DMU versus Number of DMGs.

shows that when the radius of DMG reaches up to 25m then the proposed scheme has 0.5181% and 4.667% higher sum-rate than the JUCPA and JSPA, respectively. This happened because the proposed scheme uses NOMA technique to provide the communication between DDT and their respective DMUs whereas, in JUCPA and JSPA, OFDMA technique is used for D2D communication. In NOMA, the large power is allocated to the far users due to which sum-rate of the DMG increases with an increase in its radius.

3.3.2.3 Impact on the Sum-rate of DMGs at different conditions

Fig. 3.6(a) shows the impact on the sum-rate of DMGs with an increase in the number of DMGs under different data rate requirements of CMUs. The results obtained shows that as the data rate requirement of CMUs increases along with an increase in the number of DMGs, the sum-rate of DMGs starts decreasing. The reason for such behaviour is due to the fact that with an increase in data rate requirements of CMUs, the demand to occupy the spectrum resources by the CMUs increases. As a result, the small number of spectrum resources remains available for DMGs due to which the problem of co-channel interference becomes severe.

Fig. 3.6(b) shows the impact on the sum-rate of DMGs with the number of CMUs with their different data rate requirements. The result obtained shows that when the number of CMUs in a cell increases, the problem of cross channel interference in between the CMUs and DMGs becomes severe. Also, only a few numbers of resources remain available for DMGs which results in a monotonically decrease in sum-rate of the DMGs.

Fig. 3.6(c) shows the impact on the data rate of weak DMUs to the number of DMGs in a cell. The results show that for $r_s = r_w$, data rate of weak DMUs is larger as compared to the $r_s > r_w$, and $r_s < r_w$. The reason for such behaviour is due to the fact that when $r_s = r_w$, the weak DMUs gets the services from the DDT using the NOMA technique while in rest of the cases if the number of weak DMUs is larger in number, they get the services from the BS using OFDMA.

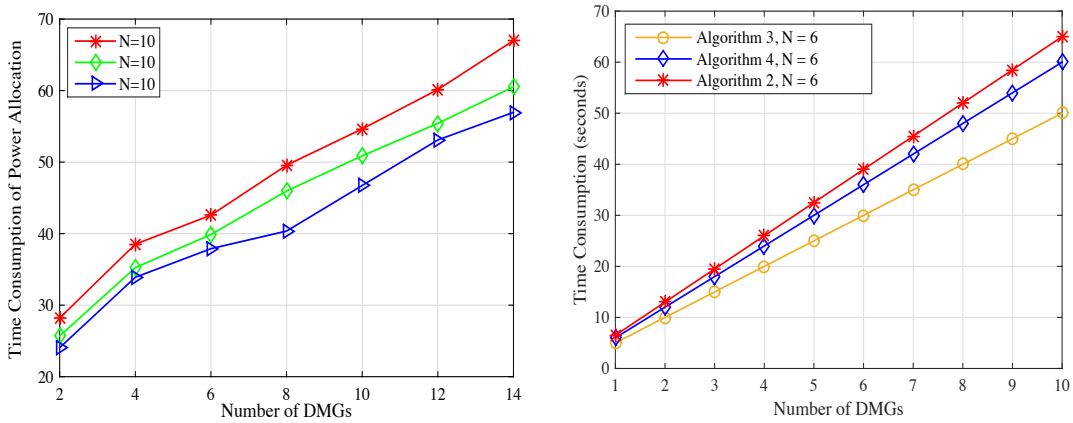

Figure 3.7: Comparative Analysis (a) Time consumed by the Algorithm 4 versus the number of DMGs (b) Time consumotion of Algorithm 2, 3, and 4 versus Number of DMGs.

3.3.2.4 Impact on time consumption

Fig. 3.7(a) shows the time consumption of the Algorithm 4 with an increase in the number of DMGs in a cell. The results show that when the number of DMGs in a cell increases, the time taken to execute the Algorithm 4 monotonically increases. This happened because with an increase in the number of DMGs, the cross and co-channel interference across each RBs increases. As a result, the time taken to optimize the power of CMUs and DDTs increases, hence, the time complexity increases.

Fig. 3.7(b) shows the time consumption of the Algorithms 1, 2, and 3 with an increase in the number of DMGs at a fixed number of RBs. The results obtained show that the time consumed by the proposed algorithms increases linearly with an increase in the number of DMGs in a cell. This is due to the fact is that with an increase in the number of DMGs, it becomes difficult among the DMGs to reuse the best possible RB.

3.4 Summary

In this chapter, we maximize the sum-rate of the DMGs while maintaining the SINR of the CMUs. To achieve the goal, the joint user grouping and resource allocation scheme are designed. For user grouping, a low complexity based sub-optimal user grouping scheme in between the DDT and DMUs is designed. Then the resource allocation is proposed for both the CMUs and DMGs. To allocate the RBs to both the CMUs and DMGs, we used the many-to-many mapping scheme. Then to fully utilize the potential benefits of DMGs, the GRSC based RB reuse algorithm is designed, in which the DMGs can exchange the RBs among each other based on their channel conditions to maximize the sum rate. Also, for power allocation of DDT, we use SCALE with DC function. The evaluated results demonstrated that the proposed scheme achieves better sum-rate than the existing JUCPA and JSPA scheme.

Chapter 4

Energy-Delay Tradeoff Scheme for NOMA-Based D2D Groups With WPCNs

Device-to-Device (D2D) is a technique which increases energy efficiency and reduces the delay by supporting short-distance communication. Also, to achieve the massive connectivity and ultra-reliable low latency in the 5G, the Non-orthogonal multiple access (NOMA) is proposed. However, an integration of NOMA in D2D mobile groups (DMGs) generates a large amount of energy and delay due to sharing the same subcarrier. In this chapter, we investigate a distributed energy-efficient and delay tradeoff scheme for NOMA-based DMGs in wireless powered communication networks.

The main contributions of this chapter are given as follows:

- To construct a system model in which Wireless-powered CMUs and DMGs co-exist. Then, SINR, average time data rate, energy buffer, data buffer, and average time energy consumption are determined to formulate the EE and delay trade-off problem. As the formulated problem is in the mixed-integer non-linear programming (MINLP) form, so we divide it into four sub-problems.
- In the first sub-problem, the weighted sum method is used to convert the non-linear fractional programming problem into a linear single-objective optimization problem. In the second-sub-problem, an optimal value of the subcarrier allocation factor is determined. To achieve the target, a many-to-one matching game is applied between the DMGs and subcarriers. Furthermore, to mitigate the effect of externalities over the subcarriers, the concept of pricing is proposed among the DMGs. In the third sub-problem, the Lyapunov optimization technique is used to transform the stochastic optimization problem into a static deterministic optimization problem. Lastly, in the fourth sub-problem, a closed-form expression of a time and power is optimized by using the Lagrangian duality function.

- Lastly, the EE and delay trade-off algorithm is designed to improve the long term average EE of the DMGs used in the network. Also, we find that the EE and delay increases with the speed of **O(V)**, where V is a control parameter used to balance the EE and delay trade-off.

This chapter-4 is organized as follows: Section 4.1 describes the network model. The problem formulation is illustrated in Section 4.2. Section 4.3 elaborate the proposed scheme through which the formulated problem is solved. Section 4.4 evaluates the performance of the proposed scheme and compared with the existing NOMA and TDMA schemes. Finally, Section 4.5 describes the conclusion and future scope of the chapter.

Table 4.1: Abbreviations used in the proposed scheme

Symbols	**Notation Used**
$\mathcal{M}$	Number of CMUs.
$\mathcal{D}$	Number of DMGs.
$\mathcal{N}$	Number of DMUs.
$\mathcal{K}$	Number of Sub-carriers.
ϕ	Subcarrier allocation factor.
τ	Time allocation factor.
α	Power allocation factor.
$\Gamma_m^k(t), \Gamma_{d,n}^k(t)$	SINR values of the m^{th} CMU & the n^{th} DMU in the d^{th} DDT.
$E_{m,b}^{h,k}, E_{d,n}^{h,k}$	Energy Harvested by the m^{th} CMU & the d^{th} DDT.
$\overline{R}_{m,b}^k(t), \overline{R}_{d,n}^k(t)$	Time-Average Data Rate of the m^{th} CMU & the n^{th} DMU in the d^{th} DDT.
$Q_m^k(t), Q_{d,n}^k(t)$	Data Buffer Queue of the m^{th} CMU & the d^{th} DDT.
$\overline{E}_{m,b}^k(t), \overline{E}_{d,n}^k(t)$	Time Average Energy Consumption of the m^{th} CMU & the d^{th} DDT.
$E_{m,b}^c, E_{d,n}^c$	Energy consumed by energy buffers of the m^{th} CMU & the d^{th} DDT.
$h_{d,n}^k(t)$, $h_{m,d,n}^k(t)$, & $h_{d',d,n}^k(t)$	Channel coefficients.
$Z_{m,b}^k(t)$, $Z_{d,n}^k(t)$	Actual admitted traffic arrival of the m^{th} CMU & the d^{th} DDT.
$P_m^c(t)$, $P_{d,n}^c(t)$	Power consumed by the internal circuitry.

4.1 Network Model

The various components used in the network model are covered in this section.

4.1.1 System Model with Assumptions

Consider a two-tier single cell in WPCN as shown in Fig. 4.1. The first-tier consists a BS and $\mathcal{M}$ CMUs, and the second-tier consists of $\mathcal{D}$ DMGs of radius R. Each DMG has one

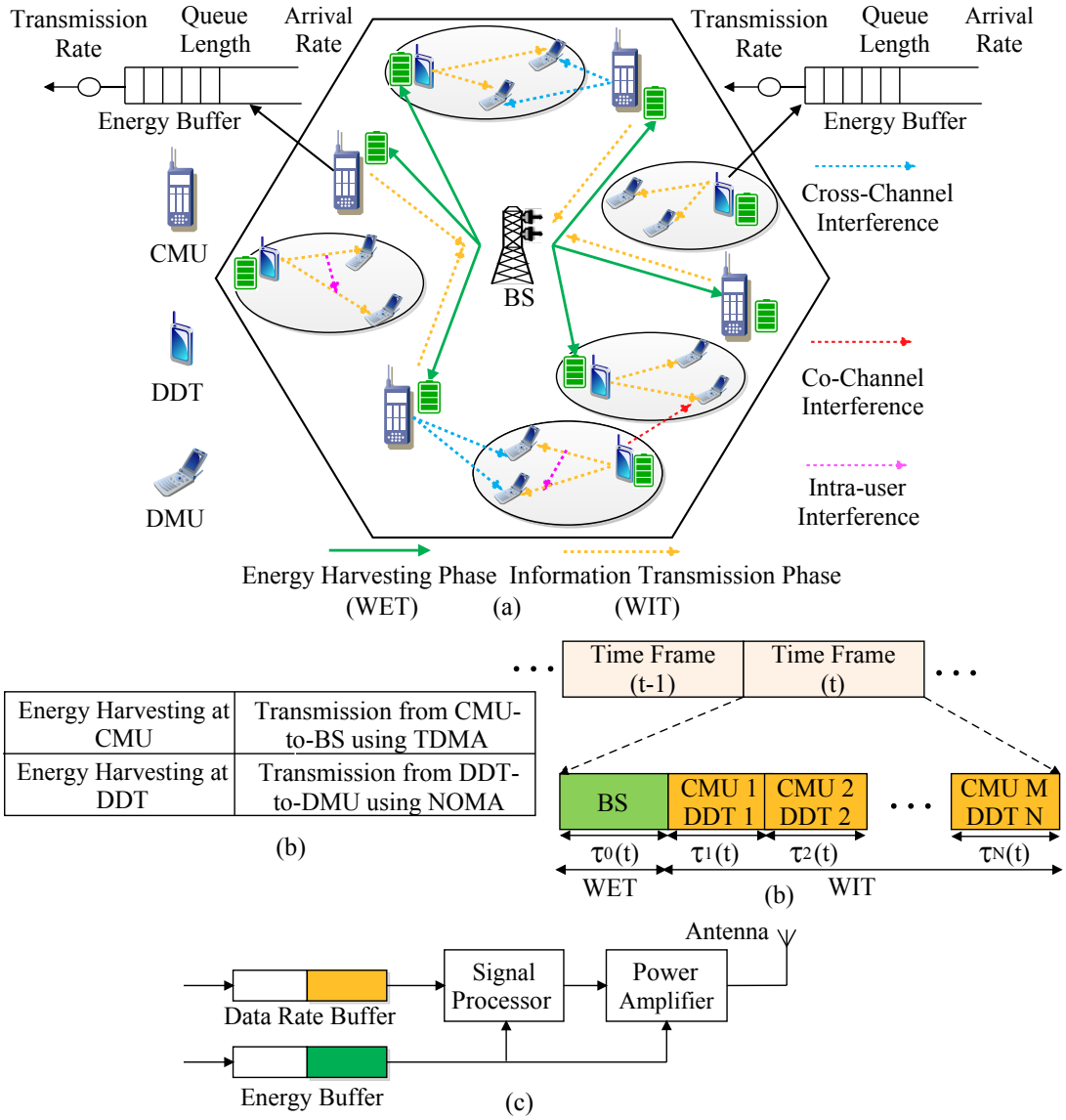

Figure 4.1: (a) System Model (b) Harvest-then-Transmit Protocol (c) Queueing Model

DDT and $\mathcal{N}$ DMUs. The DDT is situated at the centre, and $\mathcal{N}$ DMUs are uniformly distributed around it. Assume that CMUs and DDTs are equipped with a single antenna, energy buffer, and data buffer circuits. Let us assume that one subcarrier is already occupied by each CMU, where the set of subcarriers are represented as $\mathcal{K} = \{1, 2, \ldots, k, \ldots, K\}$. The CMUs used TDMA schedule to communicate with the BS to reduce energy consumption and limit the interference across the sub-carriers whereas, DDTs used NOMA to communicate with their $\mathcal{N}$ DMUs using the same subcarriers. Assume that the WPCN process is carried out in a slotted-time mode with a time slot t in a time interval $(t, t+1]$. WPCN is a combination of WET and WIT stage and used harvest-store-transmit protocol. During the downlink WET stage, the CMUs and DDTs harvest energy from the RF signals generated by the BS, and stored in the energy buffer. Then, the CMUs and DDTs used the stored harvested energy to transmit information to the BS and DMUs, respectively. Also, in this chapter, the Rayleigh fading channel model is used, where the long-term time-varying channel coefficients and random traffic arrivals are used within each time slot and follow Gaussian complex distribution $\mathcal{CN}\ (0, 1)$. The Rayleigh fading is a statistical model for a propagation environment on the radio signal. It is most suitable to the situation when no dominant propagation is available for the line of sight between the transmitter and receiver. Also, assume that the CSI of all the CMUs and DMGs are perfectly known to the BS, and the energy consumed during the transformation of CSI is set to be negligible. The list of symbols used in the chapter is described in Table 4.1.

4.1.2 WPCN Model

The process of WPCN is divided into WET and WIT stages. If τ_0 and $\tau_{d,n}$ are the time interval for WET and WIT stages, then for $\mathcal{D}$ DMGs following holds:

$$\tau_0 + \sum_{d=1}^{D} \tau_{d,n} \leq 1. \tag{4.1}$$

4.1.2.1 WET Stage

If $P_b^k(t)$ is the transmit power of the BS, then the energy harvested by the m^{th} CMU over t is given as follows:

$$E_{m,b}^{k,h}(t) = \eta_m \tau_0(t) P_b^k(t) h_{b,m}^k(t),\ \forall m \in \mathcal{M}, \tag{4.2}$$

where $\eta_m \in (0, 1]$ is the energy transformation efficiency of the m^{th} CMU, $\tau_0(t)$ is the WET time, and $h_{b,m}^k(t)$ is the channel coefficient from the BS to the m^{th} CMU.

Similarly, the energy harvested by the d^{th} DDT over t is given as follows:

$$E_{d,n}^{k,h}(t) = \eta_{d,n} \tau_0(t) P_b^k(t) h_{b,d}^k(t),\ \forall d \in \mathcal{D}, \tag{4.3}$$

where $\eta_{d,n} \in (0,1]$ is the energy transformation efficiency of the d^{th} DDT, $h^k_{b,d}(t)$ is the channel coefficient from the BS to the d^{th} DDT.

4.1.2.2 WIT Stage

Here, message signal is transmitted with time $\tau_d = (1-\tau_0)$. The performance of CMUs and DMGs are analysed separately.
(a) For CMUs: The signal transmitted by the m^{th} CMU towards the BS over the k^{th} subcarrier is given as follows:

$$y^k_{m,b}(t) = \sqrt{P^k_m(t)}h^k_{m,b}(t)x^k_{m,b}(t) + \sum_{d=1}^{D} \phi^k_{d,m}(t)\sqrt{P^k_d(t)}h^k_{d,b}(t)x^k_{d,b}(t) + \underbrace{\zeta(t)}_{\text{AWGN}}, \tag{4.4}$$

where $P^k_m(t)$ and $P^k_d(t)$ are the transmit power of the m^{th} CMU and the d^{th} DDT, respectively, $h^k_{m,b}(t)$ and $h^k_{d,b}(t)$ are the channel coefficient from the m^{th} CMU to the BS, and that between the d^{th} DDT to the BS, respectively, $x^k_{m,b}(t)$ and $x^k_{d,b}(t)$ are the transmitted message signals, $\zeta(t)$ is the additive white Gaussian noise (AWGN) with mean zero and variance σ^2, and $\phi^k_{d,m}(t)$ is the subcarrier allocation factor. If $\phi^k_{d,m}(t) = 1$, then k^{th} subcarrier is allocated to the d^{th} DDT, otherwise $\phi^k_{d,m}(t) = 0$.

According to Eq. (4.4), the signal-to-interference noise ratio (SINR) and data rate are calculated as follows:

$$\Gamma^k_{m,b}(t) = \frac{P^k_m(t)|h^k_{m,b}(t)|^2}{\sum_{d=1}^{D} P^k_d(t)|h^k_{d,b}(t)|^2 + \sigma^2(t)}, \tag{4.5}$$

$$\text{and } R^k_{m,b}(t) = \frac{B}{K}\log_2(1+\Gamma^k_{m,b}(t)). \tag{4.6}$$

(b) For DMGs: In this, the DDT transmit the information to their associated DMUs. In PD-NOMA, the superposition coding is used at the DDT to multiplex the power signal, and SIC is employed at the $\mathcal{N}$ DMUs to reduce the intra-user interference. If the channel gain of DMUs are arranged in descending order, i.e., $h^k_{d,1}(t) \leq h^k_{d,2}(t) \leq, \ldots, \leq h^k_{d,n}(t) \leq h^k_{d,l}(t), \ldots, \leq h^k_{d,N}(t)$, then the signal received at the n^{th} DMU of the d^{th} DDT over the k^{th} subcarrier is given as follows [259]:

$$\begin{aligned} y^k_{d,n}(t) &= h^k_{d,n}(t)\underbrace{\sqrt{\alpha^k_{d,n}P^k_d(t)}x^k_{d,n}(t)}_{\text{Desired Signal}} + \underbrace{\sum_{l=n+1}^{N}\sqrt{\alpha^k_{d,l}P^k_d(t)}x^k_{d,l}(t)}_{\text{NOMA Interferece } (I^{no}_{d,l}(t))} + \underbrace{\sqrt{P^k_m(t)}h^k_{m,d,n}(t)x^k_{m,d,n}(t)}_{\text{Cross channel interference } (I^{cr}_{d,n})(t)} \\ &+ \underbrace{\sum_{d'\neq d}^{D}\phi^k_{d',d}\sqrt{P^k_{d'}}(t)h^k_{d'd,n}(t)x^k_{d',d,n}(t)}_{\text{Co-channel Interference } (I^{co}_{d,n})(t)} + \underbrace{\xi(t)}_{\text{AWGN}}, \end{aligned} \tag{4.7}$$

where $h^k_{d,n}(t)$, $h^k_{m,d,n}(t)$ and $h^k_{d',d,n}(t)$ are the channel coefficient, and $x^k_{d,n}(t)$, $x^k_{m,d,n}(t)$ and $x^k_{d',d,n}(t)$ are the message signal between the d^{th} DDT to the n^{th} DMU, the m^{th} CMU to the n^{th} DMU, and that between the d'^{th} DDT to the n^{th} DMU, respectively, $P^k_{d'}$ is the transmit power of the d'^{th} DDT, $\alpha_{d,n}$ and $\alpha_{d,l}$ are the power allocation coefficients, and $\phi^k_{d',d}$ denotes the co-channel interference factor between the $(d')^{th}$ DDT and the d^{th} DDT.

According to Eq. (4.7), the SINR is calculated as follows:

$$\Gamma^k_{d,n}(t) = \left(\frac{|h^k_{d,n}(t)|^2 P^k_d \alpha^k_{d,n}(t)}{I^{no}_{d,n}(t) + I^{co}_{d,n}(t) + I^{cr}_{d,n}(t) + \sigma^2(t)} \right). \tag{4.8}$$

After successful SIC, the SINR for the l DMUs are given as follows:

$$\Gamma^k_{d,l}(t) = \sum_{l=n+1}^{N} \left(\frac{|h^k_{d,l}(t)|^2 P^k_d \alpha^k_{d,l}(t)}{I^{co}_{d,l}(t) + I^{cr}_{d,l}(t) + \sigma^2(t)} \right). \tag{4.9}$$

The data rate of the n^{th} DMU and l DMUs in the d^{th} DMG using Eq. (4.8) and (4.9) is given as follows:

$$R^k_{d,n} = \frac{B}{K} \log_2(1 + \Gamma^k_{d,n}), \tag{4.10}$$

$$\text{and } R^k_{d,l} = \sum_{l=n+1}^{N} \frac{B}{K} \log_2(1 + \Gamma^k_{d,l}). \tag{4.11}$$

4.1.3 Queueing Model

As the queue state information (QSI) of CMUs and DMUs is unknown to the BS, therefore there is a need to calculate the queuing delay. To calculate the queuing delay for the m^{th} CMU and the d^{th} DDT, we have to stabilized the traffic through queue by following the transport flow control mechanism. If $Q^{k,D}_{m,b}(t)$ and $Q^{k,D}_{d,n}(t)$ denote the queue length, $A^k_{m,b}(t)$ and $A^k_{d,n}(t)$ are the random traffic arrival data rate, $A^{max}_{m,b}(t)$ and $A^{max}_{d,n}(t)$ are the peak arrival data rate, and $R^k_{m,b}(t)$ and $R^k_{d,n}(t)$ are the departure rate of the m^{th} CMU, and the d^{th} DDT, respectively, then the queuing delay at t is given as follows:

$$Q^{k,D}_{m,b}(t+1) = \max\{Q^{k,D}_{m,b}(t) + A^k_{m,b}(t) - R^k_{m,b}(t), 0\}. \tag{4.12}$$

$$\text{and } Q^{k,D}_{d,n}(t+1) = \max\{Q^{k,D}_{d,n}(t) + A^k_{d,n}(t) - R^k_{d,n}(t), 0\}, \tag{4.13}$$

where $A^k_{d,n}(t) \leq A^{max}_{d,n}(t)$ and $A^k_{m,b}(t) \leq A^{max}_{m,b}(t)$.

If $Z^k_{m,b}(t)$ and $Z^k_{d,n}(t)$ is the actual admitted traffic arrival data rate in a queue out of random traffic arrival rate $A^k_{m,b}(t)$ and $A^k_{d,n}(t)$, then (4.12) and (4.13) is rewritten as follows:

$$Q^{k,D}_{m,b}(t+1) = \max\{Q^{k,D}_{m,b}(t) + Z^k_{m,b}(t) - R^k_{m,b}(t), 0\}. \tag{4.14}$$

$$\text{and } Q_{d,n}^{k,D}(t+1) = \max\{Q_{d,n}^{k,D}(t) + Z_{d,n}^{k}(t) - R_{d,n}^{k}(t), 0\}, \tag{4.15}$$

where $0 \leq Z_{d,n}^{k}(t) \leq A_{d,n}^{k}(t)$ and $0 \leq Z_{m,b}^{k}(t) \leq A_{m,b}^{k}(t)$.

Now, the time average data rate in terms of actual admitted traffic arrival rate for the m^{th} CMU and d^{th} DMG are given as follows:

$$\overline{R}_{m,b}^{k}(t) = \lim_{T\to\infty} \frac{1}{T} \sum_{t=0}^{T-1} \mathbb{E}(R_{m,b}^{k}(t)), \tag{4.16}$$

$$\text{and } \overline{R}_{d,n}^{k}(t) = \lim_{T\to\infty} \frac{1}{T} \sum_{t=0}^{T-1} \mathbb{E}(R_{d,n}^{k}(t)). \tag{4.17}$$

4.1.4 Energy Consumption and Energy Efficiency Model

In this model, the energy consumed by the CMUs and DMGs during the WET and WIT stage is calculated and analysed separately.

4.1.4.1 WET Stage

In this stage, the energy consumed by the energy buffers in the charging of CMUs and DMGs are calculated.

The energy consumed by the energy buffers in the charging of m^{th} CMU and the d^{th} DMG are given as follows:

$$E_{m,b}^{c}(t) = \tau_0(t)(P_b^k(t) + P_m^c) - E_{m,b}^{k,h}(t). \tag{4.18}$$

$$\text{and } E_{d,n}^{c}(t) = \tau_0(t)(P_b^k(t) + P_{d,n}^c) - E_{d,n}^{k,h}(t), \tag{4.19}$$

where $P_m^c(t)$ and $P_{d,n}^c(t)$ are the power consumed by the internal circuitry of the devices of the m^{th} CMU and the d^{th} DMG, respectively. $E_{m,b}^{k,h}(t)$ and $E_{d,n}^{k,h}(t)$ are the harvested energy already defined in Eqs. (4.2) and (4.3), respectively.

4.1.4.2 WIT Stage

In this stage, the energy consumed by the CMUs and DMGs is equal to the sum of their transmit power and constant circuit power.

(a) For CMU: The energy consumed by the m^{th} CMU is given as follows:

$$E_m^{c'}(t) = \tau_m(t) \left(P_m^k(t) + P_m^{c'} \right), \tag{4.20}$$

where $P_m^k(t)$ and $P_m^{c'}(t)$ are the transmit power and the constant circuit power consumption of the m^{th} CMU, respectively.

It should be noted that $P_m^{c'}(t) \geq P_m^c(t)$ because circuits used during the data transmission are more complex than the circuits used in energy harvesting [146].

Now, the dynamic energy queue for the m^{th} CMU is given as follows:

$$Q_m^{k,E}(t+1) = \max\{Q_m^{k,E}(t) - E_m^{c'}(t), 0\} + E_{m,b}^{k,h}(t). \tag{4.21}$$

(b) For DMG: The energy consumed by the d^{th} DMG is given as follows:

$$E_{d,n}^{c'}(t) = \tau_d(t)\left(P_d^k \alpha_{d,n}^k(t) + P_{d,n}^{c'}\right). \tag{4.22}$$

Now, the dynamic energy queue for the d^{th} DMG is given as follows:

$$Q_{d,n}^{k,E}(t+1) = \max\{Q_{d,n}^{k,E}(t) - E_{d,n}^{c'}(t), 0\} + E_{d,n}^{k,h}(t). \tag{4.23}$$

The total energy consumed by the m^{th} CMU during the WET and WIT stage is obtained by combining Eq. (4.18) and (4.20) is given as follows:

$$E_{m,b}^{k,T}(t) = E_{m,b}^{c}(t) + E_m^{c'}(t). \tag{4.24}$$

Similarly, the total energy consumed by the d^{th} DMG during the WET and WIT stage using Eq. (4.19) and (4.22) is given as follows:

$$E_{d,n}^{k,T}(t) = E_{d,n}^{c}(t) + E_{d,n}^{c'}(t). \tag{4.25}$$

Now, the time-average energy consumption for the m^{th} CMU and the d^{th} DMG are given as follows:

$$\overline{E}_{m,b}^{k,T}(t) = \lim_{T\to\infty} \frac{1}{T} \sum_{t=0}^{T-1} \mathbb{E}(E_{m,b}^{k,T}(t)), \tag{4.26}$$

$$\text{and } \overline{E}_{d,n}^{k,T}(t) = \lim_{T\to\infty} \frac{1}{T} \sum_{t=0}^{T-1} \mathbb{E}(E_{d,n}^{k,T}(t)). \tag{4.27}$$

The EE of each user's device is defined as the ratio of the long-term average transmitted data rate to the corresponding long-term average energy consumed, and is measured in bits/Hz/Joule.

Now, the long-term average energy efficiency of the m^{th} CMU and the d^{th} DMG are given as follows [329]:

$$\overline{EE}_{m,b}^{k}(t) = \frac{\overline{R}_{m,b}^{k}(\phi(t), R(t), \tau(t), p(t))}{\overline{E}_{m,b}^{k,T}(\phi(t), R(t), \tau(t), p(t))}, \tag{4.28}$$

$$\text{and } \overline{EE}_{d,n}^{k}(t) = \frac{\overline{R}_{d,n}^{k}(\phi(t), R(t), \tau(t), p(t))}{\overline{E}_{d,n}^{k,T}(\phi(t), R(t), \tau(t), p(t))}. \tag{4.29}$$

4.2 Problem Formulation

In this chapter, we propose a distributed energy-efficient and delay trade-off scheme for NOMA-based DMG with WPCN. Moreover, our goal is to maximize the long-term average EE of each DMG in a distributed manner while maintaining the long-term average EE of each CMU. To achieve this goal, an stochastic optimization problem is formulated as follows:
Let $a(t) = [\phi(t), R(t), \tau(t), \alpha(t)]$, where $\tau(t) = [\tau_0(t), \tau_d(t)]$

$$
\begin{aligned}
P1 \quad &: \quad \max_{a(t)} \sum_{d=1}^{D} \sum_{n=1}^{N} \overline{EE}_{d,n}^{k}(t), \qquad (4.30)\\
\text{s.t.} \ \mathbb{C}_1 \quad &: \quad \overline{Q}_{d,n}^{k}(t) = 0,\\
\mathbb{C}_2 \quad &: \quad \overline{R}_{d,n}^{k}(t) \geq R_{d,n}^{k,min}(t), \ \forall \mathcal{D},\\
\mathbb{C}_3 \quad &: \quad 0 \leq \overline{R}_{d,n}^{k}(t) \leq Z_{d,n}^{k}(t), \ \forall \mathcal{D},\\
\mathbb{C}_4 \quad &: \quad \phi_{d,m}^{k} \in \{0,1\},\\
\mathbb{C}_5 \quad &: \quad \sum_{k=1}^{K} \phi_{d,m}^{k}(t) \leq 1, \ \forall \mathcal{K},\\
\mathbb{C}_6 \quad &: \quad \sum_{d=1}^{D} \phi_{d,m}^{k}(t) \leq U_{max}, \ \forall \mathcal{D},\\
\mathbb{C}_7 \quad &: \quad \tau_d(t) \left(\sum_{d=1}^{D} P_d^k(t) |h_{d,m}^{k}(t)|^2 \right) \leq I_m^{th}(t), \ \forall \mathcal{M},\\
\mathbb{C}_8 \quad &: \quad E_{d,n}^{c'}(t) \leq Q_{d,n}^{k,E}(t) + E_{d,n}^{k,h}(t), \ \forall \mathcal{D},\\
\mathbb{C}_9 \quad &: \quad \tau_0(t) + \sum_{d=1}^{D} \tau_d(t) \leq 1, \ \forall \mathcal{D},\\
\mathbb{C}_{10} \quad &: \quad \tau_0(t) > 0, \tau_d(t) > 0,\\
\mathbb{C}_{11} \quad &: \quad \lim_{T \to \infty} \frac{1}{T} \sum_{t=0}^{T-1} \mathbb{E}\{E_{d,n}^{k,T}(t)\} \leq E_{d,n}^{av}(t), \ \forall \mathcal{D},\\
\mathbb{C}_{12} \quad &: \quad P_b^T \leq P_b^{\max},\\
\mathbb{C}_{13} \quad &: \quad \alpha_{d,n}^{k}(t) + \sum_{l=n+1}^{N} \alpha_{d,l}^{k}(t) \leq 1, \ \forall \mathcal{D},\\
\mathbb{C}_{14} \quad &: \quad \alpha_{d,n}^{k}(t) > 0, \alpha_{d,l}^{k}(t) > 0.
\end{aligned}
$$

In the above problem, Constraint $\mathbb{C}_1$ represents the queue stability of the d^{th} DDT, it ensures that the arrived data traffic must leave the queue in a finite time. Constraint $\mathbb{C}_2$ represents the time-average data rate of the d^{th} DDT, and must be greater than its minimum data rate requirement. $\mathbb{C}_3$ limits the admitted traffic arrival rate across the d^{th} DDT. $\mathbb{C}_4$ represents the binary integer value for sub-carrier. $\mathbb{C}_5$ ensures that at most one subcarrier is to be allocated to each DMG. In $\mathbb{C}_6$, U_{max} is the maximum number of DMGs that can be allocated to each subcarrier. It reduces the co-channel interference across each subcarrier. $\mathbb{C}_7$ implies that if d^{th}

DMG is in the information decoding time interval, then the aggregated interference received by CMU must be less than $I_m^{th}(t)$. $\mathbb{C}_8$ ensures that the energy consumed during the WIT stage of the DMG should be less than or equal to the total harvested energy available in the energy buffer. $\mathbb{C}_9$ shows that energy harvesting and data transmission time must be less than the allotted total time slot. $\mathbb{C}_{10}$ represents the non-negative time. $\mathbb{C}_{11}$ limits the time-average energy consumption of the d^{th} DMG over t. $\mathbb{C}_{12}$ represents that the $P_b^{\max}$ is the maximum transmit power of the BS in the WET stage. $\mathbb{C}_{13}$ limits the upper bound of the transmit power of the d^{th} DDT. $\mathbb{C}_{14}$ represents the non-negative transmit power allocation factors.

4.3 Proposed Scheme

The optimization problem formulated in Eq. (4.30) cannot be solved directly due to following reasons (i) it is in the fractional form (ii) stochastic due to $\mathbb{C}_1$, $\mathbb{C}_2$, $\mathbb{C}_3$ and $\mathbb{C}_7$ (iii) non-convex due to interference terms in the denominator of $\overline{R}_{d,n}^k$ and (iv) MINLP due to binary integer, the coupling of time and power variables. No systematic and tractable approach is available through which this problem can be solved directly. To solve this problem, we divided it into three sub-problems (i) Subcarrier allocation (ii) Lyapunov optimization and (iii) Joint time and power allocation. With the reuse of subcarriers between the DMGs and CMUs, the spectral efficiency of the DMGs is increased. The Lyapunov optimization approach transforms the stochastic optimization problem into a series of successive deterministic optimization problems. Now, the joint time and power allocation are further divided into (i) power allocation and (ii) time allocation.

It should be noted that the non-linear fractional programming problem is normally solved by using the Dinkelbach method, but this method is applicable only for single ratio objective function. Thus, the objective function in Eq. (4.30) cannot be solved using Dinkelbach method because it is the sum-of-ratios of EE of each DMG [330]. So, to solve this we used the weighted sum method.

4.3.1 Problem Transformation using Weighted Sum Method

In this subsection, the optimization problem $P1$ is transformed from non-linear fractional programming form to a linear single-objective optimization problem.

Theorem 2. *If $a^*(t)$ is the optimal solution of the objective function of Eq. (4.30), then there exists $\Phi^{*k} = (\Phi_{d,1}^k, \Phi_{d,2}^k, \ldots, \Phi_{d,n}^k)$ and $\Omega^{*k} = (\Omega_{d,1}^k, \Omega_{d,2}^k, \ldots, \Omega_{d,n}^k)$ such that $\Phi^k = \Phi^{*k}$ and $\Omega^k = \Omega^{*k}$.*

$$\max_{a(t)} \sum_{d=1}^{D} \sum_{n=1}^{N} \Phi_{d,n}^k (w_{d,n}^k R_{d,n}^k - \Omega_{d,n}^k E_{d,n}^k) \tag{4.31}$$

In addition, $a^*(t)$ have to satisfy the following system of equations for $\Phi^k = \Phi^{*k}$ and $\Omega^k = \Omega^{*k}$:

$$\Phi^k_{d,n} E^k_{d,n} - 1 = 0 \tag{4.32}$$

$$\Omega^k_{d,n} E^k_{d,n} - w^k_{d,n} R^k_{d,n} = 0 \tag{4.33}$$

where $w^k_{d,n}$ is the weighing factor.

Proof. For the detailed proof of Theorem 2 refer to [330] □

Based on Theorem 2, the objective function $P1$ transformed into a subtractive function which is rewritten as follows:

$$\begin{aligned} P2 \quad &: \quad \max_{a(t)} \sum_{d=1}^{D} \sum_{n=1}^{N} \Phi^k_{d,n} (w^k_{d,n} R^k_{d,n} - \Omega^k_{d,n} E^k_{d,n}) \\ s.t. \quad &\mathbb{C}_1 - \mathbb{C}_{14} \end{aligned} \tag{4.34}$$

The problem $P2$ is equivalent to $P1$, and is solved like $P1$.

4.3.2 Subcarrier Allocation

In this subsection, time and power allocated across each subcarrier is kept fixed, i.e., $\tau^k = \tau^{*K}$, and $\alpha^k_{d,n} = \alpha^{*k}_{d,n}$. Thus, we have:

$$\begin{aligned} P2 \quad &: \quad \max_{a(t)} \sum_{d=1}^{D} \sum_{n=1}^{N} \Phi^k_{d,n} (w^k_{d,n} R^k_{d,n} - \Omega^k_{d,n} E^k_{d,n}), \\ s.t. \quad &\mathbb{C}_4, \mathbb{C}_5, \mathbb{C}_6, \mathbb{C}_7. \end{aligned} \tag{4.35}$$

The optimization problem in (4.35) is non-convex due to binary integer and the existence of co-channel interference. To solve this problem, we use pricing-based dynamic many-to-one matching scheme between the set of DMGs and subcarriers.

The set of rules for the pricing-based many-to-one matching game [331], [332] are described as follows:

Definition 1. *According to the many-to-one matching scheme, a matching φ is a function of the set of all subsets of $\mathcal{K} \cup \mathcal{D}$, such that*
(a) $|\varphi(d)| = 1$, $\forall d \in \mathcal{D}$, and $\varphi(d) = \{d\}$, if the $\varphi(d) \nsubseteq \mathcal{K}$,
(b) $|\varphi(k)| \leq U_{max}$, $\forall k \in \mathcal{K}$, and $\varphi(k) = \emptyset$, if the k^{th} subcarrier is not matched with any DMG,
(c) $\varphi(d) = k$ iff $d \in \varphi(k)$.

Algorithm 7 Subcarrier Allocation Algorithm

Input: $\mathcal{D}, \mathcal{N}, \varsigma$.
Output: $\phi_{d,m}^{*k}$ or φ.
Initialization: $PL(UF_d(k))$ = PL of the d^{th} DMG on the k^{th} subcarrier ; $PL(UF_k(d))$ = PL of the k^{th} subcarrier on the d^{th} DMG; ψ = Set of not matched DMGs; $\varsigma = 0.1$; $\varphi(d) = \{\emptyset\}$; and ρ =set of conflict requests.

1: **while** $(\psi(d) \neq \emptyset$ && $\exists \varphi(d) \neq \emptyset)$ **do**
2: **for** $(d = 1, d \leq \mathcal{D}, d++)$ **do**
3: The d^{th} DDT proposes to most preferred subcarrier unit that never reject it
4: before.
5: **end for**
6: **for** $(k = 1, k \leq \mathcal{K}, k++)$ **do**
7: **if** $(\sum_{k=1}^{K} \phi_{d,n}^{k} \leq U_{max})$ **then**
8: The k^{th} subcarrier unit accept all the request proposed by DDT.
9: Delete the matched DDT from the set of ψ.
10: **else**
11: The k^{th} subcarrier accept the most preferred DDT upto U_{max} whereas
12: reject the others.
13: Delete the matched d^{th} DDT from ψ.
14: Remain the rejected DDT in ψ.
15: **end if**
16: Delete $d's$ DDT from the $(PL)_d(k)$ who sent proposals.
17: **end for**
18: Count the number of k subcarriers that have received request from more
19: than one DDT.
20: Insert the conflicting k subcarrier into ρ
21: **if** $\rho = \emptyset$ **then**
22: Repeat the step from 6-15
23: **end if**
24: **if** $(\rho \neq \emptyset)$ **then**
25: **for** $(d = 1; d \leq \mathcal{D}, d$++$)$ **do**
26: **if** (k^{th} subcarrier received request from more than one DMGs) **then**
27: k^{th} subcarrier increase their prices with price step ς till
28: conflicting not resolved.
29: Update $PL(UF_d(k))$ and $PL(UF_k(d))$.
30: Remove the d^{th} DDT from ρ that provide conflicting request.
31: **end if**
32: **end for**
33: **end if**
34: Update ρ, $PL(UF_d(k))$ and $PL(UF_k(d))$
35: **end while**

4.3.2.1 Preference List Establishment

Based on the definition 1, the preference list (PL) of subcarriers and DMGs depends on the utility functions. The utility function of the d^{th} DMG on the k^{th} subcarrier is given as follows:

$$UF_d(k) = \sum_{k=1}^{K} \phi_{d,m}^{k}[EE_{d,n}^{k}(t)]. \tag{4.36}$$

and the utility function of the k^{th} subcarrier on the d^{th} DMG is given as follows:

$$UF_k(d) = \sum_{d=1}^{D} \phi_{d,m}^{k}[EE_{d,n}^{k}(t) + EE_{m}^{k}(t)]. \tag{4.37}$$

According to the Eq. (4.36) and (4.37), the prefer relationship of the d^{th} DMG on the k^{th} subcarrier, and that of the k^{th} subcarrier on the d^{th} DMG is given as follows:

$$(k,\varphi) \succ_d (k',\varphi') \Leftrightarrow UF_d(k,\varphi) > UF_d(k',\varphi'), \tag{4.38}$$

$$\& \;\; (d,\varphi) \succ_k (d',\varphi') \Leftrightarrow UF_k(d,\varphi) > UF_k(d',\varphi'). \tag{4.39}$$

Now, the PL of the d^{th} DMG on the k^{th} subcarrier, and that of the k^{th} subcarrier on the d^{th} DMG in descending order are given as follows:

$$PL(UF_d(k)) = \{P(UF_1(k)),\ldots,P(UF_d(k)),\ldots,P(UF_D(k))\}, \tag{4.40}$$

$$\text{and } PL(UF_k(d)) = \{P(UF_1(d)),\ldots,P(UF_k(d)),\ldots,P(UF_K(d))\}. \tag{4.41}$$

$PL(UF_d(k))$ and $PL(UF_k(d))$ are updated after each matching iteration.

4.3.2.2 Matching Process Algorithm

In this process, each DMG sends the request to their most preferred subcarriers using the established PLs. Here, we also consider the effect of externalities [331], because in the proposed model we consider more than one DMG, resulting in the co-channel interference. It means that as the game proceeds further the defined PL changes. In the aforementioned situation, one DMG not only cares about the subcarrier it is matched with but also consider the set of other DMGs as per the quota who wants to share the same subcarrier. Moreover, the subcarriers also consider the effect of mutual interference produces by DMGs on it. Once a DMG is matched with a subcarrier, the defined PL of DMGs and subcarriers changes as the utility function changes with an interference. To resolve this conflict, we used "*pricing*" to represent the matching cost for DMGs. Consider that the set of prices of subcarriers for the DMGs are virtual with their initial value to be zero, and is represented as $\mathcal{V} = \{\mathcal{V}_1,\mathcal{V}_2,\ldots,\mathcal{V}_k,\ldots,\mathcal{V}_K\}, \forall k \in \mathcal{K}$. The proposed algorithm proceeds iteratively, and during each iteration, the PL of DMGs is up-

dated as $(I^{no}_{d,n}+I^{co}_{d,n}+I^{cr}_{d,n}-\mathcal{V}_k)$ and the PL of subcarrier s is to be updated accordingly. In case, if any subcarrier receives a request from more than $U_{\max}$ DMGs, then that subcarrier increases their price from a unit value of ς. This process continues until each subcarrier receives the request as per the maximum value from DMGs, and the algorithm ends when no request remains left form DMGs. The pseudocode of the matching process is described in Algorithm 7.

The computational complexity of the Algorithm 7 is approximated as $\mathcal{O}(KD)$.

4.3.3 Lyapunov Optimization

In this subsection, a Lyapunov optimization approach [333] is used to stabilize the queue of DDT in each DMG. Now, the problem describes in Eq. (4.35) is given as follows:

$$\begin{aligned} P2 \quad &: \quad \max_{R(t)} \sum_{d=1}^{D}\sum_{n=1}^{N} \Phi^k_{d,n}(w^k_{d,n}R^k_{d,n}-\Omega^k_{d,n}E^k_{d,n}), \\ s.t. \quad &\quad \mathbb{C}_1, \mathbb{C}_2, \mathbb{C}_3 \ \& \ \mathbb{C}_{11} \end{aligned} \tag{4.42}$$

To solve the time-average constraint $\mathbb{C}_2$ and $\mathbb{C}_{11}$, we used virtual queues, and for constraint $\mathbb{C}_1$ and $\mathbb{C}_3$, the Lyapunov function and Lyapunov drift are used, respectively. These techniques convert the queue stability constraint into minimum Lyapunov drift. Finally, we derive the upper bound of Lyapunov drift and propose the Lyapunov optimization algorithm.

4.3.3.1 Virtual Queues

The virtual queue of admitted data traffic and energy control at t is given as follows. $S(t)$=$\{S_1(t), S_2(t), S_3(t) \ldots, S_{N-1}(t), S_N(t)\}$, and $W(t)$= $\{W_1(t), W_2(t), W_3(t), \ldots, W_{N-1}(t), W_N(t)\}$, respectively.

The virtual queue for admitted data traffic constraint $\mathbb{C}_2$ at t is expressed as follows:

$$S^k_{d,n}(t+1) = \max\{S^k_{d,n}(t) + R^{k,min}_{d,n}(t) - R^k_{d,n}(t), 0\}, \ \forall d, n. \tag{4.43}$$

Similarly,the virtual queue for time-average energy consumption constraint $\mathbb{C}_{11}$ at t is given as follows:

$$W^k_{d,n}(t+1) = \max\{W^k_{d,n}(t) + E^{k,T}_{d,n}(t) - E^{av}_{d,n}(t), 0\}, \ \forall d, n. \tag{4.44}$$

where $S^k_{d,n}(0) = 0$ & $\alpha^k_{d,n}(0) = 0$.

Note that the constraints $\mathbb{C}_2$ & $\mathbb{C}_{11}$ are fully satisfied if its virtual queue $S^k_{d,n}(t)$ and $W^k_{d,n}(t)$ are mean rate stable [337].

Now, the constraints $\mathbb{C}_2$ and $\mathbb{C}_{11}$ used in $P2$ is reformulated as follows:

$$\begin{aligned} P2 \quad : \quad & \max_{R(t)} \sum_{d=1}^{D} \sum_{n=1}^{N} \Phi_{d,n}^{k}(w_{d,n}^{k} R_{d,n}^{k} - \Omega_{d,n}^{k} E_{d,n}^{k}), \\ s.t. \quad & \mathbb{C}_1, \mathbb{C}_3, \\ & \mathbb{C}'_2 = \lim_{T\to\infty} \mathbb{E}\{|S_{d,n}^{k}|/t\} = 0, \\ \& \quad & \mathbb{C}'_{11} = \lim_{T\to\infty} \mathbb{E}\{|W_{d,n}^{k,T}|/t\} = 0. \end{aligned} \tag{4.45}$$

4.3.3.2 Lyapunov Drift

To solve the queue stability constraints $\mathbb{C}_1, \mathbb{C}_2$ & $\mathbb{C}_{11}$ of $P2$, we used the drift-plus-penalty algorithm [333], [334]. Before, using the drift-plus-penalty algorithm, we use the following assumptions:

$$\mathbb{E}\{[R_{d,n}^{k}]^2\} \leq F; \mathbb{E}\{[Z_{d,n}^{k}]^2\} \leq F; \mathbb{E}\{[R_{d,n}^{k,min} - R_{d,n}^{k}]^2\} \leq F \tag{4.46}$$

where F represents the upper bound of the traffic arrival and transmission rate.

Let us assume that $\Psi_{d,n}^{k}(t) = [Q_{d,n}^{k}(t), S_{d,n}^{k}(t), W_{d,n}^{k}(t)]$ is the queue matrix for the DDTs in each DMG. The quadratic Lyapunov function for queue congestion in a scalar form is written as follows:

$$L_q(\Psi_{d,n}(t)) = \frac{1}{2}\left[\sum_{d=1}^{D}\sum_{n=1}^{N}\left(Q_{d,n}^{2}(t) + S_{d,n}^{2}(t) + W_{d,n}(t)^2\right)\right]. \tag{4.47}$$

Now, the one-slot conditional Lyapunov drift according to Lyapunov function is given as follows:

$$\Delta(\Psi_{d,n}^{k}(t)) = \mathbb{E}\left[L_q(\Psi_{d,n}^{k}(t)+1) - L_q(\Psi_{d,n}^{k}(t))|\Psi_{d,n}^{k}(t))\right]. \tag{4.48}$$

The Eq.(4.48) represents the expected difference between the two Lyapunov functions at two-time slots with respect to current queue state $\Psi_{d,n}^{k}(t)$. The main aim of the Lyapunov drift is to push the Lyapunov function into a lower congestion state. Thus, the actual and virtual queues can be achieved alongwith the controllable queueing delay [333], [334].

$$\Delta(\Psi_{d,n}^{k}(t)) \leq B + \sum_{d=1}^{D}\sum_{n=1}^{N} Q_{d,n}^{k}(t)\mathbb{E}\left\{Z_{d,n}^{k}(t) - R_{d,n}^{k}(t)|\Psi_{d,n}^{k}(t)\right\}$$

$$+\sum_{d=1}^{D}\sum_{n=1}^{N} S_{d,n}^{k}(t)\mathbb{E}\left\{R_{d,n}^{k,min}(t) - R_{d,n}^{k}(t)|\Psi_{d,n}^{k}(t)\right\} + \sum_{d=1}^{D}\sum_{n=1}^{N} W_{d,n}^{k}(t)\mathbb{E}\left\{E_{d,n}^{k,T}(t) - E_{d,n}^{av}(t)|\Psi_{d,n}^{k}(t)\right\}. \tag{4.49}$$

where B is a constant function that satisfies.

$$B \geq \frac{1}{2}\mathbb{E}\left\{\sum_{d=1}^{D}\sum_{n=1}^{N}\left(Z_{d,n}^{2}(t) + R_{d,n}^{2}(t)\right)\right\} + \frac{1}{2}\mathbb{E}\left\{\sum_{d=1}^{D}\sum_{n=1}^{N}\left(R_{d,n}^{k,min}(t) - R_{d,n}^{k}(t)\right)^2\right\}$$

$$+\frac{1}{2}\mathbb{E}\Bigg\{\sum_{d=1}^{D}\sum_{n=1}^{N}\left(E_{d,n}^{k,T}(t)-E_{d,n}^{av}(t)\right)^2\Bigg\} \tag{4.50}$$

4.3.3.3 Upper Bound

To determine the upper bound of (4.48), we used the Lyapunov drift-plus-penalty algorithm [334] described as follows:

$$\Delta(\Psi_{d,n}^{k}(t))-V\mathbb{E}\Bigg\{\sum_{d=1}^{D}\sum_{n=1}^{N}(\Phi_{d,n}^{k}(w_{d,n}^{k}R_{d,n}^{k}-\Omega_{d,n}^{k}E_{d,n}^{k}))|\Psi_{d,n}^{k}(t)\Bigg\}$$

$$\leq B+\sum_{d=1}^{D}\sum_{n=1}^{N}Q_{d,n}^{k}(t)\mathbb{E}\Bigg\{Z_{d,n}^{k}(t)-R_{d,n}^{k}(t)|\Psi_{d,n}^{k}(t)\Bigg\}+\sum_{d=1}^{D}\sum_{n=1}^{N}S_{d,n}^{k}(t)\mathbb{E}\Bigg\{R_{d,n}^{k,min}(t)-R_{d,n}^{k}(t)|\Psi_{d,n}^{k}(t)\Bigg\}$$

$$+\sum_{d=1}^{D}\sum_{n=1}^{N}W_{d,n}^{k}(t)\mathbb{E}\Bigg\{E_{d,n}^{k,T}(t)-E_{d,n}^{av}(t)|\Psi_{d,n}^{k}(t)\Bigg\}-V\mathbb{E}\Bigg\{\sum_{d=1}^{D}\sum_{n=1}^{N}(\Phi_{d,n}^{k}(w_{d,n}^{k}R_{d,n}^{k}-\Omega_{d,n}^{k}E_{d,n}^{k})|\Psi_{d,n}^{k}(t)\Bigg\}, \tag{4.51}$$

where V is a control parameter.

To satisfy the constraints $\mathbb{C}_1$, $\mathbb{C}'_2$, $\mathbb{C}_3$, and $\mathbb{C}'_{11}$ we have to minimize the right hand side of the above expression over all control options. As B is bounded and $Q_{d,n}^{k}(t)Z_{d,n}^{k}(t)$ has no relationship with $\tau_{d,n}^{it}$, and $\alpha_{d,n}$. The problem in $P2$ is given as follows:

$$\begin{aligned} P2 \quad : \quad & \max_{\tau,\alpha}\Bigg\{S_{d,n}^{k}(t)[R_{d,n}^{k,min}(t)-R_{d,n}^{k}(t)]-Q_{d,n}^{k}(t)R_{d,n}^{k}(t)+W_{d,n}^{k}(t)[E_{d,n}^{k,T}(t)-E_{d,n}^{av}(t)]\Bigg\} \\ & - \quad V\Bigg\{(\Phi_{d,n}^{k}(w_{d,n}^{k}R_{d,n}^{k}-\Omega_{d,n}^{k}E_{d,n}^{k})|\Psi_{d,n}^{k}(t)\Bigg\} \\ s.t. \quad & \mathbb{C}_8,\mathbb{C}_9,\mathbb{C}_{10},\mathbb{C}_{12},\mathbb{C}_{13},\ \&\ \mathbb{C}_{14}. \end{aligned} \tag{4.52}$$

Now, the stochastic optimization problem $P2$ transformed into a static deterministic problem. But, this problem is still non-convex due to $\tau_d(t)$ and $\alpha_{d,n}^{k}$ in $R_{d,n}^{k}$. So, to solve this problem, the Lagrangian method is used.

The complexity of the Algorithm 8 is $\mathcal{O}(TKD)$.

Algorithm 8 Lyapunov Optimization Algorithm

Input: Weighing parameters w_1 and w_2.
Output: $R^*(t)$.
Initialization: Set the initial time t=0.
Set the queue matrix for the d^{th} DMG as $Q_{d,n}^{k}, S_{d,n}^{k}$ & $W_{d,n}^{k}$.
Set $\alpha_{d,n}^{k}=\alpha_{d,n}^{*k}$ & $\tau_{d,n}^{it}=\tau_{d,n}^{*it}$.

1: **while** $t<T$ **do**
2: Obtain ϕ^* using Algorithm 7.
3: Update $Q_{d,n}^{k}$, $S_{d,n}^{k}$ & $W_{d,n}^{k}$ using (4.15), (4.43) and (4.44) $\forall\mathcal{D},\mathcal{N},\mathcal{K}$
4: **end while**

4.3.4 Joint Time and Power Allocation Problem

In this section, we optimize the time and power assigned to the d^{th} DDT in each DMG.

$$\begin{aligned} P2 \quad : \quad & \max_{\tau,\alpha} \sum_{d=1}^{D} \sum_{n=1}^{N} \mathbb{E}\Big\{ S_{d,n}^{k}(t)[R_{d,n}^{k,min}(t) - R_{d,n}^{k}(t)] - Q_{d,n}^{k}(t)R_{d,n}^{k}(t) + W_{d,n}^{k}(t)[E_{d,n}^{k,T}(t) - E_{d,n}^{av}(t)] \Big\} \\ & - \; V\Big\{ \Phi_{d,n}^{k}(w_{d,n}^{k}R_{d,n}^{k} - \Omega_{d,n}^{k}E_{d,n}^{k}) \Big\} \qquad (4.53) \\ s.t. \quad & \mathbb{C}_8, \mathbb{C}_9, \mathbb{C}_{10}, \mathbb{C}_{12}, \mathbb{C}_{13}, \; \& \; \mathbb{C}_{14} \end{aligned}$$

It should be noted that the inequality constraints $\mathbb{C}_8, \mathbb{C}_9, \; \& \; \mathbb{C}_{12}$ is transformed into an equality form from the theorems used in [335].

On using these theorems, we remove the constraint C_{12} and rearrange the constraints C_8 and C_9. Thus, the $P2$ is reformulated as:

$$\begin{aligned} P2 \quad : \quad & \max_{\tau,\alpha} \sum_{d=1}^{D} \Big\{ S_{d,n}^{k}(t)R_{d,n}^{k,min}(t) - (S_{d,n}^{k}(t) + Q_{d,n}^{k}(t) + \Phi_{d,n}^{k}w_{d,n}^{k}V)R_{d,n}^{k}(t) + (\Omega_{d,n}^{k}V + W_{d,n}^{k})E_{d,n}^{k,T}(t) \\ & - \; W_{d,n}^{k}(E_{d,n}^{av}(t)) \Big\} \qquad (4.54) \\ & s.t. \; \mathbb{C}_8, \mathbb{C}_9, \mathbb{C}_{10}, \mathbb{C}_{13}, \; \& \; \mathbb{C}_{14} \end{aligned}$$

In order to obtain the optimal value of power and time, we assume the following:

$$\lambda_{d,n}^{k}(t) \triangleq \eta_{d,n}P_{b}^{max}h_{b,d}^{k}(t) \qquad (4.55)$$

Now, the $P2$ is transformed as follows:

$$\begin{aligned} P2 \quad : \quad & \max_{\tau,\alpha} \sum_{d=1}^{D} \Big\{ S_{d,n}^{k}(t)R_{d,n}^{k,min}(t) - (S_{d,n}^{k}(t) + Q_{d,n}^{k}(t) + \Phi_{d,n}^{k}w_{d,n}^{k}V)R_{d,n}^{k}(t) \\ & + \; (\Omega_{d,n}^{k}V + W_{d,n}^{k})[(P_{b}^{max} + P_{d,n}^{c} - \sum_{d=1}^{D} \lambda_{d,n}^{k}(t))\tau_0(t)] \\ & + \; (\Omega_{d,n}^{k}V + W_{d,n}^{k})(P_{d}^{k}\alpha_{d,n}^{k}(t) + P_{d,n}^{c'})\tau_d(t) - W_{d,n}^{k}(E_{d,n}^{av}(t)) \Big\} \qquad (4.56) \\ & s.t. \; \mathbb{C}_8, \mathbb{C}_9, \mathbb{C}_{10}, \mathbb{C}_{13}, \; \& \; \mathbb{C}_{14} \end{aligned}$$

$P2$ is still non-convex due to the coupling of time and power allocation factors. So, to transform it into a standard convex problem, we assume that

$$e_{d,n}^{k}(t) \triangleq \tau_d P_{d}^{k}\alpha_{d,n}^{k}(t) \qquad (4.57)$$

Now, the $\mathbb{C}_8$ is transformed as follows:

$$\mathbb{C}_8 : e^k_{d,n}(t) + P^{c'}_{d,n} = Q^{k,E}_{d,n} + \lambda^k_{d,n}(t)\tau_0(t). \tag{4.58}$$

The problem $P2$ is reformulated as follows:

$$\begin{aligned} P8 : \max_{\tau,\alpha} & \sum_{d=1}^{D} S^k_{d,n}(t) R^{k,min}_{d,n}(t) - (S^k_{d,n}(t) + Q^k_{d,n}(t) + \Phi^k_{d,n} w^k_{d,n} V)\tau_d(t) \\ & \frac{B}{K}\log_2\left(1 + \frac{e^k_{d,n}(t)\delta^k_{d,n}(t)}{\tau_d(t)}\right) + (\Omega^k_{d,n}V + W^k_{d,n})[(P^{max}_b + P^c_{d,n} - \sum_{d=1}^{D}\phi^k_{d,n}(t))\tau_0] \\ & +(\Omega^k_{d,n}V + W^k_{d,n})(e^k_{d,n}(t) + P^{c'}_{d,n}\tau_d(t) - W^k_{d,n}(E^{av}_{d,n}(t)) \\ & s.t.\ \ \mathbb{C}_8, \mathbb{C}_9, \mathbb{C}_{10}, \mathbb{C}_{13}, \ \& \ \mathbb{C}_{14} \end{aligned} \tag{4.59}$$

where $\delta^k_{d,n}(t) = \left(\frac{|h^k_{d,n}|^2}{I^{no}_{d,n}(t) + I^{co}_{d,n}(t) + I^{cr}_{d,n}(t) + \sigma^2}\right), \forall d, n \neq 0.$

The Lagrangian function of Eq. (4.59) is given as follows:

$$\begin{aligned} & \mathcal{L}(\tau^{eh}_{d,n}(t), \tau_d(t), e^k_{d,n}(t), b, c, d) = (S^k_{d,n}(t) + Q^k_{d,n}(t) + \Phi^k_{d,n} w^k_{d,n} V)\tau_d(t)\frac{B}{K}\log_2\left(1 + \frac{e^k_{d,n}(t)\delta^k_{d,n}(t)}{\tau_d(t)}\right) \\ + \ & (\Omega^k_{d,n}V + W^k_{d,n})(e^k_{d,n}(t) + \tau_d(t)P^{c'}_{d,n}) - b\left(\sum_{d=1}^{D}\sum_{n=1}^{N}(\tau^{eh}_{d,n}(t) + \tau_d(t)) - 1\right) + (\Omega_{d,n}V + W^k_{d,n}) \\ & \left(P^{max}_b + P^c_{d,n} - \sum_{d=1}^{D}\sum_{n=1}^{N}\phi^k_{d,n}(t)\right)\tau_0(t) - c\sum_{d=1}^{D}\sum_{n=1}^{N}\left(e^k_{d,n}(t) + P^{c'}_{d,n} - Q^{k,E}_{d,n} - \lambda^k_{d,n}(t)\tau_0(t)\right) \end{aligned} \tag{4.60}$$

In (4.60), b, c, and d are the Lagrange multipliers for $\mathbb{C}_8$, $\mathbb{C}_9$, and $\mathbb{C}_{13}$, respectively. Note that the non-negative constraints $\mathbb{C}_{10}$ and $\mathbb{C}_{14}$ are used within the Lagrangian function to obtain the optimal solutions. Now, the dual function of Eq. (4.59) is given as follows:

$$\min_{b,c,d>0} \ \max_{\tau,e} \mathcal{L}(\tau_0(t), \tau_d(t), e^k_{d,n}(t)). \tag{4.61}$$

As the Eq. (4.59) is a convex problem, and fulfil the Slaters condition, therefore, the duality gap between Eq. (4.59) and (4.61) becomes zero [320]. Hence, the optimal solution of Eq. (4.59) is obtained by using an iterative method.

The maximization of $\mathcal{L}(\tau_0(t), \tau_d(t), e^k_{d,n}(t))$ with respect to $(\tau_0(t), \tau_d(t), e^k_{d,n}(t))$ for given (b, c, d) is solved using the Karush-Kuhn-Tucker (KKT) conditions. The partial derivative of $\mathcal{L}$ with respect to $\tau_0(t)$, $\tau_d(t)$ and $e^k_{d,n}(t)$ are given as follows:

$$\frac{\partial \mathcal{L}}{\partial \tau_0} = -b + (\Omega^k_{d,n}V + W^k_{d,n})(P^{max}_b(t) + p^c_{d,n}) + [c - (\Omega^k_{d,n}V + W^k_{d,n})]\sum_{d=1}^{D}\sum_{n=1}^{N}\lambda^k_{d,n}(t) \tag{4.62}$$

$$\frac{\partial \mathcal{L}}{\partial e^k_{d,n}} = \frac{B(S^k_{d,n}(t)+Q^k_{d,n}(t)+\Phi^k_{d,n}w^k_{d,n}V)\tau_d(t)\delta^k_{d,n}(t)}{K(\tau_d(t)+e^k_{d,n}(t)\delta^k_{d,n}(t))\ln 2} + (\Omega^k_{d,n}V + W^k_{d,n}) - b \tag{4.63}$$

$$\frac{\partial \mathcal{L}}{\partial \tau_d} = (S^k_{d,n}(t)+Q^k_{d,n}(t)+\Phi^k_{d,n}w^k_{d,n}V)\tau_d(t)\frac{B}{K}\log_2\left(1+\frac{e^k_{d,n}(t)\delta^k_{d,n}(t)}{\tau_d(t)}\right)$$

$$+\frac{e^k_{d,n}(t)\delta^k_{d,n}(t)}{\ln 2(\tau_d(t)+e^k_{d,n}(t)\delta^k_{d,n}(t))} + (\Omega^k_{d,n}V + W^k_{d,n})P^{c'}_{d,n} - b \tag{4.64}$$

To obtain the optimal value of $\alpha^{k*}_{d,n}(t)$, put $\alpha^{k*}_{d,n}(t) = \frac{e^k_{d,n}(t)}{\tau^{id}_{d,n}(t)}$, and $\frac{\partial \mathcal{L}}{\partial e^k_{d,n}} = 0$ in Eq. (4.59). Now, we get

$$\alpha^{k*}_{d,n} = \left[\frac{B(S^k_{d,n}(t)+Q^k_{d,n}(t)+\Phi^k_{d,n}w^k_{d,n}V)}{K\ln 2(b-(\Omega^k_{d,n}V+W^k_{d,n}))} - \frac{1}{\delta^k_{d,n}(t)}\right] \tag{4.65}$$

where $[x]^+$=max$\{x,0\}$. From Eq. (4.65), it is observed that $\alpha^{k*}_{d,n}$ is inversely proportional to the downlink channel gain. This means that the DDT must acquire the channel with higher gain so that less amount of power consumption provide maximum energy efficiency.

Let us assume that $f_0(b) = \frac{\partial \mathcal{L}}{\partial \tau_0(t)}$. As $\mathcal{L}$ is a linear function of τ_0 with $\tau_0(t) \geq 0$. Now the bounded value of $\tau_0(t)$ with respect to the Lagrangian function is given as follows:

$$\tau^*_0(t) = \begin{cases} \in [0,1), & \text{if } f_0(b) = 0, \\ = 0, & \text{otherwise.} \end{cases} \tag{4.66}$$

On substituting the value from (4.65) to (4.61) and taking its partial derivative with respect to $\tau_d(t)$, the optimize value of $\tau^*_d(t)$ is achieved and given as follows:

$$\begin{aligned} f(\delta^k_{d,n}(t),b) \triangleq \frac{\partial \mathcal{L}}{\partial \tau_d(t)} &= (c\ln 2 + (\Omega^k_{d,n}V + W^k_{d,n}))G\log_2\left(1+\left[G-\frac{1}{\delta^k_{d,n}(t)}\right]^+\delta^k_{d,n}(t)\right) \\ &- (c+(\Omega^k_{d,n}V+W^k_{d,n}))\left(\left[G-\frac{1}{\delta^k_{d,n}(t)}\right]^+ + p^c_{d,n}\right) - b \end{aligned} \tag{4.67}$$

where $G \triangleq \left[\frac{(S^k_{d,n}(t)+Q^k_{d,n}(t)+\Phi^k_{d,n}w^k_{d,n}V)}{\ln 2(b-(\Omega^k_{d,n}V+W^k_{d,n}))}\right]$.

The value of $\tau^*_d(t)$ is given as follows:

$$\tau^*_d(t) = \begin{cases} \left(\frac{Q^{k,E}_{d,n}(t)+\lambda^k_{d,n}(t)\tau_0(t)}{\alpha^{*k}_{d,n}+P^c_{d,n}}\right), & \text{if } \delta^k_{d,n}(t) > \beta^{k*}_{d,n}, \\ \left[0, \frac{Q^{k,E}_{d,n}(t)+\lambda^k_{d,n}(t)\tau_0(t)}{\alpha^{*k}_{d,n}+P^c_{d,n}}\right], & \text{if } \delta^k_{d,n}(t) > \beta^{k*}_{d,n}, \\ 0, & \text{if } \delta^k_{d,n}(t) < \beta^{k*}_{d,n}. \end{cases} \tag{4.68}$$

where $\beta_{d,n}^{k*}$ is the solution of

$$(S_{d,n}^k(t)+Q_{d,n}^k(t)+\Phi_{d,n}^k w_{d,n}^k V)\tau_d(t)\frac{B}{K}\log_2\left(\frac{(S_{d,n}^k(t)+Q_{d,n}^k(t)+\Phi_{d,n}^k w_{d,n}^k V)\lambda_{d,n}^k}{(\Omega_{d,n}^k V+W_{d,n}^k)\ln 2}\right)$$
$$+\quad \frac{V\Omega_{d,n}^k+W_{d,n}^k}{\lambda^k(t)_{d,n}}-\left(\frac{S_{d,n}^k(t)+Q_{d,n}^k(t)+\Phi_{d,n}^k w_{d,n}^k V}{\ln 2}\right)-(\Omega_{d,n}^k V+W_{d,n}^k)P_{d,n}^k-a \tag{4.69}$$

Furthermore, $\tau_0^*(t)$ and $\tau_d^*(t)$ should satisfy

$$\tau_0^*(t)+\sum_{d=1}^{D}\tau_d^*(t)=\begin{cases}1, & \text{if } a>0,\\ \leq 1, & \text{otherwise.}\end{cases} \tag{4.70}$$

Now, the value of Lagrangian multipliers using the gradient method is given as follows:

$$b_{d,n}^k(\iota+1)=[b_{d,n}^k(\iota)-\varepsilon_1(Q_{d,n}^{k,E}+E_{d,n}^{k,h}-E_{d,n}^{c'})]^+ \tag{4.71}$$

$$c_{d,n}^k(\iota+1)=[c_{d,n}^k(\iota)-\varepsilon_2(1-\tau_0)+\sum_{d=1}^{D}\tau_d]^+ \tag{4.72}$$

where ι is an iteration index, and ε_1 & ε_2 are the positive step sizes.

4.3.5 Updation of (Φ,Ω)

In this section, we update the value of Φ & Ω. Assume that $\upsilon_{d,n}^k(\Phi_{d,n}^k)=\Phi_{d,n}^k E_{d,n}^k-1$, and $\upsilon_{d,n}^k(\Omega_{d,n}^k)=\Omega_{d,n}^k E_{d,n}^k-w_{d,n}^k R_{d,n}^k$, where $d\in\{1,2,\ldots,D\}$. The optimal solution is obtained at (Φ,Ω), when $\upsilon(\Phi,\Omega)=0$. Now, according to damped Newton method, the value of Φ and Ω are updated as follows:

$$\Phi(\iota+1)=\Phi(\iota)+\mu(\iota)\rho(\iota), \tag{4.73}$$

$$\Omega(\iota+1)=\Omega(\iota)+\mu(\iota)\rho(\iota), \tag{4.74}$$

$$\rho(\iota)=\upsilon'(\Phi,\Omega)^{-1}\upsilon(\Phi,\Omega), \tag{4.75}$$

where $\upsilon'(\Phi,\Omega)$ is the Jacobian matrix of $\upsilon(\Phi,\Omega)$, ι is the iteration index, and $\rho(\iota)$ is the greatest of ρ satisfying.

$$||\upsilon(\Phi(\iota)+\rho\rho(\iota),\Omega(\iota)+\rho\rho(\iota))||\leq(1-\rho\chi)||(\Phi(\iota),\Omega(\iota))||, \tag{4.76}$$

where $\rho\in\{0,1\}$, $\chi\in\{0,1\}$, and $||.||$ is the standard Euclidean norm.

Now, the updated equations of Φ and Ω is expressed as follows:

$$\Phi_{d,n}^k(\iota+1)=(1-\rho(\iota))\Phi_{d,n}^k(\iota)+\rho(\iota)\frac{1}{E_{d,n}^k} \tag{4.77}$$

$$\Omega_{d,n}^{k}(\iota+1) = (1-\rho(\iota))\Omega_{d,n}^{k}(\iota) + \rho(\iota)\frac{w_{d,n}^{k}R_{d,n}^{k}}{E_{d,n}^{k}} \tag{4.78}$$

4.3.6 Energy-Delay Tradeoff Algorithm for NOMA-based DMG with WPCN

Algorithm 9 EE and Delay Tradeoff for NOMA-based DMG with WPCN

Input: ε = Accuracy Indicator; ι = Iterative index; ι_{max} = Maximum Iteration value.
Output: $\overline{EE}_{d,n}^{*k}$.
Initialization: Set $\iota = 0$; and Initialize $\Phi_{d,n}^{k}$ and $\Omega_{d,n}^{k}$;

repeat
  Compute subcarrier allocation indicator ϕ using Algorithm 7;
  Transform the stochastic optimization problem into deterministic optimization problem using Algorithm 8;
  Initialize b and c;
  repeat
    Compute the power allocation factor $\alpha_{d,n}^{*k}$ using Eq. (4.65);
    Compute the time allocation indicator $\tau_0^*(t)$ and $\tau_d^*(t)$ using Eq. (4.66) and (4.68);
    Update the dual variables b and c using Eq. (4.71) and (4.72);
  until b and c converge;
  Compute $\rho(\iota)$ using Eq. (4.75);
  Compute the ρ after satisfying Eq. (4.76);
  Update $\Phi_{d,n}^{k}$ and $\Omega_{d,n}^{k}$ using Eq. (4.77) and (4.78);
  $\iota = \iota + 1$;
until $||\upsilon(\Phi,\Omega)|| < \varepsilon$.

In this section, an iterative energy-efficient algorithm for NOMA-based D2D with WPCN is designed, as shown in algorithm 9. Firstly, the DDT allocates equal power to all DMUs in each DMG, and then use the following process to achieve the maximum EE. Compute the subcarrier allocation $\phi_{d,n}^{*k}$ using Algorithm 7. Transform the stochastic optimization problem into deterministic problem, i.e., obtain $R_{d,n}^{k}(t)$ using Algorithm 8. Compute the optimal value of power allocation coefficients and information transmission time using the Lagrangian function and KKT conditions, i.e., $\alpha_{d,n}^{*k}$ and τ_d^* using Eq. (4.65) and (4.68). In this way, the closed-form expression of $\alpha_{d,n}^{*k}$ for DDT in each DMG across each subcarrier is obtained. The time complexity of Algorithm 9 is $\mathcal{O}(\iota TKDN)$.

4.4 Performance Evaluation

In this section, performance of the proposed scheme is evaluated and discussed.

4.4.1 Numerical Settings

The parameters are chosen on the basis of 3GPP urban path loss model [336], and are listed in Table 4.2. In the proposed model, a cellular cell is taken in which the BS is located at the

Table 4.2: Simulation Parameters

Parameters	**Values**
Radius of cell	500 m
Radius of DMG	30 m
Number of CMUs ($\mathcal{M}$)	5$\sim$10
Number of DMGs ($\mathcal{D}$)	5$\sim$10
Number of DMUs in each DMG ($\mathcal{N}$)	4
Subchannel bandwidth (B/K)	25 KHz
Number of sub-carriers ($\mathcal{K}$)	5
SINR threshold of CMU (I_i^{th})	2 dBm
Max. transmission power of DDT ($P_d^{\max}$)	25 dBm
Max. transmission power of BS ($P_b^{\max}$)	50 dBm
Data Buffer Size (D_b)	1000 bits/Hz
Energy Buffer Size (E_b)	10 J
Minimum data rate of DMU ($R_{d,n}^{k,\min}$)	0.2$\sim$2 bits/slot/Hz.
Energy transformation efficiency (η)	0.9
Circuit power consumption (P_d^c)	50 mW
Weighing factor ($w_{d,n}^k$)	0.5, 1, 1.5
Control Parameter V	200
Actual admitted traffic arrival rate $Z_{d,n}^k$	0.5$\sim$ 2.5 bits/slot/Hz
Maximum number of DMGs $U_{\max}$	2

center, and CMUs and DMGs are uniformly distributed. Each DMG consist of one DDT, and $\mathcal{N}$ DMUs. Assume that D_b and E_b represent the data and energy buffer size of each CMU and DMG, respectively.

4.4.2 Results and Discussion

4.4.2.1 Comparison of the proposed Algorithms with the pre-existing schemes

In this subsection, the effectiveness of a proposed scheme is evaluated and compared with the existing NOMA, i.e., EEDRO [338] and OFDMA, i.e, TRADEOFF [337] schemes. In EEDRO, authors have studied the dynamic resource allocation in downlink NOMA networks. Also, authors proposed a suboptimal subchannel assignment algorithm based on the two-side matching method. Based on the framework of Lyapunov optimization, the problem of energy efficient optimization has been broken down into three subproblems, two of which are linear and the rest of which can be solved via Lagrangian optimization. On the other side, in TRADEOFF, investigated the EE-delay tradeoff problem in cellular network assisted D2D communication systems by a formulated stochastic optimization problem, which optimizes EE subject to the network stability, average power, and interference-control constraints. An algorithm, the TRADEOFF, has been developed to optimally solve the problem, which thus offers an important performance benchmark for other heuristic algorithms.

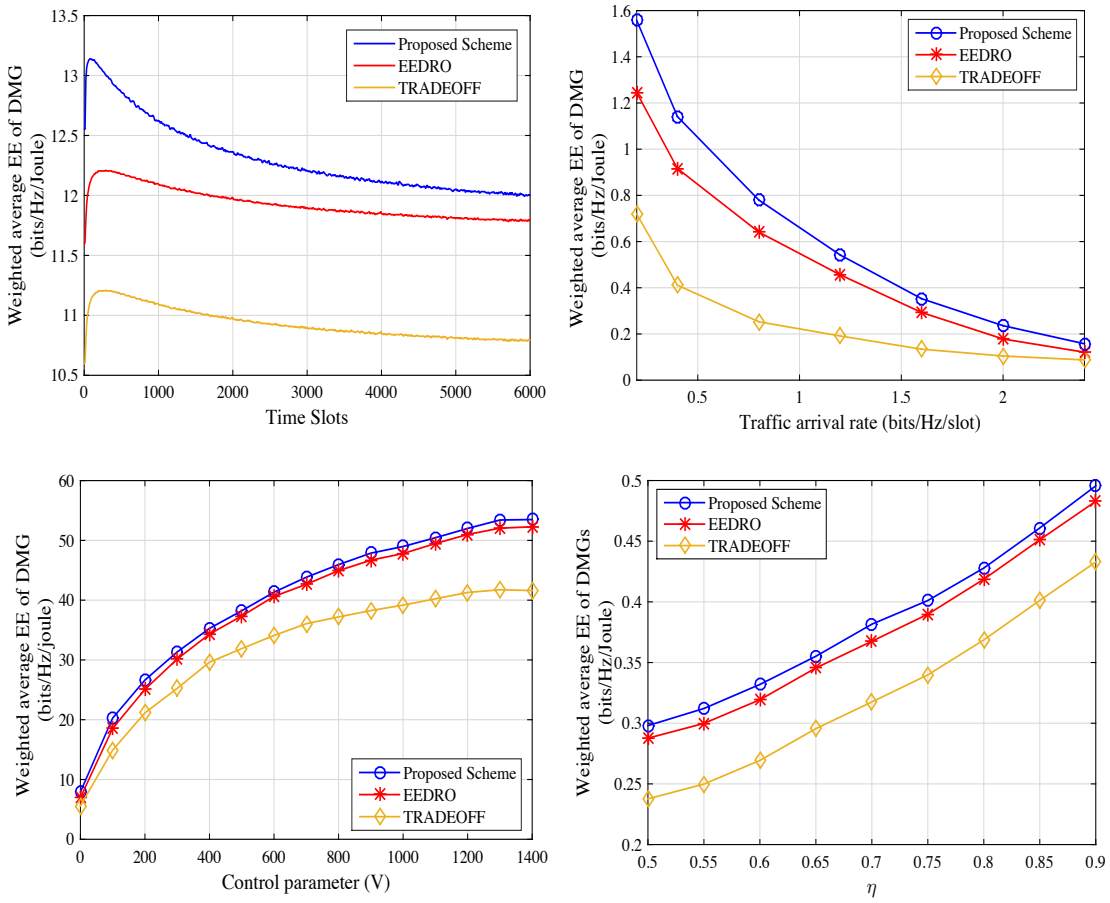

Figure 4.2: Comparative Analysis: (a) Effect on weighted average EE of DMG versus time slots $\eta = 0.9$, $P_b^c = 0.05W$ and $P_{d,n}^{c'} = 0.001W$. (b) Effect on weighted average EE of DMG with respect to traffic arrival rate (c) Effect on weighted average EE of DMG with respect to the control parameter (V) (d) Effect on weighted average EE of DMG with respect to Energy transformation efficiency (η).

Fig. 4.2(a) represent the simulated result between the weighted average EE of DMG and time slots under $\eta = 0.9$, $Z_{d,n}^k = 1.5$ $P_b^c = 0.05W$, and $P_{d,n}^{c'} = 0.001W$. The result shows that EE fluctuates gradually with an increase in time slot t. Also, the result implies that the proposed scheme achieves 2.4% and 10.6% higher average EE than the existing EEDRO and TRADEOFF schemes. This is because the proposed scheme adaptively allocates the subchannel, power, and time to harvest the energy among DMGs. Also, the proposed scheme used many-to-one matching for subcarrier allocation whereas, in EEDRO, many-to-many matching was used. It is well known that many-to-many subcarrier allocation consumes more power than the many-to-one. On the other side in TRADEOFF prismatic branch and bound was used which is more complex than the Lagrangian method.

Fig. 4.2(b) represents the graph between the weighted average EE of DMGs with respect to the actual admitted traffic arrival rate under $V = 100$, $P_b^c = 0.05W$, and $P_{d,n}^{c'} = 0.001W$. The

result shows that average EE decreases with an increase in the traffic arrival rate. This is because with an increase in the traffic arrival rate, the congestion and average power consumption increase exponentially. The result shows that when the $Z_{d,n}^{k}$=1.5, the proposed scheme achieves 5% and 55.5% higher EE than the EEDRO and TRADEOFF schemes.

Fig. 4.2(c) shows the effect on weighted average EE of DMG with respect to V under P_{b}^{c}=0.05W, $P_{d,n}^{c'}$=0.001W, $w_{d,n}^{k}$=1, $Z_{d,n}^{k}$=1.5. The result shows that the EE increases exponentially with an increase in V but after a certain value of V, the average EE becomes constant. This is because with an increase in V and fixed weight all the DMGs harvest and consume equal energy at both the downlink WET stage and uplink WIT stage. Also, the result shows that when the V reaches up 800, then the proposed scheme achieves 2.1% and 15.21% higher EE than the EEDRO and TRADEOFF, respectively.

Fig. 4.2(d) depicts the variation in weighted average EE of DMG with respect to variation η under $P_{b}^{c} = 0.05W$, $P_{d,n}^{c'} = 0.001W$, $w_{d,n}^{k} = 1$, $Z_{d,n}^{k}$=1.5. The results show that with an increase of η, the value of EE increases. This is because with an increase in η, the time to harvest the energy increases and time to transmit the information decreases. The results show that when $\eta = 0.7$, the proposed scheme achieves 2.6% and 15.78% higher EE than the EEDRO and TRADEOFF. The reason behind this is that the proposed scheme allocates adaptive time among DMGs as per the time-varying channel conditions and data queue length.

4.4.2.2 Impact on average power consumption

Fig. 4.3 (a) shows an impact on average power consumption with respect to V with an increase in the number of subcarriers. The results show that average power consumption decreases with V with an increase in the number of subcarriers. This is because, with an increase in subcarriers, the DDTs easily acquire and reuse the best subcarrier which is already occupied by the CMUs. The result shows that when V reaches to 70, then K=4 consumes 4.1% less energy as compared to K=2.

Fig.4.3 (b) shows an impact on average power consumption versus V with respect to the increase in data rate requirement of DMUs. The result shows that average power consumption increases when data rate requirements of DMUs increases. This is due to the fact that with an increase in data rate requirements of DMUs, the DDTs have to transmit information with large energy due to which power consumption increases. The result show that when V reaches to 70, then power consumed at $R_{d,n}^{k} = 2$ bits/slot/Hz is 4.823% higher than the $R_{d,n}^{k} = 1.5$ bits/slot/Hz.

4.4.2.3 Impact on weighted EE and average delay

Fig.4.3 (c) shows an impact on weighted average EE of DMG with respect to V keeping the weight constant. The result shows that the average EE increases with an increase in V. This is due to the fact that V is proportional to EE which means that a higher value of V generates more impact on EE. Also, the result shows that an average EE increases with an increase in

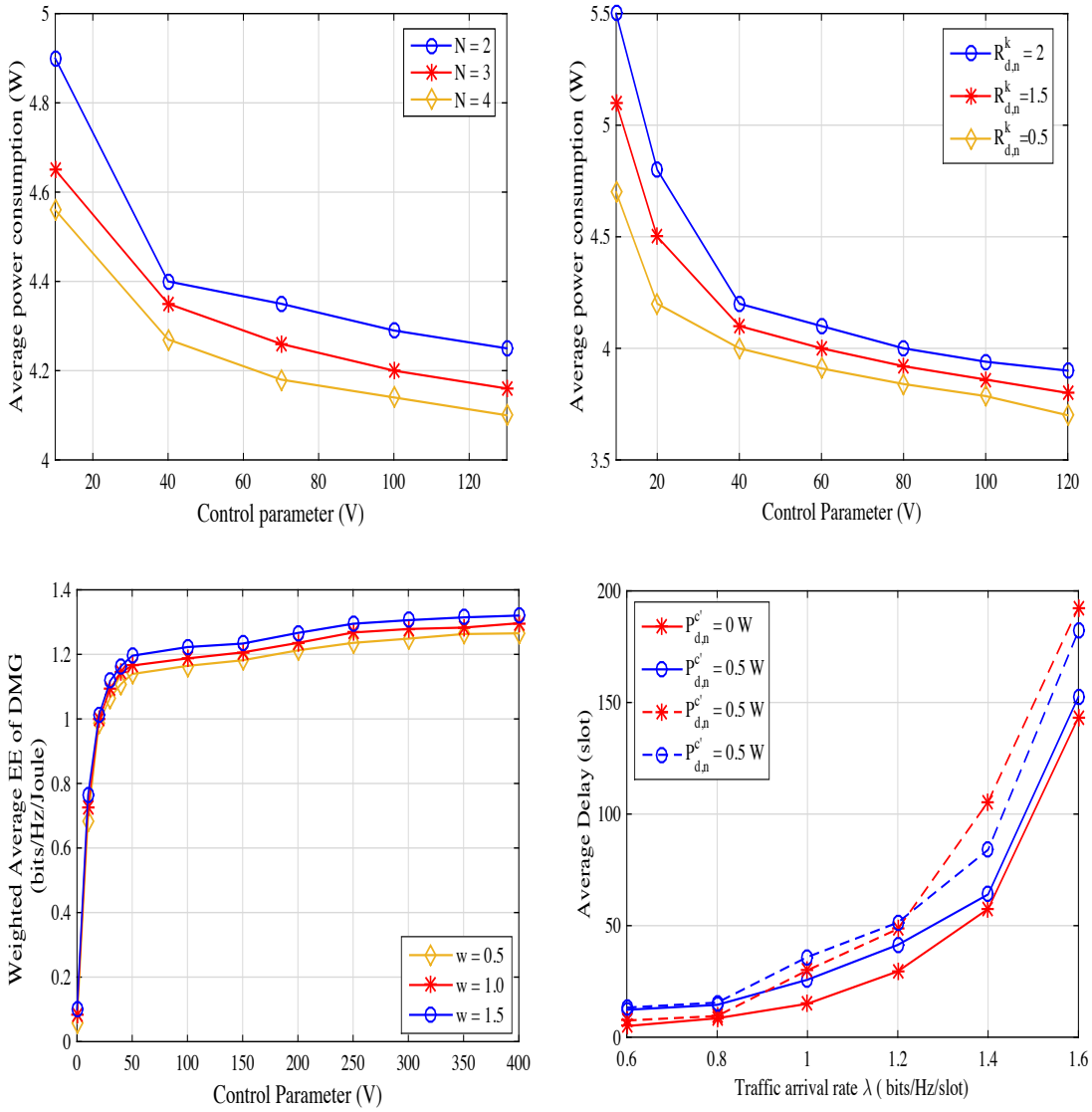

Figure 4.3: Comparative Analysis: (a) Impact on average power consumption v/s V with an increase in number of subcarriers and $\eta = 0.9$, $P_b^c = 0.05W$ and $P_{d,n}^{c'} = 0.001W$, $R_{d,n}^k = 5$ bits/slot/Hz (b) Impact on average power consumption V with varying data rate requirement of DMUs and $\eta = 0.9$, $P_b^c = 0.05W$, $P_{d,n}^{c'} = 0.001W$, and $K = 4$ (c) Impact on weighted average EE of DMG v/s V under different values of weighted factor (d) Impact on average delay v/s Z at different values of $P_{d,n}^{c'}$.

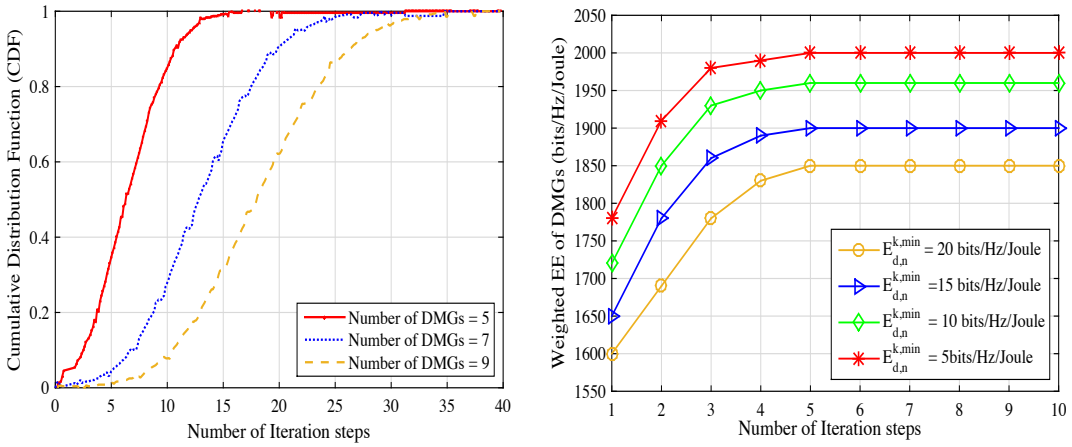

Figure 4.4: Comparative Analysis: (a) Convergence rate of the Algorithm 7 in terms of CDF at $P_d^k = 20 \sim 25dBm$ (b) Convergence testing of Algorithm 8 at $P_d^k = 20 \sim 25dBm$, $E_b = 5 \sim 10J$, and $D_b = 1000\ bits/Hz$.

weighting factor w of DMGs. This is due to the fact that with an increase in w, the energy harvesting by that DMG increases as EE is directly depended upon the weighing factor.

Fig.4.3 (d) shows an impact on an average delay with respect to change in traffic arrival rate (Z). The result shows that delay increases exponentially with an increase in actual admitted traffic arrival rate. The reason behind this is that with an increase in traffic arrival rate the queue backlog increases.

4.4.2.4 Convergence Rate Analysis

Fig.4.4(a) represents the cumulative distribution function with the number of iterations. The graph shows the convergence rate of the Algorithm 7 with different number of DMGs. The result shows that the proposed algorithm 7 takes a lesser number of iterations to converge. For example, when the number of DMGs in a cell is 9, on an average 40, the number of iterations is used by the proposed algorithm to converge. Moreover, the graph shows that when the number of DMGs in a cell increases, the number of iteration steps also increases. The reason behind such behavior is that the probability of reusing the subcarriers increases which result in an increase in the iteration steps.

Fig.4.4(b) shows the convergence rate of the Algorithm 8 at fixed data and energy buffer with respect to the variation in EE requirements of DMGs. The result shows that an optimal EE is achieved for the small number of iterations, but as the EE requirements of DMGs increases, the convergence rate also decreases. The reason behind such behaviour depends upon the availability of subcarriers and V. When the weighted average EE requirements of DMGs increases then they have to search and reuse the best possible subcarrier as per its availability to meet their EE requirements. As the number of DMGs in a cell increases, the possibility to find the best subcarrier decreases due to an increase in co-channel interference.

4.5 Summary

In this chapter, we investigate a distributed energy-efficient and delay tradeoff scheme for NOMA-based DMGs with wireless powered communication networks. Firstly, the DDTs and CMUs harvest energy from the RF signals of the BS. Then, the CMUs and DDTs transmit the information to the BS and DMUs from the harvested energy using TDMA and NOMA, respectively. Considering both stochastic traffic arrivals and time-varying channel conditions, the stochastic optimization problem is formulated whose aim is to maximize the EE and minimize the delay. To solve the problem, the weighted sum method, subcarrier allocation, Lyapunov optimization, and Lagrangian function is used. Finally, the evaluated result shows that the proposed scheme provides superior EE as compared to an existing NOMA and OFDMA schemes. In the future, we extend this work by considering imperfect channel information.

Chapter 5

Conclusion and Future Scope

D2D communication is a promising technology in which the spectrum resources are reused efficiently with CMUs in an underlay of 5G network. Using it, network capacity and spectral efficiency increases but it introduces the co-channel interference. Moreover, massive connectivity has not been fully exploited for efficient spectral efficiency usage in the existing solutions. Therefore, to address the above-mentioned challenges, PD-NOMA technique is integrated with the DMGs. Apart from spectral efficiency and massive connectivity, energy efficiency is also a challenging issue in D2D communication due to the limited energy storage capability of a battery. To overcome the aforementioned challenges, the research work focused on two different approaches.

Firstly, a “Cross-Layer Interference Management Scheme for D2D Mobile Users Using NOMA" is proposed. In this approach, the sum rate of the overall network is maximized with respect to the constraints of RB and power allocation. To achieve this goal, the DMGs are designed between the DDT and DMUs to reduce the intra-user interference using the SIC technique. Secondly, the resource allocation scheme for both the CMUs and DMGs is designed to mitigate the cross-interference using many-to-many mapping scheme. Also, to fully exploit the potential benefits of DMGs and to enhance the spectral efficiency of the DMGs, the GRSC based RB reuse algorithm among DMGs is proposed. Thirdly, for power optimization, the DC programming approach based on a SCALE is used to reduce co-channel interference. Finally, a joint user grouping, RB and power allocation scheme is designed to reduce the complexity and convergence rate, and improve the sum-rate. The proposed scheme achieves 4.54% and 22.72% higher sum-rate than the JUCPA and JSPA with respect to an increase in the number of DMGs. However, if we extend this work to a multicell scenario, the problem of intercell interference becomes severe. Hence in the next approach, we explore the issues of intercell interference in the multicell systems.

In the second approach, we investigate a distributed energy-efficient and delay tradeoff scheme for NOMA-based DMGs with wireless powered communication networks. Firstly, the DDTs and CMUs harvest energy from the RF signals of the BS. Then, the CMUs and DDTs transmit the information to the BS and DMUs from the harvested energy using TDMA and

NOMA, respectively. Considering both stochastic traffic arrivals and time-varying channel conditions, the stochastic optimization problem is formulated whose aim is to maximize the EE and minimize the delay. To solve the problem, the weighted sum method, subcarrier allocation, Lyapunov optimization, and Lagrangian function is used. Finally, the evaluated result shows that the proposed scheme provides superior EE as compared to an existing NOMA and OFDMA schemes. In the future, we extend this work by considering imperfect channel information.

Bibliography

[1] C. V. N. Index, "Global Mobile Data Traffic Forecast Update, 2016-2021,"*White Paper, Cisco, San Jose, CA, USA*, Mar. 2017.

[2] F. Jameel, Z. Hamid, F. Jabeen, S. Zeadally, and M. A. Javed, "A Survey of Device-to-Device Communications: Research Issues and Challenges,"in *IEEE Communications Surveys and Tutorials*, vol. 20, no. 3, pp. 2133-2168, Apr. 2018.

[3] A. Asadi, Q. Wang, and V. Mancuso, "A Survey on Device-to-Device Communication in Cellular Networks,"in *IEEE Communications Surveys and Tutorials*, vol. 16, no. 4, pp. 1801-1819, Apr. 2014.

[4] M. Noura and R. Nordin, "A survey on interference management for device-to-device (D2D) communication and its challenges in 5G networks,"in *Journal of Network and Computer Applications*, vol. 71, pp. 130-150, Aug. 2016.

[5] L. Dai, B.Wang, Z. Ding, Z.Wang, S. Chen, and L. Hanzo, "A Survey of Non-Orthogonal Multiple Access for 5G,"in *IEEE Communications Surveys and Tutorials*, vol. 20, no. 3, pp. 2294-2323, Jan. 2018.

[6] X. Lu, P. Wang, D. Niyato, D. I. Kim, and Z. Han, "Wireless Networks With RF Energy Harvesting: A Contemporary Survey,"in *IEEE Communications Surveys and Tutorials*, vol. 17, no. 2, pp. 757-789, Nov. 2015.

[7] Y. He, X. Cheng, W. Peng, and G. L. Stuber, "A Survey of Energy Harvesting Communications: Models and Offline Optimal Policies,"in *IEEE Communications Magazine*, vol. 53, no. 6, pp. 79-85, June 2015.

[8] M. Agiwal, A. Roy, and N. Saxena, "Next Generation Wireless Networks: A Comprehensive Survey,"in *IEEE Communications Surveys and Tutorials*, vol. 18, no. 3, pp. 1617-1655, May 2016.

[9] N. Panwar, S. Sharma, and A. K. Singh, "A Survey on 5G: The Next Generation of Mobile Communication,"in *Physical Communication*, vol. 18, no.2, pp. 64-84, Mar. 2016.

[10] P. Demestichas, A. Georgakopoulos, D. Karvounas, K. Tsagkaris, V. Stavroulaki, J. Lu, C. Xiong, and J. Yao, "5G on the Horizon: Key Challenges for the Radio Access Network,"in *IEEE Vehicular Technology Magazine*, vol. 8, no. 3, pp. 47-53, Sept. 2013. nordrum2017everything

[11] A. Nordrum and K. Clark, "Everything You Need to Know About 5G,"in *IEEE Spectrum Magazine*, vol. 27, pp. 110-118, Jan. 2017.

[12] T. Yunzheng, L. Long, L. Shang, and Z. Zhi, "A Survey: Several Technologies of Non-Orthogonal Transmission for 5G,"in *China communications*, vol. 12, no. 10, pp. 1-15, Oct. 2015.

[13] S. R. Islam, N. Avazov, O. A. Dobre, and K.-S. Kwak, "Power-Domain Non-Orthogonal Multiple Access (NOMA) in 5G Systems: Potentials and Challenges,"in *IEEE Communications Surveys and Tutorials*, vol. 19, no. 2, pp. 721-742, May 2017.

[14] Y. Liu, Z. Qin, M. Elkashlan, Z. Ding, A. Nallanathan, and L. Hanzo, "Non-orthogonal Multiple Access for 5G and Beyond,"in *Proceedings of the IEEE*, vol. 105, no. 12, pp. 2347-2381, Dec. 2017.

[15] Z. Ding, X. Lei, G. K. Karagiannidis, R. Schober, J. Yuan, and V. K. Bhargava, "A Survey on Non-Orthogonal Multiple Access for 5G Networks: Research Challenges and Future Trends,"in *IEEE Journal on Selected Areas in Communications*, vol. 35, no. 10, pp. 2181-2195, Oct. 2017.

[16] Z. Ding, Y. Liu, J. Choi, Q. Sun, M. Elkashlan, C. I, and H. V. Poor, "Application of Non-Orthogonal Multiple Access in LTE and 5G Networks,"in *IEEE Communications Magazine*, vol. 55, no. 2, pp. 185-191, Feb. 2017.

[17] L. Dai, B. Wang, Y. Yuan, S. Han, I. Chih-Lin, and Z. Wang, "Non-Orthogonal Multiple Access for 5G: Solutions, Challenges, Opportunities, and Future Research Trends,"in *IEEE Communications Magazine*, vol. 53, no. 9, pp. 74-81, Sept. 2015.

[18] M. Basharat, W. Ejaz, M. Naeem, A. M. Khattak, and A. Anpalagan, "A Survey and Taxonomy on Non-Orthogonal Multiple Access Schemes for 5G Networks,"in *Transactions on Emerging Telecommunications Technologies*, vol. 29, no. 1, p. e3202, Jan. 2018.

[19] M. Aldababsa, M. Toka, S. Gokceli, G. K. Kurt, and O. Kucur, "A Tutorial on Non-orthogonal Multiple Access for 5G and Beyond,"in *Wireless Communications and Mobile Computing*, vol. 2018, Article ID 9713450, p. 59, June 2018.

[20] Y. Cai, Z. Qin, F. Cui, G. Y. Li, and J. A. McCann, "Modulation and Multiple Access for 5G Networks,"in *IEEE Communications Surveys and Tutorials*, vol. 20, no.1, no. 1, pp. 629-646, Mar. 2018.

[21] Q. Wang, R. Zhang, L. L. Yang, and L. Hanzo, "Non-Orthogonal Multiple Access: A Unified Perspective,"in *IEEE Wireless Communications*, vol. 25, no.2, no. 2, pp. 10-16, Apr. 2018.

[22] Z. Wu, K. Lu, C. Jiang, and X. Shao, "Comprehensive Study and Comparison on 5G NOMA Schemes,"in *IEEE Access*, vol. 6, no.7, pp. 18 511-519, Mar. 2018.

[23] Z. Wei, J. Yuan, D. W. K. Ng, M. Elkashlan, and Z. Ding, "A Survey of Downlink Non-Orthogonal Multiple Access for 5G Wireless Communication Networks,"in *ZTE Communications*, vol. 14, no. 4, pp. 17-25, Oct. 2016.

[24] Y. Wang, B. Ren, S. Sun, S. Kang, and X. Yue, "Analysis of Non-Orthogonal Multiple Access for 5G,"in *China Communications*, vol. 13, no. Supplement2, pp. 52-66, Nov. 2016.

[25] C. Yan, Z. Yuan,W. Li, and Y. Yuan, "Non-Orthogonal Multiple Access Schemes for 5G,"in *ZTE Communications*, vol. 11, no. 4, pp. 11-16, Oct. 2016.

[26] S. Yang, P. Chen, L. Liang, J. Zhu, and X. She, "Uplink Multiple Access Schemes for 5G: A Survey,"in *ZTE Communications*, vol. 15, no. S1, pp. 31-40, June 2017.

[27] M. Shirvanimoghaddam, M. Dohler, and S. J. Johnson, "Massive Non-Orthogonal Multiple Access for Cellular IoT: Potentials and Limitations,"in *IEEE Communications Magazine*, vol. 55, no. 9, pp. 55-61, Sept. 2017.

[28] B. Di, L. Song, Y. Li, and Z. Han, "V2X Meets NOMA: Non-Orthogonal Multiple Access for 5G-Enabled Vehicular Networks,"in *IEEE Wireless Communications*, vol. 24, no. 6, pp.14-21, Dec. 2017.

[29] L. Zhu, Z. Xiao, X. Xia, and D. Oliver Wu, "Millimeter Wave Communication with Non-Orthogonal Multiple Access for B5G/6G,"in *IEEE Access*, vol. 7, pp. 116-123, Aug. 2019.

[30] K. Chandra, A. S. Marcano, S. Mumtaz, R. V. Prasad, and H. L. Christiansen, "Unveiling Capacity Gains in Ultra dense Networks: Using mm-Wave NOMA,"in *IEEE Vehicular Technology Magazine*, vol. 13, no. 2, pp. 75-83, June 2018.

[31] F. Zhou, Y. Wu, Y. C. Liang, Z. Li, Y. Wang, and K. K. Wong, "State of the Art, Taxonomy, and Open Issues on Cognitive Radio Networks With NOMA,"in *IEEE Wireless Communications*, vol. 25, no. 2, pp. 100-108, Apr. 2018.

[32] D. Wan, M. Wen, F. Ji, H. Yu, and F. Chen, "Non-Orthogonal Multiple Access For Cooperative Communications: Challenges, Opportunities, and Trends,"in *IEEE Wireless Communications*, vol. 25, no. 2, pp. 109-117, Apr. 2018.

[33] M. S. Ali, E. Hossain, and D. I. Kim, "Coordinated Multipoint Transmission in Downlink Multi-Cell NOMA Systems: Models and Spectral Efficiency Performance,"in *IEEE Wireless Communications*, vol. 25, no. 2, pp. 24-31, Apr. 2018.

[34] Z. Zhang, G. Yang, Z. Ma, M. Xiao, Z. Ding, and P. Fan, "Heterogeneous Ultra Dense Networks With NOMA: System Architecture, Coordination Framework, and Performance Evaluation,"in *IEEE Vehicular Technology Magazine*, vol. 13, no. 2, pp. 110-120, June 2018.

[35] Y. Huang, C. Zhang, J. Wang, Y. Jing, L. Yang, and X. You, "Signal Processing for MIMO-NOMA: Present and Future Challenges,"in *IEEE Wireless Communications*, vol. 25, no. 2, pp. 32-38, Apr. 2018.

[36] C. Zhong, X. Hu, X. Chen, D. W. K. Ng, and Z. Zhang, "Spatial Modulation Assisted Multi-Antenna Non-Orthogonal Multiple Access,"in *IEEE Wireless Communications*, vol. 25, no. 2, pp. 61-67, Apr. 2018.

[37] N. Ye, H. Han, L. Zhao, and A. h. Wang, "Uplink Non-Orthogonal Multiple Access Technologies Toward 5G: A Survey,"in *Wireless Communications and Mobile Computing*, vol. 2018, Article ID. 6187580, p. 26, June 2018.

[38] H. Marshoud, S. Muhaidat, P. C. Sofotasios, S. Hussain, M. A. Imran, and B. S. Sharif, "Optical Non-Orthogonal Multiple Access for Visible Light Communication,"in IE*EE Wireless Communications*, vol. 25, no. 2, pp. 82-88, Apr. 2018.

[39] Y. Chen, A. Bayesteh, Y.Wu, B. Ren, S. Kang, S. Sun, Q. Xiong, C. Qian, B. Yu, Z. Ding et al., "Toward the Standardization of Non-Orthogonal Multiple Access For Next Generation Wireless Networks,"in *IEEE Communications Magazine*, vol. 56, no. 3, pp. 19-27, Mar. 2018.

[40] M. B. Shahab, R. Abbas, M. Shirvanimoghaddam, and S. J. Johnson, "Grant-Free Non-Orthogonal Multiple Access for IoT: A Survey,"in *IEEE Communications Surveys Tutorials*, vol. 22, no. 3, pp. 1805-1838, May 2020.

[41] R. C. Kizilirmak, "Non-Orthogonal Multiple Access (NOMA) for 5G Networks,"in Towards 5G Wireless Networks-A Physical Layer Perspective,*InTech*, vol. 83, Dec. 2016.

[42] Z. Chen, Z. Ding, X. Dai, and R. Zhang, "An Optimization Perspective of the Superiority of NOMA Compared to Conventional OMA,"in *IEEE Transactions on Signal Processing*, vol. 65, no. 19, pp. 5191-5202, Oct. 2017.

[43] Y. Saito, Y. Kishiyama, A. Benjebbour, T. Nakamura, A. Li, and K. Higuchi, "Non-Orthogonal Multiple Access (NOMA) for Cellular Future Radio Access,"in *IEEE 77th Vehicular Technology Conference (VTC Spring), Dresden, Germany*, pp. 1-5, June 2013.

[44] M. Simsek, A. Aijaz, M. Dohler, J. Sachs, and G. Fettweis, "5G-Enabled Tactile Internet,"*IEEE Journal on Selected Areas in Communications*, vol. 34, no. 3, pp. 460-473, Mar. 2016.

[45] S. Timotheou and I. Krikidis, "Fairness For Non-Orthogonal Multiple Access in 5G Systems,"*IEEE Signal Processing Letters*, vol. 22, no. 10, pp. 1647-1651, Oct. 2015.

[46] Z. Ding, M. Peng, and H. V. Poor, "Cooperative Non-Orthogonal Multiple Access in 5G Systems,"*IEEE Communications Letters*, vol. 19, no.8, pp. 1462-1465, Aug. 2015.

[47] J. Cui and Z. Ding and P. Fan, "A Novel Power Allocation Scheme Under Outage Constraints in NOMA Systems,"in *IEEE Signal Processing Letters*, vol. 23, no. 9, pp. 1226-1230, Sept. 2016.

[48] L. Wang, X. Xu, Y. Wu, S. Xing, and Y. Chen, "Sparse Code Multiple Access-Towards Massive Connectivity and Low Latency 5G Communications,"in *China Telecommunications Network Technology*, vol. 5, no. 5, p. 005, June 2015.

[49] X. Meng, Y. Wu, Y. Chen, and M. Cheng, "Low Complexity Receiver for Uplink SCMA System via Expectation Propagation,"in *IEEE Wireless Communications and Networking Conference (WCNC), San Francisco, CA*, Mar. 2017.

[50] N. Ye, A.Wang, X. Li,W. Liu, X. Hou, and H. Yu, "On Constellation Rotation of NOMA with SIC Receiver,"in *IEEE Communications Letters*, vol. 22, no. 3, pp. 514-517, Mar. 2018. 165

[51] J. Zhao, Y. Liu, K. K. Chai, Y. Chen, M. Elkashlan, and J. Alonso- Zarate, "NOMA-Based D2D Communications: Towards 5G,"in *IEEE Global Communications Conference (GLOBECOM), Washington, DC*, Dec. 2016.

[52] A. Anwar, B. C. Seet, and X. J. Li, "Quality of Service Based NOMA Group D2D Communications,"*Future Internet*, vol. 9, no. 4, p. 73, Nov. 2017.

[53] Y. Pan, C. Pan, Z. Yang, and M. Chen, "Resource Allocation for D2D Communications Underlaying a NOMA-Based Cellular Network,"*IEEE Wireless Communications Letters*, vol. 7, no.1, pp. 130âĂŞ133, Feb. 2018.

[54] E. Chatziantoniou, Y. Ko, and J. Choi, "Non-Orthogonal Multiple Access With Multi-Carrier Index Keying,"in *VDE 23th European Wireless Conference, Dresden, Germany*, May 2017.

[55] L. Pei, Z. Yang, C. Pan, W. Huang, M. Chen, M. Elkashlan, and A. Nallanathan, "Energy-Efficient D2D Communications Underlaying NOMA-Based Networks With Energy Harvesting, "in *IEEE Communications Letters*, vol. 22, no.5, pp. 914-917, May 2018.

[56] J. B. Kim, I. H. Lee, and J. Lee, "Capacity Scaling for D2D Aided Cooperative Relaying Systems Using NOMA,"in *IEEE Wireless Communications Letters*, vol. 7, no.1, pp. 42-45, Feb. 2018.

[57] Z. Zhang, Z. Ma, M. Xiao, Z. Ding, and P. Fan, "Full-Duplex Device-to-Device-Aided Cooperative Non-Orthogonal Multiple Access,"in *IEEE Transactions on Vehicular Technology*, vol. 66, no.5, pp. 4467-4471, May 2017.

[58] C. Lim, M. Jang, and S. H. Kim, "Trellis Tone Modulation Multiple Access for Peer Discovery in D2D Networks,"*Sensors*, vol. 18, no.4, p. 1228, Apr. 2018.

[59] Z. Shi, S. Ma, H. ElSawy, G. Yang, and M. S. Alouini, "Cooperative HARQ-Assisted NOMA Scheme in Large Scale D2D Networks,"in *IEEE Transactions on Communications*, vol. 66, no.9, pp. 4286-4302, Sept. 2018.

[60] S. M. A. Kazmi, N. H. Tran, T. M. Ho, A. Manzoor, D. Niyato, and C. S. Hong, "Coordinated Device-to-Device CommunicationWith Non-Orthogonal Multiple Access in Future Wireless Cellular Networks,"in *IEEE Access*, vol. 6, no.1, pp. 39860-39875, June 2018.

[61] Y. B. Song, H. S. Kang, and D. K. Kim, "5G Cellular Systems With D2D Assisted NOMA Relay,"in *IEEE URSI Asia-Pacific Radio Science Conference (URSI AP-RASC), Seoul, South Korea*, Aug. 2016.

[62] A. Sendonaris, E. Erkip, and B. Aazhang, "Increasing Uplink Capacity via User Cooperation Diversity,"in *IEEE Proceedings on International Symposium on Information Theory, Cambridge, MA*, p. 156, Aug. 1998.

[63] J. N. Laneman, D. N. Tse, and G. W. Wornell, "Cooperative Diversity in Wireless Networks: Efficient Protocols and Outage Behavior,"in *IEEE Transactions on Information Theory*, vol. 50, no.12, pp. 3062-3080, Dec. 2004.

[64] J. I. Choi, M. Jain, K. Srinivasan, P. Levis, and S. Katti, "Achieving Single Channel, Full Duplex Wireless Communication,"in *Proceedings of the Sixteenth Annual International Conference on Mobile Computing and Networking (MobiCom), New York, NY, ACM*, Sept. 2010.

[65] L. A. Villas, A. Boukerche, H. S. Ramos, H. A. B. F. de Oliveira, R. B. de Araujo and A. A. F. Loureiro, "DRINA: A Lightweight and Reliable Routing Approach for In-Network Aggregation in Wireless Sensor Networks," in *IEEE Transactions on Computers*, vol. 62, no. 4, pp. 676-689, Apr. 2013.

[66] Z. Zhang, K. Long, A. V. Vasilakos, and L. Hanzo, "Full-Duplex Wireless Communications: Challenges, Solutions, and Future Research Directions,"*Proceedings of the IEEE*, vol. 104, no.7, pp. 1369-1409, July 2016.

[67] X. Liu and X. Wang, "Outage Probability and Capacity Analysis of the Collaborative NOMA Assisted Relaying System in 5G,"in *IEEE/CIC International Conference on Communications in China (ICCC), Chengdu, China*, July 2016.

[68] J. B. Kim and I. H. Lee, "Non-Orthogonal Multiple Access in Coordinated Direct and Relay Transmission,"*IEEE Communications Letters*, vol. 19, no.11, pp. 2037-2040, Nov. 2015.

[69] X. Liang, Y. Wu, D. W. K. Ng, Y. Zuo, S. Jin, and H. Zhu, "Outage Performance for Cooperative NOMA Transmission With an AF Relay,"*IEEE Communications Letters*, vol. 21, no.11, pp. 2428-2431, Nov. 2017.

[70] M. F. Kader and S. Y. Shin, "Coordinated Direct and Relay Transmission Using Uplink NOMA,"*IEEE Wireless Communications Letters*, vol. 7, no.3, pp. 400-403, June 2018.

[71] G. Liu, X. Chen, Z. Ding, Z. Ma, and F. R. Yu, "Hybrid Half-Duplex/Full-Duplex Cooperative Non-Orthogonal Multiple Access With Transmit Power Adaptation,"*IEEE Transactions on Wireless Communications*, vol. 17, no.1, pp. 506-519, Jan. 2018.

[72] M. F. Kader, M. B. Shahab, and S. Y. Shin, "Non-Orthogonal Multiple Access for a Full-Duplex Cooperative Network with Virtually Paired Users,"*Computer Communications*, vol. 120, pp. 1-9, May 2018.

[73] K. M. Rabie, B. Adebisi, A. M. Tonello, S. Yarkan, and M. Ijaz, "Two-Stage Non-Orthogonal Multiple Access Over Power Line Communication Channels,"*IEEE Access*, vol. 6, no.2, pp. 17368-17376, Mar. 2018.

[74] R. Wan, L. Zhu, T. Li, and L. Bai, "A NOMA-PSO Based Cooperative Transmission Method in Satellite Communication Systems,"in *IEEE 9th International Conference on Wireless Communications and Signal Processing (WCSP), Nanjing, China*, Oct. 2017.

[75] J. B. Kim and I. H. Lee, "Capacity Analysis of Cooperative Relaying Systems Using Non-Orthogonal Multiple Access,"*IEEE Communications Letters*, vol. 19, no.11, pp. 1949-1952, Nov. 2015.

[76] M. Xu, F. Ji, M. Wen, and W. Duan, "Novel Receiver Design for the Cooperative Relaying System With Non-Orthogonal Multiple Access,""*IEEE Communications Letters*, vol. 20, no.8, pp. 1679-1682, Aug. 2016.

[77] J. B. Kim, M. S. Song, and I. H. Lee, "Achievable Rate of Best Relay Selection for Non-Orthogonal Multiple Access-Based Cooperative Relaying Systems,"in *IEEE International Conference on Information and Communication Technology Convergence (ICTC), Jeju, South Korea*, pp. 960-962, Oct. 2016.

[78] M. F. Kader, M. B. Shahab, and S. Y. Shin, "Exploiting Non-Orthogonal Multiple Access in Cooperative Relay Sharing,"*IEEE Communications Letters*, vol. 21, no.5, pp. 1159-1162, May 2017.

[79] M. F. Kader, S. Y. Shin, and V. C. Leung, "Full-Duplex Non-Orthogonal Multiple Access in Cooperative Relay Sharing for 5G Systems,"*IEEE Transactions on Vehicular Technology*, vol. 67, no.7, pp. 5831-5840, July 2018.

[80] M. F. Kader and S. Y. Shin, "Cooperative Relaying Using Space-Time Block Coded Non-Orthogonal Multiple Access,"*IEEE Transactions on Vehicular Technology*, vol. 66, no.7, pp. 5894-5903, July 2017.

[81] J. Zhao, Z. Ding, P. Fan, Z. Yang, and G. K. Karagiannidis, "Dual Relay Selection for Cooperative NOMA with Distributed Space Time Coding,"*IEEE Access*, vol. 6, no.4, pp. 20440-20450, Mar. 2018.

[82] Y. Zhou, V. W. Wong, and R. Schober, "Performance Analysis of Cooperative NOMA with Dynamic Decode-and-Forward Relaying,"in *IEEE Global Communications Conference (GLOBECOM), Singapore*, Dec. 2017.

[83] Y. Wu, L. P. Qian, H. Mao, X. Yang, H. Zhou, and X. Shen, "Optimal Power Allocation and Scheduling For Non-Orthogonal Multiple Access Relay-Assisted Networks,"*IEEE Transactions on Mobile Computing*, vol. 17, no.11, pp. 2591-2606, Nov. 2018.

[84] A. Gendia, M. Elsabrouty, and A. A. Emran, "Cooperative Multi-Relay Non-Orthogonal Multiple Access for Downlink Transmission in 5G Communication Systems,"in *IEEE Wireless Days, Porto, Portugal*, pp. 89-94, May 2017.

[85] H. T. Phuoc, P. N. Son, and M. Voznak, "Exact Outage Probability of Two-Way Decode-and-Forward NOMA Scheme With Digital Network Coding,"in *IEEE 2nd International Conference on Recent Advances in Signal Processing, Telecommunications and Computing (SigTelCom), Ho Chi Minh City, Vietnam*, pp. 102-106, Jan. 2018.

[86] X. Yue, Y. Liu, S. Kang, A. Nallanathan, and Y. Chen, "Modeling and Analysis of Two-Way Relay Non-Orthogonal Multiple Access Systems,"*IEEE Transactions on Communications*, vol. 66, no.9, pp. 3784-3796, Sept. 2018.

[87] Y. Liu, G. Pan, H. Zhang, and M. Song, "Hybrid Decode-Forward and Amplify-Forward Relaying With Non-Orthogonal Multiple Access,"*IEEE Access*, vol. 4, no.6, pp. 4912-4921, Aug. 2016.

[88] H. Sun, Q. Wang, R. Q. Hu, and Y. Qian, "Outage Probability Study in a NOMA Relay System,"in *IEEE Wireless Communications and Networking Conference (WCNC), San Francisco*, CA, Mar. 2017.

[89] S. Lee, D. B. Da Costa, Q. T. Vien, T. Q. Duong, and R. T. de Sousa Jr, "Non-Orthogonal Multiple Access Schemes With Partial Relay Selection,"*IET Communications*, vol. 11, no.6, pp. 846-854, Dec. 2016.

[90] J. So and Y. Sung, "Improving Non-Orthogonal Multiple Access by Forming Relaying Broadcast Channels, "*IEEE Communications Letters*, vol. 20, no.9, pp. 1816-1819, Sept. 2016.

[91] L. Zhang, J. Liu, M. Xiao, G. Wu, Y.-C. Liang, and S. Li, "Performance Analysis and Optimization in Downlink NOMA Systems With Cooperative Full-Duplex Relaying, "*IEEE Journal on Selected Areas in Communications*, vol. 35, no.10, pp. 2398-2412, Oct. 2017.

[92] B. Xia, Y. Fan, J. Thompson, and H. V. Poor, "Buffering in a Three Node Relay Network,"*IEEE Transactions on Wireless Communications*, vol. 7, no.11, Nov. 2008.

[93] S. Luo and K. C. Teh, "Buffer State Based Relay Selection for Buffer Aided Cooperative Relaying Systems,"*IEEE Transactions on Wireless Communications*, vol. 14, no.10, pp. 5430-5439, Oct. 2015.

[94] Z. Liang, X. Chen, and J. Huang, "Non-Orthogonal Multiple Access With Buffer-Aided Cooperative Relaying,"in *IEEE 2nd International Conference on Computer and Communications (ICCC), Chengdu, China*, pp. 1535-1539, Oct. 2016.

[95] Q. Zhang, Z. Liang, Q. Li, and J. Qin, "Buffer-Aided Non-Orthogonal Multiple Access Relaying Systems in Rayleigh Fading Channels,"*IEEE Transactions on Communications*, vol. 65, no.1, pp. 95-106, Jan. 2017.

[96] S. Luo and K. C. Teh, "Adaptive Transmission for Cooperative NOMA System With Buffer-Aided Relaying,"*IEEE Communications Letters*, vol. 21, no.4, pp. 937-940, Apr. 2017.

[97] N. Nomikos, T. Charalambous, D. Vouyioukas, G. K. Karagiannidis, and R. Wichman, "Relay Selection for Buffer-Aided Non-Orthogonal Multiple Access Networks,"in *IEEE Globecom Workshops (GC Wkshps), Singapore*, Dec. 2017.

[98] I. Budhiraja and S. Tyagi and S. Tanwar and N. Kumar and J. J. P. C. Rodrigues, "DIYA: Tactile Internet Driven Delay Assessment NOMA Based Scheme for D2D communication,"*IEEE Transactions on Industrial Informatics*, vol. 15, pp. 6354-6366, Dec. 2019.

[99] J. Choi, "Non-Orthogonal Multiple Access in Downlink Coordinated Two-Point Systems,"*IEEE Communications Letters*, vol. 18, no.2, pp. 313-316, Feb. 2014.

[100] A. Beylerian and T. Ohtsuki, "Coordinated Non-Orthogonal Multiple Access (CO-NOMA),"in *IEEE Global Communications Conference (GLOBECOM), Washington, DC*, Dec. 2016.

[101] Y. Tian, A. R. Nix, and M. Beach, "On the Performance of Opportunistic NOMA in Downlink CoMP Networks, "*IEEE Communications Letters*, vol. 20, no.5, pp. 998-1001, May 2016.

[102] Y. Sun, Z. Ding, X. Dai, and G. K. Karagiannidis, "A Feasibility Study on Network NOMA,"*IEEE Transactions on Communications*, vol. 66, no.9, pp. 4303-4317, Sept. 2018.

[103] Y. Tian, A. Nix, and M. Beach, "On the Performance of a Multi-Tier NOMA Strategy in Coordinated Multi-Point Networks,"IEEE Communications Letters, vol. 21, no.11, pp. 2448-2451, Nov. 2017.

[104] Y. Tian, X.Wang, and Z.Wang, "On the Performance of Security-Based Non-orthogonal Multiple Access in Coordinated Multipoint Networks,"*Wireless Communications and Mobile Computing*, vol. 2018, Article ID 8921895, pp. 1-6, Apr. 2018.

[105] S. Tyagi, S. Tanwar, N. Kumar, and J. J. P. C. Rodrigues, "Cognitive Radio-Based Clustering For Opportunistic Shared Spectrum Access to Enhance Lifetime of Wireless Sensor Network,"*Pervasive and Mobile Computing*, vol. 22, no.5, pp. 90-112, Dec. 2015.

[106] Z. Yang, Z. Ding, P. Fan, and N. Al-Dhahir, "A General Power Allocation Scheme to Guarantee Quality of Service in Downlink and Uplink NOMA Systems,"*IEEE Transactions on Wireless Communications*, vol. 15, no.11, pp. 7244-7257, Nov. 2016.

[107] Z. Yang, J. A. Hussein, P. Xu, Z. Ding, and Y. Wu, "Power Allocation Study for Non-Orthogonal Multiple Access Networks With Multicast-Unicast Transmission,"*IEEE Transactions on Wireless Communications*, vol. 17, no.6, pp. 3588-3599, June 2018.

[108] X. Li, W. Xu, Z. Feng, X. Lin, and J. Lin, "Matching-Theory-Based Spectrum Utilization in Cognitive NOMA-OFDM Systems,"in *IEEE Wireless Communications and Networking Conference (WCNC), San Francisco, CA*, Mar. 2017.

[109] Y. Yu, H. Chen, Y. Li, Z. Ding, and L. Zhuo, "Antenna Selection in MIMO Cognitive Radio-Inspired NOMA Systems,"*IEEE Communications Letters*, vol. 21, no.12, pp. 2658-2661, Dec. 2017.

[110] X. Liu, Y. Wang, S. Liu, and J. Meng, "Spectrum Resource Optimization for NOMA-Based Cognitive Radio in 5G Communications,"*IEEE Access*, vol. 6, no.10, pp. 24904-24911, Apr. 2018.

[111] M. F. Kader and S. Y. Shin, "Performance Analysis of Cooperative Spectrum Sharing Using Non-Orthogonal Multiple Access,"*International Journal of Communication Systems*, vol. 31, no.4, p. e3481, Mar. 2018.

[112] L. Lv, J. Chen, Q. Ni, and Z. Ding, "Design of Cooperative Non-Orthogonal Multicast Cognitive Multiple Access for 5G Systems: User Scheduling and Performance Analysis, "*IEEE Transactions on Communications*, vol. 65, no.6, pp. 2641-2656, June 2017.

[113] L. Lv, L. Yang, H. Jiang, T. H. Luan, and J. Chen, "When NOMA Meets Multiuser Cognitive Radio: Opportunistic Cooperation and User Scheduling, "*IEEE Transactions on Vehicular Technology*, vol. 67, no.7, July 2018.

[114] A. Kumari, S. Tanwar, S. Tyagi, N. Kumar, M. Maasberg, and K. R. Choo, "Multimedia Big Data Computing and Internet of Things Applications: A Taxonomy and Process Model, "*Journal of Network and Computer Applications*, vol. 124, no.4, pp. 169-195, Nov. 2018.

[115] K. He, Y. Li, C. Yin, and Y. Zhang, "A Novel Compressed Sensing-Based Non-Orthogonal Multiple Access Scheme for Massive MTC in 5G Systems,"*EURASIP Journal on Wireless Communications and Networking*, vol. 2018, no.1, p. 81, Dec. 2018.

[116] Z. Yang, W. Xu, H. Xu, J. Shi, and M. Chen, "Energy Efficient Non-Orthogonal Multiple Access For Machine-to-Machine Communications,"*IEEE Communications Letters*, vol. 21, no.4, pp. 817-820, Apr.2017.

[117] H. S. Jang, H. S. Park, and D. K. Sung, "A Non-Orthogonal Resource Allocation Scheme in Spatial Group Based Random Access for Cellular M2M Communications,"*IEEE Transactions on Vehicular Technology*, vol. 66, no.5, pp. 4496-4500, May 2017.

[118] J. Choi, "NOMA-Based Random Access With Multichannel ALOHA,"*IEEE Journal on Selected Areas in Communications*, vol. 35, no.12, pp. 2736-2743, Dec. 2017.

[119] E. Balevi, F. T. Al Rabee, and R. D. Gitlin, "ALOHA-NOMA for Massive Machine-to-Machine IoT communication,"in *IEEE International Conference on Communications (ICC), Kansas City, MO*, May 2018.

[120] M. Elkourdi, A. Mazin, E. Balevi, and R. D. Gitlin, "Enabling Slotted ALOHA-NOMA for Massive M2M Communication in IoT Networks,"in *IEEE 19th Wireless and Microwave Technology Conference (WAMICON), Sand Key, FL*, Apr. 2018.

[121] N. Ye, A. Wang, X. Li, H. Yu, A. Li, and H. Jiang, "A Random Non-Orthogonal Multiple Access Scheme for mMTC,"in *IEEE 85th Vehicular Technology Conference (VTC Spring), Sydney, NSW, Australia*, June 2017.

[122] 3GPP-R1-164268, "GB and GF MA for mMTC, "

[123] Z. Ding, R. Schober, P. Fan, and H. V. Poor, "Simple Semi-Grant-Free Transmission Strategies Assisted by Non-Orthogonal Multiple Access,"*IEEE Transactions on Communications*, vol. 72, no.9, pp. 442-452, Mar. 2019.

[124] 3GPP-R1-166403, "Grant-Free Multiple Access Schemes for mMTC,"

[125] 3GPP-R1-166405, "Discussion on Grant-Free Concept for UL mMTC,"

[126] I. Budhiraja, S. Tyagi, S. Tanwar, N. Kumar, and J. J. P. C. Rodrigues, "Tactile Internet for Smart Communities in 5G: An Insight for NOMA-Based Solutions,"*IEEE Transactions on Industrial Informatics*, vol. 15, no.5, pp. 3104-3112, May 2019.

[127] L. Liu and W. Yu, "Massive Connectivity With Massive MIMO Part I: Device Activity Detection and Channel Estimation,"*IEEE Transactions on Signal Processing*, vol. 66, no.11, pp. 2933-2946, June 2018.

[128] L. Liu and W. Yu, "Massive Connectivity With Massive MIMO Part II: Achievable Rate Characterization, "*IEEE Transactions on Signal Processing*, vol. 66, no.11, pp. 2947-2959, June 2018.

[129] Y. Du, C. Cheng, B. Dong, Z. Chen, X. Wang, J. Fang, and S. Li, "Block-Sparsity-Based Multiuser Detection for Uplink Grant Free NOMA,"*IEEE Transactions on Wireless Communications*, vol. 17, no.12, pp. 7894-7909, Dec. 2018.

[130] N. Ye, A. Wang, X. Li, H. Yu, A. Li, and H. Jiang, "A Random Non-Orthogonal Multiple Access Scheme for mMTC,"in *IEEE 85th Vehicular Technology Conference (VTC Spring), Sydney, NSW, Australia*, June 2017.

[131] Y. Du, B. Dong, Z. Chen, X. Wang, Z. Liu, P. Gao, and S. Li, "Efficient Multi-User Detection for Uplink Grant-Free NOMA: Prior-Information Aided Adaptive Compressive Sensing Perspective,"*IEEE Journal on Selected Areas in Communications*, vol. 35, no.12, pp. 2812-2828, Dec. 2017.

[132] B. Wang, L. Dai, Y. Zhang, T. Mir, and J. Li, "Dynamic Compressive Sensing-Based Multi-User Detection for Uplink Grant-Free NOMA,"*IEEE Communications Letters*, vol. 20, no.11, pp. 2320-2323, Nov. 2016.

[133] H. Jiang, Q. Cui, Y. Gu, X. Qin, X. Zhang, and X. Tao, "Distributed Layered Grant-Free Non-Orthogonal Multiple Access for Massive MTC,"in *29th IEEE Annual International Symposium on Personal, Indoor and Mobile Radio Communications (PIMRC), Bologna, Italy*, Sept. 2018.

[134] Y. Liu, Z. Ding, M. Elkashlan, and H. V. Poor, "Cooperative Non-Orthogonal Multiple Access With Simultaneous Wireless Information and Power Transfer,"*IEEE Journal on Selected Areas in Communications*, vol. 34, no.4, pp. 938-953, Apr. 2016.

[135] M. Ashraf, A. Shahid, J. W. Jang, and K.-G. Lee, "Energy Harvesting Non-Orthogonal Multiple Access System With Multi-Antenna Relay and Base Station,"*IEEE Access*, vol. 5, no.12, pp. 17660-17670, Sept. 2017.

[136] R. Sun, Y. Wang, X. Wang, and Y. Zhang, "Transceiver Design For Cooperative Non-Orthogonal Multiple Access Systems With Wireless Energy Transfer,"*IET Communications*, vol. 10, no.15, pp. 1947-1955, Oct. 2016.

[137] Y. Liu, Z. Ding, M. Elkashlan, and H. V. Poor, "Cooperative Non-Orthogonal Multiple Access With Simultaneous Wireless Information and Power Transfer,"*IEEE Journal on Selected Areas in Communications*, vol. 34, no.4, pp. 938-953, Apr. 2016.

[138] N. T. Do, D. B. Da Costa, T. Q. Duong, and B. An, "A BNBF User Selection Scheme for NOMA-Based Cooperative Relaying Systems With SWIPT,"*IEEE Communications Letters*, vol. 21, no.3, pp. 664-667, Mar. 2017.

[139] N. T. Do, D. B. da Costa, T. Q. Duong, and B. An, "Transmit Antenna Selection Schemes for MISO-NOMA Cooperative Downlink Transmissions With Hybrid SWIPT Protocol, "in *IEEE International Conference on Communications (ICC), Paris, France*, May 2017.

[140] Y. Xu, C. Shen, Z. Ding, X. Sun, S. Yan, G. Zhu, and Z. Zhong, "Joint Beamforming and Power-Splitting Control in Downlink Cooperative SWIPT NOMA Systems,"*IEEE Transanctions on Signal Processing*, vol. 65, no.18, pp. 4874-4886, May 2017.

[141] Y. Zhang and J. Ge, "Performance Analysis For Non-Orthogonal Multiple Access in Energy Harvesting Relaying Networks,"*IET Communications*, vol. 11, no.11, pp. 1768-1774, May 2017.

[142] W. Han, J. Ge, and J. Men, "Performance Analysis for NOMA Energy Harvesting Relaying Networks With Transmit Antenna Selection and Maximal-Ratio Combining Over Nakagami-m Fading,"*IET Communications*, vol. 10, no.18, pp. 2687-2693, Dec. 2016.

[143] Z. Yang, Z. Ding, P. Fan, and N. Al-Dhahir, "The Impact of Power Allocation on Cooperative Non-Orthogonal Multiple Access Networks With SWIPT,"*IEEE Transactions on Wireless Communications*, vol. 16, no.7, pp. 4332-4343, July 2017.

[144] I. Budhiraja and S. Tyagi and S. Tanwar and N. Kumar and N. Guizani, "Subchannel Assignment for SWIPT-NOMA based HetNet with Imperfect Imperfect Channel State Information,"in *15th International Wireless Communications Mobile Computing Conference (IWCMC), Tangier, Morocco*, pp. 842-847, June 2019.

[145] I. Budhiraja and N. Kumar and S. Tyagi and S. Tanwar and M. Guizani, "An Energy-Efficient Resource Allocation Scheme for SWIPT-NOMA based Femtocells users with Imperfect CSI,"*IEEE Transactions on Vehicular Technology*, vol. 69, no. 7, pp. 7790-7805, July 2020.

[146] P. D. Diamantoulakis, K. N. Pappi, Z. Ding, and G. K. Karagiannidis, "Wireless-Powered Communications With Non-Orthogonal Multiple Access,"*IEEE Transactions on Wireless Communications*, vol. 15, no.12, pp. 8422-8436, Dec. 2016.

[147] H. Chingoska, Z. Hadzi-Velkov, I. Nikoloska, and N. Zlatanov, "Resource Allocation in Wireless Powered Communication Networks With Non-Orthogonal Multiple Access,"*IEEE Wireless Communications Letters*, vol. 5, no.6, pp. 684-687, Dec. 2016.

[148] Y. Yuan and Z. Ding, "The Application of Non-Orthogonal Multiple Access in Wireless Powered Communication Networks,"in *IEEE 17th International Workshop on Signal Processing Advances in Wireless Communications (SPAWC), Ednburgh, UK*, July 2016.

[149] A. F. Molisch and M. Z. Win, "MIMO Systems With Antenna Selection,"*IEEE Microwave Magazine*, vol. 5, no.1, pp. 46-56, Mar. 2004.

[150] A. P. Shrestha, T. Han, Z. Bai, J. M. Kim, and K. S. Kwak, "Performance of Transmit Antenna Selection in Non-Orthogonal Multiple Access for 5G Systems,"in *IEEE 8th International Conference on Ubiquitous and Future Networks (ICUFN), Vienna, Austria*, pp. 1031-1034, June 2016.

[151] X. Liu and X. Wang, "Efficient Antenna Selection and User Scheduling in 5G Massive MIMO-NOMA System, "in *IEEE 83rd Vehicular Technology Conference (VTC Spring), Nanjing, China*, May 2016.

[152] Y. Yu, H. Chen, Y. Li, Z. Ding, and B. Vucetic, "Antenna Selection For MIMO-NOMA Networks,"in *IEEE International Conference on Communications (ICC), Paris, France*, May 2017.

[153] M. Irfan, J. W. Kim, and S. Y. Shin, "Spectral and Energy Efficient Spatially Modulated Non-Orthogonal Multiple Access (NOMA) for 5G,"*The Journal of Korean Institute of Communications and Information Sciences*, vol. 40, no.8, pp. 1507-1514, Aug. 2015.

[154] J. Jeganathan, A. Ghrayeb, L. Szczecinski, and A. Ceron, "Space Shift Keying Modulation for MIMO Channels, "*IEEE Transactions on Wireless Communications*, vol. 8, no.7, pp. 3692-3703, May 2009.

[155] J. W. Kim, S. Y. Shin, and V. C. M. Leung, "Performance Enhancement of Downlink NOMA by Combination With GSSK,"*IEEE Wireless Communications Letters*, vol. 7, no.5, pp. 860-863, Oct. 2018.

[156] X. Su, A. Castiglione, C. Esposito, and C. Choi, "Power Domain NOMA to Support Group Communication in Public Safety Networks,"*Future Generation Computer Systems*, vol. 84, no.11, pp. 228-238, July 2018.

[157] A. Li, A. Benjebbour, X. Chen, H. Jiang, and H. Kayama, "Investigation on Hybrid Automatic Repeat Request (HARQ) Design for NOMA With SU-MIMO,"in *IEEE 26th Annual International Symposium on Personal, Indoor, and Mobile Radio Communications (PIMRC), Hong Kong, China*, pp. 590-594, Aug. 2015.

[158] N. D. Sidiropoulos, T. N. Davidson, and Z.-Q. Luo, "Transmit Beamforming for Physical-Layer Multicasting,"*IEEE Transanctions on Signal Processing*, vol. 54, no.6, pp. 2239-2251, July 2006.

[159] M. Kaliszan, E. Pollakis, and S. StaÂt'nczak, "Multigroup Multicast With Application-Layer Coding: Beamforming for Maximum Weighted Sum Rate,"in *IEEE Wireless Communications and Networking Conference (WCNC), Shanghai, China*, pp. 2270-2275, Apr. 2012.

[160] B. Kim, S. Lim, H. Kim, S. Suh, J. Kwun, S. Choi, C. Lee, S. Lee, and D. Hong, "Non-Orthogonal Multiple Access in a Downlink Multiuser Beamforming System,"in *IEEE Military Communications Conference (MILCOM), San Diego, CA*, pp. 1278-1283, Nov. 2013.

[161] J. Choi, "Minimum Power Multicast Beamforming With Superposition Coding for Multiresolution Broadcast and Application to NOMA Systems,"*IEEE Transactions on Communications*, vol. 63, no.3, pp. 791-800, Mar. 2015.

[162] Y. Hayashi, Y. Kishiyama, and K. Higuchi, "Investigations on Power Allocation Among Beams in Non-Orthogonal Access With Random Beamforming and Intra-beam SIC for Cellular MIMO Downlink,"in *IEEE 78th Vehicular Technology Conference (VTC Fall), Las Vegas, NV*, Sept. 2013.

[163] S. Ali, E. Hossain, and D. I. Kim, "Non-Orthogonal Multiple Access (NOMA) for Downlink Multiuser MIMO Systems: User Clustering, Beamforming, and Power Allocation,"*IEEE Access*, vol. 5, no. 12, pp. 565-577, Dec. 2017.

[164] Q. Zhang, Q. Li, and J. Qin, "Robust Beamforming For Non-Orthogonal Multiple-Access Systems in MISO Channels, "*IEEE Transactions on Vehicular Technology*, vol. 65, no.12, pp. 10231-10236, Dec. 2016.

[165] M. Tian, Q. Zhang, S. Zhao, Q. Li, and J. Qin, "Robust Beamforming in Downlink MIMO NOMA Networks Using Cutting-Set Method,"*IEEE Communications Letters*, vol. 22, no.3, pp. 574-577, Mar. 2018.

[166] F. Alavi, K. Cumanan, Z. Ding, and A. G. Burr, "Robust Beamforming Techniques for Non-Orthogonal Multiple Access Systems With Bounded Channel Uncertainties,"*IEEE Communications Letters*, vol. 21, no.9, pp. 2033-2036, Sept. 2017.

[167] W. Shin, M. Vaezi, B. Lee, D. J. Love, J. Lee, and H. V. Poor, "Coordinated Beamforming for Multi-Cell MIMO-NOMA,"*IEEE Communications Letters*, vol. 21, no.1, pp. 84-87, Jan. 2017.

[168] Y. I. Choi, J. W. Lee, M. Rim, and C. G. Kang, "On the Performance of Beam Division Non-Orthogonal Multiple Access for FDD Based Large-Scale Multi-User MIMO Systems,"*IEEE Transactions on Wireless Communications*, vol. 16, no.8, pp. 5077-5089, Aug. 2017.

[169] L. Bai, L. Zhu, Q. Yu, J. Choi, and W. Zhuang, "Transmit Power Minimization for Vector-Perturbation based NOMA Systems: A Sub-Optimal Beamforming Approach,"*IEEE Transactions on Wireless Communications*, vol. 18, no. 5, pp. 2679-2692, May 2019.

[170] Z. Zhao and W. Chen, "An Adaptive Switching Method for Sum Rate Maximization in Downlink MISO-NOMA Systems, "in *IEEE Global Communications Conference (GLOBECOM), Singapore*, Dec. 2017.

[171] Z. Wang, J. Cao, et al., "NOMA-Based Spatial Modulation,"*IEEE Access*, vol. 5, no.4, pp. 3790-3800, Mar. 2017.

[172] Z. Ding, R. Schober, and H. V. Poor, "A General MIMO Framework for NOMA Downlink and Uplink Transmission Based on Signal Alignment,"*IEEE Transactions on Wireless Communications*, vol. 15, no.6, pp. 4438-4454, June 2016.

[173] Z. Chen, Z. Ding, X. Dai, and G. K. Karagiannidis, "On the Application of Quasi-Degradation to MISO-NOMA Downlink,"*IEEE Transactions on Signal Processing*, vol. 64, no.23, pp. 6174-6189, Dec. 2016.

[174] Z. Chen, Z. Ding, and X. Dai, "Beamforming for Combating Inter-Cluster and Intra-Cluster Interference in Hybrid NOMA Systems,"*IEEE Access*, vol. 4, no.7, pp. 4452-4463, Aug. 2016.

[175] Z. Ding, L. Dai, and H. V. Poor, "MIMO-NOMA Design for Small Packet Transmission in the Internet of Things, "*IEEE Access*, vol. 4, no.2, pp. 1393-1405, Apr. 2016.

[176] S. Qureshi, S. A. Hassan, and D. N. K. Jayakody, "Divide-and-Allocate: An Uplink Successive Bandwidth Division NOMA System,"*Transactions on Emerging Telecommunications Technologies*, vol. 29, no.1, p. e3216, Jan. 2018.

[177] E. G. Larsson, O. Edfors, F. Tufvesson, and T. L. Marzetta, "Massive MIMO for Next Generation Wireless Systems,"*IEEE Communications Magazine*, vol. 52, no.2, pp. 186-195, Feb. 2014.

[178] G. Rajesh and A. Chaturvedi, "Correlation analysis and statistical characterization of heterogeneous sensor data in environmental sensor networks," *Computer Networks*, vol. 164, no.9, pp. 106-125, Dec. 2019.

[179] P. Kumar, and A. Chaturvedi, "Design and Development of Single & Dual Resonant Frequency Antennas for Moisture Content Measurement, " *Wireless Personal Communication*, vol. 114, pp. 565âĂŞ582, Sept. 2020.

[180] Z. Ding and H. V. Poor, "Design of Massive-MIMO-NOMA With Limited Feedback,"*IEEE Signal Processing Letters*, vol. 23, no.5, pp. 629- 633, May 2016.

[181] C. Xu, Y. Hu, C. Liang, J. Ma, and L. Ping, "Massive MIMO Non-Orthogonal Multiple Access and Interleave Division Multiple Access,"*IEEE Access*, vol. 5, no.7, pp. 14728-14748, July 2017.

[182] K. Xiao, M. Kadoch, H. Rutagemwa, and C. Li, "Opportunistic NOMA-Based Massive MIMO Precoding for 5G New Radio,"*Wireless Communications and Mobile Computing*, vol. 2018, Article ID 2328954, pp. 1-10, June 2018.

[183] X. Chen, F. K. Gong, G. Li, H. Zhang, and P. Song, "User Pairing and Pair Scheduling in Massive MIMO-NOMA Systems,"*IEEE Communications Letters*, vol. 22, no.4, pp. 788-791, Apr. 2018.

[184] L. Liu, C. Yuen, Y. L. Guan, Y. Li, and C. Huang, "Gaussian Message Passing Iterative Detection for MIMO-NOMA Systems With Massive Access,"in *IEEE Global Communications Conference (GLOBECOM), Washington, DC*, Dec. 2016.

[185] L. Liu, C. Yuen, Y. L. Guan, and Y. Li, "Capacity-Achieving Iterative LMMSE Detection for MIMO-NOMA Systems,"in *IEEE International Conference on Communications (ICC), Kuala Lumpur, Malaysia*, pp. 1-6, May 2016.

[186] D. Zhang, Y. Liu, Z. Ding, Z. Zhou, A. Nallanathan, and T. Sato, "Performance Analysis of Non-Regenerative Massive-MIMO-NOMA Relay Systems for 5G,"IEEE Transactions on Communications, vol. 65, no.11, pp. 4777-4790, Nov. 2017.

[187] P. Xu, Z. Ding, X. Dai, and H. V. Poor, "A New Evaluation Criterion for Non-Orthogonal Multiple Access in 5G Software Defined Networks,"*IEEE Access*, vol. 3, no.5, pp. 1633-1639, Sept. 2015.

[188] S. Tyagi and N. Kumar, "A Systematic Review on Clustering and Routing Techniques Based Upon LEACH Protocol for Wireless Sensor Networks,"*Journal of Network and Computer Applications*, vol. 36, no.2, pp. 623-645, Mar. 2013.

[189] V. K. Singh, M. Kumar and S. Verma, "Node Scheduling and Compressed Sampling for Event Reporting in WSNs," in *IEEE Transactions on Network Science and Engineering*, vol. 6, no. 3, pp. 418-431, Sept. 2019

[190] S. Tanwar, N. Kumar, and J. Rodrigues, "A Systematic Review on Heterogeneous Routing Protocols for Wireless Sensor Network,"*Journal of Network and Computer Applications*, vol. 53, no.2, pp. 623-645, Mar. 2015.

[191] V. Rishiwal, O. Singh, S. Tanwar, S. Tyagi, I. Budhiraja, N. Kumar, and M. S. Obaidat, "Base Station Oriented Multi Route Diversity Protocol for Wireless Sensor Networks, "in *IEEE Globecom Workshops (GC Wkshps), Abu Dhabi, United Arab Emirates*, Dec. 2018.

[192] V. K. Singh, S. Verma and M. Kumar, "ODECS: An On-Demand Explosion-Based Compressed Sensing Using Random Walks in Wireless Sensor Networks," in *IEEE Systems Journal*, vol. 13, no. 3, pp. 2466-2475, Sept. 2019.

[193] M. Song and M. Zheng, "Energy Efficiency Optimization For Wireless Powered Sensor Networks With Non-orthogonal Multiple Access,"*IEEE sensors letters*, vol. 2, no.1, pp. 1-4, Mar. 2018.

[194] A. Anwar, B. C. Seet, and Z. Ding, "Non-Orthogonal Multiple Access for Ubiquitous Wireless Sensor Networks, "*Sensors*, vol. 18, no. 2, p. 516, Feb. 2018.

[195] J. C. Li, S. Dey, and J. Evans, "Maximal Lifetime Rate and Power Allocation for Sensor Networks With Data Distortion Constraints,"in *IEEE International Conference on Communications (ICC), Glasgow, UK*, pp. 3678-3685, June 2007.

[196] J. Cheon and H. S. Cho, "Power Allocation Scheme for Non-Orthogonal Multiple Access in Underwater Acoustic Communications,"*Sensors*, vol. 17, no.11, p. 2465, Nov. 2017.

[197] W. Zhang, Z. Zhang, S. Zeadally, H. Chao and V. C. M. Leung, "Energy-efficient Workload Allocation and Computation Resource Configuration in Distributed Cloud/Edge Computing Systems With Stochastic Workloads," in *IEEE Journal on Selected Areas in Communications*, vol. 38, no. 6, pp. 1118-1132, June 2020.

[198] F. Wang, J. Xu, and Z. Ding, "Optimized Multiuser Computation Offloading With Multi-Antenna NOMA,"in *IEEE Globecom Workshops (GC Wkshps), Singapore*, Dec. 2017.

[199] Z. Ding, P. Fan, and H. V. Poor, "Impact of Non-Orthogonal Multiple Access on the Offloading of Mobile Edge Computing,"*IEEE Transactions on Communications*, vol. 67, no.1, pp. 375âĂŞ390, Jan. 2019.

[200] Z. Ding, D.W. K. Ng, R. Schober, and H. V. Poor, "Delay Minimization for NOMA-MEC Offloading,"*IEEE Signal Processing Letters*, vol. 25, no.12, pp. 1875âĂŞ1879, Dec. 2018.

[201] Z. Ding, J. Xu, O. A. Dobre, and V. Poor, "Joint Power and Time Allocation for NOMA-MEC Offloading,"*IEEE Transactions on Vehicular Technology*, vol. 75, no.10, pp. 589-599, Mar. 2019.

[202] Z. Yang, J. Hou, and M. Shikh-Bahaei, "Energy Efficient Resource Allocation for Mobile-Edge Computation Networks with NOMA,"in *IEEE Globecom Workshops (GC Wkshps), Abu Dhabi, UAE*, pp. 1-7, Dec. 2018.

[203] A. Kiani and N. Ansari, "Edge Computing Aware NOMA for 5G Networks,"*IEEE Internet of Things Journal*, vol. 5, no.2, pp. 1299-1306, Apr. 2018.

[204] Z. Yang, J. Hou, and M. Shikh-Bahaei, "Resource Allocation in Full-Duplex Mobile-Edge Computing Systems With NOMA and Energy Harvesting,"in *IEEE International Conference on Communications (ICC), Shanghai, China*, pp. 1-6, May 2019.

[205] D. Bhattacharya, S. Misra, N. Pathak, A. Mukherjee, "IDeA: IoT-Based Autonomous Aerial Demarcation and Path Planning for Precision Agriculture with UAVs," *ACM Trans. Internet Things*, vol. no.3, pp. 161-172, June 2020.

[206] S. Jeong, O. Simeone, and J. Kang, "Mobile Edge Computing via a UAV Mounted Cloudlet: Optimization of Bit Allocation and Path Planning,"*IEEE Transactions on Vehicular Technology*, vol. 67, no.3, pp. 2049-2063, Mar. 2018.

[207] P. K. Sharma and D. I. Kim, "UAV-Enabled Downlink Wireless System With Non-Orthogonal Multiple Access, "in *IEEE Globecom Workshops (GC Wkshps), Singapore*, Dec. 2017.

[208] M. F. Sohail, C. Y. Leow, and S.Won, "Non-Orthogonal Multiple Access for Unmanned Aerial Vehicle Assisted Communication,"*IEEE Access*, vol. 6, no.3, pp. 22716-22727, Apr. 2018.

[209] N. Rupasinghe, Y. Yapıcı, I. Güvenç, and Y. Kakishima, "Non-Orthogonal Multiple Access for mmWave Drone Networks With Limited Feedback,"*IEEE Transactions on Communications*, vol. 67, no.1, pp. 762-777, Jan. 2019.

[210] Y. Liu, Z. Qin, Y. Cai, Y. Gao, G. Y. Li, and A. Nallanathan, "UAV Communications Based on Non-Orthogonal Multiple Access,"*IEEE Wireless Communications*, vol. 26, no.1, pp. 52-57, Feb. 2019.

[211] T. Hou, Y. Liu, Z. Song, X. Sun, and Y. Chen, "Multiple Antenna Aided NOMA in UAV Networks: A Stochastic Geometry Approach,"*IEEE Transactions on Communications*, vol. 67, no.2, pp. 1031-1044, Feb. 2019.

[212] T. M. Nguyen, W. Ajib, and C. Assi, "A Novel Cooperative NOMA for Designing UAV-Assisted Wireless Backhaul Networks,"*IEEE Journal on Selected Areas in Communications*, vol. 36, no.11, pp. 2497-2507, Nov. 2018.

[213] W. Mei and R. Zhang, "Uplink Cooperative NOMA for Cellular-Connected UAV,"*IEEE Journal of Selected Topics in Signal Processing*, vol. 13, no.3, pp. 644-656, June 2019.

[214] L. Liu, S. Zhang, and R. Zhang, "Exploiting NOMA for Multi-Beam UAV Communication in Cellular Uplink, "in *IEEE International Conference on Communications (ICC), Shanghai, China*, pp. 1-6, May 2019.

[215] Y. Liu, X. Li, H. Ji, and H. Zhang, "A Multi-User Access Scheme for Throughput Enhancement in UDN With NOMA, "in *IEEE International Conference on Communications Workshops (ICC Workshops), Paris, France*, pp. 1364-1369, May 2017.

[216] Y. Liu, X. Li, F. R. Yu, H. Ji, H. Zhang, and V. C. Leung, "Grouping and Cooperating Aamong Access Points in User-Centric Ultra-Dense Networks With Non-Orthogonal Multiple Access,"*IEEE Journal on Selected Areas in Communications*, vol. 35, no.10, pp. 2295-2311, Oct. 2017.

[217] Z. Qin, X. Yue, Y. Liu, Z. Ding, and A. Nallanathan, "User Association and Resource Allocation in Unified NOMA Enabled Heterogeneous Ultra Dense Networks, "*IEEE Communications Magazine*, vol. 56, no.6,pp. 86-92, June 2018.

[218] H. Marshoud, V. M. Kapinas, G. K. Karagiannidis, and S. Muhaidat, "Non-Orthogonal Multiple Access for Visible Light Communications,"*IEEE Photonics Technology Letters*, vol. 28, no.1, pp. 51-54, Jan. 2016.

[219] B. Lin,W. Ye, X. Tang, and Z. Ghassemlooy, "Experimental Demonstration of Bidirectional NOMA-OFDMA Visible Light Communications,"*Optics Express*, vol. 25, no.4, pp. 4348-4355, Feb. 2017.

[220] W. Ye, J. Chen, B. Lin, X. Tang, and Y. Zhang, "Experimental Demonstration of NOMA Visible Light Communications Based on SCFDM,"in *IEEE 16th International Conference on Optical Communications and Networks (ICOCN), Wuzhen, China*, Aug. 2017.

[221] B. Lin, Z. Ghassemlooy, X. Tang, Y. Li, and M. Zhang, "Experimental Demonstration of an NOMA-PON With Single Carrier Transmission,"*Optics Communications*, vol. 396, no.6, pp. 66-70, Aug. 2017.

[222] B. Lin, K. Zhang, X. Tang, Y. Li, M. Zhang, and Z. Ghassemlooy, "Optical MIMO NOMA-PON Based on Single Carrier Transmission and Polarization Interleaving,"*Optical Fiber Technology*, vol. 36, no.8, pp. 412-416, July 2017.

[223] W. Chu, J. Dang, Z. Zhang, and L. Wu, "Effect of Clipping on the Achievable Rate of Non-Orthogonal Multiple Access With DCO-OFDM,"in *IEEE 9th International Conference on Wireless Communications and Signal Processing (WCSP), Nanjing, China*, Oct. 2017.

[224] J. Zhou, Q. Wang, J. Wei, Q. Cheng, T. Zhang, Z. Yang, A. Yang, Y. Lu, and Y. Qiao, "Faster-than-Nyquist Non-Orthogonal Frequency-Division Multiplexing for Visible Light Communications,"*IEEE Access*, vol. 6, no.7, pp. 17933-17941, Mar. 2018.

[225] Z. Pi and F. Khan, "An Introduction to Millimeter-Wave Mobile Broadband Systems," *IEEE Communications Magazine*, vol. 49, pp. 203-211, no.6, June 2011.

[226] A. Alkhateeb, J. Mo, N. Gonzalez-Prelcic, and R. W. Heath, "MIMO Precoding and Combining Solutions for Millimeter-Wave Systems,"*IEEE Communications Magazine*, vol. 52, no. 12, pp. 122-131, Dec. 2014.

[227] A. Mukherjee, S. Misra and A. Atrish,"MiND: Mind Networked Device Architecture for Attention-Gated Ambient Assisted Living Systems," *IEEE Systems Journal*, vol. 1, no. 14, pp. 1325-1332, Apr. 2020.

[228] Z. Ding, P. Fan, and H. V. Poor, "Random Beamforming in Millimeter-Wave NOMA Networks,"*IEEE Access*, vol. 5, no.1, pp. 7667-7681, Feb. 2017.

[229] J. Cui and Y. Liu and Z. Ding and P. Fan and A. Nallanathan, "Optimal User Scheduling and Power Allocation for Millimeter Wave NOMA Systems,"*IEEE Transactions on Wireless Communications*, vol. 17, no. 3, pp. 1502-1517, Mar. 2018.

[230] Z. Ding, L. Dai, R. Schober, and H. V. Poor, "NOMA Meets Finite Resolution Analog Beamforming in Massive MIMO and Millimeter-Wave Networks,"*IEEE Communications Letters*, vol. 21, no.8, pp. 1879-1882, Aug. 2017.

[231] B. Wang, L. Dai, Z. Wang, N. Ge, and S. Zhou, "Spectrum and Energy-Efficient Beamspace MIMO-NOMA For Millimeter-Wave Communications Using Lens Antenna Array, "*IEEE Journal on Selected Areas in Communications*, vol. 35, no.10, pp. 2370-2382, Oct. 2017.

[232] W. Hao, M. Zeng, Z. Chu, and S. Yang, "Energy-Efficient Power Allocation in Millimeter Wave Massive MIMO With Non-Orthogonal Multiple Access,"*IEEE Wireless Communications Letters*, vol. 6, no.6, pp. 782-785, Dec. 2017.

[233] Z. Xiao, L. Zhu, J. Choi, P. Xia, and X. G. Xia, "Joint Power Allocation and Beamforming For Non-Orthogonal Multiple Access (NOMA) in 5G Millimeter-Wave Communications, "*IEEE Transactions on Wireless Communications*, vol. 17, no.5, pp. 2961-2974, May 2018.

[234] M. A. Almasi, M. Vaezi, and H. Mehrpouyan, "Hybrid Beamforming NOMA for mmWave Communications,"*CoRR*, vol. abs/1808.00591, pp. 1-31, Aug. 2018.

[235] W. Wu and D. Liu, "Non-Orthogonal Multiple Access Based Hybrid Beamforming in 5G mmWave Systems,"in *IEEE 28th Annual International Symposium on Personal, Indoor, and Mobile Radio Communications (PIMRC), Montreal, QC, Canada*, Oct. 2017.

[236] M. A. Almasi and H. Mehrpouyan, "Non-Orthogonal Multiple Access Based on Hybrid Beamforming for mmWave Systems, "in *IEEE 88th Vehicular Technology Conference (VTC-Fall), Chicago, IL*, Aug. 2019.

[237] J. Cui and Z. Ding and P. Fan and N. Al-Dhahir, "Unsupervised Machine Learning-Based User Clustering in Millimeter-Wave-NOMA Systems,"*IEEE Transactions on Wireless Communications*, vol. 17, no. 11, pp. 7425-7440, Nov. 2018.

[238] P. Botsinis, I. Hemadeh, D. Alanis, Z. Babar, H. V. Nguyen, D. Chandra, S. X. Ng, M. El-Hajjar, and L. Hanzo, "Joint-Alphabet Space Time Shift Keying in mmwave Non-Orthogonal Multiple Access,"*IEEE Access*, vol. 6, no.2, pp. 22602-22621, Aug. 2018.

[239] R. Vanzara, P. Sharma, H. S. Bhatt, S. Tanwar, S. Tyagi, N. Kumar, and M. S. Obaidat, "ADYTIA: Adaptive and Dynamic TCP Interface Architecture for Heterogeneous Networks, "*International Journal of Communication Systems*, vol. 32, no.2, Feb. 2019.

[240] W. Zong, Y. W. Chow, W. Susilo, "Interactive three-dimensional visualization of network intrusion detection data for machine learning," *Future Generation Computer Systems*, vol. 102, pp. 292-306, Jan. 2020.

[241] V. Kalokidou, O. Johnson, and R. Piechocki, "Interference Management in Heterogeneous Networks With Blind Transmitters,"*CoRR*, vol. abs/1601.08132, pp.1-30, Jan. 2016.

[242] A. Mokdad, P. Azmi, and N. Mokari, "Radio Resource Allocation for Heterogeneous Traffic in GFDM-NOMA Heterogeneous Cellular Networks,"*IET Communications*, vol. 10, no. 12, pp. 1444-1455, Aug. 2016.

[243] Z. Zhang, Z. Ma, M. Xiao, G. Liu, and P. Fan, "Modeling and Analysis of Non-Orthogonal MBMS Transmission in Heterogeneous Networks,"*IEEE Journal on Selected Areas in Communications*, vol. 35, no.10, pp. 2221-2237, Oct. 2017.

[244] C. H. Liu and D. C. Liang, "Heterogeneous Networks With Power-Domain NOMA: Coverage, Throughput, and Power Allocation Analysis,"*IEEE Transactions on Wireless Communications*, vol. 17, no.5, pp. 3524-3539, May 2018.

[245] P. Swami, V. Bhatia, S. Vuppala, and T. Ratnarajah, "User Fairness and Performance Enhancement For Cell Edge User in NOMA-HCN With Offloading,"in *IEEE 85th Vehicular Technology Conference (VTC Spring), Sydney, NSW, Australia*, June 2017.

[246] S. A. A. Shah, E. Ahmed, M. Imran, and S. Zeadally, "5G for Vehicular Communications, "*IEEE Communications Magazine*, vol. 56, no.1, pp. 111-117, Jan. 2018.

[247] S. Chakraborty, S. Chakraborty, S. Nandi and S. Karmakar, "ADCROSS: Adaptive Data Collection from Road Surveilling Sensors,"in *IEEE Transactions on Intelligent Transportation Systems*, vol. 15, no. 5, pp. 2049-2062, Oct. 2014.

[248] A. Molinaro, C. Campolo, J. HÃd'rri, C. E. Rothenberg and A. V. Vinel, "5G-V2X Communications and Networking for Connected and Autonomous Vehicles," *Future Internet*, vol. 12, no.7, pp. 1-16, June 2020.

[249] L. Qian, Y. Wu, H. Zhou, and S. Shen, "Dynamic Cell Association for Non-Orthogonal Multiple-Access V2S Networks,"*IEEE Journal on Selected Areas in Communication*, vol. 35, no.10, pp. 2342-2356, Oct. 2017.

[250] P. K. Singh, S. K. Nandi, S. Nandi,"A tutorial survey on vehicular communication state of the art, and future research directions," *Vehicular Communications*, vol. 18, no.5, pp. 100-164, Aug. 2019.

[251] Y. Chen, L. Wang, Y. Ai, B. Jiao, and L. Hanzo, "Performance Analysis of NOMA-SM in Vehicle-to-Vehicle massive MIMO Channels,"*IEEE Journal on Selected Areas in Communications*, vol. 35, no.12, pp. 2653-2666, Dec. 2017.

[252] B. Di, L. Song, Y. Li, and G. Y. Li, "Non-Orthogonal Multiple Access for High-Reliable and Low-Latency V2X Communications in 5G Systems,"*IEEE Journal on Selected Areas in Communications*, vol. 35, no.10, pp. 2383-2397, Oct. 2017.

[253] Y. Liu, X. Wang, A. B. Sediq, G. Boudreau, and H. Li, "An Adaptive Two-Dimensional Non-Orthogonal Multiple Access Technique Using Multi-Level Modulation and Interleaving,"in *IEEE 3rd International Conference on Computer and Communications (ICCC), Chengdu, China*, pp. 57-62, Dec. 2017.

[254] J. Cui, G. Dong, S. Zhang, H. Li, and G. Feng, "Asynchronous NOMA for Downlink Transmissions,"*IEEE Communications Letters*, vol. 21, no.2, pp. 402-405, Feb. 2017.

[255] J. A. Altabas, S. Rommel, R. Puerta, D. Izquierdo, J. I. Garces, J. A. Lazaro, J. J. V. Olmos, and I. T. Monroy, "Non-Orthogonal Multiple Access and Carrierless Amplitude Phase Modulation for Flexible Multiuser Provisioning in 5G Mobile Networks,"*Journal of Lightwave Technology*, vol. 35, no. 24, pp. 5456-5463, July 2017.

[256] Z. Zhao, M. Xu, Y. Li, and M. Peng, "A Non-Orthogonal Multiple Access-Based Multicast Scheme in Wireless Content Caching Networks," *IEEE Journal on Selected Areas in Communications*, vol. 35, no.12, pp. 2723-2735, Dec. 2017.

[257] M. B. Shahab and S. Y. Shin, "On the Performance of a Virtual User Pairing Scheme to Efficiently Utilize the Spectrum of Unpaired Users in NOMA,"*Physical Communication*, vol. 25, no.10, pp. 492-501, Dec. 2017.

[258] I. Budhiraja, S. Tyagi, S. Tanwar, N. Kumar, and M. Guizani, "CR-NOMA Based Interference Mitigation Scheme for 5G Femtocells Users,"in *IEEE Global Communications Conference, GLOBECOM, Abu Dhabi, UAE*, Dec. 2018.

[259] I. Budhiraja, S. Tyagi, S. Tanwar, N. Kumar, and M. Guizani, "Cross Layer NOMA Interference Mitigation for Femtocell Users in 5G Environment,"*IEEE Transactions on Vehicular Technology*, vol. 68, no.5, pp. 4721-4733, May 2019.

[260] M. B. Shahab and S. Y. Shin, "A Time Sharing Based Approach to Accommodate Similar Gain Users in NOMA for 5G Networks,"in *IEEE 42nd Conference on Local Computer Networks Workshops (LCN Workshops), Singapore*, pp. 142-147, Oct. 2017.

[261] Z. Yang, Z. Ding, P. Fan, and Z. Ma, "Outage Performance For Dynamic Power Allocation in Hybrid Non-Orthogonal Multiple Access Systems,"*IEEE Communications Letters*, vol. 20, no.8, pp. 1695-1698, Aug. 2016.

[262] J. A. Oviedo and H. R. Sadjadpour, "A New NOMA Approach for Fair Power Allocation,"in *IEEE Conference on Computer Communications Workshops (INFOCOM WKSHPS), San Francisco, CA*, pp. 843-847, Apr. 2016.

[263] J. Farah, A. Kilzi, C. A. Nour, and C. Douillard, "Power Minimization Techniques in Distributed Base Station Antenna Systems using Non-Orthogonal Multiple Access,"*arXiv: Signal Processing*, pp.1-14, Oct. 2018.

[264] S. Baig, M. Ahmad, H. M. Asif, M. N. Shehzad, and M. H. Jaffery, "Dual PHY Layer for Non-Orthogonal Multiple Access Transceiver in 5G Networks,"*IEEE Access*, vol. 6, no.5, pp. 3130-3139, Dec. 2018.

[265] A. Li, X. Chen, and H. Jiang, "Contention Based Uplink Transmission with NOMA for Latency Reduction, "in *IEEE 85th Vehicular Technology Conference (VTC Spring), Sydney, NSW, Australia*, June 2017.

[266] L. Ping, L. Liu, K. Wu, and W. K. Leung, "On Interleave-Division Multiple-Access,"in *IEEE International Conference on Communications (ICC), Paris, France*, vol. 5, pp. 2869-2873, June 2004.

[267] 3GPP-R1-163510, "Candidate NR Multiple Access Schemes,".

[268] 3GPP-R1-164869, "Low Code Rate and Signature Based Multiple Access Scheme for NR,".

[269] L. Ping, L. Liu, K.Wu, andW. K. Leung, "Interleave Division Multiple-Access,"*IEEE Transactions on Wireless Communications*, vol. 5, no.4, pp. 938-947, Apr. 2006.

[270] K. Kusume, G. Bauch, and W. Utschick, "IDMA vs. CDMA: Analysis and Comparison of Two Multiple Access Schemes, "*IEEE Transactions on Wireless Communications*, vol. 11, no.1, pp. 78-87, Jan. 2012.

[271] L. Ping, Q. Guo, and J. Tong, "The OFDM-IDMA Approach to Wireless Communication Systems,"*IEEE Wireless Communications*, vol. 14, no.3, June 2007.

[272] L. Ping, L. Liu, K. Wu, and W. Leung, "Approaching the Capacity of Multiple Access Channels Using Interleaved Low-Rate Codes,"*IEEE Communications Letters*, vol. 8, no.1, pp. 4-6, Jan. 2004.

[273] H. Wu, L. Ping, and A. Perotti, "User-Specific Chip-Level Interleaver Design For IDMA Systems,"*Electronics Letters*, vol. 42, no.4, pp. 233-234, Feb. 2006.

[274] A. L. S. B. Nokia and L. S. Bell, "Performance of Interleave Division Multiple Access (IDMA) in Combination With OFDM Family Waveforms,"in *R1-165021, 3GPP TSG RAN WG1 Meeting*, vol. 85, May 2016.

[275] R. Zhang and L. Hanzo, "Three Design Aspects of Multicarrier Interleave Division Multiple Access, "*IEEE Transactions on Vehicular Technology*, vol. 57, no.6, pp. 3607-3617, Nov. 2008.

[276] G.T.R. WG1-163992, "Non-Orthogonal Multiple Access Candidate For NR,".

[277] 3GPP-R1-167535, "New Uplink Non-Orthogonal Multiple Access Schemes for NR,".

[278] 3GPP-R1-162385, "Multiple Access Schemes for New Radio Interface,".

[279] 3GPP-ZTE, "Discussion on Multiple Access for New Radio Interface,"*R1-162226*, Apr. 2016.

[280] E. M. Eid, M. M. Fouda, A. S. T. Eldien, and M. M. Tantawy, "Performance Analysis of MUSA With Different Spreading Codes Using Ordered SIC Methods,"in *IEEE 12th International Conference on Computer Engineering and Systems (ICCES), Cairo, Egypt*, pp. 101-106, Dec. 2017.

[281] 3GPP-R1-162517, "Considerations on DL/UL Multiple Access for NR,".

[282] H. Hu and J. Wu, "New Constructions of Codebooks Nearly Meeting the Welch Bound With Equality,"*IEEE Transactions on Information Theory*, vol. 60, no.2, pp. 1348-1355, Feb. 2014.

[283] 3GPP-R1-165019, “Non-Orthogonal Multiple Access for NR,”.

[284] J. L. Massey and T. Mittelholzer, “Welch’s Bound and Sequence Sets for Code-Division Multiple-Access Systems,”in *Sequences II, New York: Springer*, pp. 63-78, Jan. 1993.

[285] X. Dai, S. Chen, S. Sun, S. Kang, Y.Wang, Z. Shen, and J. Xu, “Successive Interference Cancellation Amenable Multiple Access (SAMA) for Future Wireless Communications, ”in *IEEE International Conference on Communication Systems (ICCS), Macau, China*, pp. 222-226, Nov. 2014.

[286] B. Ren, Y. Wang, X. Dai, K. Niu, and W. Tang, “Pattern Matrix Design of PDMA for 5G UL Applications, ”*China Communications*, vol. 13, Supplement 2, pp. 159-173, Jan. 2017.

[287] Y. Mao, J. Zeng, X. Su, L. Liu, and Y. Kuang, “Pattern Design in Joint Space Domain and Power Domain for Novel Multiple Access,”in *IEEE 83rd Vehicular Technology Conference (VTC Spring), Nanjing, China*, May 2016.

[288] J. Zeng, D. Kong, B. Liu, X. Su, and T. Lv, “RIePDMA and BP-IDD-IC Detection,”*EURASIP Journal on Wireless Communications and Networking*, vol. 2017, no.1, p. 12, Dec. 2017.

[289] H. Nikopour et al., “SCMA for downlink multiple access of 5G wireless networks,”in *IEEE Global Communications Conference (GLOBECOM), Austin, TX*, pp. 3940-3945, Dec. 2014.

[290] 3GPP-R1-162153, “Overview of Non-Orthogonal Multiple Access for 5G,”.

[291] K. Au, L. Zhang, H. Nikopour, E. Yi, A. Bayesteh, U. Vilaipornsawai, J. Ma, and P. Zhu, “Uplink Contention Based SCMA for 5G Radio Access,”in *IEEE Globecom Workshops (GC Wkshps), Austin, TX, USA*, pp. 900-905, Dec. 2014.

[292] M. Taherzadeh, H. Nikopour, A. Bayesteh, and H. Baligh, “SCMA Codebook Design,”in *IEEE 80th Vehicular Technology Conference (VTC Fall), Vancouver, BC, Canada*, Dec. 2014.

[293] H. Yu, Z. Fei, N. Yang, and N. Ye, “Optimal Design of Resource Element Mapping For Sparse Spreading Non-Orthogonal Multiple Access,”IEEE Wireless Communications Letters, vol. 7, no.5, pp. 744-747, Oct. 2018.

[294] 3GPP-R1-164329, “Initial LLS Results for UL Non-Orthogonal Multiple Access,”.

[295] R. Hoshyar, F. P. Wathan, and R. Tafazolli, “Novel Low-Density Signature for Synchronous CDMA Systems Over AWGN Channel,”*IEEE Transactions on Signal Processing*, vol. 56, no.4, pp. 1616-1626, Apr. 2008.

[296] R. Gallager, "Low-Density Parity-Check Codes,"*IRE Transactions on information theory*, vol. 8, no.1, pp. 21-28, Jan. 1962.

[297] R. Hoshyar, R. Razavi, and M. Al-Imari, "LDS-OFDM an Efficient Multiple Access Technique,"in *IEEE 71st Vehicular Technology Conference (VTC), Taipei, Taiwan*, May 2010.

[298] M. A. Naim, J. P. Fonseka, and E. M. Dowling, "A Building Block Approach for Designing Multilevel Coding Schemes,"*IEEE Communications Letters*, vol. 19, no.1, pp. 2-5, Jan. 2015.

[299] G. Thiagarajan and C. R. Murthy, "Trellis Coded Block Codes: Design and Applications,"*Journal of Communications*, vol. 7, pp. 73-85, Nov. 2012.

[300] D. Fang, Y. C. Huang, Z. Ding, G. Geraci, S. L. Shieh, and H. Claussen, "Lattice Partition Multiple Access: A New Method of Downlink Non-Orthogonal Multiuser Transmissions,"in *IEEE Global Communications Conference (GLOBECOM), Washington, DC*, Dec. 2016.

[301] M. N. Khormuji, "Generalized Semi-Orthogonal Multiple-Access for Massive MIMO,"in *IEEE 81st Vehicular Technology Conference (VTC Spring), Glasgow*, UK, May 2015.

[302] A. G. Perotti and B. M. Popovic, "Non-Orthogonal Multiple Access for Degraded Broadcast Channels: RA-CEMA, "in *IEEE Wireless Communications and Networking Conference (WCNC), New Orleans, LA*, pp. 735-740, Mar. 2015.

[303] W. H. Hsiao and C. C. Huang, "Multipath Division Multiple Access for 5G Cellular System Based on Massive Antennas in Millimeter Wave Band,"in *IEEE 18th International Conference on Advanced Communication Technology (ICACT), Pyeongchang, South Korea*, pp. 741-746, Jan. 2016.

[304] W. H. Hsiao, Y. W. Shih, and C. C. Huang, "Case Study and Performance Evaluation of MDMA-A Non-Orthogonal Multiple Access Scheme for 5G Cellular Systems,"*Mobile Networks and Applications*, vol. 23, no.4, Aug. 2018.

[305] M. Moltafet, N. Mokari, M. R. Javan, H. Saeedi, and H. Pishro-Nik, "A New Multiple Access Technique for 5G: Power Domain Sparse Code Multiple Access (PSMA),"*IEEE Access*, vol. 6, no.2, pp. 747-759, Nov. 2018.

[306] C. Berrou, A. Glavieux, and P. Thitimajshima, "Shannon Near Limit Error-Correcting Coding and Decoding: Turbo-Codes.1,"in *Proceedings of ICC'93-IEEE International Conference on Communications, Geneva, Switzerland*, vol. 2, pp. 1064-1070, May 1993.

[307] M. R. Usman, M. A. Usman, A. Khan, and S. Y. Shin, "On the Performance of Turbo Coding in Non-Orthogonal Multiple Access (NOMA),"*Annual Summer Conference of the Korean Institute of Communication Sciences, Jeju, South Korea*, June 2017.

[308] J. Dai, K. Niu, Z. Si, C. Dong, and J. Lin, "Polar-Coded Non-Orthogonal Multiple Access,"*IEEE Transactions on Signal Processing*, vol. 66, no.5, pp. 1374-1389, Mar. 2018.

[309] M. Yang, B. Li, Z. Bai, and Z. Yan, "SGMA: Semi-Granted Multiple Access For Non-Orthogonal Multiple Access in 5G Networking,"*Journal of Network and Computer Applications*, vol. 112, no.4, pp. 115-125, June 2018.

[310] J. Huang, K. Peng, C. Pan, F. Yang, and H. Jin, "Scalable Video Broadcasting Using Bit Division Multiplexing, "*IEEE Transactions on Broadcasting*, vol. 60, no.4, pp. 701âĂŞ706, Dec. 2014.

[311] T. L. Marzetta, "Non Cooperative Cellular Wireless With Unlimited Numbers of Base Station Antennas,"*IEEE Transactions on Wireless Communications*, vol. 9, no.11, pp. 3590-3600, Nov. 2010.

[312] Y. Liang, X. Li, J. Zhang, and Z. Ding, "Non-Orthogonal Random Access for 5G Networks,"*IEEE Transactions on Wireless Communications*, vol. 16, no.7, pp. 4817-4831, July 2017.

[313] A. D. Wyner, "The Wire-Tap Channel, "*Bell System Technical Journal*, vol. 54, no.8, pp. 1355-1387, Oct. 1975.

[314] A. Mukherjee and A. L. Swindlehurst, "Robust Beamforming for Security in MIMO Wiretap Channels With Imperfect CSI,"*IEEE Transactions on Signal Processing*, vol. 59, no.1, pp. 351-361, Jan. 2011.

[315] Z. Qin, Y. Liu, Z. Ding, Y. Gao, and M. Elkashlan, "Physical Layer Security for 5G Non-Orthogonal Multiple Access in Large-Scale Networks,"in *IEEE International Conference on Communications (ICC), Kuala Lumpur, Malaysia*, May 2016.

[316] Y. Liu, Z. Qin, M. Elkashlan, Y. Gao, and L. Hanzo, "Enhancing the Physical Layer Security of Non-Orthogonal Multiple Access in Large-Scale Networks, "*IEEE Transanctions on Wireless Communications*, vol. 16, no.3, pp. 1656-1672, Mar. 2017.

[317] Y. Zhang, H. M.Wang, Q. Yang, and Z. Ding, "Secrecy Sum Rate Maximization in Non-Orthogonal Multiple Access,"*IEEE Communications Letters*, vol. 20, no.5, pp. 930-933, May 2016.

[318] J. Papandriopoulos and J. S. Evans, "SCALE: A Low-Complexity Distributed Protocol for Spectrum Balancing in Multiuser DSL Networks,"IEEE Transactions on Information Theory, vol. 55, no. 8, pp. 3711âĂŞ3724, July 2009.

[319] R. Horst and N. V. Thoai, "DC Programming: Overview,"*Journal of Optimization Theory and Applications*, vol. 103, no. 1, pp. 1-43, Oct. 1999.

[320] S. Boyd and L. Vandenberghe, Convex Optimization. Cambridge university press, Mar. 2004.

[321] D. P. Bertsekas, "Nonlinear Programming, "*Journal of the Operational Research Society*, vol. 48, no. 3, pp. 334-334, Mar. 1997.

[322] 3GPP-TR-36.843, "Study on LTE Device-to-Device Proximity Services: Radio Aspects (Release 17),"July 2019.

[323] X. Cheng, Y. Li, B. Ai, X. Yin, and Q. Wang, "Device-to-Device Channel Measurements and Models: A Survey,"*IET Communications*, vol. 9, no. 3, pp. 312-325, Jan. 2015.

[324] C. H. Yu, K. Doppler, C. B. Ribeiro, and O. Tirkkonen, "Resource Sharing Optimization for Device-to-Device Communication Underlaying Cellular Networks,"*IEEE Transactions on Wireless Communications*, vol. 10, no. 8, pp. 2752-2763, June 2011.

[325] D. J. Dechene, and A. Shami, "QoS, Channel and Energy-Aware Packet Scheduling over Multiple Channels, "*IEEE Transactions on Wireless Communications*, vol. 10, no. 4, pp. 1058-1062, Apr. 2011.

[326] M. Kalil, A. Shami, A. Al-Dweik, and S. Muhaidat, "Low-Complexity Power-Efficient Schedulers for LTE Uplink With Delay-Sensitive Traffic,"*IEEE Transactions on Vehicular Technology*, vol. 64, no. 10, pp. 4551-4564, Oct. 2015.

[327] M. Kalil, A. Moubayed, A. Shami, and A. Al-Dweik, "Efficient Low-Complexity Scheduler for Wireless Resource Virtualization,"*IEEE Wireless Communications Letters*, vol. 5, no. 1, pp. 56-59, Feb. 2016.

[328] X. Li, R. Shankaran, M. A. Orgun, G. Fang, and Y. Xu, "Resource Allocation For Underlay D2D Communication With Proportional Fairness,"*IEEE Transactions on Vehicular Technology*, vol. 67, no. 7, pp. 6244-6258, Mar. 2018.

[329] J. An, Y. Zhang, X. Gao, and K. Yang, "Energy-Efficient Base Station Association and Beamforming for Multi-Cell Multiuser Systems,"*IEEE Transactions on Wireless Communications*, vol. 19, no. 4, pp. 2841-2854, Apr. 2020.

[330] Y. Jong, "An Efficient Global Optimization Algorithm for Non-Linear Sum-of-Ratios Problem,"*online: www. optimizationonline.org*, May 2012.

[331] K. Bando, "Many-to-One Matching Markets with Externalities among Firms,"*Journal of Mathematical Economics*, vol. 48, no. 1, pp. 14-20, Jan. 2012.

[332] X. Gao and D. Niyato and P. Wang and K. Yang and J. An, "Contract Design for Time Resource Assignment and Pricing in Backscatter-Assisted RF-Powered Networks, "*IEEE Wireless Communications Letters*, vol. 9, no. 1, pp. 42-46, Jan. 2020.

[333] L. Kleinrock, "Queueing Systems: Computer Applications"*Wiley New York*, vol. 2, no. 66, pp. 203-358 Apr. 1976.

[334] M. J. Neely, "Stochastic Network Optimization with Application to Communication and Queueing Systems, "*Synthesis Lectures on Communication Networks*, vol. 3, no. 1, pp. 1-211, Sept. 2010.

[335] Y. Zhang, J. Zhang, Y. Sun, and D. W. K. Ng, "Energy-Efficient Transmission for Wireless Powerec D2D Communication Networks,"in *IEEE International Conference on Communications (ICC), Paris, France*, pp. 1-7, May 2017.

[336] 3GPP-TR-36.814, "Evolved Universal Terrestrial Radio Access (EUTRA): Physical Layer Procedures, Release 11,"*Technical Report TS 36.213*, Dec. 2012.

[337] M. Sheng, Y. Li, X. Wang, J. Li, and Y. Shi, "Energy Efficiency and Delay Tradeoff in Device-to-Device Communications Underlaying Cellular Networks,"*IEEE Journal on Selected Areas in Communications*, vol. 34, no. 1, pp. 92-106, Aug. 2015.

[338] H. Zhang, B. Wang, C. Jiang, K. Long, A. Nallanathan, V. C. M. Leung, and H. V. Poor, "Energy Efficient Dynamic Resource Optimization in NOMA System,"*IEEE Transactions on Wireless Communications*, vol. 17, no. 9, pp. 5671-5683, Sept. 2018.